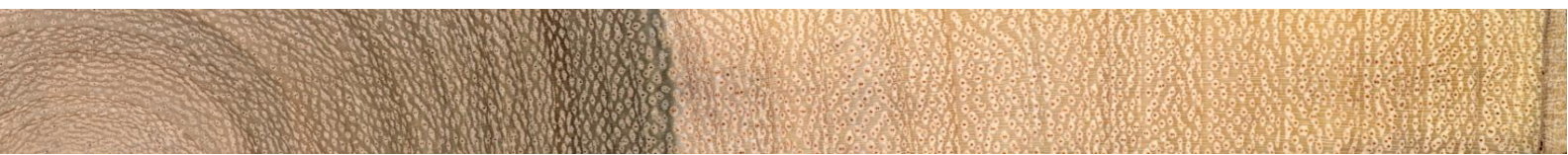
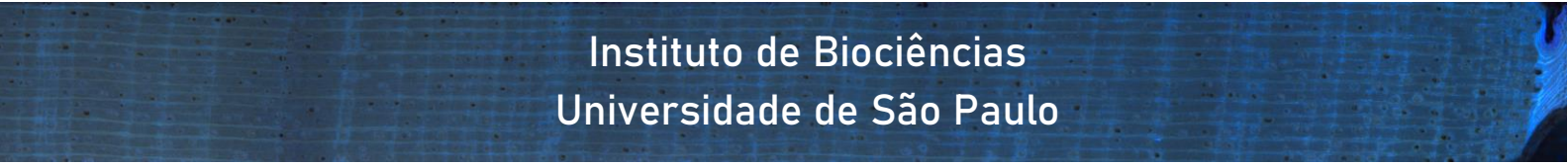


Milena de Godoy-Veiga

**Impacto das mudanças climáticas nos últimos 500 anos por meio de estudos dendroclimatológicos e isotópicos de árvores na região do Parque Nacional Cavernas do Peruaçu**



**Instituto de Biociências  
Universidade de São Paulo**





Milena de Godoy-Veiga

Impacto das mudanças climáticas nos últimos 500 anos por meio de estudos dendroclimatológicos e isotópicos de árvores na região do Parque Nacional Cavernas do Peruaçu

Assessment of climate change impacts in the last 500 years through dendroclimatological and isotopic studies from trees at the Parque Nacional Cavernas do Peruaçu region

São Paulo

2023

EXEMPLAR CORRIGIDO

Milena de Godoy-Veiga

Impacto das mudanças climáticas nos últimos 500 anos por meio de estudos dendroclimatológicos e isotópicos de árvores na região do Parque Nacional Cavernas do Peruaçu

Assessment of climate change impacts in the last 500 years through dendroclimatological and isotopic studies from trees at the Parque Nacional Cavernas do Peruaçu region

Tese apresentada ao Instituto de Biociências da Universidade de São Paulo, para a obtenção de Título de Doutora em Ciências Biológicas, na Área de Botânica.

Orientadora: Veronica Angyalossy  
Coorientador: Giuliano Maselli Locosselli

São Paulo

2023

## Ficha Catalográfica

---

De Godoy-Veiga, Milena

Impacto das mudanças climáticas nos últimos 500 anos por meio de estudos dendroclimatológicos e isotópicos de árvores na região do Parque Nacional Cavernas do Peruaçu / de Godoy-Veiga Milena ; orientadora Angyalossy Veronica ; coorientador Maselli Locosselli Giuliano -- São Paulo, 2023. 197 p.

Tese (Doutorado) - Instituto de Biociências da Universidade de São Paulo. Ciências Biológicas (Botânica). .

1. Dendrocronologia. 2. Mudanças climáticas. 3. Isótopos de oxigênio. 4. Radiocarbono. 5. Ecologia. I. Angyalossy, Veronica, orient. II. Maselli Locosselli, Giuliano, coorient. Título.

Versão corrigida

### Comissão Julgadora:

Ana Carolina Maioli Barbosa

---

Prof(a). Dr(a).

Daniela Granato Souza

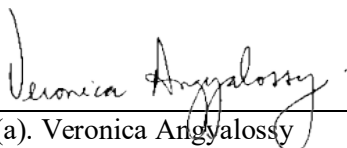
---

Prof(a). Dr(a).

Peter Stoltenborg Groenendyk

---

Prof(a). Dr(a).



---

Prof(a). Dr(a). Veronica Angyalossy

Orientador(a)



## Dedicatória

---

Dedico este trabalho primeiramente  
a meus pais,  
que me trouxeram até aqui.  
a minha esposa,  
que me manteve aqui.  
e a minha avó,  
que me ajudou nos primeiros  
passos para chegar aqui.

Epígrafe

---

Well, you roll on roads, over fresh green grass  
For your lorry loads, pumping petrol gas  
And you make them long, and you make them tough  
But they just go on and on and it seems that you can't get off

Oh, I know we've come a long way  
We're changing day to day  
But tell me, where do the children play?

Well, you've cracked the sky, scrapers fill the air  
But will you keep on building higher, until there's no more room up there?

Will you make us laugh? Will you make us cry?  
Will you tell us when to live?  
Will you tell us when to die?

*Where do the children play?*  
Composição: Cat Stevens

## Agradecimentos

---

Gostaria de agradecer a muitas pessoas e espero lembrar de todas, mas sei que será difícil e em vários momentos futuros lembrarei de alguém que não agradeceu na tese. Não se faz uma tese sem ajuda e apoio de muita gente. Obrigada por me aguentarem falando sobre anéis de crescimento por todos esses anos.

Uma pessoa fundamental para que essa tese se formasse foi minha esposa, Poca. Quem me ouviu em todas as primeiras prévias, as piores prévias, e até aprendeu muito sobre botânica e dendrocronologia no processo. Obrigada pela paciência nos momentos de ansiedade e por me lembrar de parar para comer e descansar. Você me motivou muito a acreditar em mim, ser forte e chegar até o fim. Obrigada amor.

Agradeço também a minha família. Meus pais que sempre me deram apoio e me trouxeram até aqui, mesmo que muitas vezes mais de longe do que gostaríamos. Espero que vocês gostem do resultado desse projeto e que um dia eu possa levar vocês para algum desses lugares mágicos que a dendro me levou.

Quanto aos amigos, Quarto 28 é sinônimo de muito carinho e caminhos que se encontraram e insistem em ficar juntos por aí. A todas vocês, minhas queridas, obrigada por toda a amizade, amor, conforto e desconforto que passamos. Vocês me inspiram demais e quero muito ver o que esse grupo de mulheres ainda vai fazer. Também as amigadas no Hand Barango e no karate que me deram muita força no processo.

E claro, a quem ganhou cabelos brancos junto comigo durante todo o meu processo na graduação e pós-graduação, e sem o qual esse projeto não seria o mesmo. Agradeço a você Giu. Obrigada pela orientação desde a iniciação científica em 2015 até agora. Você me ensinou a andar nessa brincadeira, obrigada por tudo e pela paciência. Aprendi muito sobre como orientar de forma leve e presente. Espero levar essa parceria por muitos projetos ainda. Também agradeço aos professores Marcos Silveira Buckeridge e Gregório Ceccantinni do departamento de Botânica do Instituto de Biociências da USP por disponibilizarem o uso de amostras e equipamentos. E finalmente ao professor Chico Bill, do Instituto de Geociências da



USP, pela brilhante coordenação e oportunidade de participar de um projeto temático como o PIRE-CREATE.

A minha orientadora Veronica que me viu crescendo pela graduação, monitorias, e na pesquisa. A quem não posso cansar de agradecer pelo exemplo de pesquisadora renomada internacionalmente, movida pelo amor ao seu objeto de estudo e uma professora que encanta e se preocupa com seus alunos. Obrigada por sua ajuda no processo dessa tese, você foi essencial para a finalização desse trabalho e sou muito grata pela sua força.

Não se faz um projeto desse tamanho sem apoio técnico. E gostaria de começar agradecendo a Paula Alecio, que me ensinou técnicas do básico ao avançado, mais do que uma vez porque eu esquecia, muito obrigada pela sabedoria na curadoria, manutenção da xiloteca e no lado pessoal também. Nossos cafés eram sempre revigorantes, saudades da equipe coração! Também agradeço as técnicas Gisele Costa e Tássia dos Santos, Eglee Igarashi, Viviane da Costa, Natalia Santos, Giselle Utida e Aparecido Siqueira. E é claro aos ajudantes de campo, que me ensinaram muito sobre o Parque, ajudaram a encontrar as árvores, vários equipamentos caros deixados para trás e a tirar trados presos nas árvores. Lucimar (e toda sua família) e Branco, vocês para mim são o coração do Peruaçu, espero mostrar essa dedicatória e esses resultados aí em Januária para vocês.

Também sou grata aos ensinamentos passados por amigos e colegas no laboratório de anatomia: Luciano Fioroto, Bruno Cintra, Luiza Teixeira, Evelyn Cardoso, Plácido Fabricio, Levi Itepan, Felipe Carvalho, Caian Gerolamo, Lui Agostinho, Mariana Victorio, Ricardo Hideaki, Leonardo Andrade, Mariana Oliveira, Edgar Lopes, Victor Sabinelli. Aos amigos e colegas da ESALQ que me receberam diversas vezes: Claudia Fontana, Bruna Hornink, Ricardo Ortega, Gabriel Pereira, Manolo Trindade, Luciana Karla, e claro ao sempre solícito professor Mario Tomazello que abriu as portas da sua equipe e laboratório sempre que preciso.

Sou muito grata a muitas professoras mulheres, fortes, que passaram pelo meu caminho da graduação a pós-graduação no instituto. Já agradei a Veronica, e também agradeço a coordenadora do programa de pós-graduação em Botânica na

época, Magdalena Rossi e a Flavia Melo de Pinna como representante do IB Acolhe, pelo apoio que me deram para finalizar meu projeto. Também fui ensinada pelas professoras, Mariana Oliveira, Estela Plastino, Renata Pardini, Adriana Martini, que muito me inspiram como modelos de professoras e pesquisadoras. Sem contar professoras e pesquisadoras que nem sabem da influência que tiveram sobre meu projeto e meu desenvolvimento como pesquisadora, como Valerie Trouet, Ana Carolina Barbosa, Alexandra Elbakyan, Daniela Granato-Souza, Laia Andrew Hayles. Obrigada pela representatividade e por abrir caminho para que outras mulheres também consigam fazer ciência.

Tive a oportunidade de visitar e trabalhar em outros laboratórios, principalmente nos laboratórios da professora Elisabetta Boaretto e Lior Regev. Fui incrivelmente recebida e apoiada por ambos e pela técnica “Genia” Mintz, e pelos amigos que fiz como Zane Stepka, Annie Melton, Jamal Ibrahim, Paula Kotli, Getta Rosenzweig, Nitsan Shalom, Filipe e Yan. E finalmente ao pessoal da Universidade Federal Fluminense, como Nicolás Strikis que me ajudou e me ensinou muito, e a Professora Kita Macario e sua aluna Izabela Hammerschlag que me receberam em seu laboratório e que me ensinaram muito sobre datação com radiocarbono.

E a todas as outras pessoas que não me lembrei de citar aqui.

Muito obrigada, essa tese não seria finalizada sem vocês.

Financiamento para este projeto foi proporcionado pela Fundação de Amparo à Pesquisa do Estado de São Paulo (FAPESP) através das bolsas de número: PIRE-CREATE 2017/50085-3; bolsa de doutorado de MG V 2018/07632-6 e Bolsa de Estágio e Pesquisa no Exterior (BEPE): 2019/09813-0. E indiretamente pela Coordenação de Aperfeiçoamento de Pessoal de Nível Superior - CAPES (Código de Financiamento 001).

## Índice

---

<b>Resumo (Geral)</b>	11
<b>Abstract</b>	12
<b>Introdução Geral</b>	13
<b>Referências Bibliográficas</b>	26
<b>Capítulo 1. <i>Improved tree-ring visualization using autofluorescence</i></b>	
Melhora na visualização de anéis de crescimento de árvores com o uso da autofluorescência	33
<b>Capítulo 2. <i>The value of climate responses of individual trees to detect areas of climate-change refugia, a tree-ring study in the Brazilian Seasonally Dry Tropical Forests</i></b>	
O valor das respostas individuais de árvores para detectar áreas de refúgio climático, um estudo dendrocronológico em mata tropical sazonalmente seca brasileira	82
<b>Capítulo 3. <i>Tree growth does not decline due to increasing VPD in seasonally dry tropical forest</i></b>	
Crescimento de árvores expostas ao aumento de VPD não é afetado floresta tropical sazonalmente seca	137
<b>Discussão Geral e Conclusões</b>	181
<b>Referências Bibliográficas</b>	192
<b>Biografia</b>	195



## Resumo

---

As mudanças climáticas causam grandes impactos nas florestas mundiais e, conseqüentemente nos ciclos biogeoquímicos. Entender as conseqüências dessas alterações antrópicas na região tropical é um desafio já que os registros instrumentais são limitados a poucas décadas. Para isso, os anéis de crescimento fornecem excelentes registros com resolução anual de variações climáticas atuais e anteriores às alterações humanas, mas poucas cronologias robustas para inferências climáticas são disponíveis nos trópicos. Assim, esta tese explorou um novo local e uma nova espécie para estudos dendrocronológicos visando avaliar o efeito de mudanças climáticas em florestas sazonalmente secas no centro leste do Brasil, um dos *hot spots* de aumento de temperatura na região tropical. Nesta tese foi: testada uma nova metodologia para aprimorar a identificação dos anéis de crescimento; construídas cronologias da largura e de isótopos estáveis de oxigênio de *Amburana cearensis* no Parque Nacional Cavernas do Peruaçu (PNCP); as quais foram analisadas em conjunto com *Cedrela fissilis*, outra espécie da Mata Seca do PNCP e espeleotemas da mesma região para avaliar os efeitos de mudanças no clima no crescimento hoje e 500 anos atrás. Com cronologias perfeitamente datadas e com forte sinal climático, vimos que as árvores de *A. cearensis* e *C. fissilis* crescem reguladas pela quantidade de chuva na estação de crescimento, e as condições de alta demanda evaporativa nos últimos anos ainda não afetam o crescimento dessas populações. Isso é corroborado com dados de amostras subfósseis e espeleotemas que mostram que eventos de aumento abrupto na demanda evaporativa durante a Pequena Idade do Gelo também não afetaram o crescimento de *A. cearensis*. Esses resultados poderão auxiliar cientistas a desenvolver cronologias com espécies de difícil interpretação da anatomia da madeira; auxiliar no desenvolvimento de novas cronologias tropicais; e entender os efeitos das mudanças climáticas no crescimento de espécies de matas tropicais secas. Os dados produzidos também podem apoiar o desenvolvimento de modelos globais de resposta da vegetação para entender o efeito de mudanças climáticas no funcionamento das florestas sazonalmente secas tropicais.

**Palavras-chave:** Dendrocronologia, ecologia, isótopos de oxigênio, radiocarbono, paleoclima.

## Abstract

---

Climate change affects forests and biogeochemical cycles globally. Assessing the effects in tropical forests is challenging because instrumental records are constrained. Thus, tree rings proxies offer excellent annually resolved records of recent and pre-industrial climate variability, however few robust chronologies are available for climate inferences in the tropics. Therefore, this thesis explored a new site in central-eastern Brazil, a hot spot of global warming in the tropics and a new tree species for dendrochronological investigations about the effects of climate change in a Seasonally Dry Tropical Forest (SDTF). In this work: we tested a new method for improving tree-ring identification; established *Amburana cearensis* tree-ring width and oxygen isotopes ratio ( $\delta^{18}\text{O}$ ) chronologies at the National Park *Cavernas do Peruaçu* (PNCP); which were analysed with records of another representative species, *Cedrela fissilis*, in the SDTF and speleothems to assess the effects of climate change in tree growth now and 500 year ago. Using the perfectly dated chronologies, with strong climate signal, we observed that trees of *A. cearensis* and *C. fissilis* grow regulated by rainfall amount during the growing season and the high evaporative demands in the recent years do not affect their growth yet. These findings are corroborated by data from subfossil samples and speleothem records that show another period of abrupt increase in evaporative demands during the Little Ice Age that did not leave traces in *Amburana cearensis* trees growth. Our results can aid scientists to develop new tree-ring chronologies with species that have complex wood anatomy; aid the development of new tropical chronologies; and understand the effects of climate change in SDTF trees growth. The data produced can also support the development of global vegetation models of SDTF responses to climate change.

**Keywords:** Dendrochronology, ecology, oxygen isotopes, radiocarbon, paleoclimate.

## Introdução Geral

---

Esta tese compõe um estudo na área de dendrocronologia na região central do Brasil que desenvolveu novas metodologias para a observação de anéis de crescimento, propôs perguntas e análises inovadoras para estudos em regiões tropicais e abriu caminho para estudos dendroclimatológicos e paleoclimáticos com uma nova espécie no Brasil. Este projeto foi uma das engrenagens centrais dentro do Projeto Temático PIRE: CREATE (*Climate Research Education in the Americas using Tree-ring and speleothem Examples*, FAPESP 2017/50085-3), para a reconstituição das condições paleoclimáticas por meio da união de indicadores de anéis de crescimento de árvores de múltiplas espécies e espeleotemas. Os estudos dendrocronológicos desta tese, em conjunto com trabalhos em espeleotemas de Strikis *et al.*, in press., coroam este projeto com o desenvolvimento de dois registros que revelaram padrões definidos de mudanças climáticas atuais em um contexto de mais de 500 anos. A utilização da dendrocronologia para investigar efeitos de mudanças climáticas em conjunto com espeleotemas em um contexto de meio milênio é algo raro e complexo na região tropical, por isto a relevância deste trabalho para a dendrocronologia nos trópicos.

Primeiramente, a dendrocronologia é o estudo dos anéis de crescimento em um contexto temporal, e cada camada de crescimento é datada com precisão anual, fornecendo informações para múltiplas perguntas relacionadas a ecologia, crescimento e história de árvores e florestas (Speer, 2010). Para que esses estudos possam ser feitos, o xilema secundário (lenho) da espécie escolhida precisa



apresentar camadas de crescimento visíveis, anuais e que registrem alguma variação ambiental regulando seu desenvolvimento (Speer, 2010). Portanto, o primeiro passo de um estudo dendrocronológico é observar a anatomia da madeira e dos anéis de crescimento, algo que pode ser muito complexo em regiões tropicais (Worbes, 1995, 2002). Dentre os problemas decorrentes da grande diversidade nos trópicos estão os anéis falsos e confluentes, que são, respectivamente, variações anatômicas que adicionam (um limite de anel a mais) ou não acrescentam anos (dois limites de anéis que parecem um) nas contagens e assim dificultam a atribuição do ano correto para cada camada (Speer, 2010). Além disso, a maioria das espécies arbóreas tropicais são angiospermas, que em sua maioria possuem mais tipos celulares no xilema secundário do que as gimospermas que predominam nas regiões temperadas (Simpson, 2019). Dada a dificuldade presente no dia-a-dia de estudos dendrocronológicos, uma técnica para auxiliar no entendimento e observação das variações anatômicas que delimitam os anéis de crescimento foi desenvolvida no primeiro capítulo desta tese. Testamos um método prático para explorar a grande diversidade anatômica encontrada nas espécies do local de estudo que aprimorou o contraste entre os diferentes tipos celulares e, em alguns casos, possibilitou a diferenciação entre anéis de crescimento verdadeiros e falsos (Godoy-Veiga *et al.*, 2019).

Após entender e visualizar as camadas de crescimento anuais, é preciso comprovar sua anualidade e entender quais fatores climáticos limitam e regulam o crescimento de cada espécie (Fritts, 1976, 1966). Nesta tese exploramos principalmente os sinais de *Amburana cearensis* (Allemão) A.C. Sm, uma espécie

amplamente distribuída e utilizada na América do Sul, com grande potencial dendroclimático (Brienen & Zuidema, 2005; López, Villalba & Bravo, 2013; Baker *et al.*, 2015; Paredes-Villanueva *et al.*, 2015; López, Villalba & Stahle, 2022), porém sem cronologias publicadas no Brasil até este trabalho. Assim, selecionamos uma área de florestas secas sazonais no norte de Minas Gerais, uma região de ocorrência da espécie e potencial para a formação de anéis de crescimento anuais e com forte sinal de chuva (Barbosa *et al.*, 2018; Pereira *et al.*, 2018; Fritts, 1976; Stahle, 1999). De fato, foi observado que essa espécie possui um excelente registro nos anéis de crescimento da variabilidade climática associada à chuva e temperatura na área, permitindo até que inferências a nível individual pudessem ser exploradas. Essas diferenças individuais são importantes, tanto para o uso dessa espécie como um registro natural quanto para a manutenção da espécie em um local sujeito a mudanças climáticas abruptas como é o Parque Nacional Cavernas do Peruaçu (PNCP).

A região do PNCP é um ponto estratégico para estudos dendrocronológicos e climatológicos no Brasil, pois contém a maior extensão de florestas sazonais secas contínuas da América do Sul (Apgaua *et al.*, 2015; Prado, 2000). A sazonalidade climática se deve à sua posição sob influência da Zona de Convergência do Atlântico Sul (ZCAS), no Sistema de Monção da América do Sul (SMAS) (Marengo *et al.*, 2012; Vera *et al.*, 2006). Além disso, a paisagem cárstica também propicia a ocorrência de cavernas com espeleotemas e eventual presença de madeiras subfósseis preservadas. Tanto os espeleotemas quanto os anéis de crescimento de árvore são excelentes registros de mudanças climáticas passadas e atuais (Brienen

*et al.*, 2015; Cruz *et al.*, 2009). Porém a sua aplicação em conjunto, apesar de notória, ainda foi pouco explorada em nível global (e.g. Trouet *et al.*, 2009; Managave, 2014), e sem aplicações no Brasil. Assim, no terceiro capítulo, os sinais climáticos registrados em árvores vivas, mortas e subfósseis são analisados em conjunto com os provenientes dos espeleotemas da região para avaliar as mudanças no déficit hídrico da região (Godoy-Veiga *et al.*, in prep). As inferências que podem ser feitas com base em registros naturais independentes e utilizando isótopos estáveis de oxigênio como indicadores de mudanças no sistema hidroclimático são robustas (Trouet *et al.*, 2009), mas pouco exploradas em regiões tropicais, o que torna o último capítulo da tese um grande avanço para a dendrocronologia e paleoclimatologia no Brasil.

### **Porque esta tese se fez necessária?**

#### *Breve contextualização e introdução dos tópicos abordados*

Entender a resposta da vegetação à variabilidade climática é de extrema importância dado o atual cenário de aquecimento global (IPCC WGI, 2021). As mudanças climáticas causadas pela intensa queima de combustíveis fósseis vêm causando rápidos aumentos de temperatura e déficit de pressão de vapor (VPD) que são importantes reguladores na fisiologia e evapotranspiração das árvores (Rawson, Begg & Woodward, 1977; Franks & Farquhar, 1999). Essas alterações climáticas são especialmente alarmantes na região central do Brasil e do PNCP, um dos “hot spots” na região tropical com aumentos de temperatura atingindo 2°C nos últimos 100 anos. Por isso são necessários estudos com anéis de crescimento nessa área,

para fornecer informações sobre o funcionamento do sistema no presente e passado, para que medidas para o futuro possam ser planejadas de forma embasada.

Portanto, este foi um dos principais objetivos dessa tese: estabelecer novas e longas cronologias de largura e isótopos de oxigênio de anéis de uma espécie de mata seca. Para desenvolver esta tese, novas metodologias (Capítulo 1), novas abordagens nas análises (Capítulo 2) e uso de diversos indicadores ambientais (Capítulo 3) foram explorados. Uma breve contextualização e introdução dos tópicos de cada capítulo são apresentados a seguir.

Uma breve contextualização e introdução dos tópicos de cada capítulo são resumidos na Figura 1 e apresentados a seguir.

### **Capítulo 1** – Desafio: *Dificuldade de visualização dos anéis de crescimento em áreas com grande diversidade anatômica*

Estudos dendrocronológicos são necessários em regiões tropicais devido ao lento desenvolvimento dessa área da ciência em locais com pouca sazonalidade de temperatura (Schongart *et al.*, 2017; Worbes, 2002). Por muito tempo acreditava-se que o câmbio, o meristema secundário responsável pela formação da madeira e consequentemente dos anéis de crescimento, somente entrava em estado de dormência sob condições de baixa temperatura durante o inverno das regiões temperadas (Worbes, 2002). Apesar de estudos pioneiros (Coster 1927, Berlage 1931, Mariaux 1967) e reuniões internacionais (Bormann & Berlyn 1981) já demonstrarem o potencial da região tropical, a ausência de uma variação considerável de temperatura desviou a atenção de muitos cientistas para as regiões

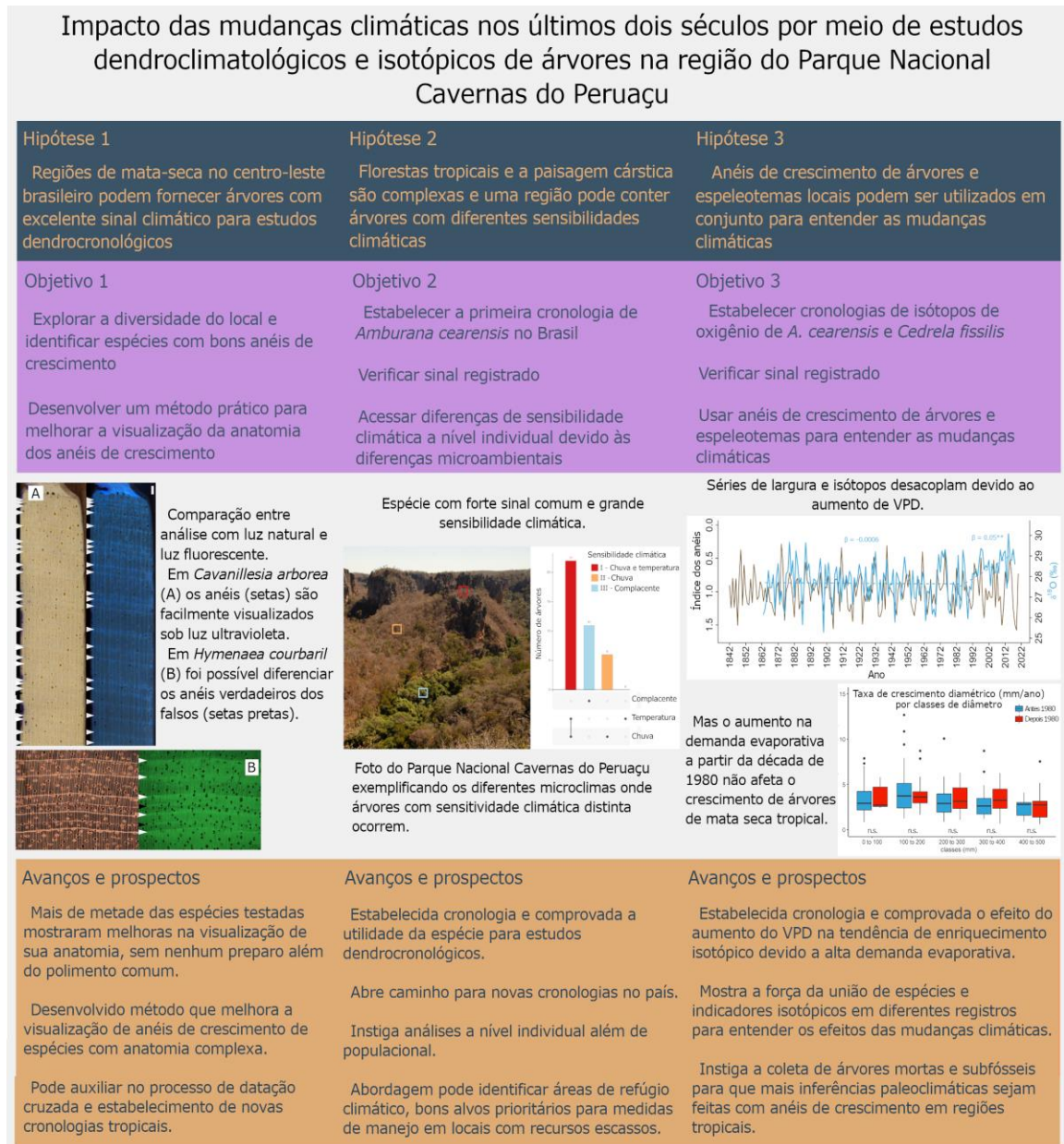


**Figura 1** - Infograma resumindo as hipóteses, objetivos, resultados e os avanços esperados a partir de cada capítulo desta tese

com clima temperado (Worbes, 2002). Entretanto, variações de precipitação são comuns por toda a região tropical e mais de 284 espécies apresentam anéis anuais que podem ser explorados para estudos dendrocronológicos (Locosselli *et al.*, 2020). Como consequência, as regiões temperadas ainda possuem mais cronologias de anéis, espacialmente e temporalmente (Zuidema *et al.*, 2013b), apesar do recente aumento no número de cronologias disponíveis nos trópicos que fornecem a base

para inferências climáticas a nível globais (Locosselli *et al.*, 2020; Zuidema *et al.*, 2022).

O desenvolvimento tardio da dendrocronologia tropical também resultou da diversidade e complexidade da anatomia das madeiras tropicais (Worbes & Fichtler, 2010). Devido a esta diversidade de espécies e anatômica, foram desenvolvidas várias técnicas para a discriminação dos anéis de crescimento, como a micro densitometria de raio-x (de Andrade *et al.*, 2017), análise anatômica (Quintilhan *et al.*, 2021), mensuração da variação de elementos traço com ablação a laser (Amais *et al.*, 2021), variações intra-anuais na composição de isótopos estáveis (Verheyden *et al.*, 2006) e micro tomografia de raios-x (Van Den Bulcke *et al.*, 2019), de forma independente ou até mesmo de forma conjunta (Ortega-Rodriguez *et al.*, 2022). Entretanto, para investigar a presença de camadas de crescimento em muitas espécies coletadas em estudos prospectivos e selecionar as melhores candidatas para estudos avançados, é preciso uma técnica que não necessitasse de processamentos adicionais e que utilizasse máquinas comumente encontradas em institutos de pesquisa.

Dessa forma exploramos um método alternativo para aprimorar visualização das camadas de crescimento sem preparos adicionais usando um estereomicroscópio de fluorescência (Godoy-veiga *et al.*, 2019). Esse equipamento emite uma luz de alta intensidade que induz a autofluorescência de componentes da madeira como lignina, antocianinas, óleos e resinas (Murphy, 2001) e seu potencial foi indicado em um estudo prévio com baobás (Slota *et al.*, 2017). Nesta tese o método foi sistematizado e testado em várias espécies com diferentes tipos de anéis de

crescimento para verificar quais características anatômicas tinham seu contraste aumentado pela técnica. Essa nova metodologia para observação e interpretação de camadas de crescimento em madeira mostrou-se útil para cientistas no processo de contagem dos anéis, datação cruzada e localização de anéis falsos, além de oferecer imagens de qualidade e com grande contraste para estudos anatômicos quantitativos.

## **Capítulo 2** – Desafio: *Estabelecer uma nova cronologia em região tropical*

Após observar as camadas de crescimento de uma espécie, o próximo passo é contá-las e aplicar a metodologia da datação cruzada, garantindo com que todos os anéis sejam perfeitamente datados (Speer, 2010). O sucesso da datação cruzada, que é a sincronização dos padrões de crescimento entre diversas árvores, depende de um fator comum limitando o crescimento da população (Douglass, 1941). Se um mesmo fator, como a ausência de chuvas no inverno, faz com que o câmbio reduza ou pare sua atividade na formação da madeira, esse sinal pode ser recuperado por meio da medida da largura dos anéis de crescimento, e será similar em toda a população (Douglass, 1941; Fritts, 1971).

Entretanto, ainda é necessário definir a periodicidade da formação dessas camadas para provar que os anéis de crescimento são anuais. Para comprovar a anualidade, ou definir a periodicidade da formação dos anéis de crescimento, algumas técnicas podem ser utilizadas, como: datação por radiocarbono dos anéis no período do “pico-da-bomba” (Hogg *et al.*, 2013); datação cruzada e correlações climáticas (Stahle, 1999); ou marcações cambiais periódicas e análise anatômicas (Speer, 2010). Já que por muitos anos se acreditava que a região tropical não produzia anéis anuais, em muitos casos ainda são necessárias pelo menos duas

dessas metodologias para estabelecer uma nova cronologia. Nesta tese, para o estabelecimento da primeira cronologia de *Amburana cearensis* no Brasil, a anualidade dos seus anéis foi comprovada por datações de radiocarbono e pela excelente correlação entre as séries e com variáveis climáticas. Dado que a cronologia produzida estava muito robusta foi possível inferir respostas do crescimento ao clima a nível individual, sendo que normalmente essas inferências são feitas a nível populacional (Trouillier *et al.*, 2018; Zuidema *et al.*, 2013a). Dessa forma foi possível identificar locais onde as árvores são menos sensíveis ao clima, nos chamados refúgios climáticos (Morelli *et al.*, 2020). Entretanto em anos de condições extremas de pouca chuva e temperaturas muito altas, todas as árvores, mesmo em diferentes condições pelo Parque Nacional Cavernas do Peruaçu (PNCP), apresentam uma resposta negativa no crescimento. Essas diferenças individuais na sensibilidade das árvores ao clima condizem com a grande complexidade da paisagem cárstica na qual as árvores foram coletadas.

O PNCP está inserido dentro dos limites da Bacia do Rio São Francisco, é marcado pela presença de rochas calcárias erodidas pela ação das chuvas e do baixo curso do Rio Peruaçu (Coelho, *et al.*, 2013). O clima no local é definido por um inverno seco (Aw na classificação Köppen), verão chuvoso e temperaturas ao redor dos 25°C (Peel, *et al.*, 2007). Essa comunhão de fatores edáficos e climáticos torna a área um excelente local para estudos climáticos na América do Sul, já que no local ocorrem tanto árvores que podem ter seus anéis de crescimento analisados, quanto espeleotemas e troncos preservados dentro das cavernas formadas pelo rio Peruaçu.



Com o estabelecimento da cronologia de *Amburana cearensis* e a verificação do forte sinal climático registrado, até mesmo em nível individual, o próximo passo foi a avaliação de novos indicadores além da largura dos anéis e sua análise em conjunto com os espeleotemas locais e troncos subfósseis para contextualizar os efeitos das mudanças climáticas recentes.

### **Capítulo 3** – Desafio: *Aumentar o poder de inferências paleoclimáticas em regiões tropicais unindo diferentes arquivos naturais*

Com cronologias longas e robustas de largura de anéis, é possível fazer inferências sobre a relação entre o clima e o crescimento das árvores, e assim explorar quais os efeitos das mudanças climáticas sobre o funcionamento dessas florestas (Boninsegna *et al.*, 2009). Entretanto, a construção de longas séries que englobem o período pré-instrumental é um desafio na região tropical onde as árvores vivem em média 200 anos e podem não ter um sinal climático tão claro (Locosselli *et al.*, 2020; Zuidema *et al.*, 2022).

Cronologias mais longas requerem amostras mortas e preservadas sob condições específicas muito raras em florestas tropicais. Entretanto, na região central do Brasil, condutos dentro de cavernas formam um ambiente que permitiu com que madeiras ficassem preservadas. Essas madeiras provavelmente foram removidas e transportadas por eventos de mega inundação que as deslocaram para altos condutos dentro de cavernas, onde permaneceram após o nível do rio voltar ao normal (Coelho, *et al.*, 2013). Com o auxílio de datações de radiocarbono essas amostras puderam ser utilizadas para melhor entender as mudanças climáticas presentes e passadas na região.

Nessas cavernas também ocorrem espeleotemas, as estalactites e estalagmites, que formam camadas de crescimento e podem ser utilizadas para análises paleoclimáticas (Cruz *et al.*, 2009; Novello *et al.*, 2018; Orrison *et al.*, 2022; Stríkis *et al.*, 2011), inclusive em conjunto com os anéis de crescimento de árvores (Managave, 2014). Nos dois registros naturais, os isótopos estáveis de oxigênio ( $\delta^{18}\text{O}$ ) são um indicador (proxy) que pode registrar as alterações no sistema hídrico da região. Nos espeleotemas de fundo de caverna na região, os isótopos de oxigênio registram a quantidade de chuva (Novello *et al.*, 2018; Novello *et al.*, 2012; Stríkis *et al.*, 2011). Esses registros podem ter milhares de anos, como um no sul da Bahia que mostrou que a região já passou por um período de seca intenso durante a Pequena Idade do Gelo (entre 1450 e 1850, IPCC WGI, 2021) e atualmente está em um período de estiagem sem precedentes nos últimos 3 mil anos (Novello *et al.*, 2012). Já em espeleotemas formados mais próximos à entrada das cavernas no PNCP, um outro sinal foi encontrado (Stríkis *et al.*, in press), o qual mostra um claro enriquecimento nos valores de  $\delta^{18}\text{O}$  que refletem o aumento das taxas evaporativas locais a partir dos anos 1980. Na série que vai de 1298 a 2016, mudanças de magnitude semelhantes são observadas durante o período da Pequena Idade do Gelo, o que indica que a região já passou por outros momentos de aumento da demanda evaporativa devido às mudanças em forçantes radiativas (Novello *et al.*, 2012; Stríkis *et al.*, in press). Essas forçantes podem ser alterações na composição atmosférica (*e.g.* sulfatos de vulcões, gás carbônico de combustíveis fósseis), ou mudanças de irradiância solar, que provocam gradientes de temperatura entre os hemisférios e deslocam a Zona de Convergência Intertropical (ZCIT), afetando

assim o Sistema de Monção da América do Sul e alterando a quantidade e periodicidade das nuvens na região (posicionamento da Zona de Convergência do Atlântico Sul – ZCAS) (Novello *et al.*, 2018; Strikis *et al.*, 2012; Vera *et al.*, 2006). O período da Pequena Idade do Gelo é caracterizado por temperaturas mais baixas no hemisfério norte e intensa atividade vulcânica em todo o globo (IPCC WGI, 2021), entretanto, ainda existem poucos registros longos com resolução anual nos trópicos. Dada a geografia complexa da América do Sul, os modelos e registros nessa época mostram variações nas respostas do regime de chuvas no Sistema de Monção da América do Sul dentro do continente (Novello *et al.*, 2018, Orrison *et al.*, 2022). Ainda são necessários mais registros especialmente nas bordas da ZCAS para entender as variações na quantidade de chuva na região durante esses eventos de mudanças climáticas (Novello *et al.*, 2018). Estas variações podem ser compreendidas em escalas anuais, decadais, seculares e milenares. Variações de baixa frequência como as multi-decadais, seculares e milenares podem ser acessadas por meio da análise dos espeleotemas, enquanto os anéis de crescimento são uma fonte confiável de informações de alta frequência como as decadais, anuais e até sub-aneis. Estas características distintas dos registros os tornam complementares no estudo das condições paleoclimáticas de um local.

Para permitir a comparação entre os dois registros analisamos a razão dos isótopos estáveis de oxigênio ( $\delta^{18}\text{O}$ ), um indicador hidroclimático que pode ter um sinal compartilhado nos dois registros. Nos espeleotemas, o sinal de  $\delta^{18}\text{O}$  pode registrar a quantidade de chuva, como em Novello *et al.*, (2012), ou condições evaporativas, como nos espeleotemas mais próximos a entrada das cavernas em

Strikis et al., *in press*. Já nos anéis de crescimento, os isótopos de oxigênio podem registrar tanto o sinal isotópico da chuva sem nenhuma alteração, quanto sinais de déficit de vapor de pressão (ou VPD na sigla em inglês Vapour Pressure Deficit). Uma atmosfera mais quente e seca pode aumentar o fracionamento (evaporação preferencial dos isótopos mais leves, no caso  $^{16}\text{O}$  em relação ao  $^{18}\text{O}$ ) nas folhas devido a aumentos na taxa de transpiração, ou evaporação da água no solo (Cintra *et al.*, 2019; van der Sleen *et al.*, 2017). Portanto, o sinal registrado na celulose dos anéis de crescimento depende de qual desses estímulos é o dominante no local de estudo, e um sinal dominante da evapotranspiração nas folhas é esperado em locais mais secos (Barbour, 2007; Cintra *et al.*, 2019) como a região do PNCP. Como o PNCP contém tanto os espeleotemas anuais quanto uma vasta área de mata sazonalmente seca, a área é ideal para estudos com múltiplos registros e indicadores para auxiliar a entender as consequências do aquecimento global e aumento na demanda evaporativa nos ciclos biogeoquímicos da região.

Assim, para entender os efeitos do aumento do déficit de pressão de vapor nas matas secas da região nós investigamos as cronologias de largura e  $\delta^{18}\text{O}$  dos anéis de crescimento de árvores de *Amburana cearensis*, e de *Cedrela fissilis*. Cronologias dessas duas espécies são extensivamente usadas na região tropical (Brienen & Zuidema, 2005; Pereira *et al.*, 2018; Granato-Souza *et al.*, 2020; Godoy-Veiga *et al.*, 2021; López, Villalba & Stahle, 2022), e neste local de estudo ambas contêm sinal semelhante nos seus indicadores. Portanto, para tornar a cronologia mais robusta e assim aumentar o poder de inferência dos dados, as duas espécies foram usadas para a construção de uma única cronologia, e assim foram verificados

os efeitos das mudanças climáticas no crescimento das árvores da região. Esta é a primeira vez que as duas espécies de gêneros diferentes são utilizadas em conjunto para a construção de uma única cronologia, um método nunca utilizado em regiões tropicais. Dessa forma, este trabalho abre portas para que estudos sejam produzidos unindo diferentes espécies, registros naturais e indicadores, aumentando o número de inferências e reconstruções climáticas robustas em regiões tropicais.

## Referências Bibliográficas

---

- Amáis, R. S., Moreau, P. S., Francischini, D. S., Magnusson, R., Locosselli, G. M., Godoy-Veiga, M., Ceccantini, G., Ortega Rodriguez, D. R., Tomazello-Filho, M., & Arruda, M. A. Z. (2021). Trace elements distribution in tropical tree rings through high-resolution imaging using LA-ICP-MS analysis. *Journal of Trace Elements in Medicine and Biology*, 68(October). <https://doi.org/10.1016/j.jtemb.2021.126872>
- Apgaua, D. M. G., Pereira, D. G. S., Santos, R. M., Menino, G. C. O., Pires, G. G., Fontes, M. A. L., & Tng, D. Y. P. (2015). Floristic variation within seasonally dry tropical forests of the Caatinga Biogeographic Domain, Brazil, and its conservation implications. *International Forestry Review*, 17(Special Issue 2), 33–44. <https://doi.org/10.1505/146554815815834840>
- Baker, J. C. A., Hunt, S. F. P., Clerici, S. J., Newton, R. J., Bottrell, S. H., Leng, M. J., Heaton, T. H. E., Helle, G., Argollo, J., Gloor, M., & Brienen, R. J. W. (2015). Oxygen isotopes in tree rings show good coherence between species and sites in Bolivia. *Global and Planetary Change*, 133, 298–308. <https://doi.org/10.1016/j.gloplacha.2015.09.008>
- Barbosa, A. C. M., Pereira, G. A., Granato-Souza, D., Santos, R. M., & Fontes, M. A. L. (2018). Tree rings and growth trajectories of tree species from seasonally dry tropical forest. *Australian Journal of Botany*, 66(5), 414–427. <https://doi.org/10.1071/BT17212>
- Barbour, M. M. (2007). Stable oxygen isotope composition of plant tissue: a review. *Functional Plant Biology*, 34, 83–94. <https://doi.org/10.1071/FP06228>

- Berlage HP, (1931). Over het verband tusschen de dikte der jaarringen van djatiboomen (*Tectona grandis* L. f.) en den regenval op Java. *Tectona*, 24: 939±953.
- Boninsegna, J. A., Argollo, J., Aravena, J. C., Barichivich, J., Christie, D., Ferrero, M. E., Lara, A., Le Quesne, C., Luckman, B. H., Masiokas, M., Morales, M., Oliveira, J. M., Roig, F., Srur, A., & Villalba, R. (2009). Dendroclimatological reconstructions in South America: A review. *Palaeogeography, Palaeoclimatology, Palaeoecology*, 281(3–4), 210–228. <https://doi.org/10.1016/j.palaeo.2009.07.020>
- Bormann FH, Berlyn G, 1981. Age and growth rate of tropical trees. New directions for research. New Haven, Yale University Press: 137 pp
- Brienen, R. J. W., Schöngart, J., & Zuidema, P. A. (2016). *Tree Rings in the Tropics: Insights into the Ecology and Climate Sensitivity of Tropical Trees*. [https://doi.org/10.1007/978-3-319-27422-5\\_19](https://doi.org/10.1007/978-3-319-27422-5_19)
- Brienen, R. J. W., & Zuidema, P. A. (2005). Relating tree growth to rainfall in Bolivian rain forests: a test for six species using tree ring analysis. *Oecologia*, 146(1), 1–12. <https://doi.org/10.1007/s00442-005-0160-y>
- Brienen, R.J.W., Phillips, O.L., Feldpausch, T.R., Gloor, E., Baker, T.R., Lloyd, J., Lopez-Gonzalez, G., Monteagudo-Mendoza, A., Malhi, Y., Lewis, S.L., Vásquez Martínez, R., Alexiades, M., Álvarez Dávila, E., Alvarez-Loayza, P., Andrade, A., Aragaõ, L.E.O.C., Araujo-Murakami, A., Arets, E.J.M.M., Arroyo, L., Aymard C., G.A., Bánki, O.S., Baraloto, C., Barroso, J., Bonal, D., Boot, R.G.A., Camargo, J.L.C., *et al.*, Thomas-Caesar, R., Toledo, M., Torello-Raventos, M., Umetsu, R.K., Van Der Heijden, G.M.F., Van Der Hout, P., Guimarães Vieira, I.C., Vieira, S.A., Vilanova, E., Vos, V.A., Zagt, R.J., 2015. Long-term decline of the Amazon carbon sink. *Nature* 519, 344–348. <https://doi.org/10.1038/nature14283>.
- Cintra, B. B. L., Gloor, M., Boom, A., Schöngart, J., Locosselli, G. M., & Brienen, R. (2019). Contrasting controls on tree ring isotope variation for Amazon floodplain and terra firme trees. *Tree Physiology*, 39(5), 845–860. <https://doi.org/10.1093/treephys/tpz009>
- Coelho, M., Fernandes, G., & Sánchez-Azofeifa, A. (2013). Brazilian Tropical Dry Forest on Basalt and Limestone Outcrops. *Tropical Dry Forests in the Americas*, January 2014, 55–68. <https://doi.org/10.1201/b15417-5>
- Coster C, 1927. Zur Anatomie und Physiologie der Zuwachszonen und Jahresringbildung in den Tropen I. *Ann. Jard. Bot. Buitenzorg*, 37: 49±161.
- Cruz, F. W., Vuille, M., Burns, S. J., Wang, X., Cheng, H., Werner, M., Edwards, R. L., Karmann, I., Auler, A. S., & Nguyen, H. (2009). Orbitally driven east – west antiphasing of South American precipitation. *Nature Geosciences*, 2(3), 210–214. <https://doi.org/10.1038/ngeo444>

- de Andrade, E. S., Garcia, S. dos S. C., Albernaz, A. L. K. M., Filho, M. T., & Moutinho, V. H. P. (2017). Análise dos anéis de crescimento de *Euxylophora paraensis* por meio da microdensitometria de raios-x. *Ciencia Rural*, 47(4).  
<https://doi.org/10.1590/0103-8478cr20150895>
- Douglass, A. E. (1941a). Crossdating in Dendrochronology. *Journal of Forestry*, 39(10), 825–831.
- Franks, P. J., & Farquhar, G. D. (1999). A relationship between humidity response, growth form and photosynthetic operating point in C3 plants. *Plant, Cell and Environment*, 22(11), 1337–1349. <https://doi.org/10.1046/j.1365-3040.1999.00494.x>
- Fritts, H.C. (1976). Dendrochronology and Dendroclimatology. *Tree Rings and Climate*, 1–54. <https://doi.org/10.1016/b978-0-12-268450-0.50006-9>
- Fritts, Harold C. (1966). Growth-rings of trees: Their correlation with climate. *Science*, 154(3752), 973–979. <https://doi.org/10.1126/science.154.3752.973>
- Fritts, Harold C. (1971). Dendroclimatology and dendroecology. *Quaternary Research*, 1(4), 419–449. [https://doi.org/10.1016/0033-5894\(71\)90057-3](https://doi.org/10.1016/0033-5894(71)90057-3)
- Godoy-Veiga, M., Cintra, B. B. L., Stríkis, N. M., Cruz, F. W., Grohmann, C. H., Santos, M. S., Regev, L., Boaretto, E., Ceccantini, G., & Locosselli, G. M. (2021). The value of climate responses of individual trees to detect areas of climate-change refugia, a tree-ring study in the Brazilian seasonally dry tropical forests. *Forest Ecology and Management*, 488(January). <https://doi.org/10.1016/j.foreco.2021.118971>
- Godoy-Veiga, M., Slotta, F., Alecio, P. C., & Ceccantini, G. (2019). Improved tree-ring visualization using autofluorescence. *Dendrochronologia*, 55(April), 33–42. <https://doi.org/10.1016/j.dendro.2019.03.003>
- Granato-Souza, D., Stahle, D. W., Torbenson, M. C. A., Howard, I. M., Barbosa, A. C., Feng, S., Fernandes, K., & Schöngart, J. (2020). Multidecadal Changes in Wet Season Precipitation Totals Over the Eastern Amazon. *Geophysical Research Letters*, 47(8), 1–9. <https://doi.org/10.1029/2020GL087478>
- Grossiord, C., Buckley, T. N., Cernusak, L. A., Novick, K. A., Poulter, B., Siegwolf, R. T. W., Sperry, J. S., & McDowell, N. G. (2020). Plant responses to rising vapor pressure deficit. *New Phytologist*, 226(6), 1550–1566. <https://doi.org/10.1111/nph.16485>
- Hogg, A. G., Hua, Q., Blackwell, P. G., Niu, M., Buck, C. E., Guilderson, T. P., Heaton, T. J., Palmer, J. G., Reimer, P. J., Reimer, R. W., Turney, C. S. M., & Zimmerman, S. R. H. (2013). SHCAL13 Southern Hemisphere Calibration, 0–50,000 years cal BP. *Radiocarbon*, 55(3), 1–5.

- IPCC WGI, I. A. (2021). Climate Change 2021 The Physical Science Basis WGI. In Bulletin of the Chinese Academy of Sciences (Vol. 34, Issue 2).
- Locosselli, G. M., Brienen, R. J. W., de Souza Leite, M., Gloor, M., Krottenthaler, S., de Oliveira, A. A., Barichivich, J., Anhof, D., Ceccantini, G., Schöngart, J., & Buckeridge, M. (2020). Global tree-ring analysis reveals rapid decrease in tropical tree longevity with temperature. *Proceedings of the National Academy of Sciences of the United States of America*, 117(52), 33358–33364. <https://doi.org/10.1073/PNAS.2003873117>
- López, L., Villalba, R., & Bravo, F. (2013). Cumulative diameter growth and biological rotation age for seven tree species in the Cerrado biogeographical province of Bolivia. *Forest Ecology and Management*, 292, 49–55. <https://doi.org/10.1016/j.foreco.2012.12.011>
- López, L., Villalba, R., & Stahle, D. (2022). High-fidelity representation of climate variations by *Amburana cearensis* tree-ring chronologies across a tropical forest transition in South America. *Dendrochronologia*, 72(December 2021). <https://doi.org/10.1016/j.dendro.2022.125932>
- Managave, S. R. (2014). Model evaluation of the coherence of a common source water oxygen isotopic signal recorded by tree-ring cellulose and speleothem calcite. *Geochemistry, Geophysics, Geosystems*, 15(4), 905–922. <https://doi.org/10.1002/2013GC004983>
- Marengo, J. A., Liebmann, B., Grimm, A. M., Misra, V., Silva Dias, P. L., Cavalcanti, I. F. A., Carvalho, L. M. V., Berbery, E. H., Ambrizzi, T., Vera, C. S., Saulo, A. C., Noguez-Paegle, J., Zipser, E., Seth, A., & Alves, L. M. (2012). Recent developments on the South American monsoon system. *International Journal of Climatology*, 32(1), 1–21. <https://doi.org/10.1002/joc.2254>
- Mariaux A, 1967. Les cernes dans les bois tropicaux africains, nature et periodicite. *Rev. Bois For. Trop.*, 113: 3± 14/114: 23±37
- Murphy, D. B. (2001). *Fundamentals of Light Microscopy and Electronic Imaging*. In John Wiley & Sons, Inc. USA. <https://doi.org/10.1259/bjr/21753020>
- Novello, V. F., Cruz, F. W., Moquet, J. S., Vuille, M., de Paula, M. S., Nunes, D., Edwards, R. L., Cheng, H., Karmann, I., Utida, G., Strikis, N. M., & Campos, J. L. P. S. (2018). Two millennia of south atlantic convergence zone variability reconstructed from isotopic proxies. *Geophysical Research Letters*, 45(10), 5045–5051. <https://doi.org/10.1029/2017GL076838>
- Novello, Valdir F., Cruz, F. W., Karmann, I., Burns, S. J., Strikis, N. M., Vuille, M., Cheng, H., Lawrence Edwards, R., Santos, R. V., Frigo, E., & Barreto, E. A. S. (2012). Multidecadal climate variability in Brazil's Nordeste during the last 3000 years



based on speleothem isotope records. *Geophysical Research Letters*, 39(23), 1–6.  
<https://doi.org/10.1029/2012GL053936>

- Orrison, R., Vuille, M., Smerdon, J. E., Apaestegui, J., Azevedo, V., Campos, J. L. P. S., Cruz, F. W., Della Libera, M. E., & Strikis, N. M. (2022). South American Summer Monsoon variability over the last millennium in paleoclimate records and isotope-enabled climate models. *Climate of the Past*, 18(9), 2045–2062.  
<https://doi.org/10.5194/cp-18-2045-2022>
- Ortega Rodriguez, D. R., Hevia, A., Sánchez-Salguero, R. Santini, L., de Carvalho, H. W. P., Roig, F. A., Tomazello-Filho, M. (2022). Exploring wood anatomy, density and chemistry profiles to understand the tree-ring formation in Amazonian tree species. *Dendrochronologia* 71, 125915.
- Paredes-Villanueva, K., López, L., Brookhouse, M., & Cerrillo, R. M. N. (2015). Rainfall and temperature variability in Bolivia derived from the tree-ring width of *Amburana cearensis* (Fr. Allem.) A.C. Smith. *Dendrochronologia*, 35, 80–86.  
<https://doi.org/10.1016/j.dendro.2015.04.003>
- Peel, M. C., Finlayson, B. L., & McMahon, T. A. (2007). Updated world map of the Köppen-Geiger climate classification. *Hydrology and Earth System Sciences*, 11(5), 1633–1644. <https://doi.org/10.5194/hess-11-1633-2007>
- Pereira, G. de A., Barbosa, A. C. M. C., Torbenson, M. C. A., Stahle, D. W., Granato-Souza, D., Santos, R. M. Dos, & Barbosa, J. P. D. (2018). The Climate Response of *Cedrela Fissilis* Annual Ring Width in the Rio São Francisco Basin, Brazil. *Tree-Ring Research*, 74(2), 162–171. <https://doi.org/10.3959/1536-1098-74.2.162>
- Prado, D. E. (2000). Seasonally dry forests of tropical South America: From forgotten ecosystems to a new phytogeographic unit. *Edinburgh Journal of Botany*, 57(3), 437–461. <https://doi.org/10.1017/S096042860000041X>
- Quintilhan, M. T., Santini, L., Ortega Rodriguez, D. R., Guillemot, J., Cesilio, G. H. M., Chambi-Legoas, R., Nouvellon, Y., & Tomazello-Filho, M. (2021). Growth-ring boundaries of tropical tree species: Aiding delimitation by long histological sections and wood density profiles. *Dendrochronologia*, 69(September).  
<https://doi.org/10.1016/j.dendro.2021.125878>
- Rawson, H. M., Begg, J. E., & Woodward, R. G. (1977). The effect of atmospheric humidity on photosynthesis, transpiration and water use efficiency of leaves of several plant species. *Planta*, 134(1), 5–10. <https://doi.org/10.1007/BF00390086>
- Schongart, J., Bräuning, A., Barbosa, A. C. M. C., Lisi, C. S., & de Oliveira, J. M. (2017). *Dendroecological Studies in the Neotropics: History, Status and Future Challenges*. [https://doi.org/10.1007/978-3-319-61669-8\\_8](https://doi.org/10.1007/978-3-319-61669-8_8)
- Simpson, M. G. (2019). *Plant systematics*. Academic press.

- Slotta, F., Helle, G., Heussner, K. U., Shemang, E., & Riedel, F. (2017). Baobabs on Kubu Island, Botswana – A dendrochronological multi-parameter study using ring width and stable isotopes ( $\delta^{13}\text{C}$ ,  $\delta^{18}\text{O}$ ). *Erdkunde*, 71(1), 23–43. <https://doi.org/10.3112/erdkunde.2017.01.02>
- Speer, B. J. H. (2010). *Fundamentals of Tree-Ring Research*. 509. <https://doi.org/10.1002/gea.20357>
- Stahle, D. W. (1999). Useful strategies for the development of tropical tree-ring chronologies. *IAWA Journal*, 20(3), 249–253. <https://doi.org/10.1163/22941932-90000688>
- Stríkis, N. M., Cruz, F. W., Cheng, H., Karmann, I., Edwards, R. L., Vuille, M., Wang, X., de Paula, M. S., Novello, V. F., & Auler, A. S. (2012). Abrupt variations in South American monsoon rainfall during the Holocene based on a speleothem record from central-eastern Brazil. *Geology*, 39(11), 1075–1078. <https://doi.org/10.1130/G32098.1>
- Trouet, V., Esper, J., Graham, N. E., Baker, A., Scourse, J. D., Frank, D. C., (2009) Persistent positive north atlantic oscillation mode dominated the medieval climate anomaly. *Science*. 324, 78–80.
- Trouillier, M., van der Maaten-Theunissen, M., Harvey, J. E., Würth, D., Schnittler, M., & Wilmking, M. (2018). Visualizing individual tree differences in tree-ring studies. *Forests*, 9(4), 1–14. <https://doi.org/10.3390/f9040216>
- Van Den Bulcke, J., Boone, M. A., Dhaene, J., Van Loo, D., Van Hoorebeke, L., Boone, M. N., Wyffels, F., Beeckman, H., Van Acker, J., & De Mil, T. (2019). Advanced X-ray CT scanning can boost tree ring research for earth system sciences. *Annals of Botany*, 124(5), 837–847. <https://doi.org/10.1093/aob/mcz126>
- van der Sleen, P., Zuidema, P. A., & Pons, T. L. (2017). Stable isotopes in tropical tree rings: theory, methods and applications. *Functional Ecology*, 31(9), 1674–1689. <https://doi.org/10.1111/1365-2435.12889>
- Vera, C., Higgins, W., Amador, J., Ambrizzi, T., Garreaud, R., Gochis, D., Gutzler, D., Lettenmaier, D., Marengo, J., Mechoso, C. R., Nogues-Paegle, J., Silva Dias, P. L., & Zhang, C. (2006). Toward a unified view of the American monsoon systems. *Journal of Climate*, 19(20), 4977–5000. <https://doi.org/10.1175/JCLI3896.1>
- Worbes, M. (1995). How to Measure Growth Dynamics in Tropical Trees a Review. *IAWA Journal*, 16(4), 337–351. <https://doi.org/10.1163/22941932-90001424>
- Worbes, M. (2002). One hundred years of tree-ring research in the tropics-a brief history and an outlook to future challenges. *Dendrochronologia*, 20, 217–231.
- Worbes, M., & Fichtler, E. (2010). Wood Anatomy and Tree-Ring Structure and Their Importance for Tropical Dendrochronology (pp. 329–346). Springer. [https://doi.org/10.1007/978-90-481-8725-6\\_17](https://doi.org/10.1007/978-90-481-8725-6_17)

- Zuidema, P. A., Babst, F., Groenendijk, P., Trouet, V., Abiyu, A., Acuña-Soto, R., Adenesky-Filho, E., Alfaro-Sánchez, R., Aragão, J. R. V., Assis-Pereira, G., Bai, X., Barbosa, A. C., Battipaglia, G., Beeckman, H., Botosso, P. C., Bradley, T., Bräuning, A., Brienen, R., Buckley, B. M., ... Zhou, Z. K. (2022). Tropical tree growth driven by dry-season climate variability. *Nature Geoscience*, 15(4), 269–276. <https://doi.org/10.1038/s41561-022-00911-8>
- Zuidema, P. A., Baker, P. J., Groenendijk, P., Schippers, P., van der Sleen, P., Vlam, M., & Sterck, F. (2013a). Tropical forests and global change: filling knowledge gaps. *Trends in Plant Science*, 18(8), 413–419. <https://doi.org/10.1016/j.tplants.2013.05.006>
- Zuidema, P. A., Baker, P. J., Groenendijk, P., Schippers, P., van der Sleen, P., Vlam, M., & Sterck, F. (2013b). Tropical forests and global change: Filling knowledge gaps. *Trends in Plant Science*, 18(8), 413–419. <https://doi.org/10.1016/j.tplants.2013.05.006>.

## Capítulo 1

---

*Improved tree-ring visualization using autofluorescence.*

Melhora na visualização de anéis de crescimento de árvores com o uso da autofluorescência

Milena Godoy-Veiga, Franziska Slotta, Paula Christiani Alecio, Gregório Ceccantini, Marcos Silveira Buckeridge, Giuliano Maselli Locosselli

Artigo publicado no periódico *Dendrochronologia* em 2019, Volume 55, pág. 33-42

## Abstract

The great diversity of wood anatomical features found in trees worldwide results in a broad variety of growth-ring boundary types that are not always easy to recognize, especially in tropical woods. However, the presence of clearly visible limits between tree rings is essential for any tree-ring studies. Here, we propose the use of autofluorescence of wood in order to enhance tree-ring visualization. The multispectral light emitted from the fluorescence stereomicroscope can be filtered in specific wavelengths to improve the visualization of wood anatomical features. To evaluate the effectiveness of this technique, we compared visualization under natural light, GFP (green fluorescent protein) filter, RFP (red fluorescent protein) filter and UV filter. We tested this technique with a set of 38 tree species with different types of growth-ring boundaries. Although results are species-specific, fluorescence has been shown to improve the visualization of growth-ring boundaries by enhancing the contrast among cell types. It may highlight fibrous zones (e.g. *Cavanillesia arborea*, *Aspidosperma polyneuron*), different porosity patterns (e.g. *Myracrodruon urundeuva*), secretory canals (e.g. *Copaifera langsdorffii*), and parenchyma bands (e.g. *Tipuana tipu*). Fluorescence allows the visualization of growth-ring boundaries in species that were previously described as having indistinct growth rings under natural light. For species with clear tree-ring boundaries such as *Cedrela fissilis* and *Hymenaea courbaril*, this approach aids the identification of false rings. In addition to the visualization of growth-ring boundaries, autofluorescence may be useful for other qualitative and quantitative analyses of wood anatomy, such as wood identification and automated measurements of anatomical features. Scientists struggling with tree-ring counting and cross-dating due to difficult tree-ring visualization may find fluorescence useful. It may also aid to identify new species suitable for tree-ring studies.

**Keywords:** dendrochronology, wood anatomy, GFP, RFP, UV light, ultraviolet

## Resumo

A grande diversidade de padrões anatômicos encontrado na madeira de espécies arbóreas pelo mundo resulta em uma grande diversidade de limites de camadas de crescimento que nem sempre são fáceis de interpretar, especialmente em espécies tropicais. Entretanto a presença de camadas visíveis delimitando anéis de crescimento é essencial para estudos dendrocronológicos. Aqui nós propomos o uso da autofluorescência da madeira para melhorar a visualização dos anéis de crescimento. A luz multiespectral que é emitida através do estereomicroscópio pode ser filtrada em comprimentos de onda específicos para melhorar a visualização de caracteres anatômicos. Para avaliar a eficiência desta técnica, foram comparados a visualização da madeira entre imagens obtidas com luz natural, filtro GFP (proteína fluorescente verde), filtro RFP (proteína fluorescente vermelha) e filtro UV (ultravioleta). Foram testadas 38 espécies arbóreas com diferentes tipos de camada de crescimento. Apesar dos resultados serem específicos de cada espécie, a fluorescência melhorou a visualização das camadas de crescimento aumentando o contraste entre os tipos celulares. O método pode destacar zonas fibrosas (e.g. *Cavanillesia arborea*, *Aspidosperma polyneuron*), padrões de porosidade diferentes (e.g. *Myracrodruon urundeuva*), canais secretores (e.g. *Copaifera langsdorffii*), e faixas de parênquima (e.g. *Tipuana tipu*). A fluorescência também permitiu a visualização de camadas de crescimento em espécies que foram previamente descritas como não possuindo camadas em luz natural. Já nas espécies com anéis de crescimento visíveis, como *Cedrela fissilis* e *Hymenaea courbaril*, essa abordagem auxiliou na identificação de anéis falsos. Além de melhorar a identificação dos limites de camadas de crescimento, a autofluorescência também pode ser útil para outros estudos quantitativos e qualitativos de anatomia da madeira, como para identificação de espécies e para medições automatizadas de características anatômicas. Cientistas com dificuldade na contagem de anéis e na datação cruzada, devido a dificuldades na visualização dos anéis, podem achar a técnica de fluorescência útil. Ela também pode ajudar a identificar novas espécies potenciais para estudos dendrocronológicos.

**Palavras-chave:** dendrocronologia, anatomia de madeira, GFP, RFP, luz UV, ultravioleta

## Introduction

Growth rings have been largely used to study species' age and growth rate (Brienen and Zuidema, 2006; Godoy-Veiga *et al.*, 2018; Maes *et al.*, 2018; Worbes *et al.*, 2003), forest dynamics (Bergeron *et al.*, 2002; Splechtna *et al.*, 2005; Vlam *et al.*, 2017; Xu *et al.*, 2017), forest management (Brienen and Zuidema, 2006; Schöngart, 2008), palaeoclimate (Buntgen *et al.*, 2011; Esper *et al.*, 2002; Fang *et al.*, 2018; Palmer *et al.*, 2016), and for predicting tree responses to climate change (Babst *et al.*, 2018; Cook *et al.*, 2015; Fonti *et al.*, 2010; Groenendijk *et al.*, 2015; Locosselli *et al.*, 2016b, 2013; van der Sleen *et al.*, 2014; Zuidema *et al.*, 2013). The majority of these studies were conducted in temperate and boreal regions, where many species produce distinct tree rings (Worbes, 2002). The tropics still lag behind, partially because of the past belief that tropical regions lacked the climate seasonality to promote cambium dormancy, resulting in the formation of annual growth increments (Worbes, 2002). Tree rings have now been described for over 230 tree species in the tropics (Brienen *et al.*, 2016). However, the identification of the growth-ring boundaries in some tropical tree species is still an issue that hampers the further development of tropical tree-ring studies. The high diversity of tree species found in the tropics (Slik *et al.*, 2015) reflects in the proportional diversity of wood anatomy and growth-ring boundaries (Worbes, 1989).

The proper visualization of the tree rings is a key step in any dendrochronological study (Fritts, 1976). Tree rings are identified as regular changes in the patterns of wood anatomy as a result of the seasonal cambium activity. This activity may display sensitivity to external factors such as climate (Fritts, 1976), which promotes changes in the arrangement and proportion of cell types (vessel elements, tracheids, fibres, axial, and/or radial parenchyma) resulting in concentric layers. Some tropical genera like *Tectona* L. f. (Lamiaceae), *Cedrela* L. (Meliaceae), *Pterocarpus* Jacq. and *Hymenaea* L. (Fabaceae) were successfully used in dendrochronological studies due to their tree-rings clear boundaries (Barbosa *et al.*, 2018; Borgaonkar *et al.*, 2010; Locosselli *et al.*, 2017; Therrell *et al.*, 2007). Tree rings may be identified by changes in vessel patterns as for *Cedrela* spp. (Meliaceae), *Tectona grandis* L.f. (Lamiaceae), *Pterocarpus angolensis* DC. (Fabaceae) that are characterized by a gradual change in vessel diameter from earlywood to latewood, regarded as semi-ring

porous woods (Dünisch *et al.*, 2002; Worbes, 1989). These species also exhibit the presence of a marginal parenchyma band at the tree-ring boundary. Other species, including *Acacia cochliacantha* Willd., *Copaifera langsdorffii* Desf., *Hymenaea courbaril* L., *Lonchocarpus sericeus* (Poir.) DC., are diffuse porous, but their tree rings are clearly delimited by the presence of a marginal parenchyma band (Mainieri and Chimelo, 1989; Wheeler, 2011). However, even these species may not be easy to cross-date because of the presence of false rings, which are often not distinguishable from tree rings in less detailed analyses (Baker *et al.*, 2017; Worbes, 2002).

The use of some other tree species have been less successful, not because they lack annual cambial activity, but due to the poor definition of the tree-ring boundaries (Brienen *et al.*, 2016; Lisi *et al.*, 2008; Worbes, 1995). For instance, tree rings delimited by radially flattened fibres with thickened cell walls may require a greater effort to identify the precise position of the tree-ring boundary. This anatomical pattern is common to families such as Lauraceae (*Nectandra amazonum* Nees, *Ocotea porosa* (Nees & Mart.) Barroso) (Reis-Avila and Oliveira, 2017), Annonaceae (*Guatteria aeruginosa* Standl., *Rollinia jimenezii* Saff.) (Brienen *et al.*, 2009; Fichtler *et al.*, 2003) and Apocynaceae (*Aspidosperma polyneuron* Müll. Arg., *Thevetia ahouai* (L.) A.DC.) (Mainieri and Chimelo, 1989; Wheeler, 2011). The precise delimitation of the tree rings is also an issue in a few tree species from Lecythidaceae (*Bertholletia excelsa* Bonpl., *Cariniana estrellensis* (Raddi) Kuntze), Sapotaceae (*Manilkara bidentata* (A.DC.) A.Chev.), and Moraceae (*Ficus insipida* Willd.) that produce tree rings characterized by alternating parenchyma and fibre bands (Worbes and Fichtler, 2010). Due to their complicated tree-ring anatomy, the potential of these species was underestimated in past studies.

Some technological solutions have been developed to solve problems related to growth-ring boundary visualization and identification of false rings. X-ray micro densitometry is one of them, and differences in the apparent density profile of the wood, at up to 40µm of resolution, are used to aid the identification of growth rings (Worbes, 1995; Amaral and Tomazello Filho, 1998; Andrade *et al.*, 2017). High-resolution measurements of wood anatomical features in micro slides or on the wood surface may also aid the identification of growth rings boundaries (Gärtner *et al.*, 2015; Verheyden *et al.*, 2004) as well as high resolution analyses of stable carbon or oxygen isotopes



(Schleser *et al.*, 1999; Verheyden *et al.*, 2006). Despite the proven effectiveness of these methods, such approaches require expensive equipment frequently restricted to a few specialized laboratories. Sample preparation may also be laborious and time-consuming as for the cellulose extraction, dissection and weighing required for stable isotope analyses. Less laborious techniques that require facilities commonly found in laboratories at universities and research institutes may bring important advances in tree-ring studies.

In order to enhance the visualization of growth-ring boundaries in the wood of different species, we propose the use of fluorescence imaging. Fluorescence occurs when an electron of an atom or molecule is excited by radiant energy and almost immediately collapses back to its initial ground state, while releasing the absorbed energy as a fluorescent photon (Murphy, 2001). The fluorescent molecules exhibit distinct excitation and emission spectra depending on their atomic structure and electron resonance properties (Murphy, 2001). Autofluorescence in wood, when exposed to UV light, is known since the XIX century (Vodr zka, 1929), but the systematic use of wood fluorescence for identification began much later (e.g. Krishna & Chowdhury, 1935; Dyer, 1988; Avella *et al.*, 1988; Han & Kywe, 1991, Miller, 2007). The Committee of the International Association of Wood Anatomists (IAWA 1989) standardized UV ( $\lambda=365$  nm) for computer-based identification as a reliable approach because anthocyanins and lignin respond to light excitation. Distinct fluorescence properties also help to distinguish structural differences revealing growth layers in other natural archives. UV induced fluorescence is already used with other environmental records to enhance the visibility of growth layers of e.g. corals, speleothems or sediment cores (Barnes & Taylor, 2001; McGarry & Baker, 2000). In corals, fluorescent bands are the result of variations in skeletal architecture, probably caused by reduced salinity conditions (Barnes and Taylor, 2001) and in speleothems fluorescence is caused by organic acids incorporated into the speleothem calcite (McGarry and Baker, 2000). Regarding tree-ring studies, UV light has already been used to enhance the visualization of tree rings from *Adansonia digitata* L., (Slotta *et al.*, 2017) with promising results.

Based on the previous applications of UV light, we scrutinized the use of fluorescence to enhance growth-ring boundary visualization. To validate the

applicability of this technique we tested: 1) filters with distinct combinations of excitation and emission wavelengths; 2) different types of tree-ring boundaries; 3) false ring identification; and 4) additional applications in qualitative and quantitative wood anatomy studies.

## **Material & Methods**

In order to test the use of fluorescence to improve growth-ring visualization, 38 species from 14 families were tested for their autofluorescence properties. Samples of these species were selected in the wood collection “Nanuza Luiza de Menezes - SPFw” from the Department of Botany of the Institute of Biosciences of the University of São Paulo to represent a variety of anatomical delimitations of growth rings. Although a small fraction of the tree species diversity is reported here, it satisfactorily represents the range of wood anatomy often found in tropical tree-ring studies (Barbosa *et al.*, 2018; Lisi *et al.*, 2008; Marcati *et al.*, 2006; Worbes and Fichtler, 2010). The samples were prepared using sandpapers with different grits (from 50 to 2000, the latter under water) to produce a smooth transversal surface, allowing a clear observation of the wood cells. The specimens were analysed using a Leica Fluorescence stereomicroscope M205FA, coupled with a Leica DFC 7000T camera head, using the following fluorescence filters: Filter set ET GFP (Green Fluorescent Protein - excitation 470/40 nm, emission 525/50 nm); Filter set ET RFP (Red Fluorescent Protein - excitation 546/10 nm, emission 605/70 nm); and Filter set UV LP (Ultraviolet - excitation 350/50 nm, emission 420 nm Long Pass). This system takes advantage of the autofluorescence of different substances found in the wood. It uses a shortwave light that is filtered by the excitation filter, and a dichromatic mirror then transmits the longwave light to the barrier filter, which removes any residual short excitation wavelengths and transmits it to the camera (Murphy, 2001). The proper mechanisms of light interaction with wood substances is only well described for GFP. Lignin, for instance, absorbs the selected short wavelengths filtered by GFP and emits an excitation light that is selected by the emission filter as green light (Murphy, 2001). Therefore, cell-walls with high lignin content produce a higher intensity green light when compared to cell-walls with low lignin content. These differences allow us to identify distinct cell types in the wood, or similar cells with distinct cell-wall composition and/or lumen content.

## Application and discussion of the technique

Poor definition of the growth-ring boundaries is a common problem in tropical tree-ring studies (Brienen *et al.*, 2016; Lisi *et al.*, 2008; Worbes, 2002). Previous studies successfully addressed this issue using different approaches that may be cost restrictive or laborious, like x-ray micro densitometry (Amaral and Tomazello Filho, 1998; Andrade *et al.*, 2017) and high resolution analyses of stable isotopes (Schleser *et al.*, 1999; Verheyden *et al.*, 2006), to name a few. In the present study, we evaluated the potential of using a stereomicroscope with fluorescence to enhance growth-ring visualization. Such equipment is likely present in laboratories of cell biology, since it is required for immunolocalization studies. It may also be found in other laboratories that also require fluorescence for other applications, which will likely include growth-ring visualization in the near future.

From the set of 38 species used in the present study (Table 1), growth-ring boundaries became clearer in 22 of them (58%). Fluorescence improved their visualization by enhancing the contrast of vessels, fibres and parenchyma. Porosity became clearer under fluorescence specially by highlighting wide earlywood vessels and/or narrow latewood vessels. The wider earlywood vessels became evident for *Machaerium vilosum* Vogel (Fig.1A-D) and *Myracrodruon urundeuva* Allemão (Fig. 1E-H) compared to the evaluation under natural light. Narrow latewood vessels became evident in *Peltogyne* sp. Vogel at the tree-ring boundaries (Fig. 1I-L) (Soliz-Gamboa *et al.*, 2011). In some cases, the contrast among vessels, parenchyma, and fibres improves the overall tree-ring visualization, as shown for *Tipuana tipu* (Benth.) Kuntze (Fig. 1M-P) (Locosselli *et al.*, 2019). This technique also enhances the contrast between vessels and a fibrous zone at the tree-ring boundary of *Aspidosperma polyneuron* (Fig. 1Q-T). Although this species has already been used in tree-ring studies (Godoy-Veiga *et al.*, 2018; Lisi *et al.*, 2008), its tree rings have been considered indistinct by some authors because of their unclear delimitation under natural light (Tomazello Filho *et al.*, 2004).

The use of fluorescence also improves the interpretation of wood density variations and compensates for changes in wood colour that can be misinterpreted as growth-rings boundaries (Fig. 2). For instance, only 4 tree rings can be clearly seen in

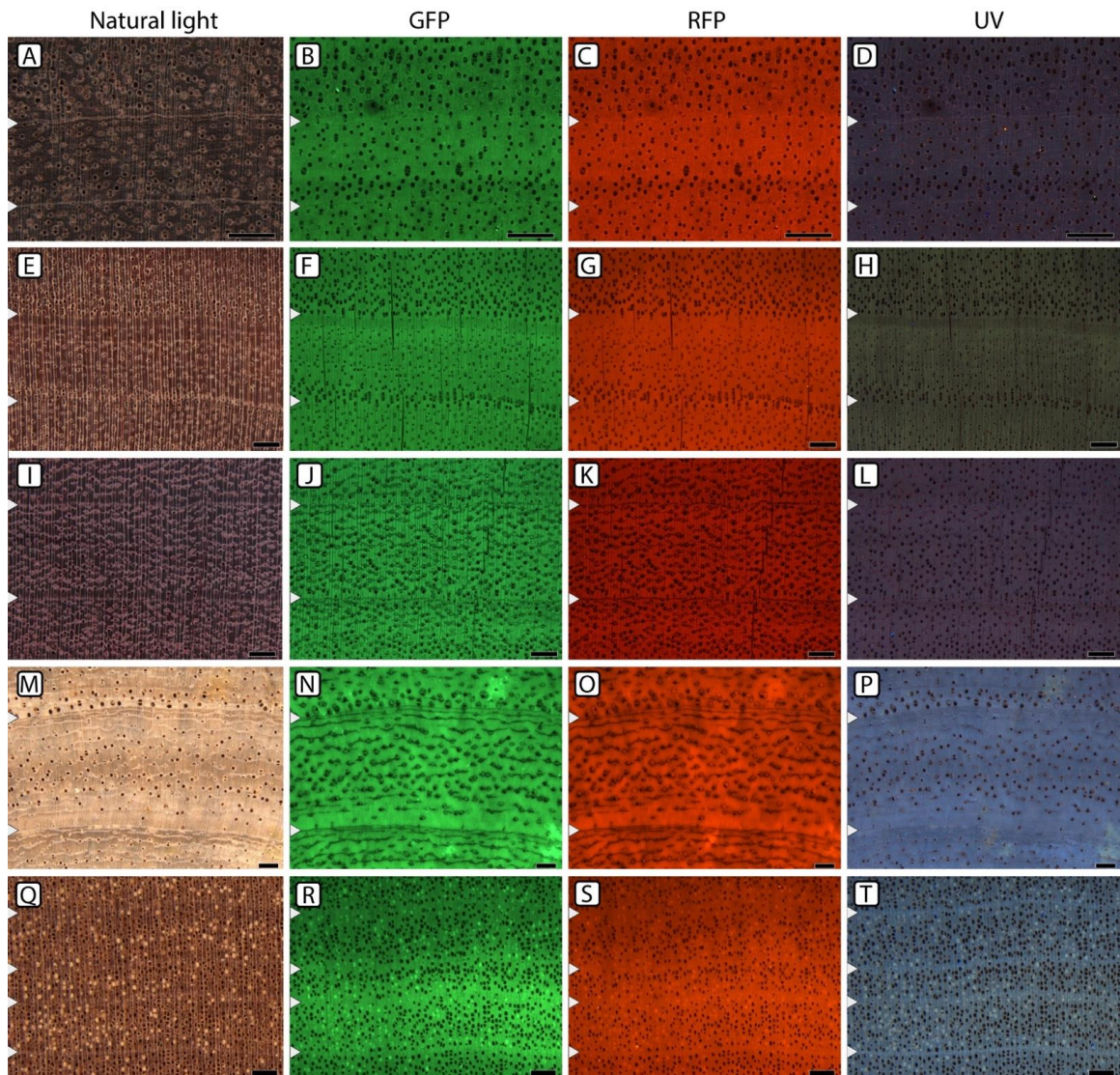


**Figure 1** - Macroscopic view of growth-rings using different sets of fluorescence filters. Visualization was compared under natural light, GFP, RFP and UV, respectively in the following species: A-D *Machaerium vilosum*, filters remove axial parenchyma noise and highlight differences in vessel density; E-H: *Myracrodruon urundeuva*, contrast between fibres, parenchyma and vessels emphasize this species porosity; I-L: *Peltogyne* sp., presence of vessels and enhanced contrast improve boundary visualization; M-P: *Tipuana tipu*, parenchyma (dark green/red/blue) and fibre (light green/red/blue) contrast enhanced visualization of marginal parenchyma bands; Q-T: *Aspidosperma polyneuron*, growth rings are demarked by fibres zones (lighter bands) and visualization was improved in all filters. White arrowheads: growth-ring boundaries; scale bar: 1 mm.

the *Centrolobium tomentosum* Benth. sample (Fig. 2A) if the changes in wood colour are considered. Nonetheless, fluorescence (Fig. 2B, C and D) revealed the existence of

an additional growth ring, characterized by changes in the wood anatomy. In *Copaifera langsdorffii* (Fig. 2E-H), fluorescence not only enhanced the contrast among cell types, but highlighted secretory canals associated with some parenchyma bands. These marginal parenchyma bands are the actual tree-ring boundaries for this species (Marcati *et al.*, 2000; Rodrigues and Machado, 2009). Those rings containing no secretory canals could be readily identified as false rings (black arrowheads). Also, the interpretation of vessel density, vessel size, and wood density fluctuations has been improved in *Commiphora leptophloeos* (Mart.) J. B. Gillett (Fig. 2I-L).

In light-coloured woods such as *Ceiba petandra* (L.) Gaertn. (Fig. 2M-P) and *Cavanillesia arborea* (Willd.) K. Schum. (2Q-T), the filters enhanced the contrast between thin- and thick-walled fibres and improved the visualisation of growth rings. Under natural light, the growth rings of *C. arborea* have been considered as indistinguishable due to the low contrast among cell types (Barbosa *et al.*, 2018). Nonetheless, growth-ring boundaries were highlighted as brighter bands (the fibrous zones) when using fluorescence, especially with the GFP and UV filters. Figure 3 shows an increment core of *C. arborea*, where the growth-ring boundaries became clear under UV light. When using a stereomicroscope with a moving table, the images taken could be stitched together and used for tree-ring width measurements.

Fluorescence may also aid the identification of false rings for species that are known to produce clear tree-rings boundaries. Sometimes, false rings can only be identified during cross-dating (Stahle, 1999). These rings are not continuous through the stem and may have a slightly different anatomical pattern (Fritts, 1971). For example, false rings in *Hymenaea* sp., *Cedrela odorata* L. and *Goniorrhachis marginata* Taub. (Fig. 4) are composed of parenchyma cells with different fluorescence emission intensity compared to tree rings. In *Cedrela odorata* and *Goniorrhachis marginata* (Fig. 4E-L) paratracheal parenchyma and fibres showed the same fluorescence characteristics, in contrast to the low fluorescence of marginal parenchyma bands. The distinction between tree rings and false rings is also helpful in slow growing species or periods of suppressed growth that result in very narrow rings. Especially when using 5 mm increment cores that only allow the evaluation of a small surface (but see Krottenthaler *et al.*, 2015), these false rings might not be identified as



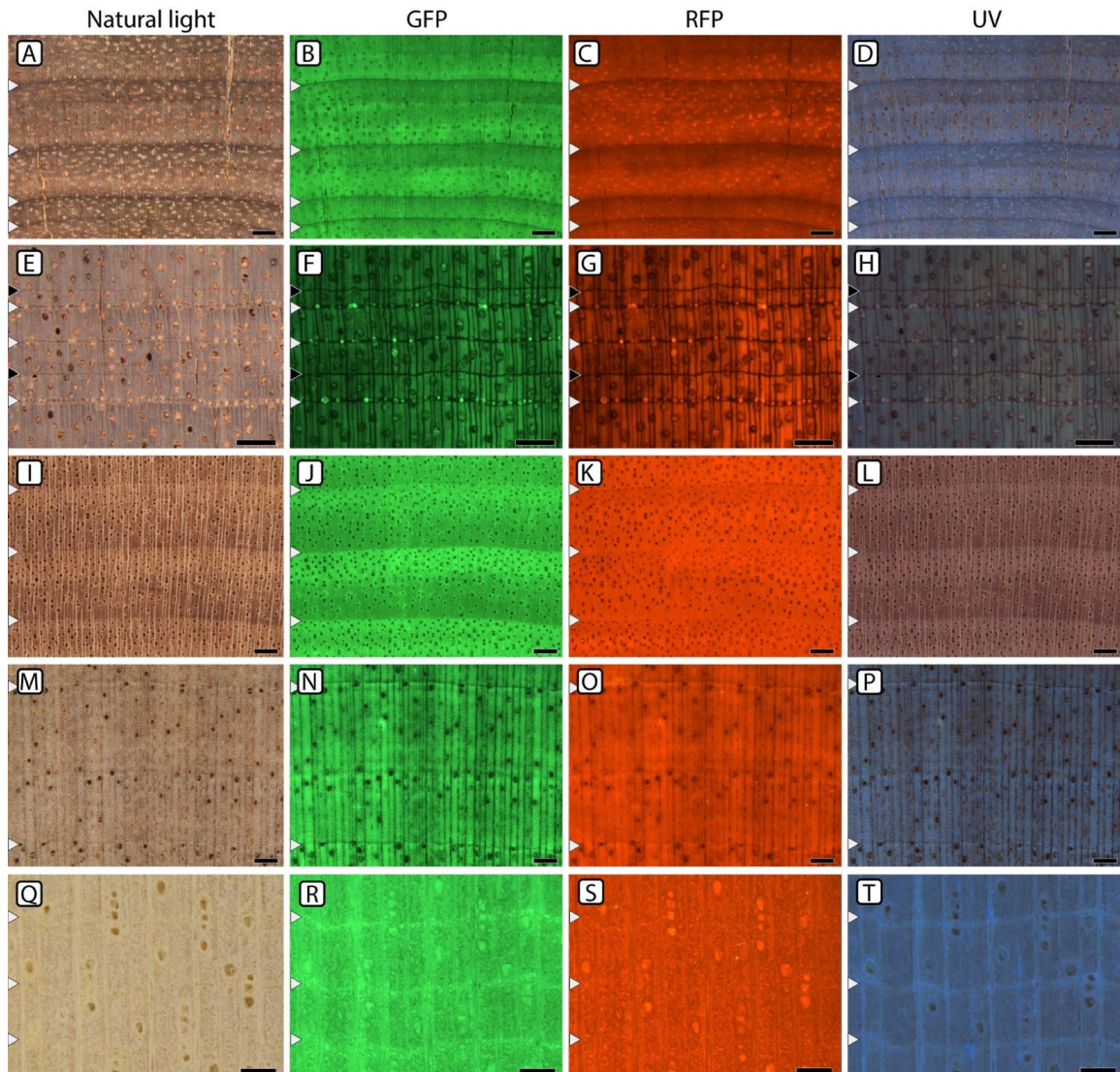


**Figure 2** - Macroscopic view of growth-rings using different sets of fluorescence filters. Visualization was compared under natural light, GFP, RFP and UV, respectively in the following species; A-D: *Centrolobium tomentosum*, growth-rings boundaries are clearer in fluorescence (darker lines); E-H: *Copaifera langsdorffii*, secretory canals and contrast between fibre (light green/red/blue) and parenchyma (dark green/red/blue) become highlighted with all filters; I-L: *Commiphora leptophloeos*, visualization improvements of density fluctuations and vessel lumen aids boundary delimitation; M-P: *Ceiba petandra*, another light coloured wood favoured by higher contrast amongst cell types with different lignin content; Q-T: *Cavanillesia arborea*, fibre bands are shown in fluorescence as brighter lines, enhancing tree ring visualization. White arrowheads: growth-ring boundaries; black arrowheads: false ring boundary; scale bar: 1 mm.

such. Distinct fluorescence emission between real and false rings may be due to differences in cell structure and / or composition. For instance, in *Hymenaea courbaril*, the marginal parenchyma band is formed by flattened parenchyma cells which are different from those of false rings that resemble the more rounded and larger aliform parenchyma cells (refer to Figure 3 from Locosselli *et al.*, 2016).

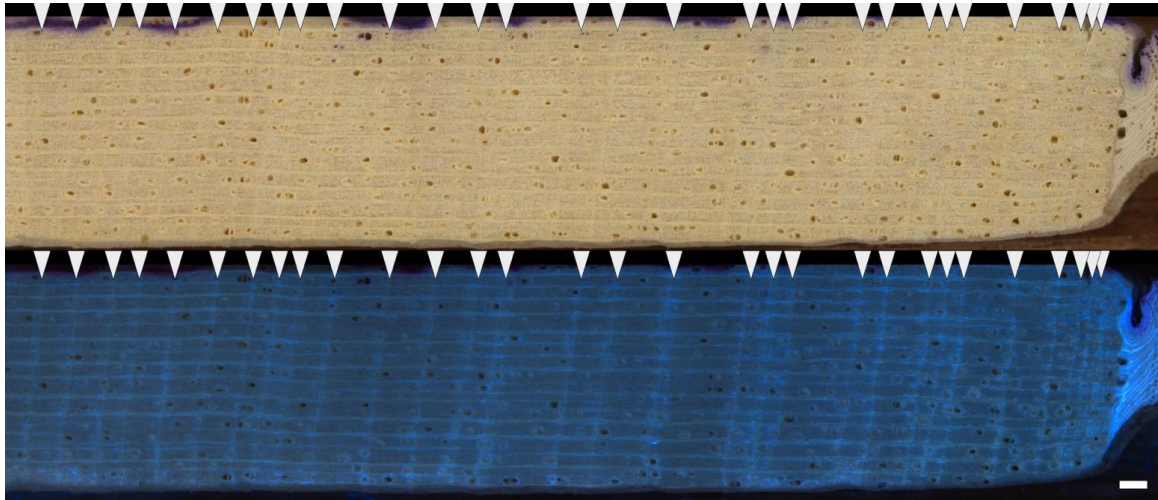


**Figure 3** - Growth-ring visualization under natural light and using an UV filter on a 10 mm core of *Cavanillesia arborea*. Under natural light (upper image) the boundaries are not clearly distinct. With the application of fluorescence (bottom image) the fibrous zones become distinct as lighter bands. White arrowheads: growth-ring boundaries; scale bar: 1 mm.

On the other hand, fluorescence may not be suitable for all species (Fig. 5). The parenchyma bands of *Swietenia macrophylla* King turned out to be indistinguishable from fibre density fluctuations when using GFP and RFP filters. Although the UV filter maintains the parenchyma bands distinct, the best results are obtained under natural light. In addition, the fibrous zone delimiting the tree rings of *Ocotea* sp. Aubl. (Fig. 5E-H) became indistinguishable when using GFP and RFP filters. The same result was observed in other *Ocotea* species and in *Aniba canelilla* (Kunth) Mez (all members of the Lauraceae family). Similar results were also found with *Amburana cearensis* (Allemão) A.C.SM. (Fig. 5I-L), a species whose tree rings are characterized either by a change in the paratracheal parenchyma from vasicentric to aliform, the formation of a fibrous zone, and/or the reduction in vessel diameter towards the end of the tree ring (Brienen and Zuidema, 2005; Paredes-Villanueva *et al.*, 2015). We therefore



recommend previous verification of the viability of use of this technique with species other than those presented here, including species with clear tree-ring boundaries.

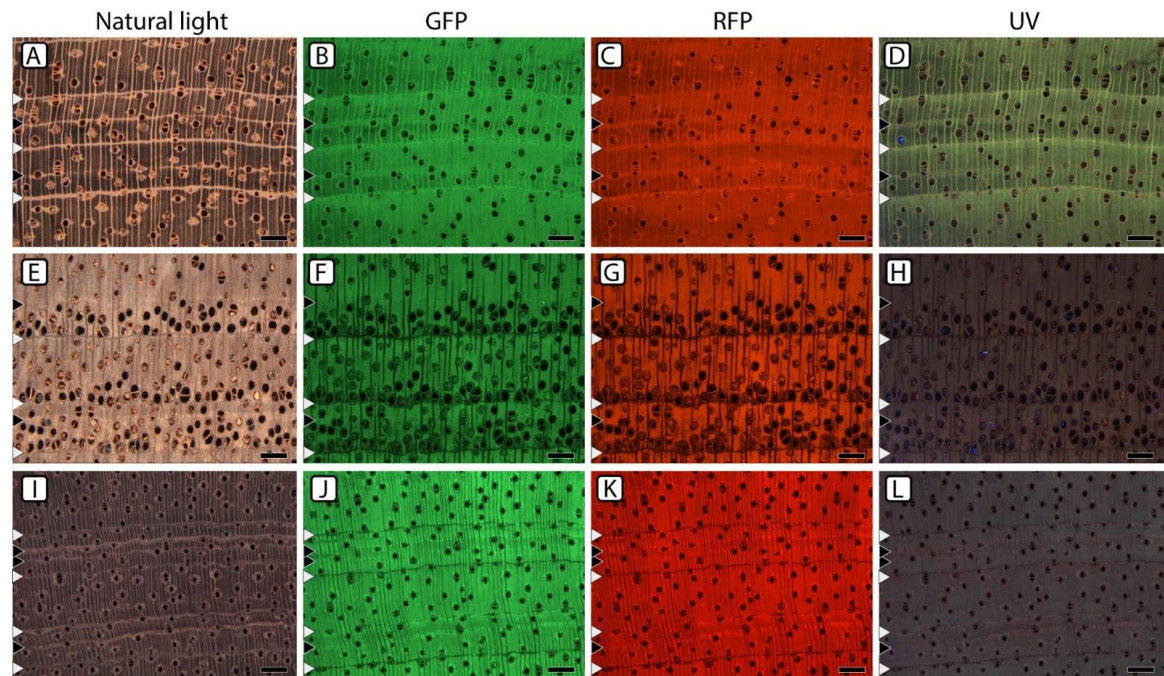


**Figure 4** - Identification of false tree rings using fluorescence. Visualization was compared under natural light, GFP, RFP and UV, respectively in the following species; A-D: *Hymenaea* sp., both true and false rings marked by marginal parenchyma bands are quite distinct under natural light. However, using the fluorescence filters, false rings disappear, and tree rings remain as brighter bands; E-H: *Cedrela odorata*, false rings are characterized by a whitish parenchyma band under natural light, but turn into small black dots using GFP and RFP filters. The parenchyma bands of *Goniorrhachis marginata* (I-L) look all very similar under natural light but show different fluorescent properties when using the filters: false rings are composed of parenchyma cells similar to paratracheal parenchyma while the parenchyma bands of the tree rings are similar to rays. White arrowheads: tree-ring boundaries; black arrowheads: false tree ring boundary; scale bar: 1 mm.

The use of this technique is not restricted to tree-ring studies but can be extended to other applications that require a better visualisation of wood anatomical features. On one hand, it can be used to aid wood identification, as cited above. For instance, the only two genera of conifers in Brazil, namely *Araucaria* and *Podocarpus*, can be differentiated due to the exclusive presence of axial parenchyma in *Podocarpus* spp.



(Wheeler, 2011). These thin-walled cells appeared as darker spots on the transversal wood surface of *Podocarpus lambertii* Klotzsch ex Endl. using the GFP filter (Fig.6E-H), which are not seen in *Araucaria angustifolia* (Bertol.) Kuntze (Fig. 6A-D). Fluorescence also highlights the oil/mucilage cells as lighter green spots in the Lauraceae species (Loureiro, 1976; Wheeler, 2011) analysed here in a unique distribution close to vessels (Fig. 6I-L and Supplementary Material). This result is similar to the visualization of the resin canals in *Copaifera langsdorffii* (Fig.2E-H). On the other hand, quantitative anatomy that allows understanding environmental variability through xylem structure (Fonti *et al.*, 2010; Islam *et al.*, 2018; Jono *et al.*, 2013; Locosselli *et al.*, 2013) may benefit from wood autofluorescence (e.g. Martin-Benito *et al.*, 2017), because automated measurements on digital images require a high contrast among target cells and background (Fonti *et al.*, 2010). Overall, vessels became clearer using the fluorescence as highlighted in this study for a variety of species. For *Erismia uncinatum* Warm. (Fig.6 M-P) the filters allowed a clear differentiation among vessels, parenchyma bands (darker bands), and the lighter background of fibres, crossed by rays (darker lines). Although the focus of this study was to improve the growth visualization, fluorescence may also aid other applications, including qualitative and quantitative wood anatomy.

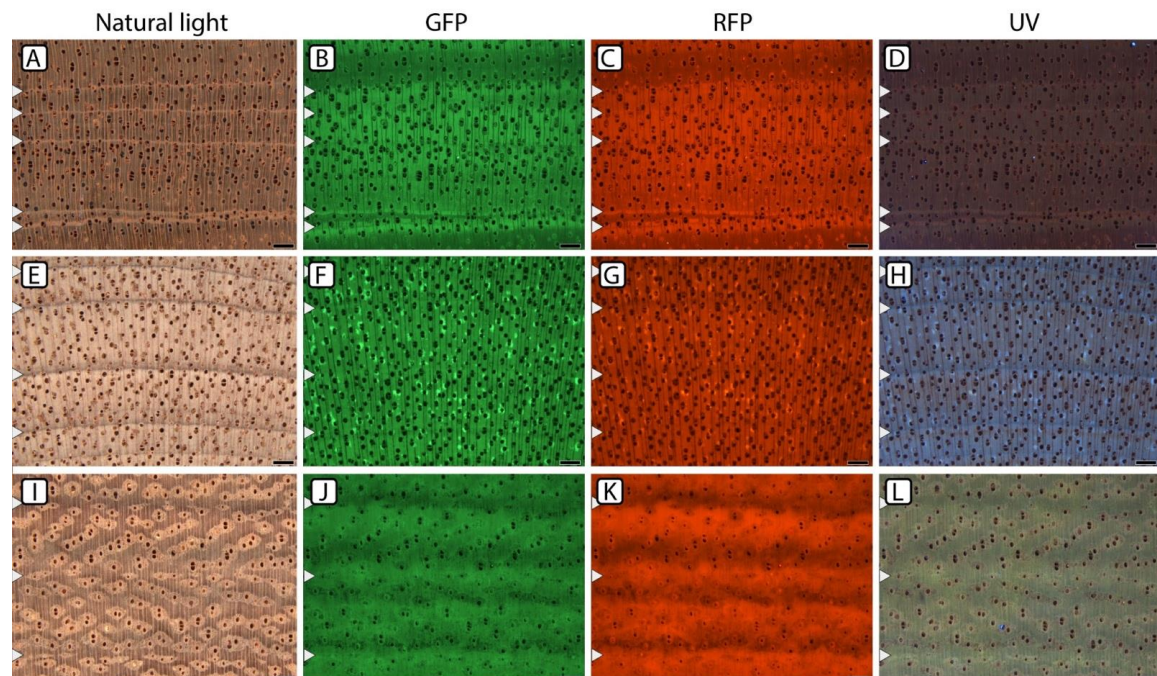


**Figure 5** - Growth-ring visualization hampered by the use of fluorescence. Visualization was compared under natural light, GFP, RFP and UV, respectively in the following species;

A-D: *Swietenia macrophylla*, marginal parenchyma bands are distinct they disappear in density fluctuations when using the filters; E-H: *Ocotea* sp., fibrous zones at the growth ring boundaries become indistinct with GFP and RFP filters; I-L: *Amburana cearensis* tree-rings are characterized by a change in the axial parenchyma configuration and the formation of a fibrous zone, neither highlighted through fluorescence. White arrowheads: tree-ring boundaries; scale bar: 1 mm.

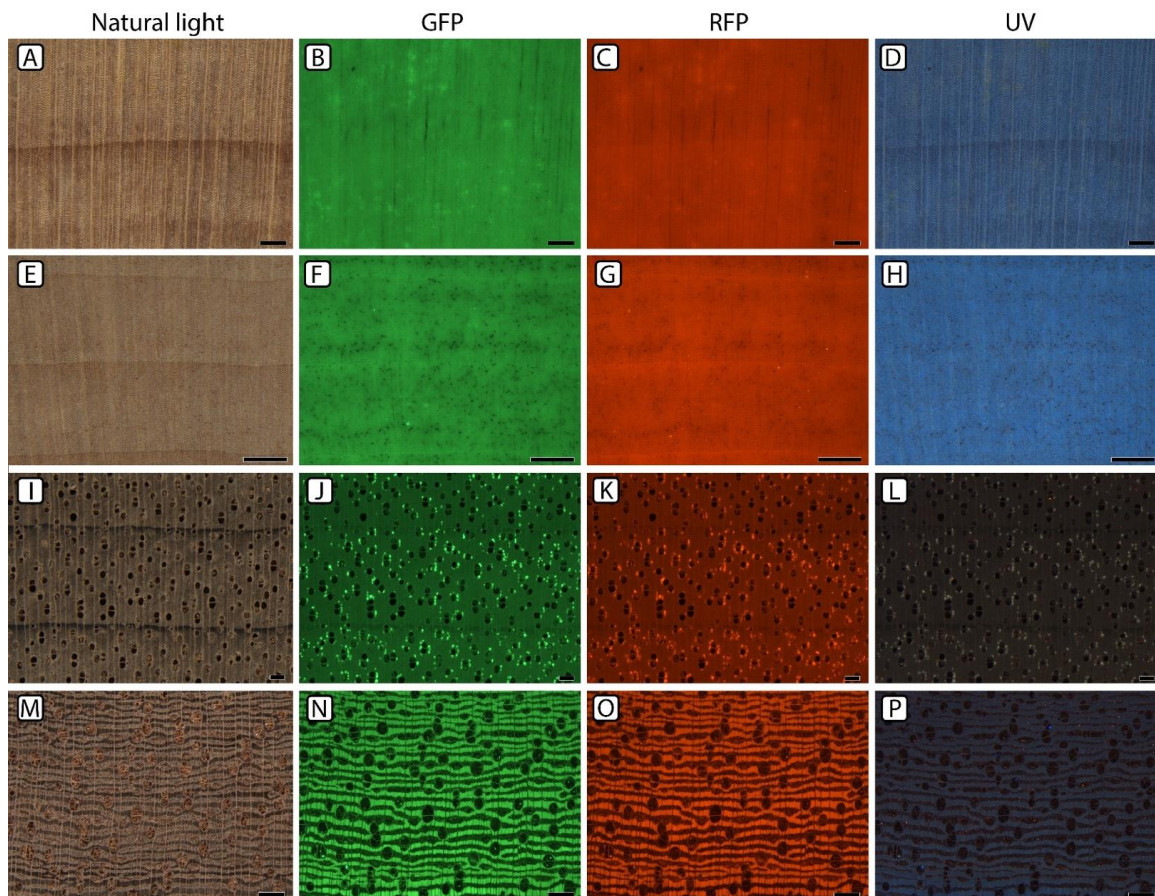


**Figure 6** - Other applications of fluorescence in wood anatomy. Species are compared under natural light, GFP, RFP and UV, respectively. The first two species, *Araucaria angustifolia* (A-D) and *Podocarpus lambertii* (E-H), are the only two extant genera of Brazilian gymnosperms and the presence of axial parenchyma (black dots) in *P. lambertii* is an easy way separate them. Fluorescence is a useful tool to improve some characteristics for image analyses software; I-L: *Ocotea porosa*, oil cells are highlighted by fluorescence (brighter dots). In *Erisma uncinatum* (M-P) the contrast between different cell types enhances the visualization for parenchyma/fibre/vessel measurements. Scale bar: 0.5 mm.

One important aspect to consider for the selection of the fluorescence filters is the exposure time for image acquisition (Fig. 7). The filters GFP and RFP require

similar exposures, on average  $3.62 \pm 2.46$ s and  $2.62 \pm 1.92$ s, respectively, while the exposure time for the UV filter is considerably higher, on average  $13.87 \pm 4.87$ s. Exposure time may change according to species and magnification and is usually higher in dark-coloured wood species and under lower magnification. The difficulty imposed by the higher exposure time is related to the time needed to acquire the images and how it impacts the routines of the analyses. About two seconds of exposure for each image does not really affect the routine in tree-ring studies, especially considering that it aids tree-ring visualization. In addition, image acquisition is not always necessary, as samples can be analysed directly on the stereomicroscope using the different filters. If the exposure time becomes too high, fluorescence might be only suitable for improving the cross-dating in specific regions of the samples. Results may also change to an extent between sapwood and heartwood, and except for a few species (e.g. *Commiphora leptophloeos*), growth-ring visualization was considerably improved in almost the whole sample. When taking these issues into consideration, fluorescence can be used either for the entire process of growth-ring identification and measurements or just for specific segments of the samples to improve the detection of false rings.

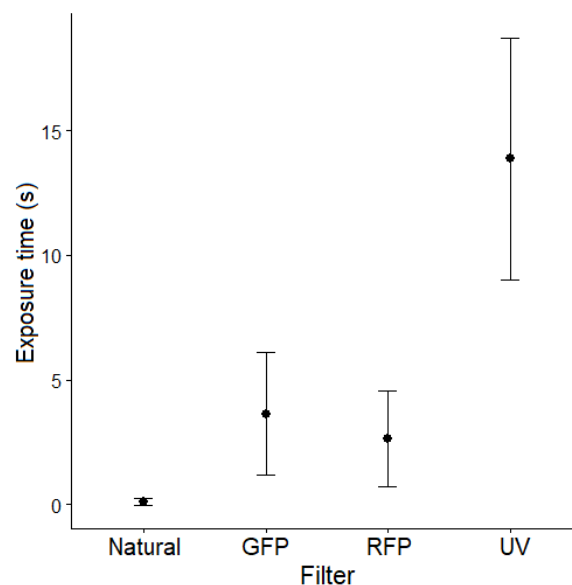


**Figure 7** - Mean exposure time and standard error (95% confident interval) required for image acquisition using a Leica DFC 7000T camera using natural light and the following fluorescence filters: GFP, RFP and UV, all under 10x magnification.



## **Conclusion**

With this technical note we demonstrated that the use of fluorescence can improve the growth-ring visualization and false ring identification in several species. This method is highly recommended for species with more complex wood anatomy (frequently found in tropical regions). To our knowledge, this is the first study that systematically explores fluorescence for improving tree-ring counting and cross-dating in different tree species. Although the sample size was relatively small, it has covered a great diversity of anatomical features. We expect fluorescence to assist those struggling with tree-ring counting and cross-dating. In addition, this technique may also be used for other applications in qualitative and quantitative wood anatomy. Other filters with different combinations of excitation and emission wavelengths are available on the market and they also have the potential to aid tree-ring studies. Therefore, we encourage future studies to explore different possibilities of using fluorescence, to search for other filter sets and to expand the available set of species useful for tree-ring studies.

## **Acknowledgments**

We thank Dr. Federico David Brown Almeida for helping with the early tests of this technique. Authors thank the Instituto Nacional de Ciência e Tecnologia do Bioetanol (FAPESP 2008/57908-6 and CNPq 574002/2008-1) for allowing the use of the stereomicroscope. Funding for this project was provided by São Paulo Research Foundation – FAPESP (2013/21728-2, 2015/25511-3, 2017/50085-3, and 2018-07632-6).

**Authors' contributions:** GML, MSB, FS, GC and MGV designed the research; MGV and PCA prepared and collected the data; MGV and GML analysed and interpreted the data; MGV and GML led the writing of the manuscript. All authors contributed in the discussions, revisions, drafts and gave approval for publication.

**Conflict of interest:** Authors declare that they have no conflict of interest.

**Table 1:** Species employed for testing fluorescence in growth-ring visualization, the respective features highlighted by the method (-, no feature highlighted). It also shows if the annuality of the tree rings of each species have been proven before, or if there is no information (-); and if tree rings have been considered distinct, distinct to indistinct (distinct with difficulties), or indistinct.

Species	Family	Feature improved	Annual / Visualization	Reference
<i>Acacia polyphylla</i> DC.	Fabaceae	-	- / -	Willians and León (2008)
<i>Amburana cearensis</i> (Allemão) A.C.SM.	Fabaceae	-	Yes / Distinct	Paredes-Villanueva et al. (2015)
<i>Anadenanthera colubrina</i> (Vell.) Brenan	Fabaceae	Parenchyma bands	Yes / Distinct	Mendivelso et al. (2014)
<i>Aniba canelilla</i> (Kunth) Mez	Lauraceae	-	Yes / Distinct to indistinct	Reis-Avila and Oliveira (2017)
<i>Araucaria angustifolia</i> (Bertol.) Kuntze	Araucariaceae	-	Yes / Distinct	Prestes et al. (2018)
<i>Aspidosperma desmanthum</i> Benth. Ex Müll.Arg.	Apocynaceae	Fibrous zone	- / Indistinct	Alves and Angyalossy-Alfonso (2000)
<i>Aspidosperma polyneuron</i> Müll.Arg.	Apocynaceae	Fibrous zone and vessel density	Yes / Difficult to indistinct	Lisi et al. (2008); Tomazello Filho et al. (2004)
<i>Aspidosperma pyriformium</i> Mart.	Apocynaceae	Fibrous zone and vessel density	- / Indistinct	Alves and Angyalossy-Alfonso (2000)
<i>Brosimum rubescens</i> Taub.	Moraceae	-	- / Distinct to indistinct	Alves and Angyalossy-Alfonso (2000)
<i>Cariniana estrellensis</i> (Raddi) Kuntze	Lecythidaceae	Contrast among fibres and parenchyma	Yes / Distinct to indistinct	Lisi et al. (2008)
<i>Cavanillesia arborea</i> (Willd.) K.Schum.	Malvaceae	Fibrous zone	- / Indistinct	Barbosa et al. (2018)
<i>Cedrela fissilis</i> Vell.	Meliaceae	Porosity and parenchyma band	Yes / Distinct	Pereira et al. (2018)
<i>Cedrela odorata</i> L.	Meliaceae	Porosity and parenchyma band	Yes / Distinct	Baker et al. (2017)
<i>Ceiba petandra</i> (L.) Gaertn.	Malvaceae	Contrast among fibres and parenchyma	Yes / Distinct to indistinct	Worbes et al. (2003)
<i>Centrolobium tomentosum</i> Benth.	Fabaceae	Contrast among fibres and parenchyma	Yes / Distinct	Lisi et al. (2008)
<i>Commiphora leptophloeos</i> (Mart.) J.B.Gillett	Burseraceae	Density fluctuation and vessel density	- / Distinct to indistinct	Unpublisehd data
<i>Copaifera langsdorffii</i> Desf.	Fabaceae	Parenchyma bands and secretory canals	Yes / Distinct	Carvalho et al. (2018)
<i>Dimorphandra mollis</i> Benth.	Fabaceae	-	- / Distinct to indistinct	Marcati et al. (2006)
<i>Dryobalanops</i> sp. C.F. Gaertn.	Dipterocarpaceae	Vessels at ring boundary	No / Distinct	Sass et al. (1995)
<i>Erythrina speciosa</i> Andrews	Fabaceae	Fibres at ring boundary	- / Distinct to indistinct	Wheeler (2011)
<i>Eucalyptus</i> sp.L'Hér.	Myrtaceae	-	Yes / Distinct to indistinct	Schulze et al. (2006)
<i>Goniorrhachis marginata</i> Taub.	Fabaceae	Contrast among fibres and parenchyma	- / Distinct	Mainieri and Chimelo (1989)
<i>Guibourtia</i> sp.Benn.	Fabaceae	-	- / Distinct to indistinct	Wheeler (2011)
<i>Handroanthus</i> sp.Mattos	Bignoniaceae	Parenchyma bands	Yes / Distinct	da Fonseca et al. (2009)

<i>Hymenaea</i> sp. L.	Fabaceae	Parenchyma bands	Yes / Distinct	Westbrook et al. (2006); Locosselli et al. (2013)
<i>Lecythis pisonis</i> Cambess.	Lecythidaceae	-	- / Distinct	Mainieri and Chimelo (1989)
<i>Machaerium villosum</i> Vogel	Fabaceae	Vessel density	- / Distinct to indistinct	Marcati et al. (2006); Tomazello-Filho et al. (2004)
<i>Myracrodruon urundeuva</i> Allemão	Anacardiaceae	Vessel density and porosity	- / Distinct	Alves and Angyalossy-Alfonso (2000)
<i>Ocotea odorifera</i> (Vell.) Rohwer	Lauraceae	-	Yes / Distinct	Reis-Avila and Oliveira (2017)
<i>Ocotea porosa</i> (Nees & Mart.) Barroso	Lauraceae	-	Yes / Distinct	Reis-Avila and Oliveira (2017)
<i>Ocotea</i> sp. Aubl. / <i>Nectandra</i> sp. Rol. ex. Rottb.	Lauraceae	-	Yes / Distinct	Reis-Avila and Oliveira (2017)
<i>Parapiptadenia rigida</i> (Benth.) Brenan	Fabaceae	-	Yes / Distinct	Boninsegna et al. (1989)
<i>Peltogyne</i> sp. Vogel	Fabaceae	Vessel density	Yes / Distinct to indistinct	Brienen and Zuidema (2005)
<i>Plathymenia foliolosa</i> Benth.	Fabaceae	-	- / Distinct to indistinct	Manieri and Chimelo (1989)
<i>Podocarpus lambertii</i> Klotzsch ex Endl.	Podocarpaceae	Tracheids at ring boundary	Yes / Distinct to indistinct	Locosselli et al. (2016)
<i>Pseudobombax</i> sp. Dugand	Malvaceae	-	Yes / Distinct	Devall et al. (1995)
<i>Swietenia macrophylla</i> King	Meliaceae	-	Yes / Distinct	Dünisch et al. (2003)
<i>Tipuana tipu</i> (Benth.) Kuntze	Fabaceae	Contrast among fibres and parenchyma	Yes / Distinct to indistinct	Ferrero et al. (2014); Locosselli et al. 2019

## Referências Bibliográficas

---

- Alves, E.S., Angyalossy-Alfonso, V., 2000. Ecological trend in the wood anatomy of some Brazilian species. 1. Growth rings and vessels. IAWA Journal. Vol 21 (1): 3-30  
<https://doi.org/10.1163/22941932-90000311>
- Amaral, A.C.B. and Tomazello Filho, M., 1998. Avaliação das características dos anéis de crescimento de *Pinus taeda* pela técnica de microdensitometria de raios X. Revista de Ciência e Tecnologia, 6(11/12), pp.17-23.
- Andrade, E.S., Garcia, S.S.C., Albernaz, A.L.K.M., Tomazello Filho, M., Moutinho, V.H.P., 2017. Growth ring analysis of *Euxylophora paraensis* through x-ray microdensitometry. Ciência Rural 47, 1–6. <http://dx.doi.org/10.1590/0103-8478cr20150895>
- Avella, T., R. Dechamps and M. Bastin., 1988. Fluorescence study of 10610 woody species from the Tervurin (T W) Collection, Belgium. IAWA Bull. 9: 346-352.  
<https://doi.org/10.1163/22941932-90001094>
- Babst, F., Bodesheim, P., Charney, N., Friend, A.D., Girardin, M.P., Klesse, S., Moore, D.J.P., Seftigen, K., Björklund, J., Bouriaud, O., Dawson, A., DeRose, R.J., Dietze, M.C., Eckes, A.H., Enquist, B., Frank, D.C., Mahecha, M.D., Poulter, B., Record, S., Trouet, V., Turton, R.H., Zhang, Z., Evans, M.E.K., 2018. When tree rings go global: Challenges and opportunities for retro- and prospective insight. Quat. Sci. Rev. 197, 1–20. <https://doi.org/10.1016/j.quascirev.2018.07.009>
- Baker, J.C.A., Santos, G.M., Gloor, M., Brienen, R.J.W., 2017. Does *Cedrela* always form annual rings? Testing ring periodicity across South America using radiocarbon dating. Trees - Struct. Funct. 31, 1999–2009. <https://doi.org/10.1007/s00468-017-1604-9>
- Barbosa, A.C.M., Pereira, G.A., Granato-Souza, D., Santos, R.M., Fontes, M.A.L., 2018. Tree rings and growth trajectories of tree species from seasonally dry tropical forest. Aust. J. Bot. 66, 414–427. <https://doi.org/10.1071/BT17212>
- Barnes, D.J., Taylor, R.B., 2001. On the nature and causes of luminescent lines and bands in coral skeletons. Coral Reefs 19, 221–230. <https://doi.org/10.1007/PL00006958>
- Bergeron, Y., Denneler, B., Charron, D., Girardin, M.-P., 2002. Using dendrochronology to reconstruct disturbance and dynamics, Quebec. Dendrochronologia 2, 175–189.  
<https://doi.org/10.1078/1125-7865-00015>

- Boninsegna, J.A., Villalba, R., Amarilla, L., Ocampo, J., 1989. Studies on tree rings, growth rates and age-size relationships of tropical tree species in misiones, argentina. *IAWA J.* 10, 161–169. <https://doi.org/10.1163/22941932-90000484>
- Borgaonkar, H.P., Sikder, A.B., Ram, S., Pant, G.B., 2010. El Niño and related monsoon drought signals in 523-year-long ring width records of teak (*Tectona grandis* L.F.) trees from south India. *Palaeogeogr. Palaeoclimatol. Palaeoecol.* 285, 74–84. <https://doi.org/10.1016/j.palaeo.2009.10.026>
- Brienen, R.J.W., Lebrija-Trejos, E., Van Breugel, M., Pérez-García, E.A., Bongers, F., Meave, J.A., Martínez-Ramos, M., 2009. The potential of tree rings for the study of forest succession in Southern Mexico. *Biotropica* 41, 186–195. <https://doi.org/10.1111/j.1744-7429.2008.00462.x>
- Brienen, R.J.W., Schöngart, J., Zuidema, P.A., 2016. Tree rings in the tropics: insights into the ecology and climate sensitivity of tropical trees. *Trop. Tree Physiol.* 6, 439–461. [https://doi.org/10.1007/978-3-319-27422-5\\_20](https://doi.org/10.1007/978-3-319-27422-5_20)
- Brienen, R.J.W., Zuidema, P.A., 2006. Lifetime growth patterns and ages of Bolivian rain forest trees obtained by tree ring analysis. *J. Ecol.* 94, 481–493. <https://doi.org/10.1111/j.1365-2745.2005.01080.x>
- Brienen, R.J.W., Zuidema, P.A., 2005. Relating tree growth to rainfall in Bolivian rain forests: a test for six species using tree ring analysis. *Oecologia* 146, 1–12. <https://doi.org/10.1007/s00442-005-0160-y>
- Büntgen, U., Tegel, W., Nicolussi, K., McCormick, M., Frank, D., Trouet, V., Kaplan, J.O., Herzig, F., Heussner, K.-U., Wanner, H., Luterbacher, J., Esper, J., 2011. 2500 Years of European Climate. *Science*. 331, 578–582. <https://doi.org/10.1126/science.1197175>
- Carvalho, D.C., Pereira, M.G., Latorraca, J.V., Pace, J.H., da Silva, L.D., Carmo, J.F., 2018. Estoque de carbono em áreas de restauração florestal da Mata Atlântica. *Floresta* 48, 183–194. <https://doi.org/10.5380/rf.v48>
- Cook, E.R., Seager, R., Kushnir, Y., Briffa, K.R., Büntgen, U., Frank, D., Krusic, P.J., Tegel, W., Schrier, G., Van Der, Andreu-hayles, L., Baillie, M., Baittinger, C., Bleicher, N., Bonde, N., Brown, D., Carrer, M., Cooper, R., Čufar, K., Dittmar, C., Esper, J., Griggs, C., Heussner, K., Hofmann, J., Janda, P., Kontic, R., Köse, N., Kyncl, T., Levani, T., Nola, P., Panayotov, M., Popa, I., Rothe, A., Seftigen, K., Seim, A., Svarva, H., Gutierrez, E., Haneca, K., Helama, S., Herzig, F., Heussner, K., Hofmann, J., Janda, P., Kontic, R., Linderholm, H., Manning, S., Melvin, T.M.,



- Miles, D., Neuwirth, B., Nicolussi, K., Nola, P., Panayotov, M., Popa, I., Rothe, A., Seftigen, K., Seim, A., Svarva, H., Svoboda, M., Thun, T., Timonen, M., Touchan, R., Trotsiuk, V., Trouet, V., Walder, F., Wilson, R., Zang, C., 2015. Old World megadroughts and pluvials during the Common Era. *Science Adv.* 1–10. <https://doi.org/10.1126/sciadv.1500561>
- da Fonseca Júnior, S.F., Piedade, M.T.F., Schöngart, J., 2009. Wood growth of *Tabebuia barbata* (E. Mey.) Sandwith (Bignoniaceae) and *Vatairea guianensis* Aubl. (Fabaceae) in Central Amazonian black-water (igapó) and white-water (várzea) floodplain forests. *Trees* 23, 127–134. <https://doi.org/10.1007/s00468-008-0261-4>
- Devall, M.S., Parresol, B.R., Wright, S.J., 1995. Dendroecological Analysis of *Cordia Alliodora*, *Pseudobombax Septenatum* and *Annona Spraguei* in Central Panama. *IAWA J.* 16, 411–424. <https://doi.org/10.1163/22941932-90001430>
- Dünisch, O., Bauch, J., Gasparotto, L., 2002. Formation of increment zones and intraannual growth dynamics in the xylem of *Swietenia macrophylla*, *Carapa guianensis*, and *Cedrela odorata* (Meliaceae). *IAWA J.* 23, 101–119. <https://doi.org/10.1163/22941932-90000292>
- Dünisch, O., Montóia, V.R., Bauch, J., 2003. Dendroecological investigations on *Swietenia macrophylla* King and *Cedrela odorata* L. (Meliaceae) in the central Amazon. *Trees* 17, 244–250. <https://doi.org/10.1007/s00468-002-0230-2>
- Dyer, S.T., 1988. Wood fluorescence of indigenous South African trees. *IAWA Bulletin n.s.*, Vol. 9 (1), 15-87. <https://doi.org/10.1163/22941932-90000472>
- Esper, J., Cook, E.R., Schweingruber, F.H., 2002. Low-frequency signals in long tree-ring chronologies for reconstructing past temperature variability. *Science* (80-. ). 295, 2250–2253. <https://doi.org/10.1126/science.1066208>
- Fang, K., Cook, E., Guo, Z., Chen, D., Ou, T., Zhao, Y., 2018. Synchronous multi-decadal climate variability of the whole Pacific areas revealed in tree rings since 1567. *Environ. Res. Lett.* 13. <https://doi.org/10.1088/1748-9326/aa9f74>
- Ferrero, M.E., Villalba, R., Rivera, S.M., 2014. Na assessment of growth ring identification in subtropical forests from northwestern Argentina. *Dendrochronologia*, 32: 113-119. <http://dx.doi.org/10.1016/j.dendro.2014.01.003>
- Fichtler, E., Clark, D.A., Worbes, M., 2003. Age and long-term growth of trees in an old-growth tropical rain forest, based on analyses of tree rings and <sup>14</sup>C. *Biotropica* 35, 306. <https://doi.org/10.1646/03027>

- Fonti, P., Von Arx, G., García-González, I., Eilmann, B., Sass-Klaassen, U., Gärtner, H., Eckstein, D., 2010. Studying global change through investigation of the plastic responses of xylem anatomy in tree rings. *New Phytol.* 185, 42–53.  
<https://doi.org/10.1111/j.1469-8137.2009.03030.x>
- Fritts, H. C., (1976) *Tree-ring and climate*. Academic Press, London, p 567
- Gärtner, H., Cherubini, P., Fonti, P., von Arx, G., Schneider, L., Nievergelt, D., Verstege, A., Bast, A., Schweingruber, F.H., Büntgen, U., 2015. A technical perspective in modern tree-ring research-how to overcome dendroecological and wood anatomical challenges. *J. Vis. Exp.* <https://doi.org/10.3791/52337>
- Godoy-Veiga, M., Ceccantini, G., Pitsch, P., Krottenthaler, S., Anhuf, D., Locosselli, G.M., 2018. Shadows of the edge effects for tropical emergent trees: the impact of lianas on the growth of *Aspidosperma polyneuron*. *Trees - Struct. Funct.* 32, 1073–1082.  
<https://doi.org/10.1007/s00468-018-1696-x>
- Groenendijk, P., van der Sleen, P., Vlam, M., Bunyavejchewin, S., Bongers, F., Zuidema, P.A., 2015. No evidence for consistent long-term growth stimulation of 13 tropical tree species: Results from tree-ring analysis. *Glob. Chang. Biol.* 21, 3762–3776.  
<https://doi.org/10.1111/gcb.12955>
- Han, D.Y.Y., Kywe, U.T., 1991. Wood fluorescence of indigenous myanmar timbers. Forest Research Institute, Leaflet No. 9, Yezin.
- Islam, M., Rahman, M., Bräuning, A., 2018. Impact of extreme drought on tree-ring width and vessel anatomical features of *Chukrasia tabularis*. *Dendrochronologia* 53, 63–72. <https://doi.org/10.1016/j.dendro.2018.11.007>
- IAWA Committee IAWA, 1989. List of microscopic features for hardwood identification. *IAWA Bull*, 10(3), 201- 232
- Jono, V., Locosselli, G.M., Ceccantini, G., 2013. The influence of tree size and microenvironmental changes on the wood anatomy of *Roupala rhombifolia*. *IAWA Journal*. Vol 34 (1): 88-106. <https://doi.org/10.1163/22941932-00000008>
- Krishna, S.L., Chowdhury, K.A., 1935. Fluorescence of wood under ultraviolet light. *Indian Forester* 61: 221 – 228
- Krottenthaler, S., Pitsch, P., Helle, G., Locosselli, G.M., Ceccantini, G., Altman, J., Svoboda, M., Dolezal, J., Schleser, G., Anhuf, D., 2015. A power-driven increment borer for sampling high-density tropical wood. *Dendrochronologia* 36, 40–44.  
<https://doi.org/10.1016/j.dendro.2015.08.005>

- Lisi, C.S., Tomazello Filho, M., Botosso, P.C., Roig, F.A., Maria, V.R.B., Ferreira-Fedele, L., Voigt, A.R.A., 2008. Tree-ring formation, radial increment periodicity, and phenology of tree species from a seasonal semi-deciduous forest in southeast Brazil. *IAWA J.* 29, 189–207. <https://doi.org/10.1163/22941932-90000179>
- Locosselli, G.M., Buckeridge, M.S., Moreira, M.Z., Ceccantini, G., 2013. A multi-proxy dendroecological analysis of two tropical species (*Hymenaea* spp., Leguminosae) growing in a vegetation mosaic. *Trees - Struct. Funct.* 27, 25–36. <https://doi.org/10.1007/s00468-012-0764-x>
- Locosselli, G.M., Camargo E., Moreira, T., Todesco E., Andrade M., de André, C.D.S., de André, P.A., Singer, J.M., Ferreira, L.S., Saldiva, P.H.N., Buckeridge, M.S., 2019. The role of air pollution and climate on the growth of urban trees. *Science of the Total Environment.* 666, 652–661. <https://doi.org/10.1016/j.scitotenv.2019.02.291>
- Locosselli, G.M., Cardim, R.H., Ceccantini, G., 2016a. Rock outcrops reduce temperature-induced stress for tropical conifer by decoupling regional climate in the semiarid environment. *Int. J. Biometeorol.* 60, 639–649. <https://doi.org/10.1007/s00484-015-1058-y>
- Locosselli, G.M., Krottenthaler, S., Pitsch, P., Anhof, D., Ceccantini, G., 2017. Age and growth rate of congeneric tree species (*Hymenaea* spp. - Leguminosae) inhabiting different tropical biomes. *Erdkunde* 71. <https://doi.org/10.3112/erdkunde.2017.01.03>
- Locosselli, G.M., Schöngart, J., Ceccantini, G., 2016b. Climate/growth relations and teleconnections for a *Hymenaea courbaril* (Leguminosae) population inhabiting the dry forest on karst. *Trees - Struct. Funct.* 30, 1127–1136. <https://doi.org/10.1007/s00468-015-1351-8>
- Loureiro, A.A., 1976. Estudo anatômico macro e microscópico de 10 espécies do Gênero *Aniba* (Lauraceae) da Amazônia. *Acta Amaz.* 6. <http://dx.doi.org/10.1590/1809-43921976062s005>
- Maes, S.L., Perring, M.P., Vanhellefont, M., Depauw, L., Van den Bulcke, J., Brūmelis, G., Brunet, J., Decocq, G., den Ouden, J., Härdtle, W., Hédli, R., Heinken, T., Heinrichs, S., Jaroszewicz, B., Kopecký, M., Máliš, F., Wulf, M., Verheyen, K., 2018. Environmental drivers interactively affect individual tree growth across temperate European forests. *Glob. Chang. Biol.* <https://doi.org/10.1111/gcb.14493>
- Mainieri, C., Chimelo J.P. (1989) Fichas das características das principais madeiras brasileiras. 2. ed. São Paulo. Instituto de Pesquisas Tecnológicas (IPT).

- Marcati, C.R., Angyalossy-alfonso, V., Benetati, L., 2000. Anatomia comparada do lenho de *Copaifera langsdorffii* Desf. (Leguminosae-Caesalpinoideae) de floresta e cerrado. *Brazilian Journal of Botany* 24: 311–320.  
<http://dx.doi.org/10.1590/S0100-84042001000300010>
- Marcati, C.R., Oliveira, J.S., Machado, S.R., 2006. Growth rings in cerrado woody species: occurrence and anatomical markers. *Biota Neotrop.* 6, 0–0.  
<https://doi.org/10.1590/S1676-06032006000300001>
- Martin-Benito, D., Anchukaitis, K.J., Evans, M.N., Del Río, M., Beeckman, H., Cañellas, I., (2017). Effects of drought on xylem anatomy and water-use efficiency of two co-occurring pine species. *Forests*, 8: 332. <https://doi.org/10.3390/f8090332>
- McGarry, S.F., Baker, A., 2000. Organic acid fluorescence: applications to speleothem palaeoenvironmental reconstruction. *Quat. Sci. Rev.* 19, 1087–1101.  
[https://doi.org/10.1016/S0277-3791\(99\)00087-6](https://doi.org/10.1016/S0277-3791(99)00087-6)
- Mendivelso, H.A., Camarero, J.J., Gutiérrez, E., Zuidema, P.A., 2014. Time-dependent effects of climate and drought on tree growth in a Neotropical dry forest: Short-term tolerance vs. long-term sensitivity. *Agric. For. Meteorol.*  
<https://doi.org/10.1016/j.agrformet.2013.12.010>
- Miller, R.B., 2007. Fluorescent wood of the world. In: Flynn Jr., J.H., ed. *A guide to more useful woods of the world*. Madison, WI: Forest Products Society. 358 p.
- Murphy, D.B., 2001. *Fundamentals of light microscopy and electronic imaging*, John Wiley & Sons, Inc. USA. <https://doi.org/10.1259/bjr/21753020>
- Palmer, J.G., Turney, C.S.M., Cook, E.R., Fenwick, P., Thomas, Z., Helle, G., Jones, R., Clement, A., Hogg, A., Southon, J., Bronk Ramsey, C., Staff, R., Muscheler, R., Corrège, T., Hua, Q., 2016. Changes in El Niño – Southern Oscillation (ENSO) conditions during the Greenland Stadial 1 (GS-1) chronozone revealed by New Zealand tree-rings. *Quat. Sci. Rev.* 153, 139–155.  
<https://doi.org/10.1016/j.quascirev.2016.10.003>
- Paredes-Villanueva, K., López, L., Brookhouse, M., Cerrillo, R.M.N., 2015. Rainfall and temperature variability in Bolivia derived from the tree-ring width of *Amburana cearensis* (Fr. Allem.) A.C. Smith. *Dendrochronologia* 35, 80–86.  
<https://doi.org/10.1016/j.dendro.2015.04.003>
- Pereira, G. de A., Barbosa, A.C.M.C., Torbenson, M.C.A., Stahle, D.W., Granato-Souza, D., Santos, R.M. Dos, Barbosa, J.P.D., 2018. The Climate Response of *Cedrela fissilis*

- Annual Ring Width in the Rio São Francisco Basin, Brazil. *Tree-Ring Res.* 74, 162–171. <https://doi.org/10.3959/1536-1098-74.2.162>
- Prestes, A., Klausner, V., Rojahn Da Silva, I., Ojeda-González, A., Lorensi, C., 2018. *Araucaria* growth response to solar and climate variability in South Brazil. *Ann. Geophys.* 36, 717–729. <https://doi.org/10.5194/angeo-36-717-2018>
- Reis-Avila, G., Oliveira, J.M., 2017. Lauraceae: A promising family for the advance of neotropical dendrochronology. *Dendrochronologia* 44, 103–116. <https://doi.org/10.1016/j.dendro.2017.04.002>
- Rodrigues, T.M., Machado, S.R., 2009. Developmental and structural features of secretory canals in root and shoot wood of *Copaifera langsdorffii* desf. (leguminosae-caesalpinioideae). *Trees - Struct. Funct.* 23, 1013–1018. <https://doi.org/10.1007/s00468-009-0343-y>
- Sass, U., Killmann, W., Eckstein, D., 1995. Wood Formation in Two Species of Dipterocarpaceae in Peninsular Malaysia. *IAWA J.* 16, 371–384. <https://doi.org/10.1163/22941932-90001427>
- Schleser, G.H., Helle, G., Lücke, A., Vos, H., 1999. Isotope signals as climate proxies: the role of transfer functions in the study of terrestrial archives. *Quat. Sci. Rev.* 18, 927–943. [https://doi.org/10.1016/S0277-3791\(99\)00006-2](https://doi.org/10.1016/S0277-3791(99)00006-2)
- Schöngart, J., 2008. Growth-Oriented Logging (GOL): A new concept towards sustainable forest management in Central Amazonian várzea floodplains. *For. Ecol. Manage.* 256, 46–58. <https://doi.org/10.1016/j.foreco.2008.03.037>
- Schulze, E.D., Turner, N.C., Nicolle, D., Schumacher, J., 2006. Leaf and wood carbon isotope ratios, specific leaf areas and wood growth of *Eucalyptus* species across a rainfall gradient in Australia. *Tree Physiol.* 26, 479–492. <https://doi.org/10.1093/treephys/26.4.479>
- Segala Alves, E., Angyalossy-Alfonso, V., 2000. Ecological trends in the wood anatomy of some Brazilian species. 1. Growth rings and vessels. *IAWA J.* 21, 3–30. <https://doi.org/10.1078/0367-2530-0058>
- Slik, J.W.F., Arroyo-Rodríguez, V., Aiba, S.-I., Alvarez-Loayza, P., Alves, L.F., Ashton, P., Balvanera, P., Bastian, M.L., Bellingham, P.J., van den Berg, E., Bernacci, L., da Conceição Bispo, P., Blanc, L., Böhning-Gaese, K., Boeckx, P., Bongers, F., Boyle, B., Bradford, M., Brearley, F.Q., Breuer-Ndoundou Hockemba, M., Bunyavejchewin, S., Calderado Leal Matos, D., Castillo-Santiago, M., Catharino, E.L.M., Chai, S.-L., Chen, Y., Colwell, R.K., Chazdon, R.L., Robin, C.L., Clark,

C., Clark, D.B., Clark, D.A., Culmsee, H., Damas, K., Dattaraja, H.S., Dauby, G., Davidar, P., DeWalt, S.J., Doucet, J.-L., Duque, A., Durigan, G., Eichhorn, K.A.O., Eisenlohr, P. V, Eler, E., Ewango, C., Farwig, N., Feeley, K.J., Ferreira, L., Field, R., de Oliveira Filho, A.T., Fletcher, C., Forshed, O., Franco, G., Fredriksson, G., Gillespie, T., Gillet, J.-F., Amarnath, G., Griffith, D.M., Grogan, J., Gunatilleke, N., Harris, D., Harrison, R., Hector, A., Homeier, J., Imai, N., Itoh, A., Jansen, P.A., Joly, C.A., de Jong, B.H.J., Kartawinata, K., Kearsley, E., Kelly, D.L., Kenfack, D., Kessler, M., Kitayama, K., Kooyman, R., Larney, E., Laumonier, Y., Laurance, S., Laurance, W.F., Lawes, M.J., Amaral, I.L. do, Letcher, S.G., Lindsell, J., Lu, X., Mansor, A., Marjokorpi, A., Martin, E.H., Meilby, H., Melo, F.P.L., Metcalfe, D.J., Medjibe, V.P., Metzger, J.P., Millet, J., Mohandass, D., Montero, J.C., de Morisson Valeriano, M., Mugerwa, B., Nagamasu, H., Nilus, R., Ochoa-Gaona, S., Onrizal, N., Page, N., Parolin, P., Parren, M., Parthasarathy, N., Paudel, E., Permana, A., Piedade, M.T.F., Pitman, N.C.A., Poorter, L., Poulsen, A.D., Poulsen, J., Powers, J., Prasad, R.C., Puyravaud, J.-P., Razafimahaimodison, J.-C., Reitsma, J., Dos Santos, J.R., Roberto Spironello, W., Romero-Saltos, H., Rovero, F., Rozak, A.H., Ruokolainen, K., Rutishauser, E., Saiter, F., Saner, P., Santos, B.A., Santos, F., Sarker, S.K., Satdichanh, M., Schmitt, C.B., Schöngart, J., Schulze, M., Suganuma, M.S., Sheil, D., da Silva Pinheiro, E., Sist, P., Stevart, T., Sukumar, R., Sun, I.-F., Sunderland, T., Sunderand, T., Suresh, H.S., Suzuki, E., Tabarelli, M., Tang, J., Targhetta, N., Theilade, I., Thomas, D.W., Tchouto, P., Hurtado, J., Valencia, R., van Valkenburg, J.L.C.H., Van Do, T., Vasquez, R., Verbeeck, H., Adekunle, V., Vieira, S.A., Webb, C.O., Whitfeld, T., Wich, S.A., Williams, J., Wittmann, F., Wöll, H., Yang, X., Adou Yao, C.Y., Yap, S.L., Yoneda, T., Zahawi, R.A., Zakaria, R., Zang, R., de Assis, R.L., Garcia Luize, B., Venticinque, E.M., 2015. An estimate of the number of tropical tree species. *Proc. Natl. Acad. Sci. U. S. A.* 112, 7472–7. <https://doi.org/10.1073/pnas.1423147112>

Slotta, F., Helle, G., Heussner, K.U., Shemang, E., Riedel, F., 2017. Baobabs on Kubu Island, Botswana – A dendrochronological multi-parameter study using ring width and stable isotopes ( $\delta^{13}\text{C}$ ,  $\delta^{18}\text{O}$ ). *Erdkunde* 71, 18–39. <https://doi.org/10.3112/erdkunde.2017.01.02>

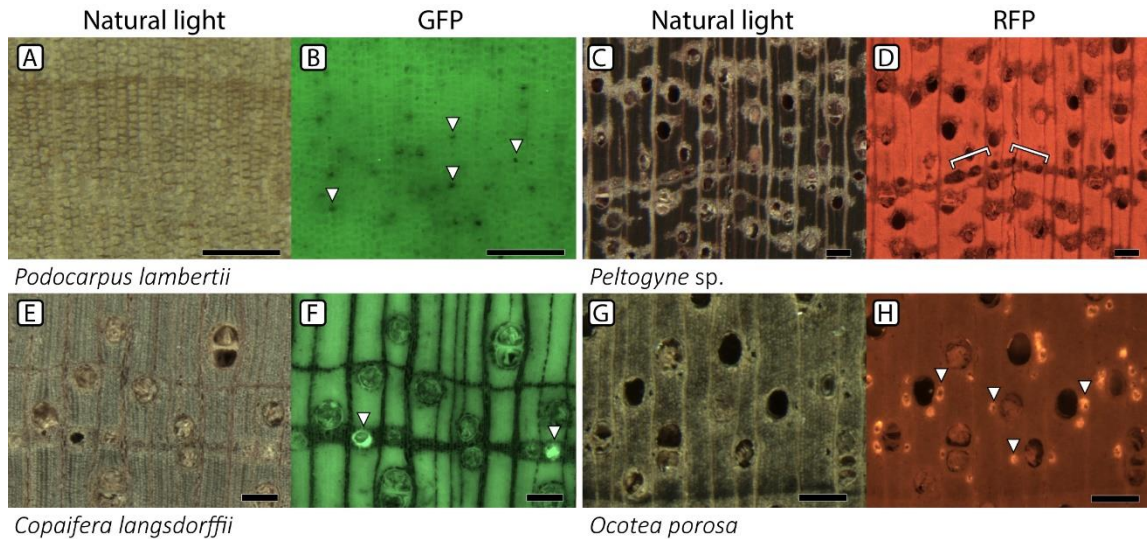
Soliz-Gamboa, C.C., Rozendaal, D.M.A., Ceccantini, G., Angyalossy, V., van der Borg, K., Zuidema, P.A., 2011. Evaluating the annual nature of juvenile rings in Bolivian tropical rainforest trees. *Trees - Struct. Funct.* 25, 17–27. <https://doi.org/10.1007/s00468-010-0468-z>

- Splechtna, B., Gratzner, G., Black, B. a, 2005. Disturbance history of a European old-growth mixed-species forest – A spatial dendro-ecological analysis. *J. Veg. Sci.* 16, 511–522. <https://doi.org/10.1111/j.1654-1103.2005.tb02391.x>
- Stahle, D.W., 1999. Usefull strategies for the development of tropical tree-ring chronology. *IAWA J.* 20, 249–253. <https://doi.org/10.1163/22941932-90000688>
- Therrell, M.D., Stahle, D.W., Mukelabai, M.M., Shugart, H.H., 2007. Age, and radial growth dynamics of *Pterocarpus angolensis* in southern Africa. *For. Ecol. Manage.* 244, 24–31. <https://doi.org/10.1016/j.foreco.2007.03.023>
- Tomazello Filho, M., Lisi, C.S., Hansen, N., Cury, G., 2004. Anatomical features of increment zones in different tree species in the State of São Paulo, Brazil. *Sci. For.* 66, 46–55.
- van der Sleen, P., Groenendijk, P., Vlam, M., Anten, N.P.R., Boom, A., Bongers, F., Pons, T.L., Terburg, G., Zuidema, P.A., 2014. No growth stimulation of tropical trees by 150 years of CO<sub>2</sub> fertilization but water-use efficiency increased. *Nat. Geosci.* 8, 24–28. <https://doi.org/10.1038/ngeo2313>
- Verheyden, A., Helle, G., Schleser, G.H., Beeckman, H., 2006. High-resolution carbon and oxygen isotope profiles of tropical and temperate liana species. *Schr Forsch Jülich R.* 4, 31–35.
- Verheyden, A., Kairo, J.G., Beeckman, H., Koedam, N., 2004. Growth rings, growth ring formation and age determination in the mangrove *Rhizophora mucronata*. *Ann. Bot.* 94, 59–66. <https://doi.org/10.1093/aob/mch115>
- Vlam, M., van der Sleen, P., Groenendijk, P., Zuidema, P.A., 2017. Tree age distributions reveal large-scale disturbance-recovery cycles in three tropical forests. *Front. Plant Sci.* 7, 1–12. <https://doi.org/10.3389/fpls.2016.01984>
- Vodrázka, O., 1929. Das Mikroskopieren von Holz in filtriertem Ultraviolettlicht. Botanisches Institut der Hochschule Für Bodenkultur, Brünn, Czechoslovakia.
- Westbrook, J.A., Guilderson, T.P., Colinvaux, P.A., 2006. Annual growth rings in a sample of *Hymenaea courbaril*. *IAWA Journal.* Vol. 27 (2): 193-197 <https://doi.org/10.1163/22941932-90000148>
- Wheeler, E.A., (2011). InsideWood - a web resource for hardwood anatomy. *IAWA Journal* 32 (2): 199-211. <https://doi.org/10.1163/22941932-90000051>

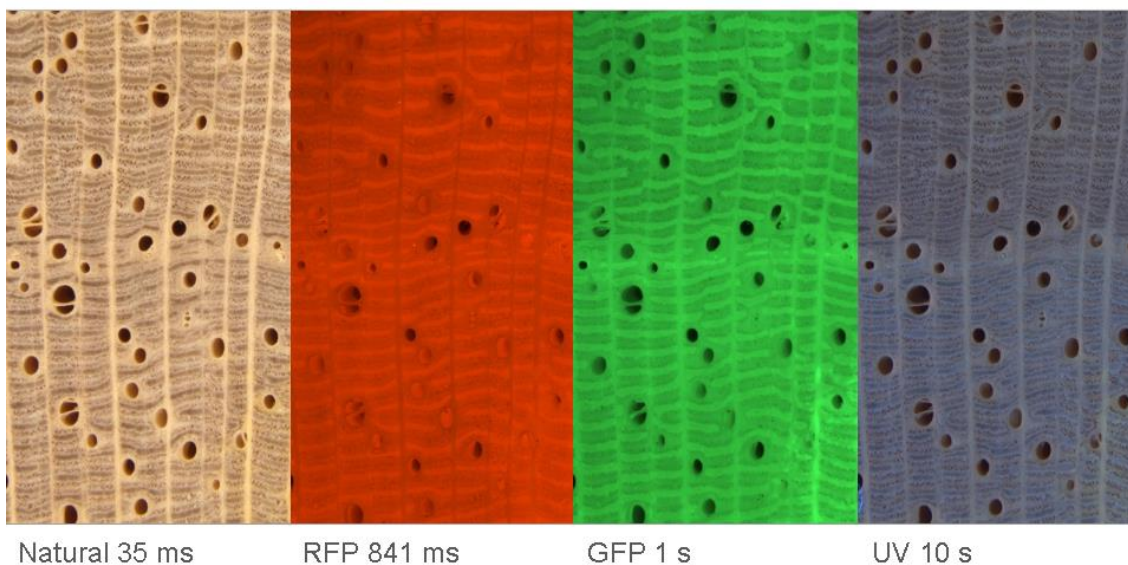
- Willians, J., León, H., 2008. Anatomía de madera en 31 especies de la subfamilia Mimosoideae (Leguminosae) en Venezuela. *Colomb. For.* 11, 113–135. ISSN 0120-0739
- Worbes, M., 2002. One hundred years of tree-ring research in the tropics-a brief history and an outlook to future challenges. *Dendrochronologia* 20, 217–231. <https://doi.org/10.1078/1125-7865-00018>
- Worbes, M., 1995. How to measure growth dynamics in tropical trees a review. *IAWA J.* 16, 337–351. <https://doi.org/10.1163/22941932-90001424>
- Worbes, M., 1989. Growth rings, increment and age of trees in inundation forests, savanna and a mountain forest in the neotropics. *IAWA Bull.* 10, 109–122. <https://doi.org/10.1163/22941932-90000479>
- Worbes, M., Fichtler, E., 2010. Wood anatomy and tree-ring structure and their importance for tropical dendrochronology. Springer, pp. 329–346. [https://doi.org/10.1007/978-90-481-8725-6\\_17](https://doi.org/10.1007/978-90-481-8725-6_17)
- Worbes, M., Staschel, R., Roloff, A., Junk, W., 2003. Tree ring analysis reveals age structure, dynamics and wood production of a natural forest stand in Cameroon. *For. Ecol. Manage.* 173, 105–123. [https://doi.org/10.1016/S0378-1127\(01\)00814-3](https://doi.org/10.1016/S0378-1127(01)00814-3)
- Xu, K., Wang, X., Liang, P., An, H., Sun, H., Han, W., Li, Q., 2017. Tree-ring widths are good proxies of annual variation in forest productivity in temperate forests. *Sci. Rep.* 7, 1–8. <https://doi.org/10.1038/s41598-017-02022-6>
- Zuidema, P.A., Baker, P.J., Groenendijk, P., Schippers, P., van der Sleen, P., Vlam, M., Sterck, F., 2013. Tropical forests and global change: filling knowledge gaps. *Trends Plant Sci.* 18, 413–419. <https://doi.org/10.1016/j.tplants.2013.05.006>



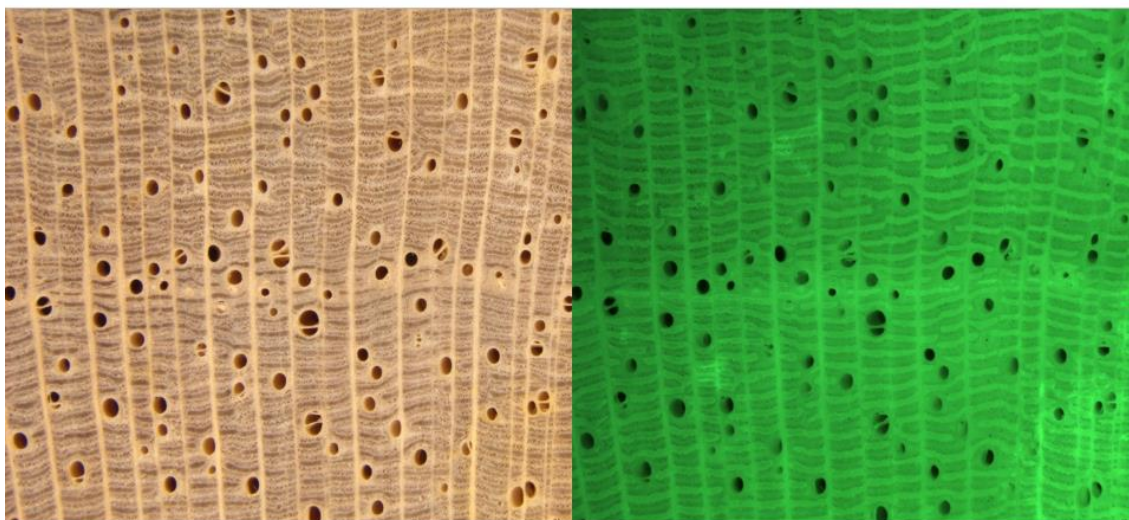
## Supplementary Material



**Figure S1** - Details of macroscopic features highlighted using different sets of fluorescence filters. Visualization under natural light is compared with GFP for *Podocarpus lambertii* and *Copaiifera langsdorffii*, and with RFP for *Peltogyne* sp. and *Ocotea porosa*. A-B: *Podocarpus lambertii* axial parenchyma are visualized as black dots (white arrowheads) and tracheid cell walls in light green; C-D: *Peltogyne* sp. presence of small vessels (inside brackets) in growth-ring boundary; E-F: *Copaiifera langsdorffii* secretory canals (white arrowheads) emits light green fluorescence, contrasting with the low fluorescent marginal parenchyma band. G-H: *Ocotea porosa* oil cells (white arrowheads) emits light red fluorescence contrasting with fibres and other parenchymatic cells. Scale bar: 0.2 mm.

*Erythrina speciosa*

**Figure S2** - Macroscopic view of *Erythrina speciosa* tree rings comparing different sets of fluorescence filters and their exposure time. Growth-ring visualization was compared under natural light, RFP, GFP and UV, respectively.

*Erythrina speciosa*

GFP: enhanced contrast between fibres and parenchyma; brighter fibres at tree-ring boundary

**Figure S3** - Example of *Erythrina speciosa* anatomical feature highlighted with the application of the technique.



*Brosimum rubescens*

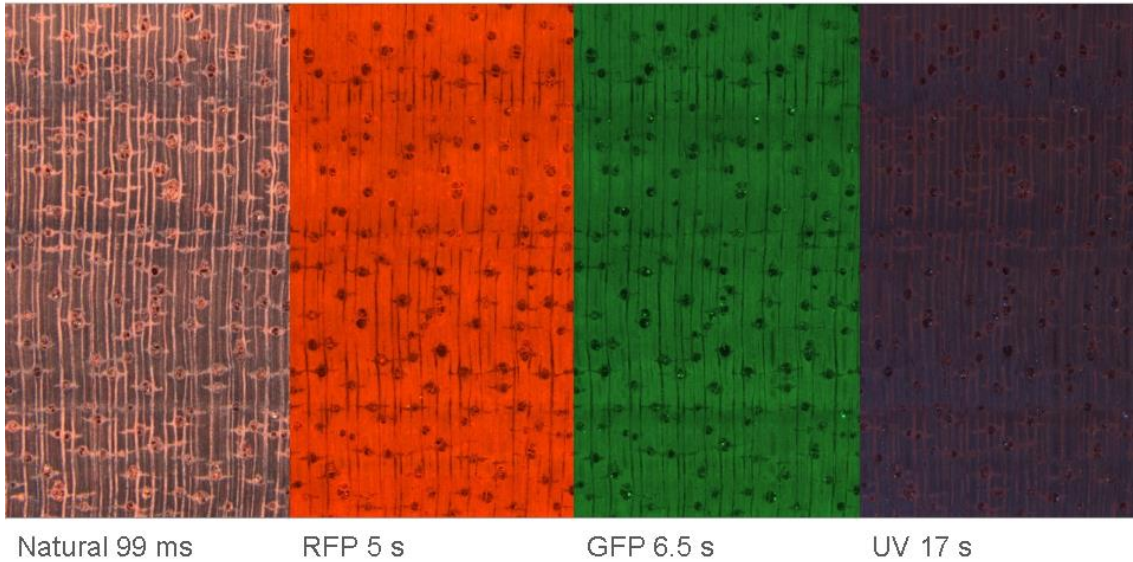
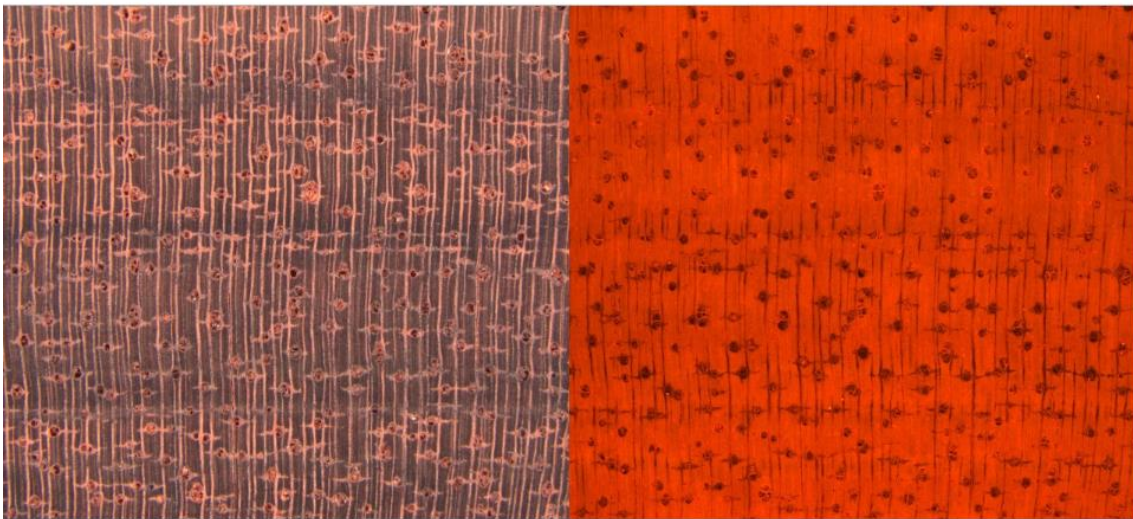


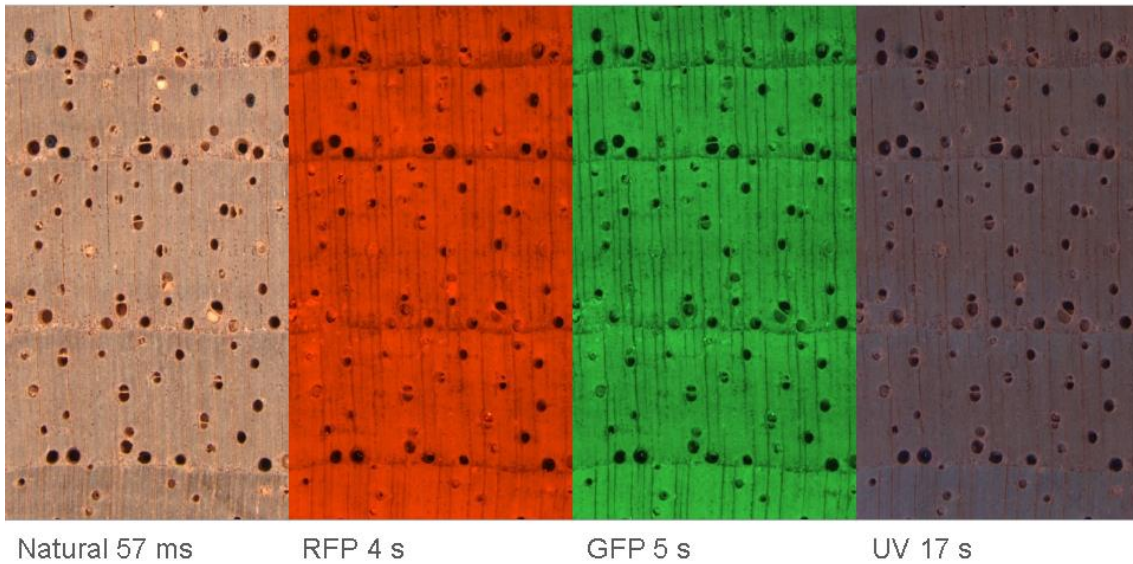
**Figure S4** - Macroscopic view of *Brosimum rubescens* tree rings comparing different sets of fluorescence filters and their exposure time. Growth-ring visualization was compared under natural light, RFP, GFP and UV, respectively.

*Brosimum rubescens*

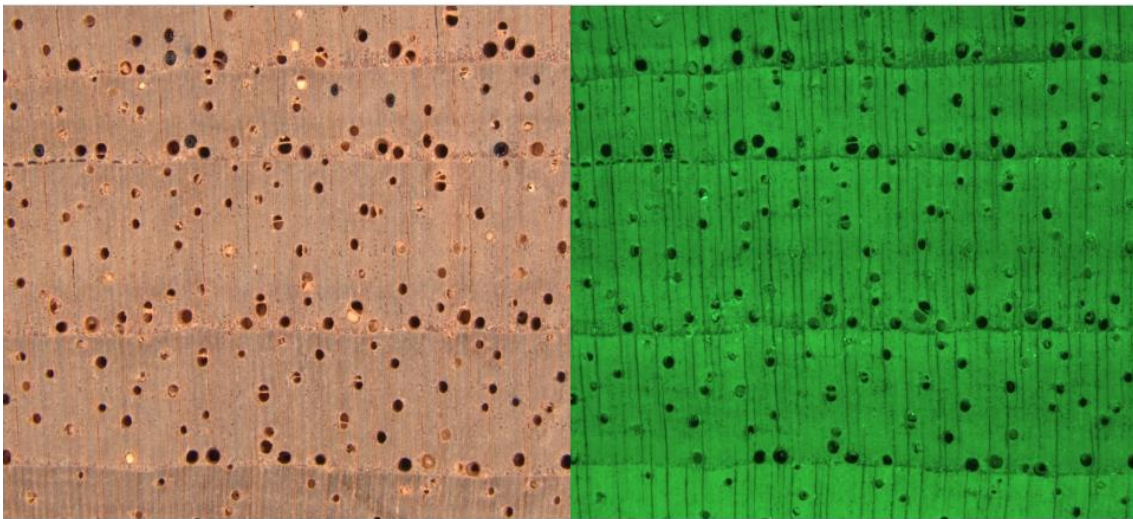


RFP higher contrast between vessels and background

**Figure S5** - Example of *Brosimum rubescens* anatomical feature highlighted with the application of the technique.

*Cedrela fissilis*

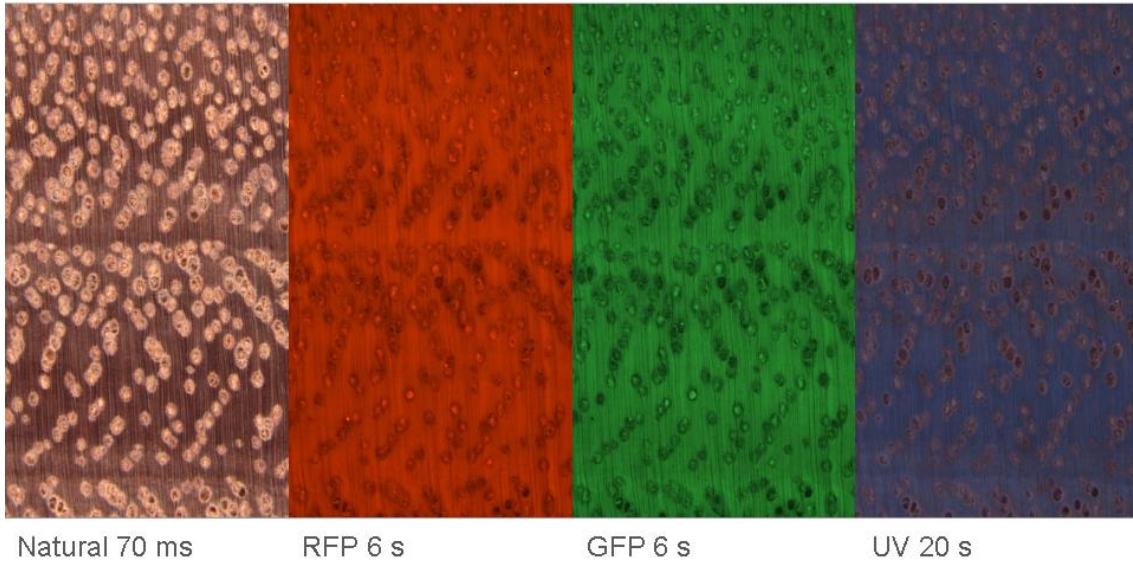
**Figure S6** - Macroscopic view of *Cedrela fissilis* tree rings comparing different sets of fluorescence filters and their exposure time. Growth-ring visualization was compared under natural light, RFP, GFP and UV, respectively.

*Cedrela fissilis*

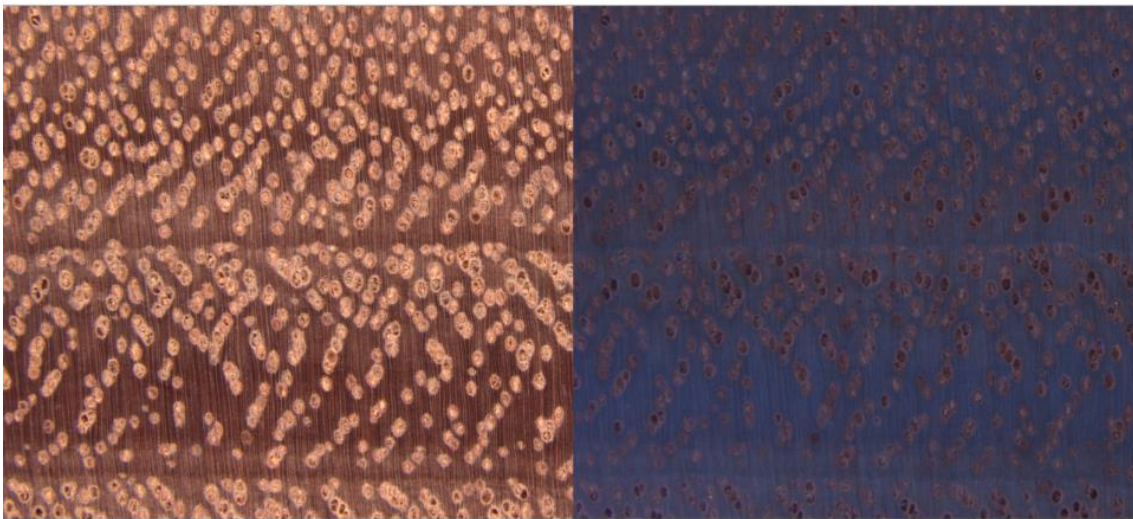
Easier to see boundary and semi porosity due to contrast amongst cells

**Figure S7** - Example of *Cedrela fissilis* anatomical feature highlighted with the application of the technique.



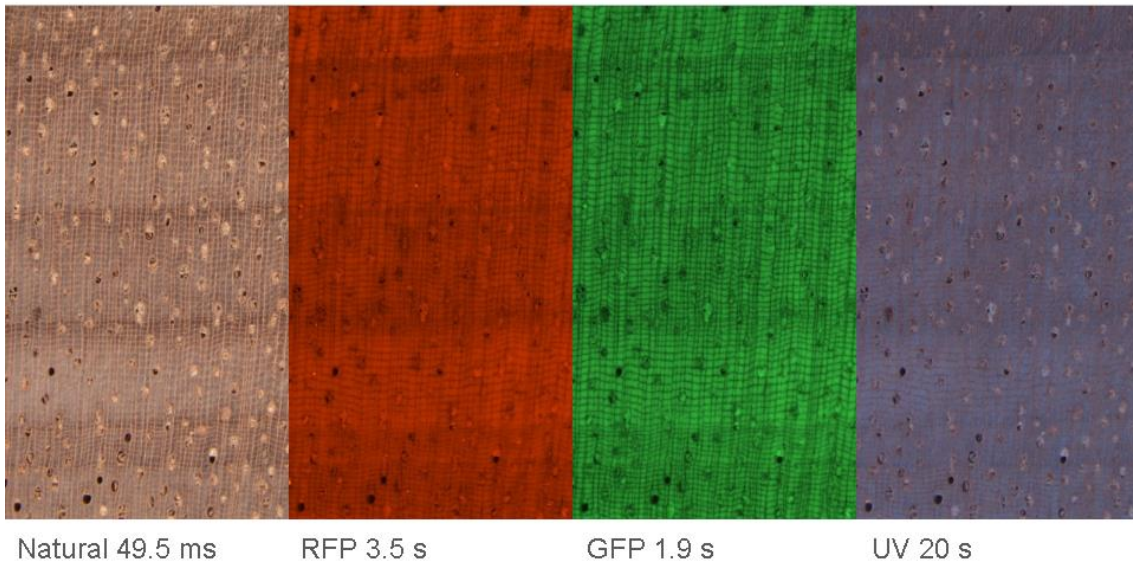
*Eucalyptus* sp.

**Figure S8** - Macroscopic view of *Eucalyptus* sp. tree rings comparing different sets of fluorescence filters and their exposure time. Growth-ring visualization was compared under natural light, RFP, GFP and UV, respectively.

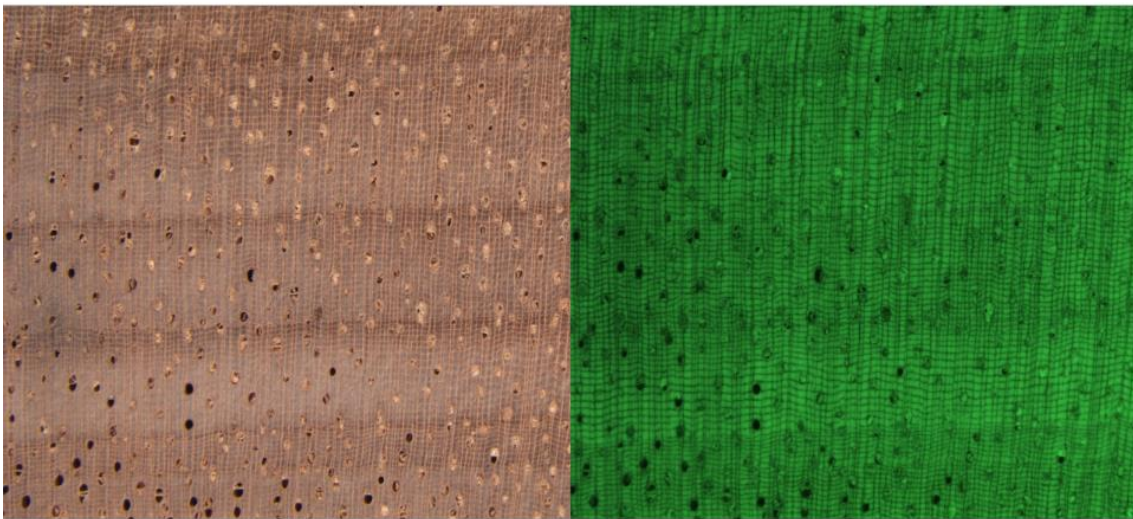
*Eucalyptus* sp.

Filters do not influence tree-ring visualisation

**Figure S9** - Example of *Eucalyptus* sp. anatomical feature highlighted with the application of the technique.

*Acacia polyphylla*

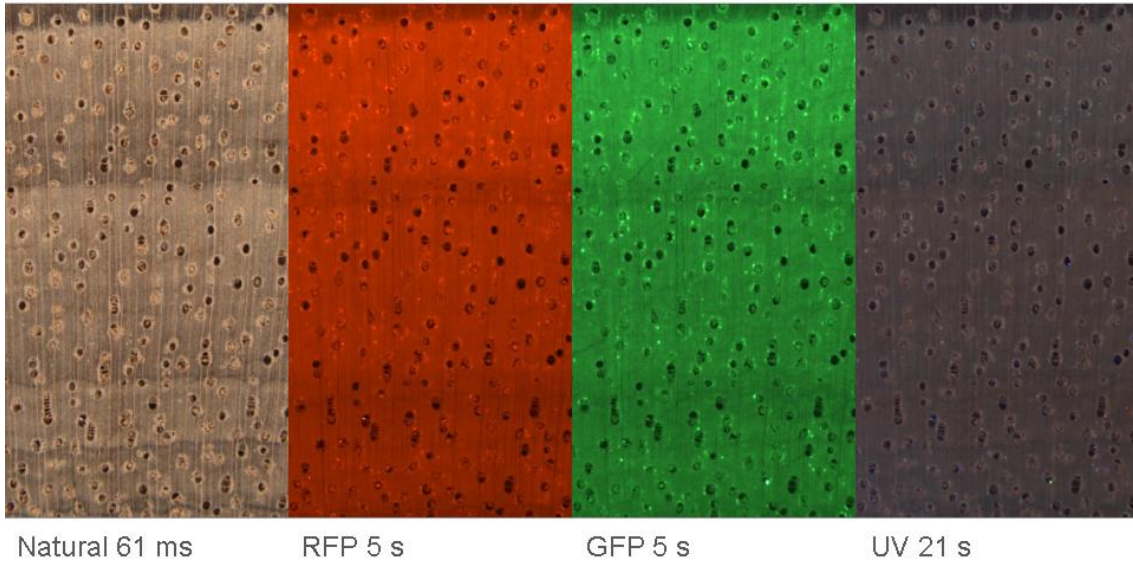
**Figure S10** - Macroscopic view of *Acacia polyphylla* tree rings comparing different sets of fluorescence filters and their exposure time. Growth-ring visualization was compared under natural light, RFP, GFP and UV, respectively.

*Acacia polyphylla*

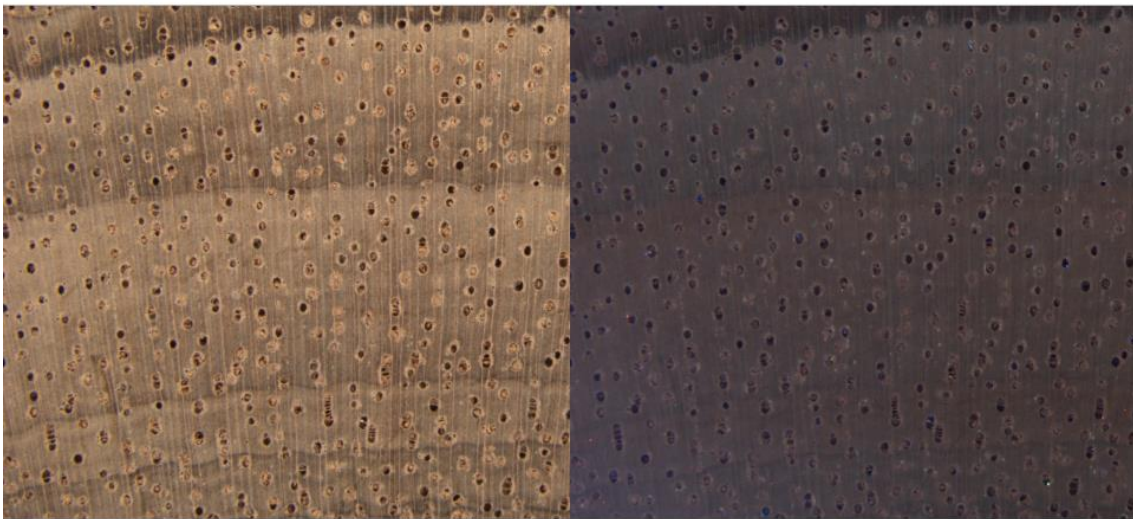
The use of filters do not add or disturb tree-ring visualization, but improves visualization of parenchyma bands in early wood.

**Figure S11** - Example of *Acacia polyphylla* anatomical feature highlighted with the application of the technique.



*Aniba canelilla*

**Figure S12** - Macroscopic view of *Aniba canelilla* tree rings comparing different sets of fluorescence filters and their exposure time. Growth-ring visualization was compared under natural light, RFP, GFP and UV, respectively.

*Aniba canelilla*

Filters make tree-ring boundary less clear

**Figure S13** - Example of *Aniba canelilla* anatomical feature highlighted with the application of the technique.

*Anadenanthera macrocarpa*

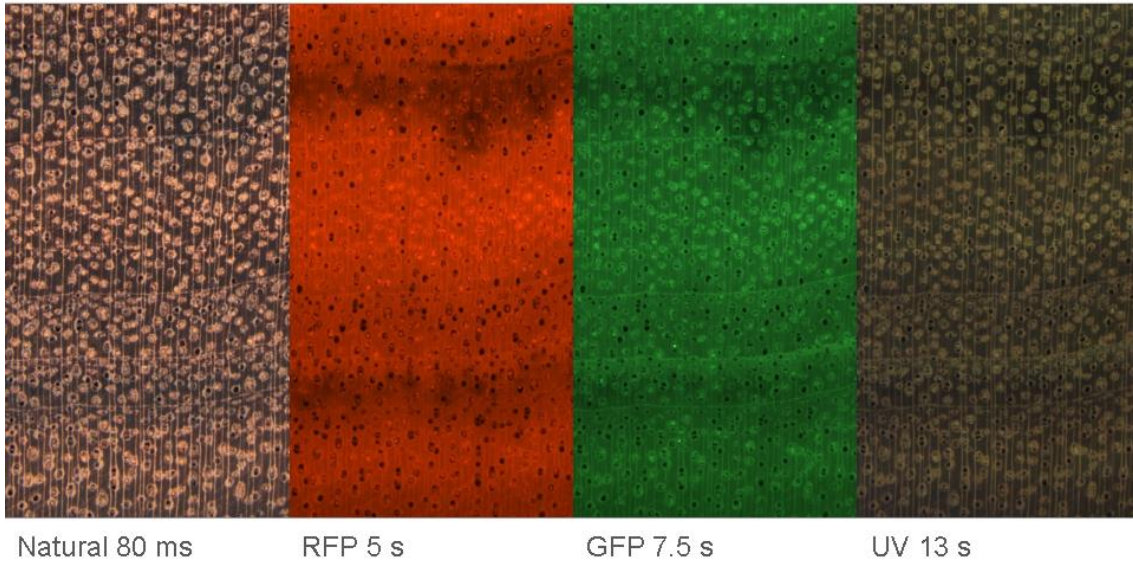
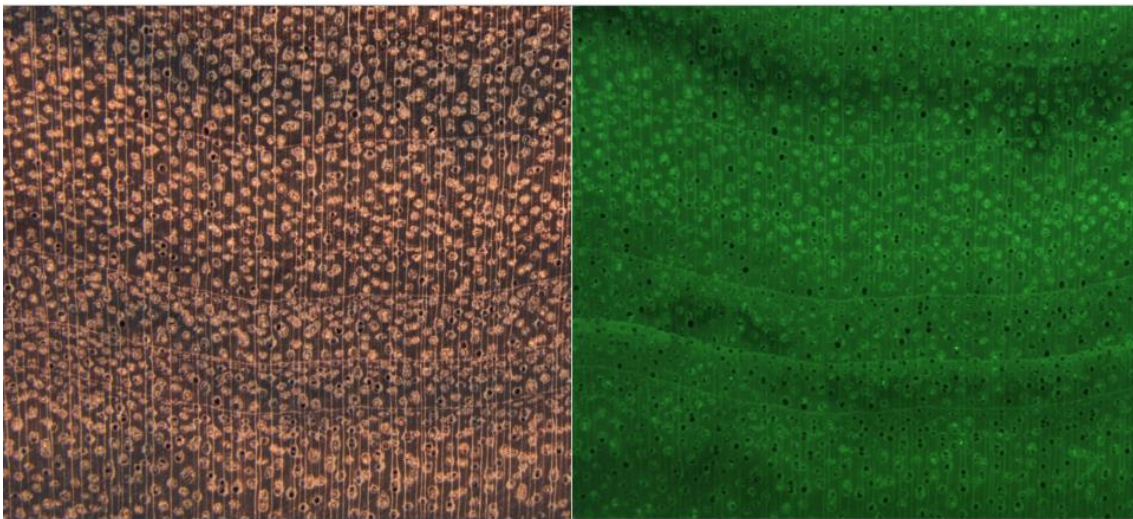


**Figure S14** - Macroscopic view of *Anadenanthera macrocarpa* tree rings comparing different sets of fluorescence filters and their exposure time. Growth-ring visualization was compared under natural light, RFP, GFP and UV, respectively.

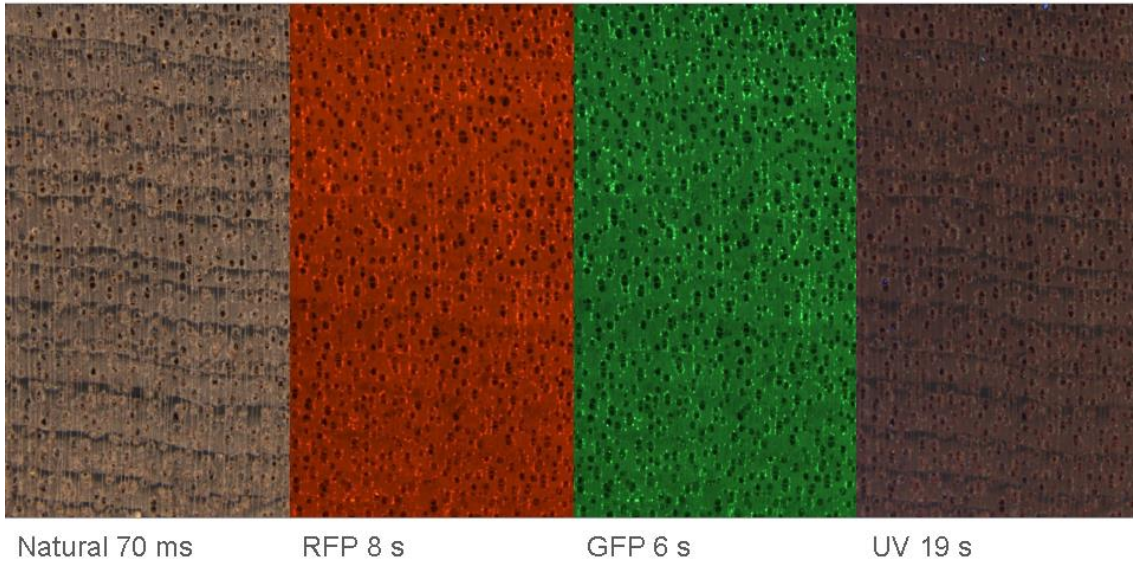
*Anadenanthera macrocarpa*



GFP cleared the boundary, enhanced the difference between paratracheal and parenchyma band

**Figure S15** - Example of *Anadenanthera macrocarpa* anatomical feature highlighted with the application of the technique.



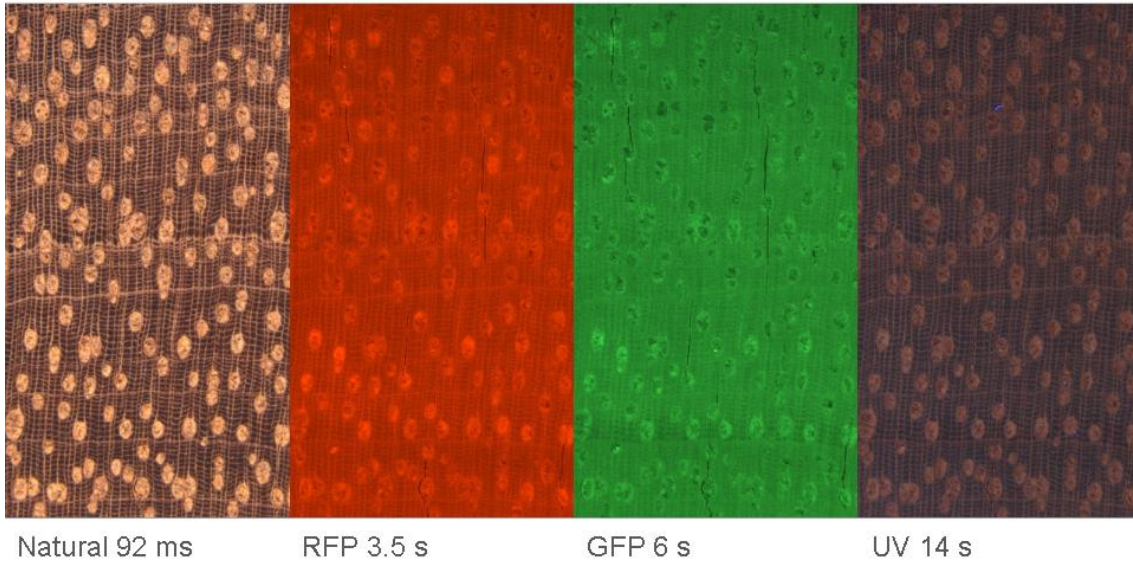
*Ocotea odorifera*

**Figure S16** - Macroscopic view of *Ocotea odorifera* tree rings comparing different sets of fluorescence filters and their exposure time. Growth-ring visualization was compared under natural light, RFP, GFP and UV, respectively.

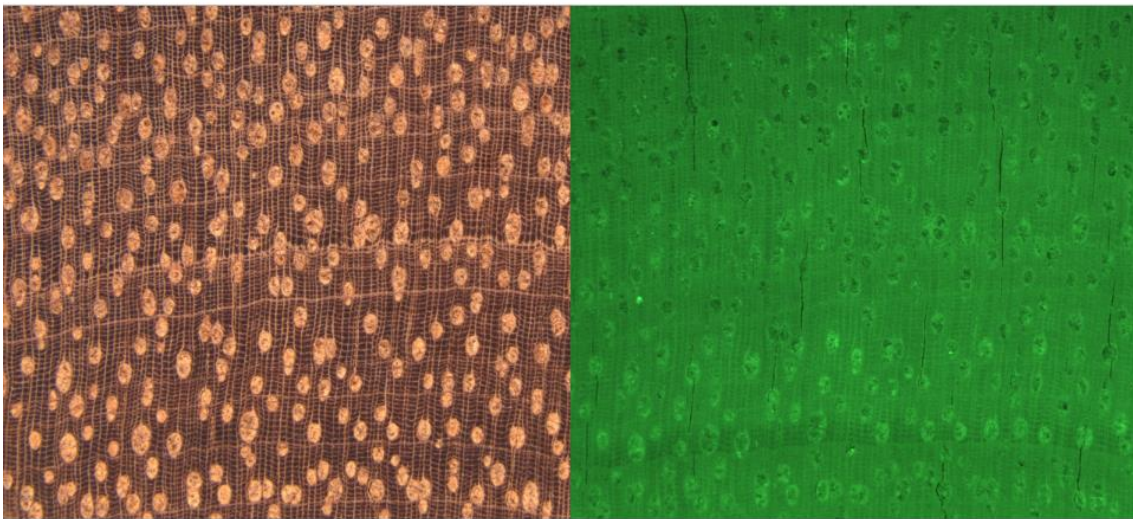
*Ocotea odorifera*

Tree-ring delimitation hampered, but other oil cells are highlighted

**Figure S17** - Example of *Ocotea odorifera* anatomical feature highlighted with the application of the technique.

*Lecythis paraensis*

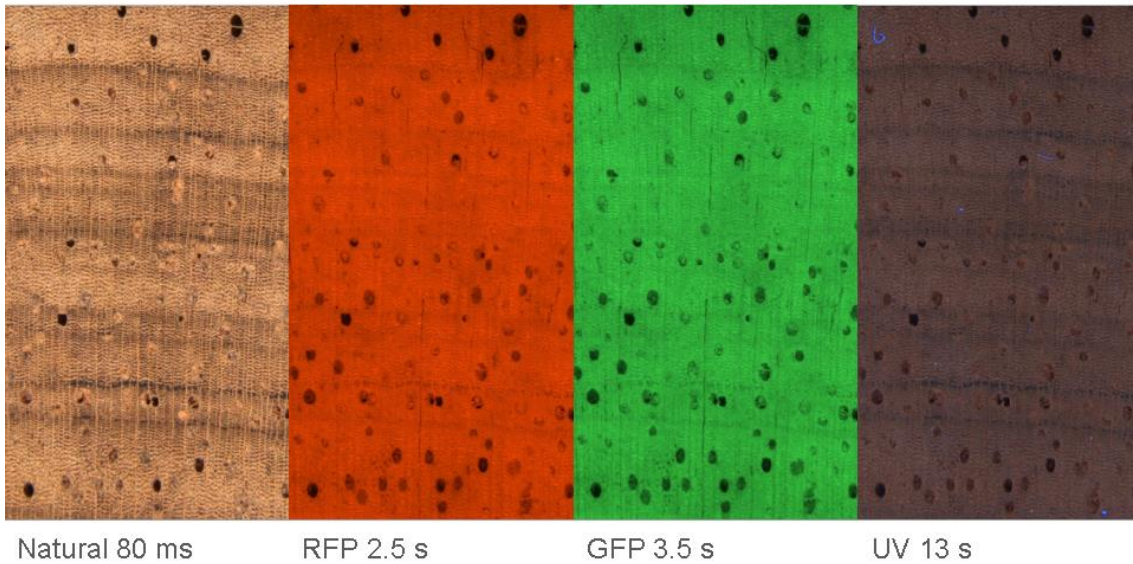
**Figure S18** - Macroscopic view of *Lecythis paraensis* tree rings comparing different sets of fluorescence filters and their exposure time. Growth-ring visualization was compared under natural light, RFP, GFP and UV, respectively.

*Lecythis paraensis*

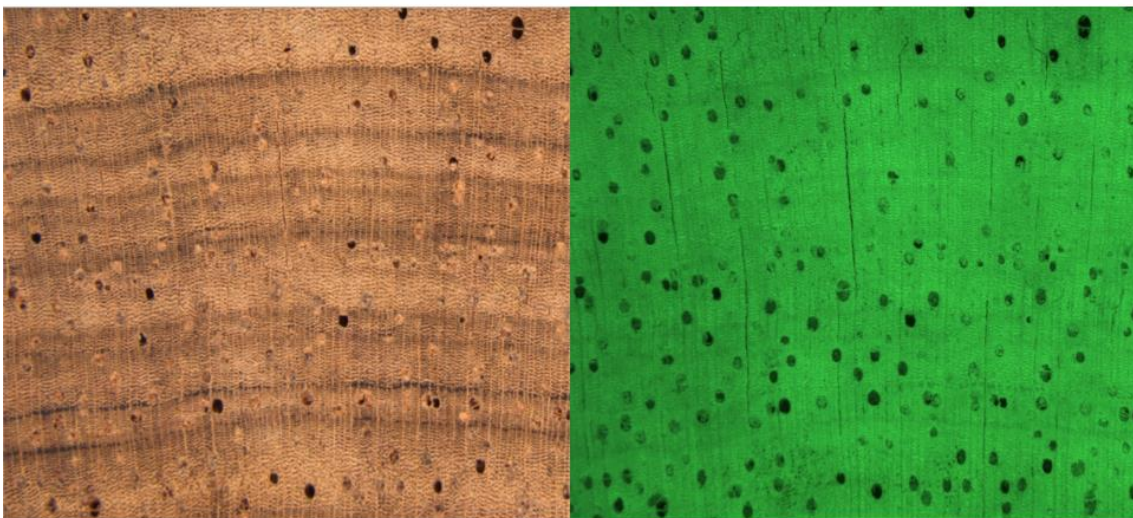
Filter make tree-ring boundary less clear

**Figure S19** - Example of *Lecythis paraensis* anatomical feature highlighted with the application of the technique.



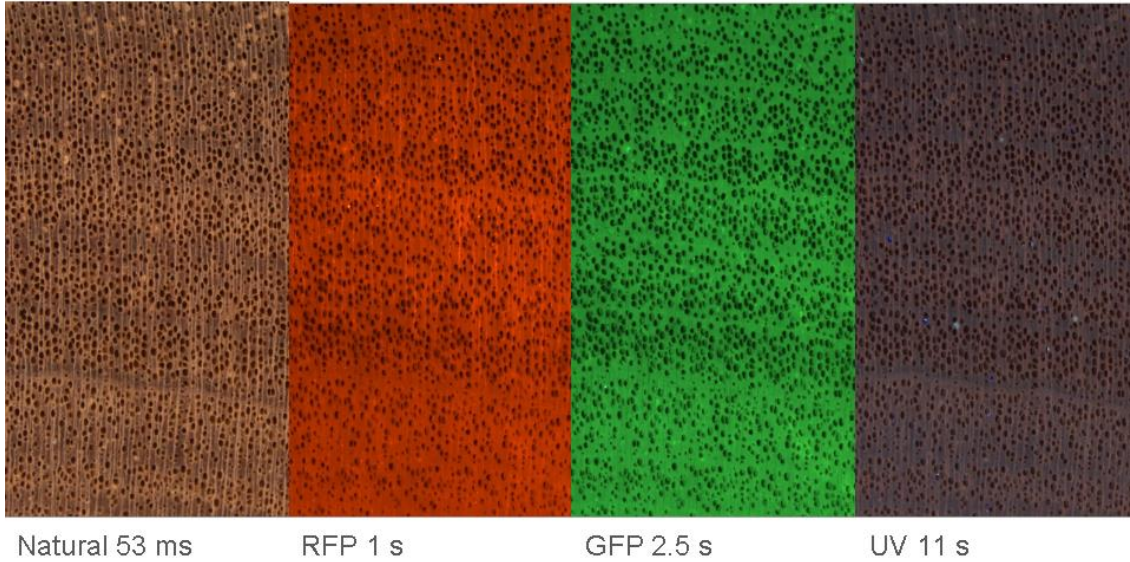
*Pseudobombax* sp.

**Figure S20** - Macroscopic view of *Pseudobombax* sp. tree rings comparing different sets of fluorescence filters and their exposure time. Growth-ring visualization was compared under natural light, RFP, GFP and UV, respectively.

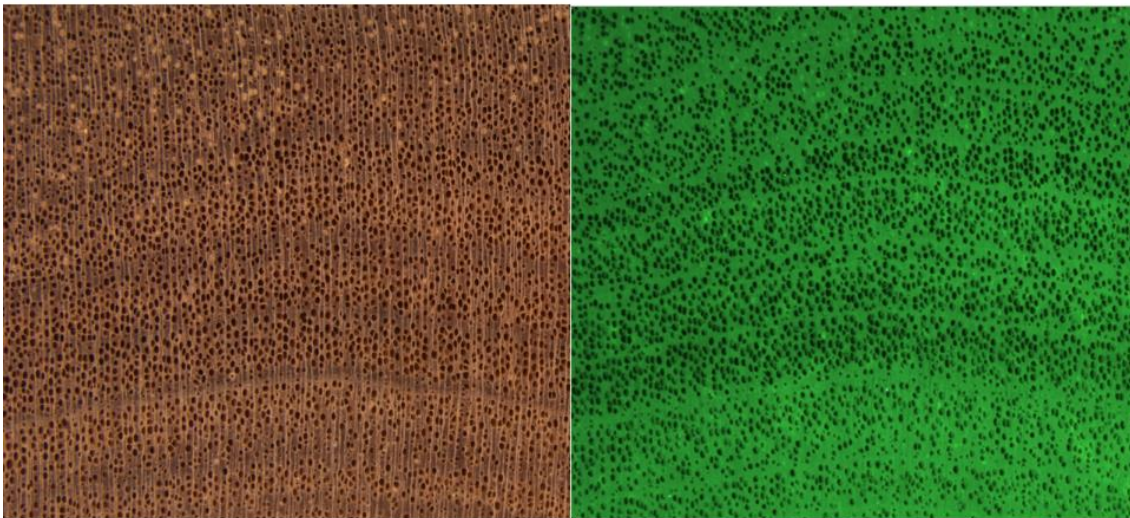
*Pseudobombax* sp.

**Figure S2** - Example of *Pseudobombax* sp. anatomical feature highlighted with the application of the technique.



*Aspidosperma pyriformium*

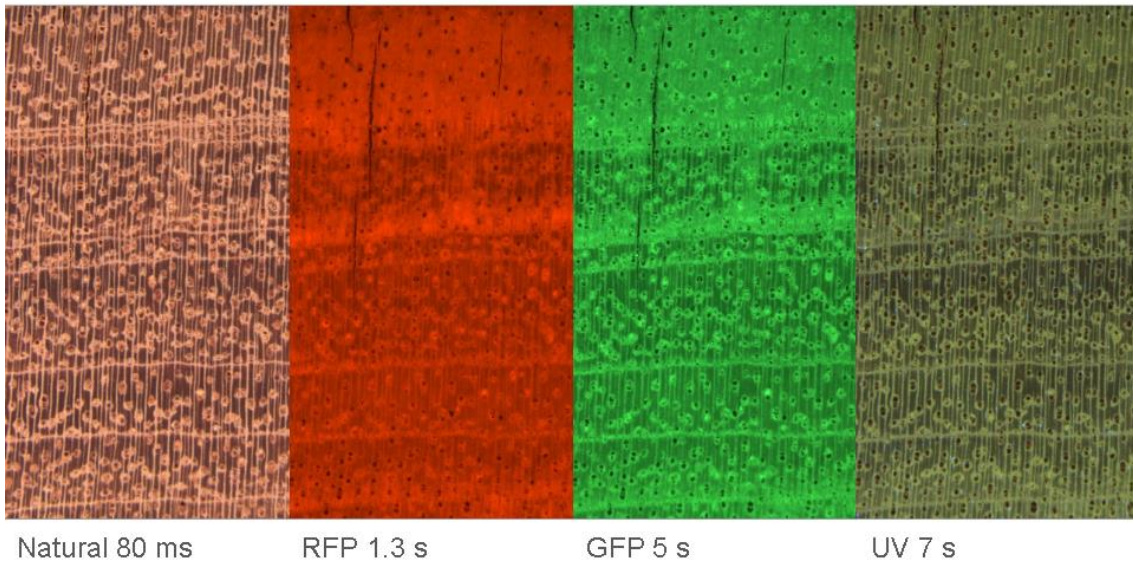
**Figure S22** - Macroscopic view of *Aspidosperma pyriformium*. tree rings comparing different sets of fluorescence filters and their exposure time. Growth-ring visualization was compared under natural light, RFP, GFP and UV, respectively.

*Aspidosperma pyriformium*

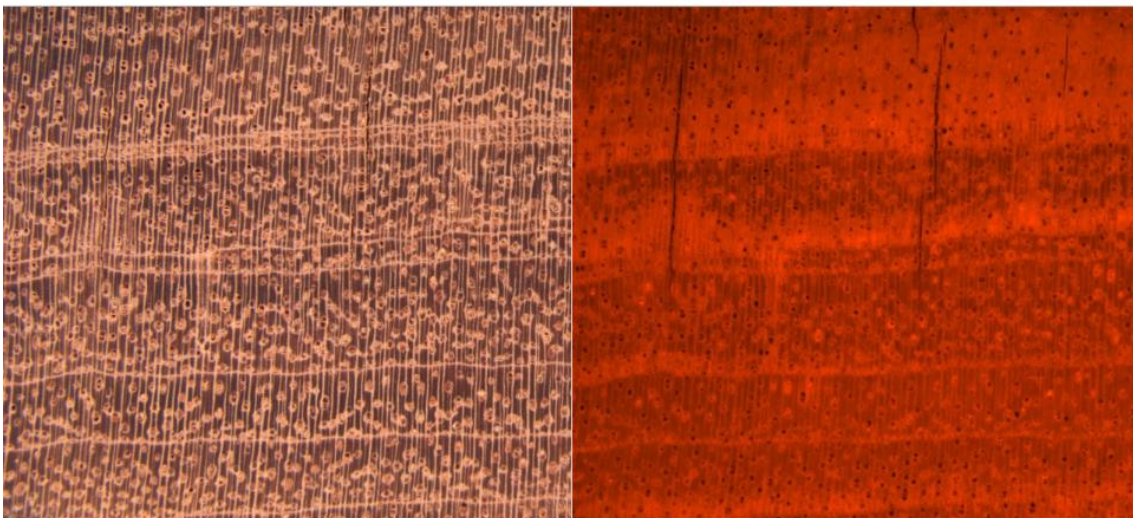
All filters improved tree-ring visualization with low exposure time

**Figure S23** - Example of *Aspidosperma pyriformium* anatomical feature highlighted with the application of the technique.



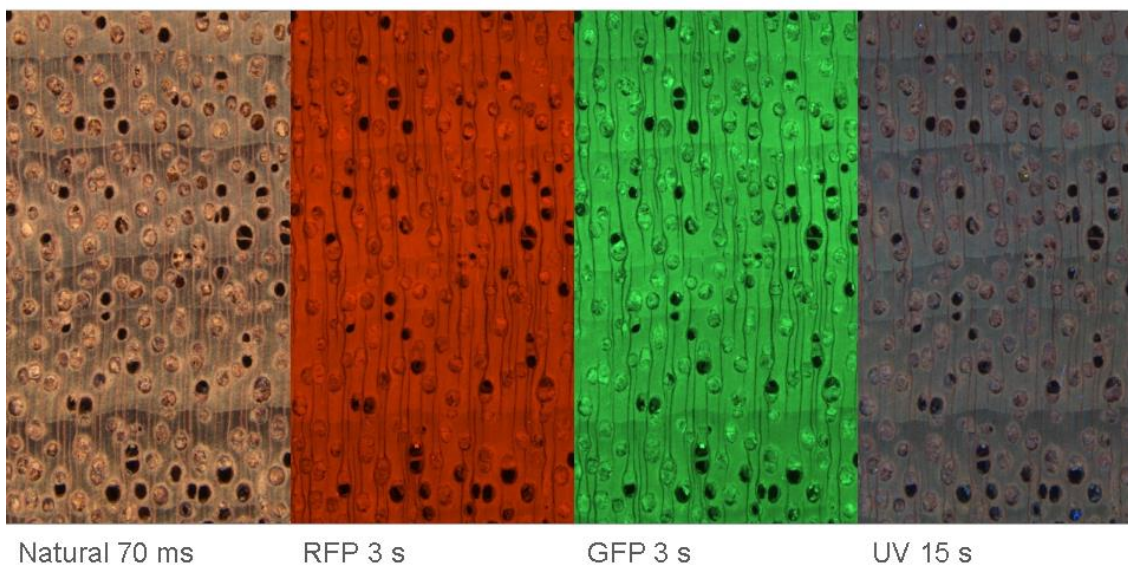
*Guibourtia* sp.

**Figure S24** - Macroscopic view of *Guibourtia* sp. tree rings comparing different sets of fluorescence filters and their exposure time. Growth-ring visualization was compared under natural light, RFP, GFP and UV, respectively.

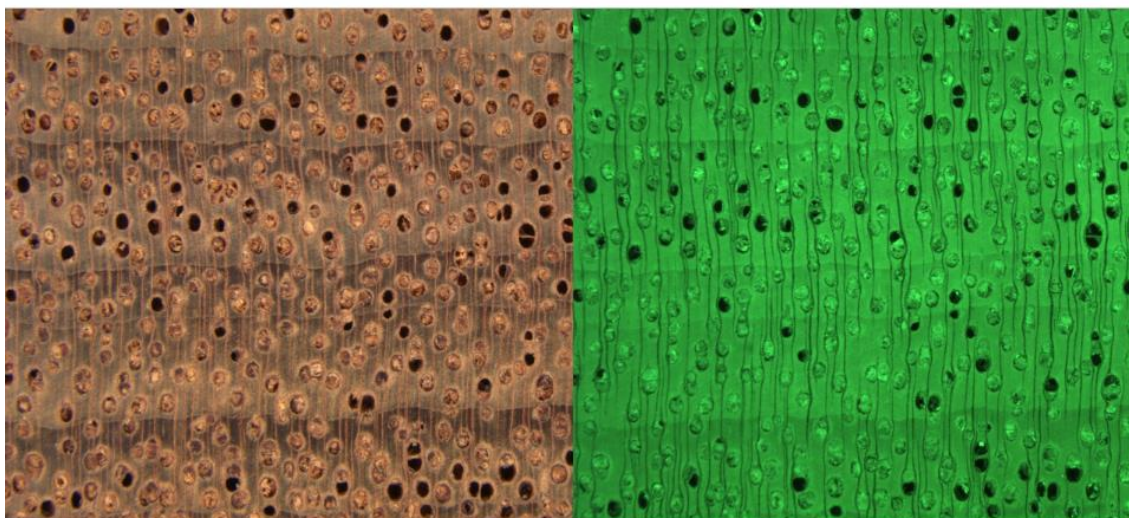
*Guibourtia* sp.

Filter make tree-ring boundary less clear

**Figure S25** - Example of *Guibourtia* sp. anatomical feature highlighted with the application of the technique.

*Plathymenia foliosa*

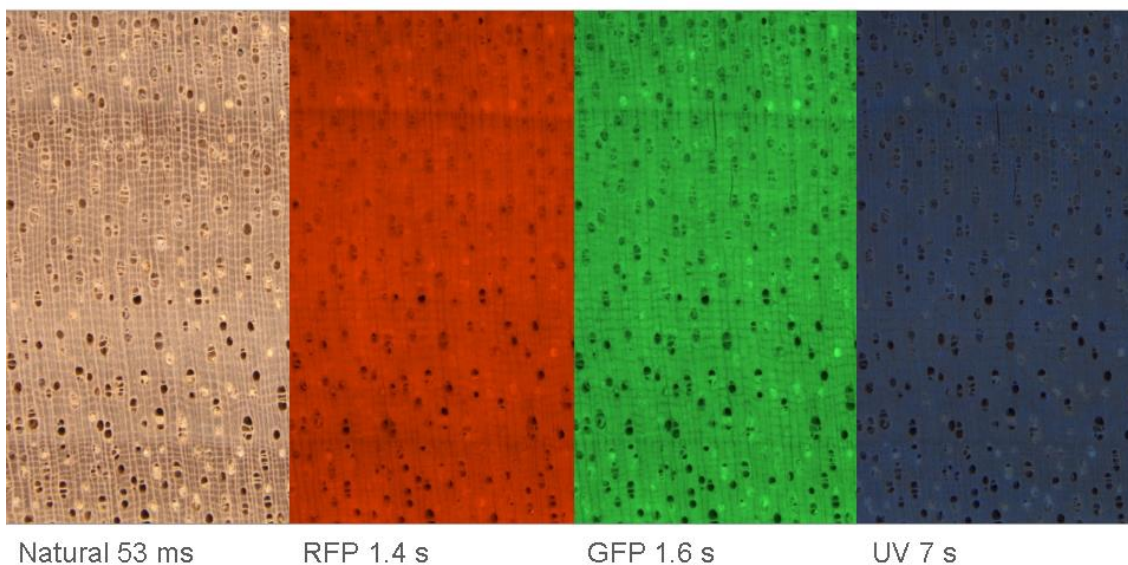
**Figure S26** - Macroscopic view of *Plathymenia foliosa* tree rings comparing different sets of fluorescence filters and their exposure time. Growth-ring visualization was compared under natural light, RFP, GFP and UV, respectively.

*Plathymenia foliosa*

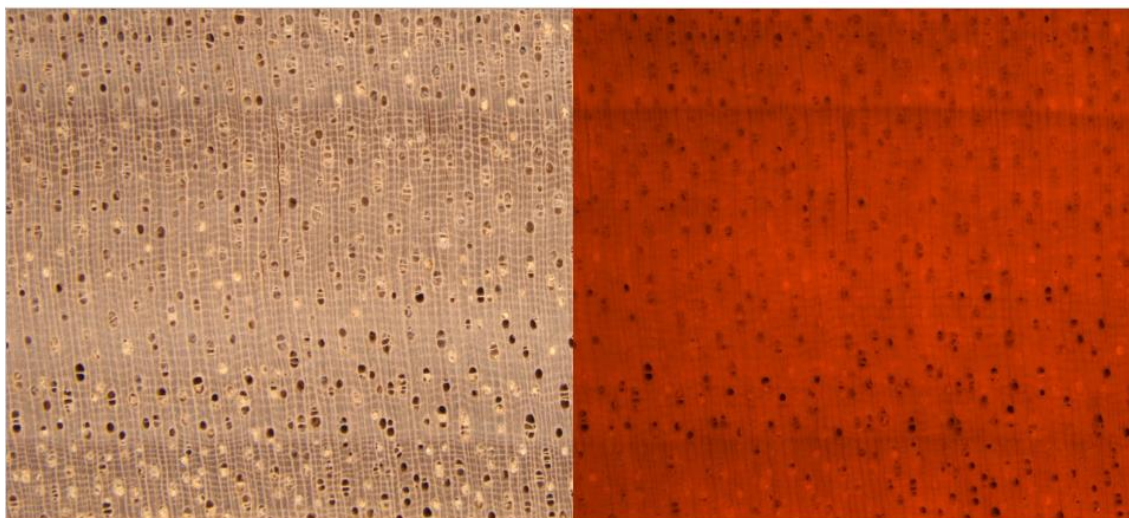
Filters do not influence tree-ring visualization

**Figure S27** - Example of *Plathymenia foliosa* anatomical feature highlighted with the application of the technique.



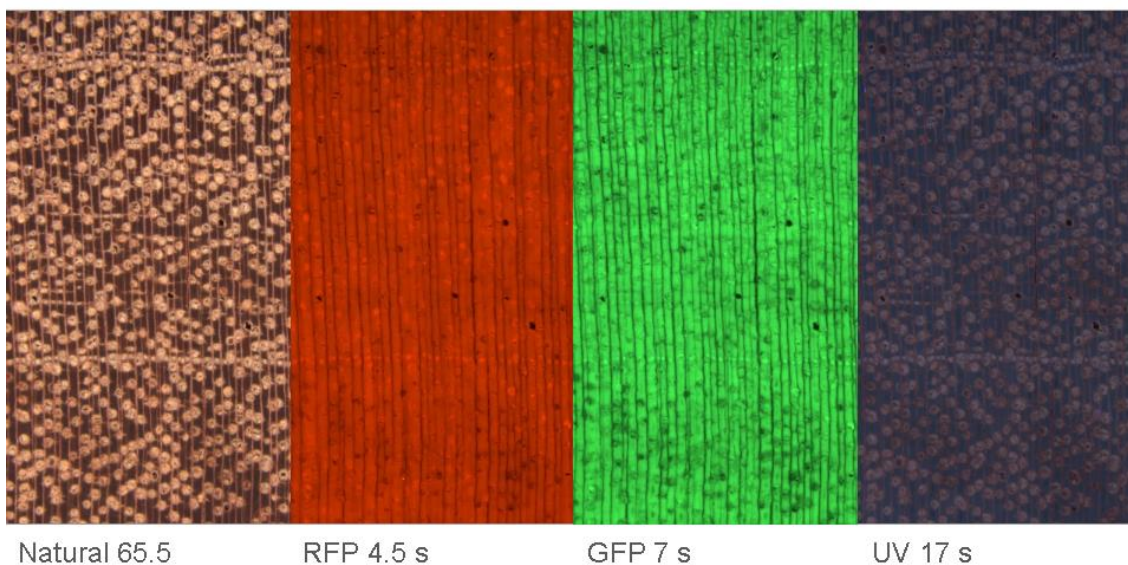
*Cariniana estrellensis*

**Figure S28** - Macroscopic view of *Cariniana estrellensis* tree rings comparing different sets of fluorescence filters and their exposure time. Growth-ring visualization was compared under natural light, RFP, GFP and UV, respectively.

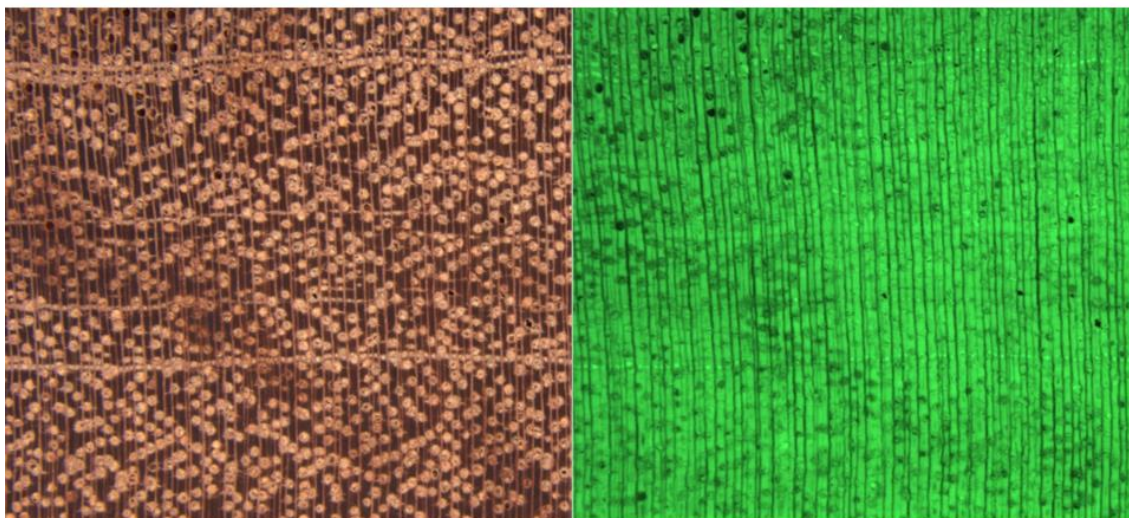
*Cariniana estrellensis*

Filters improve visualization of density variations and contrast between parenchyma and fibres

**Figure S29** - Example of *Cariniana estrellensis* anatomical feature highlighted with the application of the technique.

*Dryobalanops* sp.

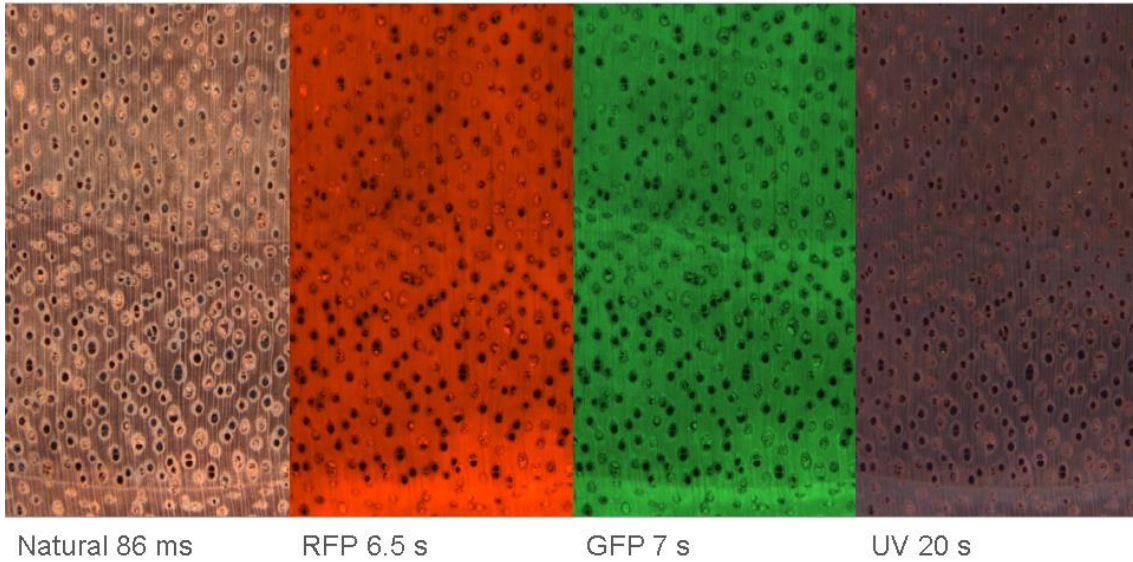
**Figure S30** - Macroscopic view of *Dryobalanops* sp. tree rings comparing different sets of fluorescence filters and their exposure time. Growth-ring visualization was compared under natural light, RFP, GFP and UV, respectively.

*Dryobalanops* sp.

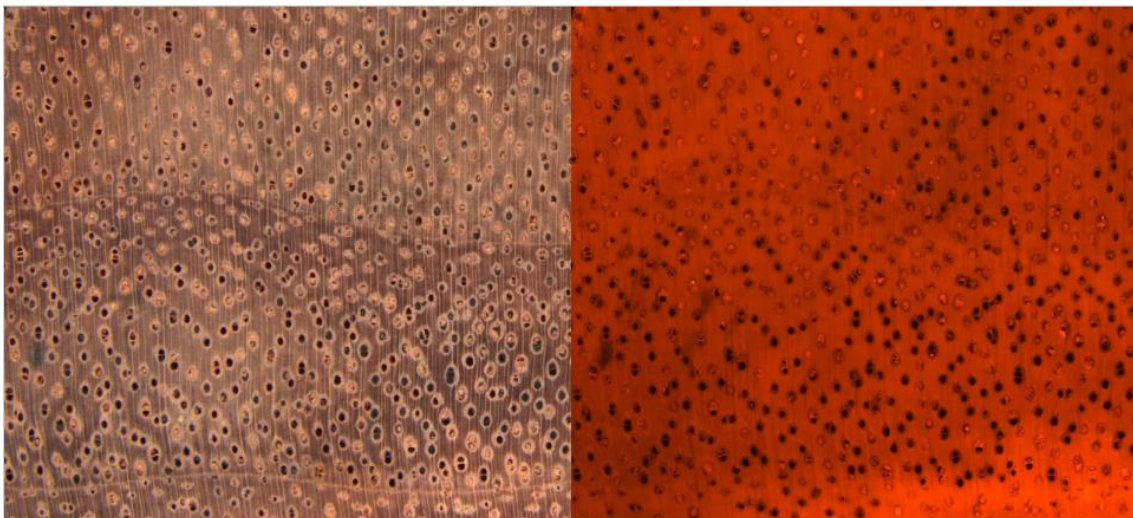
Filter removed the noise added by the axial parenchyma and highlighted the presence of two types of boundaries.

**Figure S31** - Example of *Dryobalanops* sp. anatomical feature highlighted with the application of the technique.



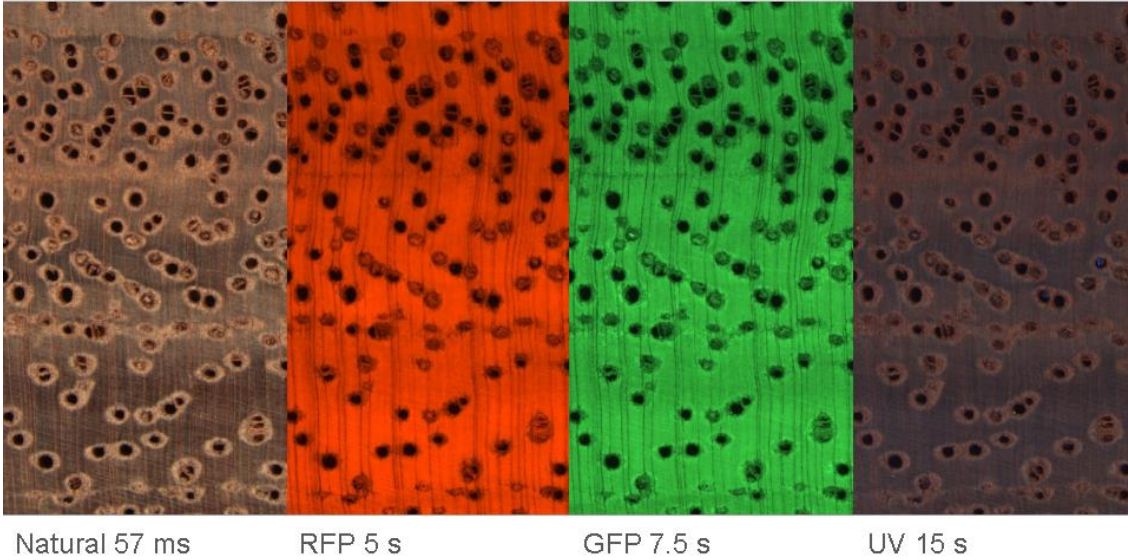
*Parapiptadenia rigida*

**Figure S32** - Macroscopic view of *Parapiptadenia rigida* tree rings comparing different sets of fluorescence filters and their exposure time. Growth-ring visualization was compared under natural light, RFP, GFP and UV, respectively.

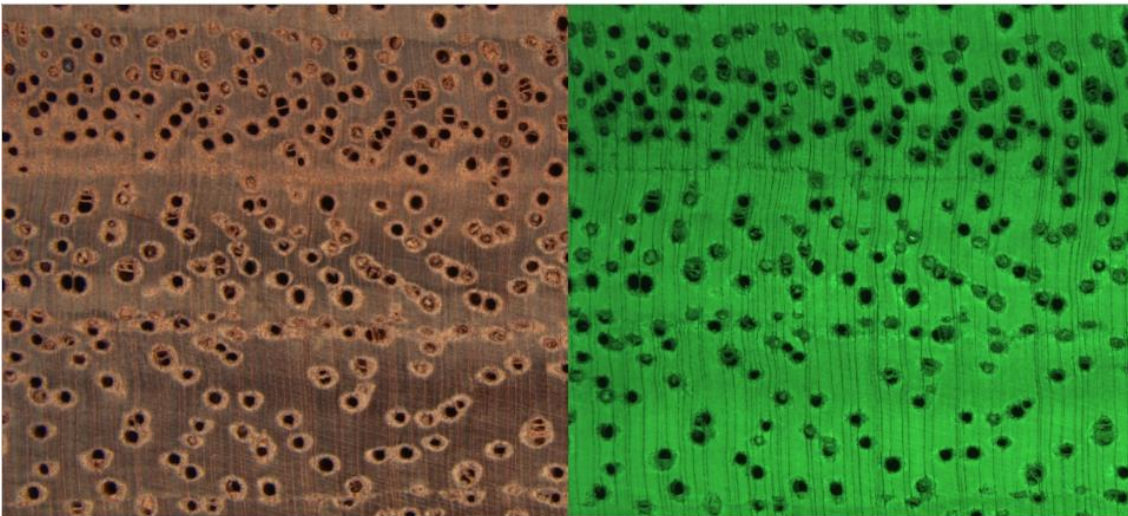
*Parapiptadenia rigida*

Filter make tree-ring boundaries less clear

**Figure S33** - Example of *Parapiptadenia rigida* anatomical feature highlighted with the application of the technique.

*Dimorphandra mollis*

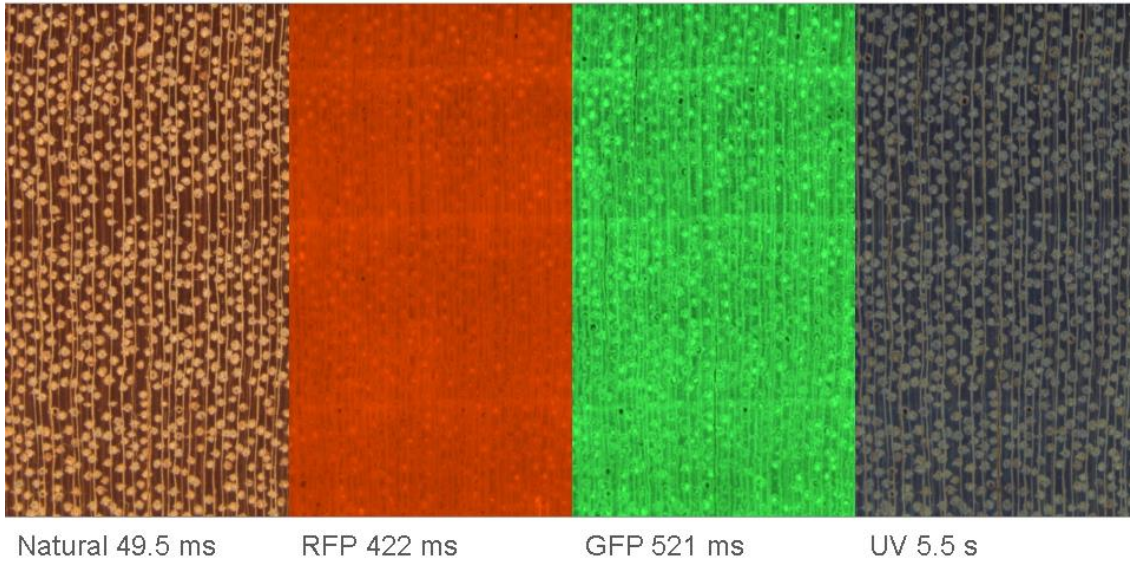
**Figure S34** - Macroscopic view of *Dimorphandra mollis* tree rings comparing different sets of fluorescence filters and their exposure time. Growth-ring visualization was compared under natural light, RFP, GFP and UV, respectively.

*Dimorphandra mollis*

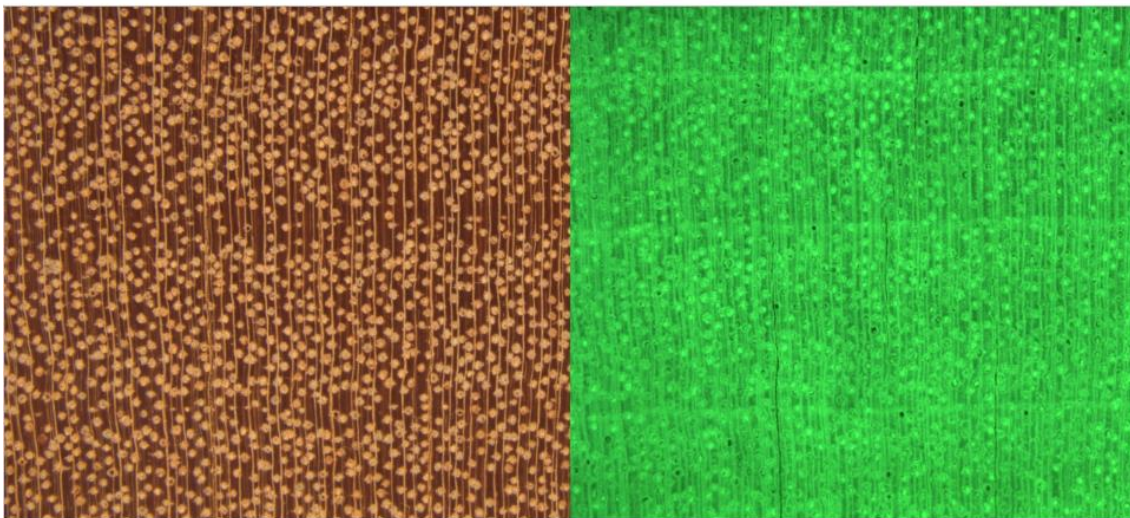
Filter removed the noise added by the axial parenchyma and highlighted the presence of two types of boundaries.

**Figure S35** - Example of *Dimorphandra mollis* anatomical feature highlighted with the application of the technique.



*Aspidosperma desmanthum*

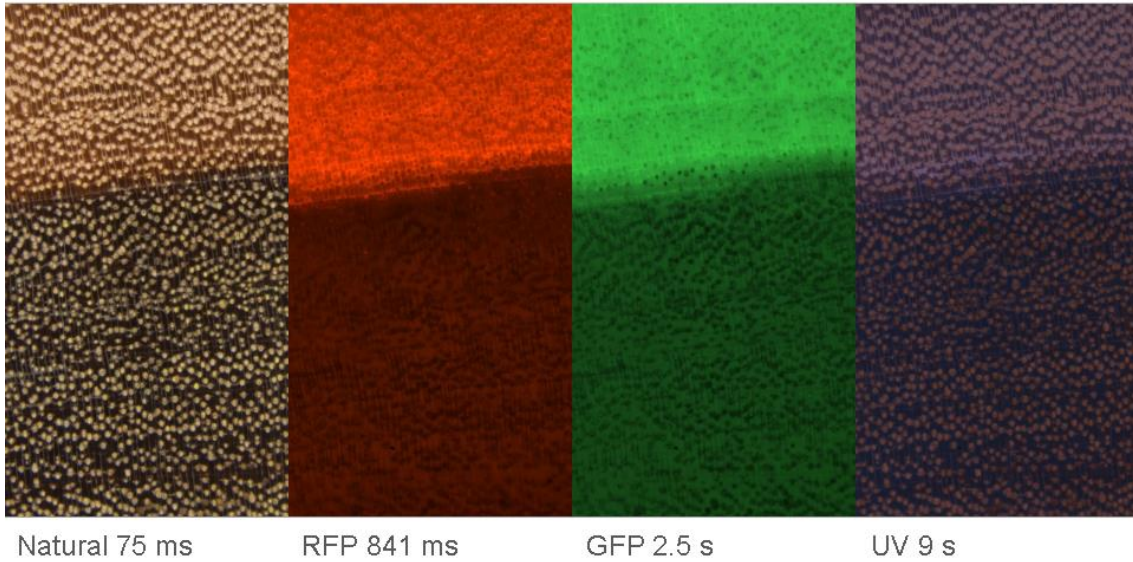
**Figure S36** - Macroscopic view of *Aspidosperma desmanthum* tree rings comparing different sets of fluorescence filters and their exposure time. Growth-ring visualization was compared under natural light, RFP, GFP and UV, respectively.

*Aspidosperma desmanthum*

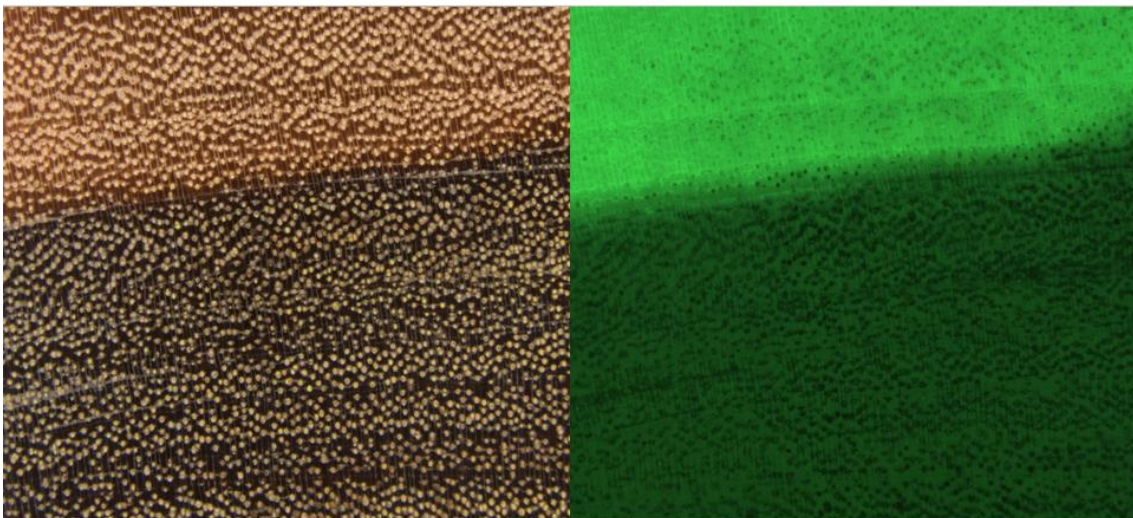
All filters improved tree-ring visualization with low exposure time

**Figure S37** - Example of *Aspidosperma desmanthum* anatomical feature highlighted with the application of the technique.



*Handroanthus* sp.

**Figure S38** - Macroscopic view of *Handroanthus* sp. tree rings comparing different sets of fluorescence filters and their exposure time. Growth-ring visualization was compared under natural light, RFP, GFP and UV, respectively.

*Handroanthus* sp.

Parenchyma bands are clearer among vessels and paratracheal parenchyma

**Figure S39** - Example of *Handroanthus* sp. anatomical feature highlighted with the application of the technique.



## Capítulo 2

---

*The value of climate responses of individual trees to detect  
areas of climate-change refugia, a tree-ring study in the Brazilian  
Seasonally Dry Tropical forests*

O valor das respostas individuais de árvores para detectar  
áreas de refúgio climático, um estudo dendrocronológicos  
em mata tropical sazonalmente seca brasileira

Milena de Godoy-Veiga, Bruno Barçante Ladvocat Cintra, Nicolas Misailidis Stríkis,  
Francisco William Cruz, Carlos Henrique Grohman, Matheus Simões Santos, Lior  
Regev, Elisabetta Boaretto, Gregório Ceccantini, Giuliano Maselli Locosselli

## Abstract

Forests worldwide are facing increasingly frequent climate extremes due to global warming. Its negative effects on tropical forests have been extensively reported by both permanent plots and tree-ring studies that targeted forest's responses to climate. While this has been done mostly at community and population levels, the effects of landscape heterogeneity on trees' sensitivity to climate is often not accounted for, overlooking the diverse responses of individual trees to climate variation. We tested the hypotheses that trees may differ in sensitivity to climate and that some microenvironmental conditions may exert the role of climate-change refugia. We built the first tree-ring chronology of *Amburana cearensis* trees sampled across a Seasonally Dry Tropical Forest (SDTF) in Brazil. We ensure a robust tree-ring dating using dendrochronological methods and  $^{14}\text{C}$  dating of trees inhabiting various conditions characterized here through the seasonality of the local Normalized Difference Vegetation Index. At the population level, the standard tree-ring chronology suggests that tree growth depends on rainfall and temperature, leading to a common conclusion that drier and warmer conditions would impact interannual tree growth in the tropics. However, the cluster analyses revealed groups of individual trees with distinct growth sensitivities to climate. The most sensitive trees were the individuals located in the highly seasonal vegetation of the epikarst, in contrast to the complacent (non-sensitive to regular interannual climate variability) trees, which inhabited the less-seasonal vegetation in the deep soil epikarst and valley. Using the groups of trees revealed by the cluster, we built two mean chronologies and assessed their climate-growth relationships. Similar to the patterns observed in the individual analysis, the growth of complacent trees showed no association with wet season precipitation and only moderate association with temperature. The areas supporting these complacent trees of *A. cearensis* in the less seasonal vegetation correspond to a quarter of the entire sampling area. The climate buffering capacity of these refugia may only be compromised in years of climate extremes when all sampled trees share low growth rates during years with anomalous low rainfall and high temperature. Assessing individual's climate sensitivity is therefore

paramount for a comprehensive understanding of the heterogeneous responses of tropical forests to climate change. The hidden individual tree responses in the population can help identify priority areas of management in a rapidly changing environment.

**Keywords:** Climate change, dendrochronology, karst, microenvironment, radiocarbon ( $^{14}\text{C}$ ), tropics.

### **Resumo**

Florestas de todo o mundo estão experienciando cada vez mais extremos climáticos devido ao aquecimento global. Os impactos negativos em florestas tropicais foram extensamente reportados tanto em estudos em parcelas permanentes quanto por anéis de crescimento que investigavam a resposta de florestas ao clima. Enquanto isso foi investigado a nível de comunidades e populações, os efeitos de uma paisagem complexa na sensibilidade de árvores ao clima normalmente não são considerados, negligenciando a diversidade de resposta individuais ao nível individual. Nós testamos a hipótese de que árvores podem ter diferentes sensibilidades ao clima e de que condições microambientais específicas podem exercer o papel de refúgios as mudanças climáticas. Para isso construímos a primeira cronologia de *Amburana cearensis* em uma floresta sazonalmente seca no Brasil. Nós garantimos uma datação robusta usando métodos dendrocronológicos e datação por radiocarbono ( $^{14}\text{C}$ ) de árvores crescendo em diversas condições caracterizadas pelo Índice Normalizado de Diferença de Vegetação (NDVI). A nível populacional, a cronologia de anéis de crescimento sugere que o crescimento das árvores depende da quantidade de chuva e temperatura, o que leva a comum conclusão de que condições quentes e secas podem impactar o crescimento interanual de árvores nos trópicos. Entretanto, análises de agrupamento revelaram diferentes grupos de árvores cuja sensibilidade do crescimento ao clima é diferente. Os indivíduos mais sensíveis eram os localizados nas áreas com maior sazonalidade da

vegetação no epicarste, contrastando com as árvores complacentes (não sensitivas a variabilidade interanual regular), que habitam as áreas menos sazonais da paisagem cárstica, como os vales e regiões com solo mais profundo. Usando os grupos de árvores revelados pela análise cluster, foram construídas duas cronologias e sua relação entre clima e crescimento foi investigada. De forma similar aos padrões observados nas análises individuais, o crescimento das árvores complacentes não mostrou associação com a precipitação nos meses de crescimento e fraca correlação com temperatura. As áreas que abrigam essas árvores complacentes de *A. cearensis* na porção de floresta menos sazonal correspondem a um quarto de toda a área investigada. A capacidade de buffer desses refúgios é comprometida apenas em anos de eventos climáticos extremos, no qual todas as árvores coletadas compartilham a mesma resposta de baixa taxa de crescimento quando expostas a pouca chuva e altas temperaturas. Investigar as respostas individuais é, portanto, essencial para um melhor entendimento da heterogeneidade das respostas de florestas tropicais as mudanças climáticas. Essas respostas individuais ocultas dentro da população podem ajudar a identificar áreas prioritárias de manejo e conservação nas condições atuais de mudanças climáticas.

**Palavras-chave:** Mudanças climáticas, dendrocronologia, cárste, microambiente, radiocarbono ( $^{14}\text{C}$ ), trópicos.



## 1. Introduction

Trees are widely threatened in many ecosystems around the world due to the numerous consequences of climate change (Allen *et al.*, 2010; IPCC, 2018). Harsher climate conditions have been reported worldwide putting large areas of forest ecosystems at risk (Allen *et al.*, 2010; Ault 2020; Brienen *et al.*, 2010). There is growing evidence from forest plots and tree-ring studies that global warming is changing the dynamics of forests by affecting tree growth (DeSoto *et al.*, 2020) and mortality rates (Aleixo *et al.*, 2019; Brienen *et al.*, 2015). However, most analyses at the population or community levels underestimate how forest structure and dynamics are influenced by diverse interactions of individual trees within the forest assembly (Albert *et al.*, 2010; Levine *et al.*, 2016; Paine *et al.*, 2011). For example, individual responses to climate fluctuations vary with microenvironmental conditions (Stillman *et al.*, 2015), which often create forest enclaves that shelter individual trees of given species from the regional effects of global warming (Carrol *et al.*, 2017). These forest enclaves can become climate-change refugia that act as “slow lanes” to changes in climate condition, supporting the growth of individuals that do not fully develop in the surrounding landscape (Morelli et al 2020). Knowledge on the individual responses to climate variability, especially in these enclaves of climate-change refugia, is crucial for understanding future carbon assimilation in tropical forests and planning effective conservation management actions (Morelli *et al.*, 2020; Trouillier *et al.*, 2018; Zuidema *et al.*, 2013).

Tropical forests are naturally heterogeneous in terms of microenvironmental conditions (Chen *et al.*, 1999, Townsend *et al.*, 2008, Uriarte *et al.*, 2017) pointing to a possible diversity in tree responses to climate variability. This is especially the case of Seasonally Dry Tropical Forests (SDTF) due to the combination of seasonal climate and complex landscape. In this case, the SDTF is a particular one, that occurs in a transitional area of two Brazilian Biomes (the typical SDTF, named ‘*Caatinga*’ and the Brazilian savanna, the ‘*Cerrado*’), but locally conditioned by the limestone bedrock and derived karstic formation. Diverse landscape features with variations in i.e. altitude, soil depth, presence of ravines, rock outcrops (Locosselli *et al.*, 2016) and watercourses, to name a few (Coelho *et al.*, 2013; Pennington *et al.*, 2006), can sustain consistently different vegetation

structures and functions (Murphy & Lugo 1986) and might create climate-change refugia (Morelli *et al.*, 2020). In these forest enclaves, the negative effects imposed by adverse climate conditions on key physiological mechanisms are less intense and frequent when compared to the surrounding landscape (Locosselli *et al.*, 2016, McLaughlin *et al.*, 2017). The heterogeneity of microenvironmental conditions from tropical forest formations is likely maximized in the SDTF turning it into a reliable model for exploring the range of climate responses of growth in the individuals of a population.

Tree's responses to climate in SDTF, as in any other forests of the world, can be accurately assessed using tree-ring analyses (Douglas 1941, Fritts, 1966). Tree rings are known to be reliable records of trees' growth response to climate variability across different climate regimes, including the tropics (e.g. Schöngart *et al.*, 2017; Brienen *et al.*, 2016; Worbes, 2002). As a standard defined early on by tree-ring studies (Douglas 1941, Fritts 1966), the focus of most dendrochronological investigations relies on the mean population growth patterns (Carrer, 2011; Zuidema *et al.*, 2013) from the most sensitive trees to climate variability, avoiding conditions where the growth of trees may be complacent and not subject to climate variability (Fritts, 1966; Stahle 1999). Such strategies employed for building a robust tree-ring chronology may deliberately remove key information about the growth signal of individual trees. The diversity in the growth responses of individual trees is inherent to tree populations and may be related to competition (Trouillier *et al.*, 2018), genetics (Mori *et al.*, 2020), site provenance (Akhmetzyanov *et al.*, 2020), and climate sensitivity (Galván *et al.*, 2014). However, it is unclear to what extent trees with complacent growth represent a significant share of the population, and if these trees growing in supposedly more favorable conditions may still be subject to more extreme climate events in tropical regions. Such knowledge on individual trees is considered paramount to assess the possible responses of vegetation dynamics to climate change (Zuidema *et al.*, 2013).

As key information is likely being missed from an ecological perspective in studies focusing only on the population response, we propose the evaluation of the individual climate sensitivity to better predict future changes in forests dynamics. The individual tree responses could also help to reveal enclaves of climate change refugia which can be used

to guide effective management practices in a changing climate. Here we assessed the presence of possible enclaves of climate-change refugia in an SDTF by evaluating the climate sensitivity of individual trees using tree rings. We tested the following hypothesis: I) trees' responses to climate variability differ at population and individual levels, II) groups of trees may be more or less sensitive to climate according to the microenvironmental conditions, III) enclaves of climate-refugia in the SDTF may buffer trees' responses to regular interannual climate variability as well as to extreme climate conditions. Our findings show that there are different climate responses at the individual tree level that cannot be revealed from simple population analyses. Moreover, our results show a significant variability of climate responses at individual level, evidencing the presence of potential enclaves of climate-change refugia in the less-seasonal microenvironments found in the SDTFs.

## 2. Material and methods

### 2.1. Species and study site

We sampled trees of *Amburana cearensis* (Allemão) A.C. Sm., a deciduous tree species, partly light-demanding, widely distributed and commonly found in the driest forests of South America (Figure S1). Trees of *A. cearensis* can reach up to 25m in height and 110cm of diameter at breast height (DBH) with straight and cylindrical trunks (Leite, 2005; López, 1987, Lorenzi, 2008). It produces distinct annual tree rings with great potential for recording interannual climate variation (Baker *et al.*, 2015; Brienen & Zuidema, 2006; López & Villalba, 2016; López *et al.*, 2012, 2013; Paredes-Villanueva *et al.*, 2015). The tree rings of *A. cearensis* are characterized by the presence of small vessels surrounded by half-flattened aliform axial parenchyma, sometimes associated with a fibrous zone without vessels (Figure S2). Marginal parenchyma bands may be present in the oldest individuals with relatively lower growth rates.

*Amburana cearensis* is usually found in calcareous and limestone-rich soil, common to karstic areas (Leite, 2005). We sampled trees in a SDTF located in the largest karstic area in Central-Eastern Brazil (Auler & Farrant, 1996), at the Cavernas do Peruaçu National Park in Northwestern Minas Gerais State (14°54' and 15°15'S / 44°03' and

44°22'W). The area is at the São Francisco craton, formed by Proterozoic Bambuí limestone rocks and crossed by the lesser course of the Peruaçu river (MMA 2002) a perennial left-bank tributary of the Rio São Francisco. The climate in this region is tropical savanna-like with dry winters (Aw) according to the Köppen system (Peel *et al.*, 2007). The mean total annual precipitation is 930 mm with rainfall distributed during the year as a typical monsoon system (Zhou and Lau, 1998) (Figure S3). Out of the total annual rainfall, 90% falls in the spring and summer months (ONDJF) and it is almost absent (less than 50 mm per month) during winter (JJA) (Vera *et al.*, 2006).

The local precipitation and temperature time-series used in this study were calculated based on the mean monthly values from local meteorological stations from Agência Nacional de Águas (ANA) and Instituto Nacional de Meteorologia (INMET) (Figure S4). The meteorological stations compiled cover an area of nearly 1.5° X 1.5°, centered over the Cavernas do Peruaçu National Park (Figure S5). The list of meteorological station used in this study is shown in (Table S1).

## **2.2. Tree sampling**

We sampled trees within a gradient of microenvironmental conditions (Chen *et al.*, 1999), from the highest areas of epikarst to the valley (Figure S6 and S7). The karstic landscape is highly complex (Figure S7) and thus with different microenvironmental conditions that harbor diverse vegetation (Rodet *et al.*, 2015), ranging from xerophytic to flood-adapted species (a detailed list of species is found at Lombardi *et al.*, 2005). The epikarst is covered by dry forests, an open formation with short trees (between 15 and 25 meters tall), associated with limestone rocks not connected to the water table (Coelho & Sánchez-Azofeifa, 2013; Prous & Rodet, 2009). Soil depth in the epikarst varies through the sampling site, with shallow soil close to the ravines and rocky outcrops while the karstic pavements have a deeper soil layer. The valley includes, but it is not restricted to, the riparian forest from the Peruaçu river. It has deeper soil than the epikarst and support a dense and tall vegetation, with canopy height ranging between 20 and 25m mostly composed by evergreen and brevi-deciduous species (Prous & Rodet, 2009). Besides, there

is a near 200-meter difference in altitude between the valley and the epikarst (Coelho *et al.*, 2013).

We sampled trees with various diameters at breast height, ranging from 10cm to 70cm, to have a better representation of the tree population (Speer 2010). We obtained two to four cores from each individual tree using manual increment borers or a special borer coupled to a motor drill (Krottenthaler *et al.*, 2015). After sampling, we applied a solution of copper sulfate and calcium carbonate in the sampling hole and closed it with natural cork to avoid bacterial or fungal infection and to prevent insect attacks. Information about the geographical location, diameter at breast height (DBH), and tree height were recorded in the field. All wood samples were included in the Xylarium Nanuza Luiza de Menezes (SPFw, for further information refer to <http://splink.cria.org.br/>) and herbarium reproductive vouchers were stored in the herbarium SPF. Increment cores were fixed on wood supports and left to dry for a couple of weeks. After air-drying, we sanded the samples using sandpaper with different grits (80 to 400) to obtain a clean cross-section for proper tree-ring observation. All radii were scanned at 2400dpi resolution (EPSON Expression 12000XL) for measuring the tree-ring width in WinDendro™ (Regents Instruments Inc., Canada). We used a modified version of the protocol proposed by Hietz (2011) to estimate the age of trees from cores that missed the pith or central trunk area.

### ***2.3. Chronology construction and confirmation of tree ring annual formation***

In this study, we combined three different methods to check tree-ring annual formation of *Amburana cearensis*: i) cross-dating and the establishment of a robust chronology (section 2.3.1.); ii) inter and intra-annual radiocarbon dating of the years relative to the bomb-peak (section 2.3.2.); iii) correlation analysis with climatic variables (section 2.3.3.).

#### ***2.3.1. Cross-dating and chronology establishment***

The cross-dating is the process of matching tree-ring width patterns among trees (Douglass, 1941). This procedure aids the identification of false and locally absent tree rings that are corrected before the final chronology is built (Speer, 2010). We attributed the calendar year according to the year in which tree rings started to be produced (Schulman,

*et al.*, 1956). First, we conducted a visual cross-dating in WinDendro<sup>TM</sup> (Regents Instruments Inc., Canada). For that, all the radii of a tree were visualized simultaneously, allowing identification of false and missing rings. During this stage, we identified possible pointer years, or years characterized by low growth rates, that were used to cross-date different trees. We then used the software COFECHA (Holmes, 1983) for checking the dating quality.

The signal extraction and index calculation were performed using the Dendrochronology Program Library - dplR (Bunn, 2008) in R (R Core Team 2020). We used a 20-year cubic smoothing spline curve to remove non-climatic signals, such as the age- and size-related trends, while retaining the high-frequency variability (Cook, 1987). We also calculated the  $\bar{r}$  to quantify the common-growth signal, which is the mean correlation coefficient of all pairwise combinations of all trees in the dataset (Briffa *et al.*, 1995), and the EPS (Expressed Population Signal) that shows how well the samples represent an infinitely replicated chronology (Briffa and Jones, 1990). For this study, we used both the standard tree-ring chronology, to represent the population growth signal, and the detrended individual mean series to evaluate growth signals at the individual level.

### **2.3.2. Radiocarbon dating**

To independently test tree-ring annual formation and confirm tree-ring dating, we applied high-precision radiocarbon ( $^{14}\text{C}$ ) dating for the tree rings in the bomb-peak period (Baker *et al.*, 2017; Soliz-Gamboa *et al.*, 2011; Worbes 1989). The number of available samples to date was constrained because few trees presented growth rings that date back to the bomb-peak years (i.e. over 55 growth rings). Therefore, we were able to select only one tree from each sensitivity group (please refer to the results section 3.2. to see the different sensitivity groups) to date the tree-rings and make sure the distinct responses were not the result of dating problems. From the three selected trees, we dated two to four key years each (1960, 1964, 1965, 1970, 1980, 2001). The tree rings were separated using a scalpel under a stereomicroscope. To explore the high variability in the bomb-peak period (Hua *et al.*, 2013) and test tree-ring annual formation, we performed intra-annual analyses. Also, to confirm the length of the growing season, we attempt to

verify if the intra-annual shifts in  $^{14}\text{C}$  followed the expected wet season months (from October until April). For that, we selected a tree with the highest growth rate in 1965 and divided the corresponding tree ring into eight parts.

We extracted the  $\alpha$ -cellulose from the whole wood to perform the measurements (Linick *et al.*, 1986) with an acid-base-acid extraction in individual rings as described in Ehrlich *et al.* (2017). Between 2-3mg of  $\alpha$ -cellulose were graphitized using an EA-IRMS-AGE3 system, composed of an elemental analyzer (EA, 'vario ISOTOPE SELECT' by Elementar), coupled to an isotope ratio mass spectrometer for  $\delta^{13}\text{C}$  measurement (IRMS, isoprime precisION by Elementar), and to a third generation of the Automated Graphitization Equipment (AGE3, by Ionplus). The  $^{14}\text{C}$  content determination was made in an Accelerator Mass Spectrometry and results were calibrated and modelled using OxCal v 4.3.2 (Ramsey, 2009; Ramsey *et al.*, 2001) to the Southern Hemisphere calibration curve, zones 1-2 (Hua *et al.*, 2013). The  $^{14}\text{C}$  measurements sometimes provide ambiguous results caused by the shape of peak in the calibration curve, but this can be corrected using a tree-ring sequence model (Hammerschlag, *et al.*, 2019; Ramsey 2008; Ramsey *et al.*, 2001). These procedures were carried out at the Dangoor Research Accelerator Mass Spectrometry (D-REAMS) laboratory at the Weizmann Institute (Regev *et al.*, 2017).

### 2.3.3. Climate / growth relationship

To understand the relationship between climatic variables and the average growth signal in the sampled population, we correlated the standard tree-ring chronology with historical climate data from 1961 to 2017 (the period covered by more than five trees). Rainfall and temperature are commonly used together in dendrochronological studies, and despite some level of covariance between them in the present sampling site, we used both variables to turn our study comparable with the current literature. Climate/growth relationships were assessed by calculating Pearson's correlation coefficients (Blasing *et al.*, 1984). As tree growth can also be influenced by the climate of previous years, we analyzed the monthly correlations with the previous and current growing (24 months from May -1 to April +1). We also analyzed seasonal correlations by averaging the climate during the wet season (months with precipitation above 50mm, from October to March).

## 2.4. Analysis of individual trees

Correlations between interannual climate variation and detrended individual tree-ring series were used as a tool to objectively group trees according to their sensitivity to climate. The individual detrended tree-ring series were correlated with the interannual climate data and clustered according to their correlation scores. For that, we used the Ward method of hierarchical clustering using the correlation coefficients between each individual series and monthly climate (Ward and Hook, 1963). We used the common period to all tree-ring series and climate data to make the correlation coefficients comparable and assure the robustness of the individual inferences (from 2002-2016).

We further compared the groups of trees retrieved from the cluster analyses using the individual-tree metadata to characterize the possible drivers of the observed climate-growth clusters (Trouillier *et al.*, 2018). We evaluated differences in microenvironmental conditions, site elevation, trees' estimated age, Diameter at Breast Height (DBH) and Basal Area Increment (BAI). BAI was calculated using dplR (Bunn, 2008) that transform tree-ring width (mm) to tree-ring area (mm squared) to enable comparison of trees with different sizes (Peters *et al.*, 2015). We checked for statistical difference between two groups using the non-parametric Wilcoxon signed-rank test, and the Kruskal-Wallis test for more than 2 groups. We use the Dunn test as a *post-hoc* analysis to verify the difference between the groups (Zar, 2010). In addition, we evaluated the linear relationship between the correlation coefficients calculated before and trees' age to access any age dependence on the climatic responses of the sampled trees.

We then used the results of the cluster analyses to build two separate mean chronologies using sensitive and non-sensitive trees (refer to the results for further details). We used the same methodology described in Section 2.3. for the population chronology and verified the climate-growth relationships during the previous and current wet season. We finally performed a pointer year analysis (Cropper, 1979; van der Maaten-Theunissen *et al.*, 2015), to explore the common growth signals of the trees from different clusters during years with extreme climate conditions. All analyses were performed in R (R Core Team 2017) using the packages ggplot2 (Wickham, 2016) FSA (Ogle *et al.*, 2020), and gplots (Warnes *et al.*, 2015).



We characterized the vegetation seasonality as an indirect assessment of the microenvironmental conditions in the vicinity of each sampled tree. For that, we calculated the Normalized Difference Vegetation Index (NDVI) (Kriegler *et al.*, 1969; Rouse *et al.*, 1974) based on LANDSAT 8 OLI satellite images taken in the wet and dry season - December 20<sup>th</sup> 2018 and July 16<sup>th</sup> 2019, respectively (Figure S5) - downloaded from the Brazilian National Institute of Space Research web catalogue (INPE - <http://www.dgi.inpe.br/catalogo/>). The images have 30m of spatial resolution and were corrected for the top-of-atmosphere reflectance values according to the United States Geological Survey (USGS) standards to enable comparison. To calculate the NDVI ratio, we divided the NDVI of the wet season by the dry season one (Figure 1). We then reclassified the NDVI ratio image according to the range of the NDVI values in each of the groups retrieved from the cluster analyses, using the interquartile range of the NDVI ratio values of the trees in each group using QGIS 3.4.2 (QGIS Development Team, 2015) and used the Point Sampling Tools.

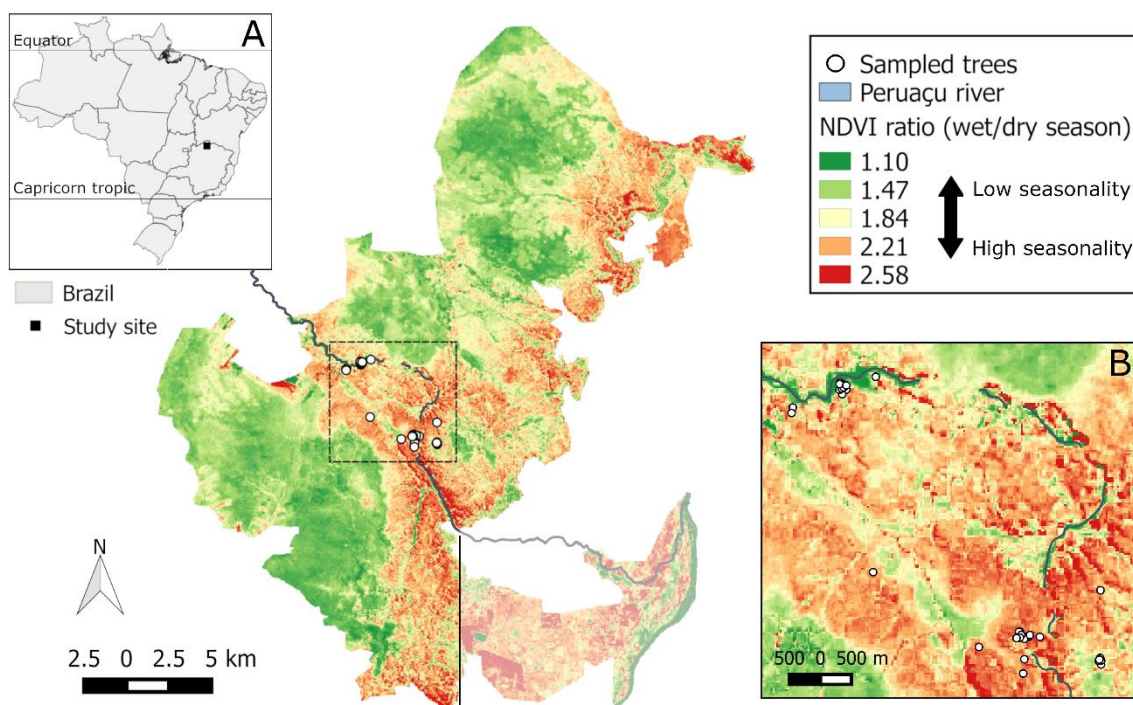


**Figure 1** – Map showing the ratio between the NDVI from wet season (summer) and dry season (winter) at the “Cavernas do Peruaçu” National Park, Central-Eastern

Brazil (A). Green areas correspond to the less seasonal vegetation from the valley and karstic pavements (epikarst areas with deeper soil), while red areas correspond to the highly seasonal vegetation from the epikarst with shallow soil cover. A detail of the distribution of the sampled trees (white circles) is given on panel B. The Southeastern portion of the National Park (dull area) suffered from intense land-use changes characterizing it as a non-natural area.

### 3. Results:

#### 3.1. Tree-ring series and cross-dating quality

Out of the 51 sampled trees of *A. cearensis*, 39 were cross-dated and included in the analyses. Trees not included in the chronology presented inconsistent growth patterns caused by a high number of false rings, local growth anomalies, intra-annual density fluctuations or overall poor tree-ring delimitation (Figure S8).

The maximum age of the trees included in the chronology was 78 years, and the mean annual diameter increment rate was  $0.70 \pm 0.43$  cm yr<sup>-1</sup>. The final mean chronology (Figure 2) showed a strong common-growth signal in the population ( $r_{bar} = 0.45$  and  $EPS = 0.93$ , see Table 1). Dating was further tested using radiocarbon (<sup>14</sup>C) dating in trees from different microenvironments. Figures 2 and S9 show that the year attributed using cross-dating had the expected <sup>14</sup>C content from 1965 until 2018. The high-resolution analysis showed an intra-annual <sup>14</sup>C variation corresponding to the expected growing season at the end of the cross-dated year (October-November) until the beginning of the following year (April-May), which corresponds to the wet season (Figure 2C). The <sup>14</sup>C results and modelled age for the 20 measurements are available in Supplementary Material (Table S2 and Figure S9). For the earlier years, outside the period used in this study, there is still a minor dating error, only one year off in one of the measured trees which can only be corrected with the addition of older trees to the chronology.

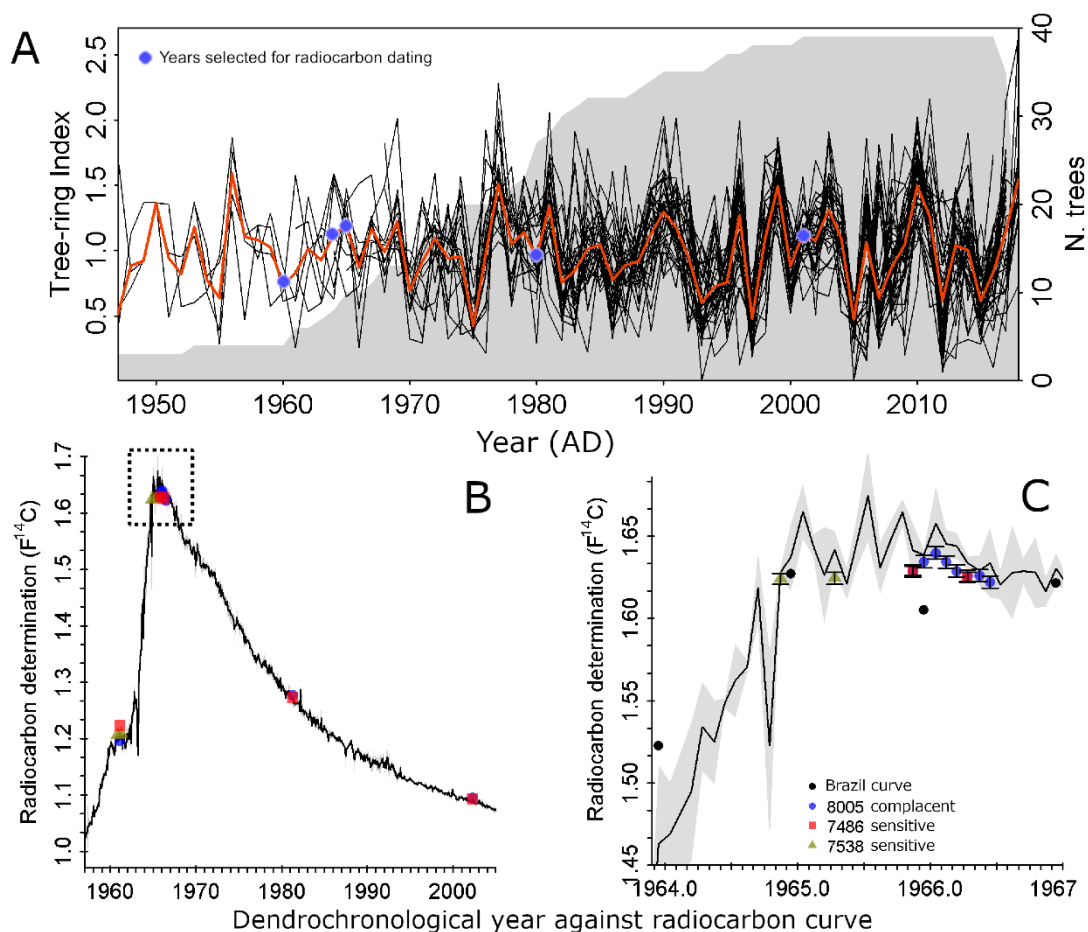


**Figure 2** - Tree-ring width chronology of *Amburana cearensis* and radiocarbon dating of “bomb-peak” years. A) The mean chronology is highlighted by the thick orange line while mean individual tree series are plotted as black lines. The sample depth is displayed as the shaded gray area. The blue circles on the mean chronology indicate the years selected for radiocarbon dating. B) Radiocarbon “bomb-peak” period with the 3 measured trees plotted on the curve according to their dendrochronological year. The values of standard deviation of the measurements are smaller than the symbols. The dotted square in panel B is highlighted in C, detailing the intra-annual analysis performed in the year of 1965 (8 measurements) from the complacent tree number 8005 that captured the growing season in the wet season (summer). The tree rings from the other two trees were divided in half. The black line is the reference curve used for calibration (Hua *et al.*, 2013) and black dots are from the Brazil curve (Santos *et al.*, 2015).

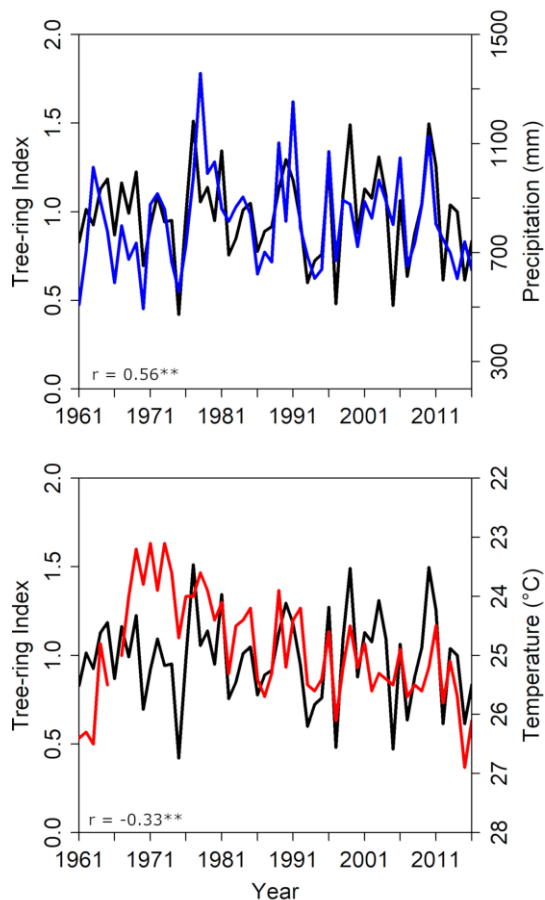
**Table 1**Diagnostics of *Amburana cearensis* tree-ring width chronology

Sampled trees	51
Dated trees (radii)	39/112
Mean diameter growth-rate $\pm$ SD (cm)	0.70 $\pm$ 0.43
Mean tree-ring width $\pm$ SD (cm)	0.35 $\pm$ 0.21
Maximum age (years)	78
Series intercorrelation <sup>a</sup>	0.62
Sensitivity <sup>a</sup>	0.51
Absent rings (%) <sup>a</sup>	0.46
Time Span	1947-2018
rbar	0.45
EPS	0.93

<sup>a</sup>data from COFECHA

### ***3.2. Climate response at the population and individual level***

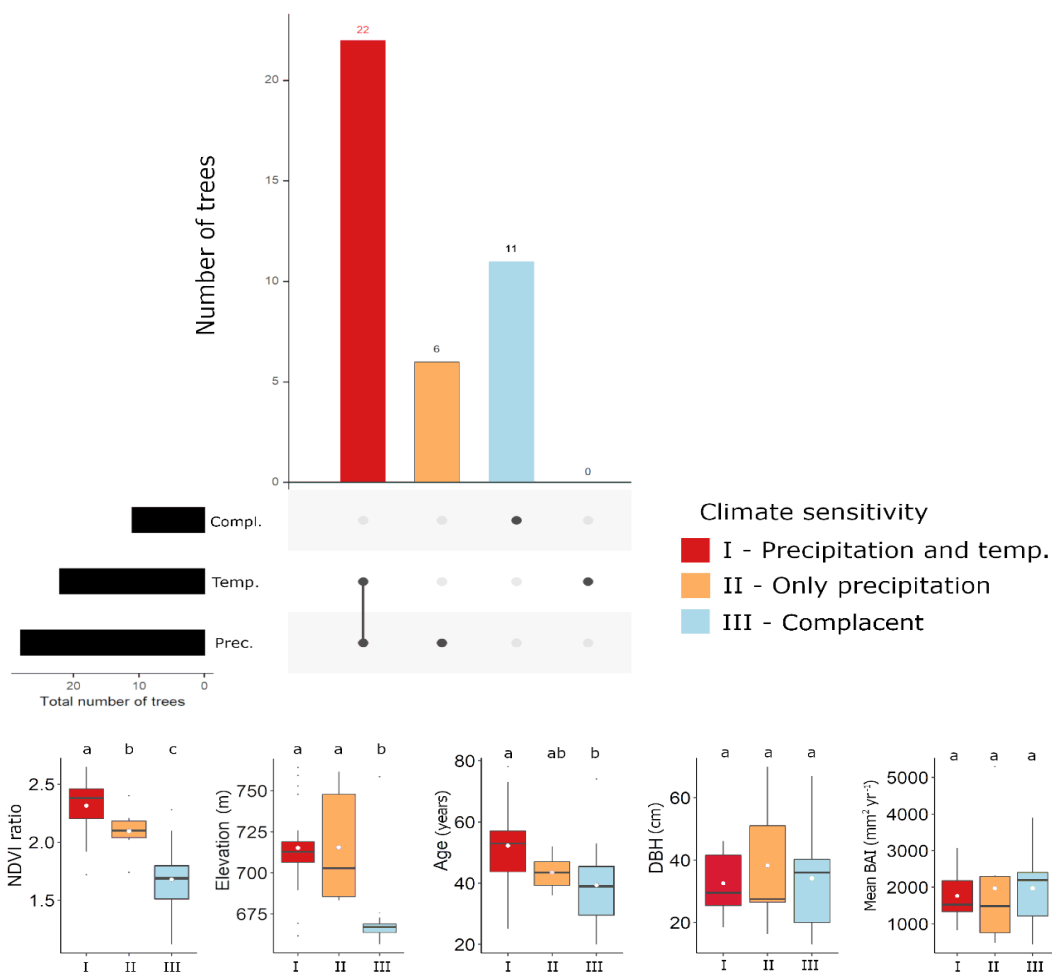
We calculated the correlation values between the population tree-ring width chronology and precipitation and temperature for each month, and during the wet season (Figure S10 and Figure 3). The tree-ring chronology is strongly associated with the sum of precipitation during the wet season, from October to March ( $r = 0.56$ ,  $p < 0.001$ ), but not with the monthly precipitation values. On the other hand, temperature is significantly associated with tree growth mostly at the end of the wet season, from January to March, with the highest correlation values in February ( $r = -0.42$ ,  $p < 0.001$ ).



**Figure 3** – Synchrony and correlation values ( $r$ ) between the mean population chronology and both rainfall and mean temperature from the wet season (from October until March). Precipitation (blue line) has a positive correlation and temperature (red line) has negative correlation with population tree-growth (black lines). Asterisks indicate statistical significance,  $** p < 0.01$ .

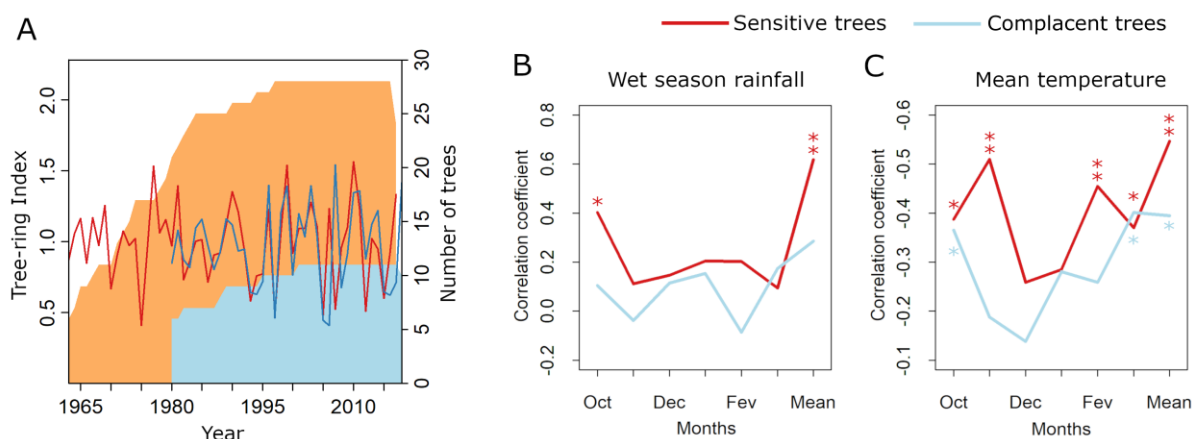
In addition to the population analysis, we also evaluated the climate signal at the individual tree level. The cluster analyses of individual climate sensitivity revealed three groups that represent the association between interannual growth and monthly precipitation (A, B and C in Figure S11). Out of the 39 dated trees, 22 are sensitive to temperature and precipitation variations, six are sensitive only to precipitation and 11 trees showed no sensitivity to regular interannual climate variability, from now on referred to as complacent trees (Figure 4). Trees sensitive to both temperature and precipitation inhabit the most seasonal conditions, mainly at the highest elevations. They are also the oldest trees in the

sampling site. Trees only sensitive to precipitation, inhabit sites with intermediate seasonality, at high to medium elevation. The complacent trees, in turn, are the ones at the less seasonal sites, at low altitude, and also correspond to relatively young trees (Figure 4 and Figure S13). Nonetheless, there is no evidence that young trees are less sensitive to climate and the old complacent trees showed even lower correlation scores (Figure S14). In addition, trees' dimension and growth rate are similar among groups (Figure 4 and S13).



**Figure 4** - Upset plot of observed individual tree climate sensitivities. The boxplots on the lower panel are the individual trees' value of NDVI ratio (value from the wet season divided by dry season), elevation (m), age (years), Diameter at Breast Height – DBH (cm) and Basal Area Increment – BAI (mm<sup>2</sup> yr<sup>-1</sup>) compared per group. Red boxplots are the group sensitive to temperature and precipitation, light-red is the group sensitive only to precipitation and blue is the complacent group. Different letters (“a”, “b” and “c”) indicate statistically different groups.

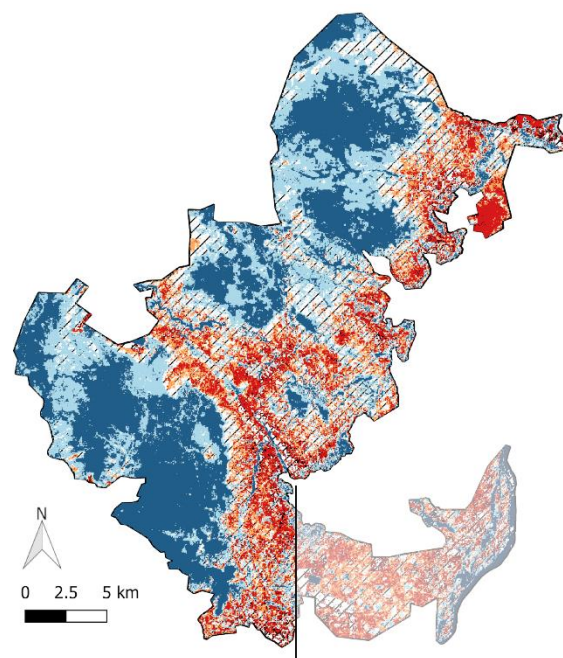
Using the results of the cluster analyses to objectively group the trees according to their sensitivity to climate, we built two mean chronologies and assessed their climate-growth relationship from 1980 to 2016 (Figure 5, Table S3). Similar to the individual-tree analyses (Figure 4, Figures S11 and S12), the complacent trees showed no significant correlation with mean wet season rainfall, and only moderate correlations with mean temperature during the onset and the end of the wet season, as well as for the mean temperature of the wet season (Figure S15). These correlations are only sustained because of three specific years, 1997, 2005, and 2015, that present the highest temperatures for the studied period. Sensitive trees, on the other hand showed rather strong correlations with temperature and precipitation during the months of the wet season (Figure 5). Even for the shorter period from 2002 to 2016 used in the individual analyses (Figure S16 compared to Figure S11 and S12), we observed consistent results with the ones obtained using the mean chronology of the sensitive and complacent trees (Figure S16).









**Figure 5** – Mean chronology of sensitive (red) and complacent (blue) trees and the correlation coefficients of their climate-growth relationship. A) tree-ring width chronologies and sample depth (number of trees). B) and C) correlation coefficients of the monthly and seasonal (mean wet season) association between tree-ring index and precipitation and temperature for the period from 1980 to 2016. Asterisks indicate statistically significant: \* $p < 0.05$ , \*\*  $p < 0.01$ .



The range of NDVI ratio values of each sensitivity group was then used to classify the NDVI ratio map from the sampling site (Figure 8). Due to the presence of crops and other land-use changes in the Southeastern portion of the National Park, these areas were not included in the analysis. A significant share of the “Cavernas do Peruaçu National Park” might harbor *Amburana cearensis* trees that are complacent (25.45% of the National Park area). Some areas show values of the NDVI ratio below the lowest values of the interquartile interval correspondent to complacent trees (34.38%), where trees are also expected to be complacent. On the other hand, 12.03% of the area may potentially support trees sensitive to both precipitation and temperature, and 9.66% of the area may support trees only sensitive to precipitation. Because we observed a gap between the quartiles of the *A. cearensis* trees affected and not affected by climate variation, about 16.88% of the area of the Park has NDVI ratio values that fall within a transition zone likely harboring both sensitive and complacent trees. In this gap between the quartiles of NDVI ratio values is where the trees that were removed from the analysis are located (Figure S17). The NDVI values of their sites of provenance showed intermediary values between the groups of trees defined by the cluster analyses, as if they were in a transitional area.



Individual *A. cearensis* tree climate sensitivity (% of area)

34.38		Likely complacent
25.45		Complacent
16.88		Undefined*
9.66		Precipitation
12.03		Prec. and temperature
1.61		Likely to prec. and temp.

**Figure 6** – Reclassification of the NDVI ratio map of the National Park highlighting areas with different individual *Amburana cearensis* tree sensitivity. The Southeastern portion of the National Park (dull area) were not accounted due to the presence intense land-use changes characterizing it as a non-natural area. The bar plots on the lower panel are the relative coverage (% of area) of each class. The sampled trees correspond to the complacent (light blue) and sensitive (light and dark red) areas. The dark blue and black areas are likely to have the same response as the sensitive and complacent trees, respectively. \* The hatched area in the temperature map refers to transitional areas with no clear classification based on the present data.

The individual analysis also revealed that trees from the sensitive and complacent groups share some pointer-years, always related to harsher climates conditions (Figure 7). For instance, pointer years like 1997 are marked by relatively high temperatures (wet season mean temperature more than one standard deviation above the last 56 years' average), and rainfall below average or unevenly distributed during the wet season. Such similarity is not observed for other years, as trees from the various groups show distinct tree-ring width variability.

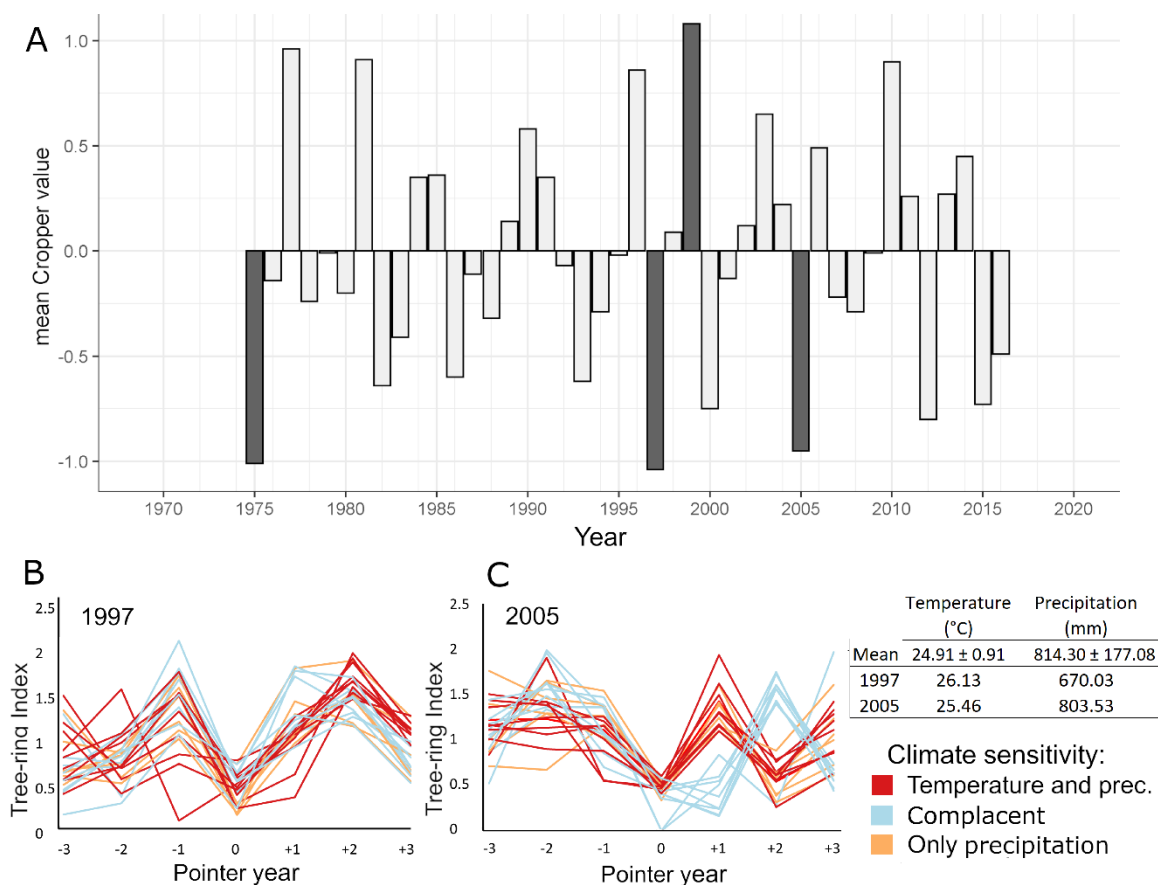


**Figure 7** – Pointer year analysis of the population (A). Gray filled bar plots indicate number of standard deviations from local mean, dark gray bars are years with >75% of the population showing significant deviation (Cropper 1979). On B and C, we verified the common growth among individual series for two most recent negative pointer years. Main climate characteristics of the site and selected years are shown in the table with standard deviations ( $\pm$ ) on the right.

## Discussion

Tropical forests are highly diverse ecosystems (Wiegand *et al.*, 2007; Wright, 2002) and the assessment of tree-growth responses to climate across microenvironmental conditions is usually performed at the population level (Albiero-Júnior *et al.*, 2019; Godoy-Veiga *et al.*, 2018; Locosselli *et al.*, 2016; López *et al.*, 2019), while responses of individual trees remain poorly explored. Overlooking the individual signal is a standard procedure in dendrochronology, as well as in other fields concerning trees and forests dynamics, whose statistical methods aim to improve the population climate signal (Cook, 1987; Douglas, 1941; Fritts, 1966; Trouillier *et al.*, 2018). Few standard procedures have to be employed to maximize the population climate signal and remove the “individual noise”, such as the choice of the most sensitive trees based on provenance characteristics, and the later removal of individual series for presenting a weaker climate signal (Douglas, 1941). The latter is usually attributed to a possible lack of precision in the tree-ring dating of tropical trees. To ensure the precision in the tree-ring dating is, therefore, a key issue that should be addressed by any study that aims to explore the different signals at the individual tree level. In this work, the individual tree analysis was used as the first step to identify trees with different degrees of climate sensitivity that could indicate possible areas of climate change refugia for this tree species.

The framework used in this study allowed us to use a consistently dated set of tree-ring series. Such quality of dating was attested by a tree-ring chronology that meets cross-dating standards comparable to temperate sites. The calculated inter-series correlation (0.62) and  $r_{bar}$  (0.45) was significantly higher than in any other chronologies built with *Amburana cearensis* in South America ( $r_{bar}$  value of 0.33 in Brienen & Zuidema, 2005, and 0.34 in Paredes-Villanueva *et al.* 2015), and on par to temperate studies (e.g.  $r_{bar}$  values from 0.43 to 0.62 in Friedrichs *et al.* 2009). The quality of our tree-ring dating was then independently supported by  $^{14}C$  dating of trees from different sensitivity groups in the period covered by the climate analyses (Figure 2B and 2C). The intra-annual shifts in the measured  $^{14}C$  further allowed us to confirm the growing season during the wet summer for these trees. Altogether, these results gave us the certainty that the individual analyses were not subject to bias due to dating mistakes.

### ***Climate response at the population level***

Similar to other studies in tropical areas (e.g. Brienen & Zuidema, 2005; Paredes-Villanueva *et al.*, 2015), our results indicate climate as a key factor modulating *A. cearensis* tree growth, with a predominant control of rainfall during the wet season and a negative effect of temperature in few months of the growing season (Figure 3). Dry and warm conditions favor the downregulation of photosynthesis while increasing photorespiration and evaporative demands that can reduce carbon net gain (Brienen *et al.*, 2015; Doughty & Goulden, 2009; Lloyd & Farquhar, 2008). This result can be interpreted as the expected response of trees in a population to climate variability and further used to infer how this species may respond to future climate changes. Nonetheless, climate signal may vary according to the local microenvironmental conditions, and the individual tree correlations may be further used as a filter for tree sensitiveness among a population.

### ***Climate response in the individual level***

The cluster analyses indeed revealed groups of sensitive and complacent trees in the same population. A surprising result was that within the group of sensitive trees, tree age seems to affect how trees respond to rainfall variations, which could be related to different strategies of carbon allocation between structural and non-structural carbon pools in relatively old and young trees (Konter *et al.*, 2016; Locosselli & Buckeridge, 2017; Sala *et al.*, 2012). However, the lack of climate sensitivity of the complacent trees is not dependent on tree age. Both young and old trees may show complacent behavior depending on the local microenvironment conditions (Figure 4 and Figure S13). Tree size and growth rate were also not associated with the tree's sensitivity to either temperature or rainfall.

We then used the clusters of sensitive and complacent trees to build two mean chronologies and assess their climate-growth relationships (Figure 5). The two new chronologies support the overall patterns revealed by the analyses of individual trees (Figure 4) with changes in the months with significant correlations probably because of the non-stationary noise present in individual tree-ring series (Cook, 1987). The mean chronology of the complacent trees showed no response to wet season precipitation and only a moderate association with temperature, supported only by the presence of specific



years with more extreme climate conditions. The same is not valid for the sensitive trees that retained a significant association between growth and climate even without these years with extreme climate conditions.

As a general pattern, the sensitive trees of *A. cearensis* mainly inhabit the more seasonal microhabitats formations in the SDTF, as indicated by the values of NDVI ratio (Figures 4 and S13). This pattern points to the role of the microenvironmental conditions shaping the sensitivity of trees to climate variability. Such differences in the NDVI ratio are due to a series of factors including site elevation forests structure and dynamics, microclimate, and soil characteristics. Overall, the more seasonal forest on top of the epikarst presents a more open formation, likely with less tree competition, higher temperature, lower air humidity, and shallower soils which are not connected with the water tables (Coelho, 2013; Prous & Rodet, 2009 and field observations). Such conditions are very different from the ones found in the karstic pavement, at the bottom of the valley and near ravines, which may decouple the microclimate from the macroclimate, and likely create forest enclaves that can act as climate-change refugia (Carrol *et al.*, 2017; Morelli *et al.*, 2020) that favors tree growth (Boakye *et al.*, 2016; Locosselli *et al.*, 2016). These “slow-lanes” for plant species in a changing climate are strategic places for effective conservation management efforts in the near and long-term (Morelli *et al.* 2020).

The capacity of specific microenvironmental conditions to act as a climate refugia, such as those found in the valley, karstic pavements, and ravines, may not always be sufficient to protect trees from climate variability. The results from this study show that both sensitive and complacent trees share consistent narrow rings in some specific years with anomalous low rainfall and high temperature (Figure 7). For instance, the year of 1997 was particularly warm and dry in the region, affecting not only the growth of both sensitive and complacent *Amburana cearensis* trees but also the growth of other tree species such as the *Cedrela fissilis* (Pereira *et al.*, 2018). The presence of these narrow rings in the complacent *A. cearensis* trees indicate that even the trees growing in protected areas are susceptible to climate extremes. They are likely the reason why we observed moderate correlations with climate for the mean chronology of complacent trees, which become non-significant after removing these extreme years. Therefore, despite the possible role of specific landscape

features of the SDTF as climate refugia for *A. cearensis*, that we estimated to cover at least 25% of the National Park area (Figure 6), the gradually more frequent climate extremes (Anderegg *et al.*, 2015; Kitoh *et al.*, 2013; Murphy and Lugo, 1986) may jeopardize this role to some extent in the future.

## **Conclusion**

We demonstrated the potential role of less-seasonal forest enclaves as climate-change refugia in Seasonally Dry Tropical Forests (SDTF) based on individual trees' growth sensitivity to climate. Such forest enclaves buffer the local climate reducing the sensitivity of *A. cearensis* trees' growth to the interannual climate variability. Although this result cannot be retrieved from the population level analyses commonly employed in the literature, we estimate that these complacent trees cover about 25% of the entire sampling area. This buffering capacity, however, is not sufficient to decouple the growth of trees during years with extreme rainfall and temperature conditions. Such extreme years affect all trees in the population regardless of their microenvironmental conditions.

These key nuances in the responses of trees to climate variability could not be obtained from the usual population analyses, and it was only possible through the evaluation of individual tree-ring series. The framework employed in the present study, although tested in only one deciduous, light demanding trees species from this SDTF, indicates new avenues for future research that aim to improve our current understanding of trees and forests responses to climate change. We believe that retrieving information at the individual level from new and well-established chronologies will improve our current understanding of forest dynamics, resource allocation of management practices and the predictability of vegetation responses to climate change.

## **Acknowledgments**

Funding: this work was supported by the São Paulo Research Foundation – FAPESP (grant numbers: PIRE-CREATE project 2017/50085-3; MGV grant 2018/07632-6 and BEPE 2019/09813-0; 2019/08783-0; 2019/25636-1; 2020/09251-0). The National Council for Scientific and Technological Development (CNPq) (grant numbers: 423481/2018-5, 304413/2018-6). The radiocarbon research was supported by the Exilarch

Foundation that supports the Dangoor Research Accelerator Mass Spectrometer (D-REAMS) Laboratory. We wish to thank the Kimmel Center for Archaeological Science and the George Schwartzman Fund for the laboratory and funding support for MGV in Israel. E.B. is the incumbent of the Dangoor Professorial Chair of Archaeological Sciences at the Weizmann Institute of Science. This study was partially financed by the Coordenação de Aperfeiçoamento de Pessoal de Nível Superior - CAPES (Finance Code 001). The authors are deeply indebted to fieldwork support personnel, such as our cooks, Mrs. Anita and Nildinha dos Santos and our field guides, Mr. Lucimar dos Santos and Mr. Vandey Batista de Jesus who helped a lot the sampling. The authors also thank Paula Alecio, Luciano Fioroto Redondo and Eugenia Mintz for helping with sample preparation and laboratory procedures, Yael Ehrlich for discussing the methods for tree-ring  $^{14}\text{C}$  dating and the anonymous reviewers for valuable inputs in the article.

**CRedit author statement:** MGV: Conceptualization, Methodology, Formal analysis, Investigation, Writing – Original Draft. BBLC: Methodology, Software, Writing – Review & Editing. NMS: Methodology, Formal analysis, Validation. FWC: Funding acquisition, Project administration. CHG: Formal analysis, Data Curation. MSS: Formal analysis, Data Curation. LR: Methodology, Validation. EB: Methodology, Funding acquisition, Resources. GC: Supervision, Project administration. GML: Conceptualization, Formal analysis, Writing – Review & Editing, Supervision.

### **Conflict of interest**

The authors declare that they have no conflict of interest.

## Referências Bibliográficas

---

- Akhmetzyanov, L., Sánchez-Salguero, R., García-González, I., Buras, A., Dominguez-Delmás, M., Mohren, F., den Ouden, J., Sass-Klaassen, U., 2020. Towards a new approach for dendroprovenancing pines in the Mediterranean Iberian Peninsula. *Dendrochronologia* 60, 125688. <https://doi.org/10.1016/j.dendro.2020.125688>.
- Albert, C.H., Thuiller, W., Yoccoz, N.G., Soudant, A., Boucher, F., Saccone, P., Lavorel, S., 2010. Intraspecific functional variability: Extent, structure and sources of variation. *J. Ecol.* 98, 604–613. <https://doi.org/10.1111/j.1365-2745.2010.01651.x>.
- Albiero-Júnior, A., Camargo, J.L.C., Roig, F.A., Schöngart, J., Pinto, R.M., Venegas-González, A., Tomazello-Filho, M., 2019. Amazonian trees show increased edge effects due to Atlantic Ocean warming and northward displacement of the Intertropical Convergence Zone since 1980. *Sci. Total Environ.* 693, 133515. <https://doi.org/10.1016/j.scitotenv.2019.07.321>.
- Aleixo, I., Norris, D., Hemerik, L., Barbosa, A., Prata, E., Costa, F., Poorter, L., 2019. Amazonian rainforest tree mortality driven by climate and functional traits. *Nat. Clim. Chang.* 9, 384–388. <https://doi.org/10.1038/s41558-019-0458-0>.
- Allen, C.D., Macalady, A.K., Chenchouni, H., Bachelet, D., McDowell, N., Vennetier, M., Kitzberger, T., Rigling, A., Breshears, D.D., Hogg, E.H., Ted., Gonzalez, P., Fensham, R., Zhang, Z., Castro, J., Demidova, N., Lim, J.H., Allard, G., Running, S.W., Semerci, A., Cobb, N., 2010. A global overview of drought and heat-induced tree mortality reveals emerging climate change risks for forests. *For. Ecol. Manage.* 259, 660–684. <https://doi.org/10.1016/j.foreco.2009.09.001>.
- Anderegg, W.R.L., Schwalm, C., Biondi, F., Camarero, J.J., Koch, G., Litvak, M., Ogle, K., Shaw, J.D., Shevliakova, E., Williams, A.P., Wolf, A., Ziaco, E., Pacala, S., 2015. Pervasive drought legacies in forest ecosystems and their implications for carbon cycle models. *Science* 349, 528–532. <https://doi.org/10.1126/science.aab1833>.
- Auler, A.S., Farrant, A.R., 1996. A brief introduction to karst and caves in Brazil. *Proc. Univ. Bristol. Spelacol.Soc.* 20, 187–200.
- Ault, T. R., 2020. On the essentials of drought in a changing climate. *Science*, 368(6489), 256–260. <https://doi.org/10.1126/SCIENCE.ABC4034>.
- Baker, J. C. A., Hunt, S. F. P., Clerici, S. J., Newton, R. J., Bottrell, S. H., Leng, M. J., ... Brienen, R. J. W., 2015. Oxygen isotopes in tree rings show good coherence between

species and sites in Bolivia. *Global and Planetary Change*, 133, 298–308. <https://doi.org/10.1016/j.gloplacha.2015.09.008>.

- Baker, J.C.A., Santos, G.M., Gloor, M., Brienen, R.J.W., 2017. Does *Cedrela* always form annual rings? Testing ring periodicity across South America using radiocarbon dating. *Trees - Struct. Funct.* 31, 1999–2009. <https://doi.org/10.1007/s00468-017-1604-9>.
- Bhandari, A.K., Kumar, A., Singh, G.K., 2012. Feature Extraction using Normalized Difference Vegetation Index (NDVI): A Case Study of Jabalpur City. *Procedia Technol.* 6, 612–621. <https://doi.org/10.1016/j.protcy.2012.10.074>.
- Blasing, T.J., Solomon, A.M., Duvick, D.N., 1984. Response Functions Revisited. *Tree-Ring Bull.* 44, 1–15.
- Boakye, E.A., Gebrekirstos, A., Hyppolite, D.N., Barnes, V.R., Kouamé, F.N., Kone, D., Porembski, S., Bräuning, A., 2016. Influence of climatic factors on tree growth in riparian forests in the humid and dry savannas of the Volta basin, Ghana. *Trees - Struct. Funct.* 30, 1695–1709. <https://doi.org/10.1007/s00468-016-1401-x>.
- Brienen, R. J. W., Gloor, E., Clerici, S., Newton, R., Arppe, L., Boom, A., ... Timonen, M. 2017. Tree height strongly affects estimates of water-use efficiency responses to climate and CO<sub>2</sub> using isotopes. *Nature Communications*, 8(1), 288. <https://doi.org/10.1038/s41467-017-00225-z>.
- Brienen, R.J.W., Lebrija-Trejos, E., Zuidema, P.A., Martínez-Ramos, M., 2010. Climate-growth analysis for a Mexican dry forest tree shows strong impact of sea surface temperatures and predicts future growth declines. *Glob. Chang. Biol.* 16, 2001–2012. <https://doi.org/10.1111/j.1365-2486.2009.02059.x>.
- Brienen, R.J.W., Phillips, O.L., Feldpausch, T.R., Gloor, E., Baker, T.R., Lloyd, J., Lopez-Gonzalez, G., Monteagudo-Mendoza, A., Malhi, Y., Lewis, S.L., Vásquez Martínez, R., Alexiades, M., Álvarez Dávila, E., Alvarez-Loayza, P., Andrade, A., Aragañ, L.E.O.C., Araujo-Murakami, A., Arets, E.J.M.M., Arroyo, L., Aymard C., G.A., Bánki, O.S., Baraloto, C., Barroso, J., Bonal, D., Boot, R.G.A., Camargo, J.L.C., *et al.*, Thomas-Caesar, R., Toledo, M., Torello-Raventos, M., Umetsu, R.K., Van Der Heijden, G.M.F., Van Der Hout, P., Guimarães Vieira, I.C., Vieira, S.A., Vilanova, E., Vos, V.A., Zagt, R.J., 2015. Long-term decline of the Amazon carbon sink. *Nature* 519, 344–348. <https://doi.org/10.1038/nature14283>.



- Brienen, R.J.W., Schöngart, J., Zuidema, P.A., 2016. Tree rings in the tropics: insights into the ecology and climate sensitivity of tropical trees. [https://doi.org/10.1007/978-3-319-27422-5\\_19](https://doi.org/10.1007/978-3-319-27422-5_19).
- Brienen, R.J.W., Zuidema, P.A., 2005. Relating tree growth to rainfall in Bolivian rain forests: a test for six species using tree ring analysis. *Oecologia* 146, 1–12. <https://doi.org/10.1007/s00442-005-0160-y>
- Brienen, R. J. W., & Zuidema, P. A. 2006. Lifetime growth patterns and ages of Bolivian rain forest trees obtained by tree ring analysis. *Journal of Ecology*, 94(2), 481–493. <https://doi.org/10.1111/j.1365-2745.2005.01080.x>.
- Briffa, K.R., Jones, P.D., Schweingruber, F.H., Shiyatov, S.G., Cook, E.R., 1995. Unusual twentieth-century summer warmth in a 1, 000-year temperature record from siberia. *Nature* 376, 156–159. <https://doi.org/10.1038/376156a0>.
- Briffa, K. R. and Jones, P. D. 1990. Basic chronology statistics and assessment. In: *Methods of Dendrochronology: Applications in the Environmental Sciences*. Kluwer Academic Publishers, pp. 137-152. ISBN 978-0-7923-0586-6.
- Bunn, A.G., 2008. A dendrochronology program library in R (dplR). *Dendrochronologia* 26, 115–124. <https://doi.org/10.1016/j.dendro.2008.01.002>.
- Carrer, M., 2011. Individualistic and time-varying Tree-Ring growth to climate sensitivity. *PLoS One* 6. <https://doi.org/10.1371/journal.pone.0022813>.
- Carroll, C., Roberts, D. R., Michalak, J. L., Lawler, J. J., Nielsen, S. E., Stralberg, D., ... Wang, T., 2017. Scale-dependent complementarity of climatic velocity and environmental diversity for identifying priority areas for conservation under climate change. *Global Change Biology*, 23(11), 4508–4520. <https://doi.org/10.1111/gcb.13679>.
- Chen, J., Saunders, S.C., Crow, T.R., Naiman, R.J., Brososke, K.D., Mroz, G.D., Brookshire, B.L., Franklin, J.F., J, W.I.R., Franklin, J.F., 1999. in *Forest Microclimate and Ecosystem Ecology Landscape Variations in local climate can be used to monitor and compare the effects of different management regimes*. *Bioscience* 49, 288–297.
- Coelho, A. H. F. 2013. Registros de grandes alagamentos no cânion do rio Peruaçu, Parque Nacional Cavernas do Peruaçu – PNCP, MG. Master Thesis defended at the Geography department of the University of Minas Gerais.
- Coelho, M., Fernandes, G., & Sánchez-Azofeifa, A., 2013. Brazilian tropical dry forest on basalt and limestone outcrops. *Tropical dry forests in the americas*, 55–68. <https://doi.org/10.1201/b15417-5>.

- Cook, E.R., 1987. The decomposition of tree-ring series for environmental studies. *Tree-Ring Bull.* 47, 37–59. <https://doi.org/S>.
- Cropper, J.P., 1979. Tree-ring skeleton plotting by computer. *Tree Ring Bull.* 39, 47–59.
- DeSoto, L., Cailleret, M., Sterk, F., Jansen, S., Kramer, K., Robert, E.M.R., Aakala, T., Amoroso, M.M., Bigler, C., Camarero, J.J., Cufar, K., Gea-Izquierdo, G., Gillner, S., Haavik, L.J., Hereş, A.M., Kane, J.M., Kharuk, V.I., Kitzberger, T., Tamir Klein, Levanič, T., Linares, J.C., Mäkinen, H., Oberhuber, W., Papadopoulos, A., Rohner, B., Sangüesa-Barreda, G., Stojanović, D.B., Suarez, M.L., Villalba, R., Martínez-Vilalta, J., 2020. Low growth resilience to drought is related to future mortality risk in trees. *Nat. Commun.* 1–9. <https://doi.org/10.1038/s41467-020-14300-5>.
- Doughty, C.E., Goulden, M.L., 2009. Are tropical forests near a high temperature threshold? *J. Geophys. Res. Biogeosciences* 114, 1–12. <https://doi.org/10.1029/2007JG000632>.
- Douglass, A., 1941. Crossdating in Dendrochronology. *J. For.* 39, 825–831. <https://doi.org/10.1093/jof/39.10.825>.
- Ehrlich, Y., Regev, L., Kerem, Z., Boaretto, E., 2017. Radiocarbon dating of an olive tree cross-section: New insights on growth patterns and implications for age estimation of olive trees. *Front. Plant Sci.* 8, 1–9. <https://doi.org/10.3389/fpls.2017.01918>.
- Friedrichs, D. A., Trouet, V., Büntgen, U., Frank, D. C., Esper, J., Neuwirth, B., & Löffler, J. 2009. Species-specific climate sensitivity of tree growth in Central-West Germany. *Trees - Structure and Function*, 23(4), 729–739. <https://doi.org/10.1007/s00468-009-0315-2>.
- Fritts, H. C., 1966. Growth-rings of trees: Their correlation with climate. *Science*, 154 (3752), 973–979. <https://doi.org/10.1126/science.154.3752.973>.
- Fritts, H.C., 1976. *Tree-ring and climate*. Academic Press, London p 567.
- Galván, J.D., Camarero, J.J., Gutiérrez, E., 2014. Seeing the trees for the forest: Drivers of individual growth responses to climate in *Pinus uncinata* mountain forests. *J. Ecol.* 102, 1244–1257. <https://doi.org/10.1111/1365-2745.12268>.
- Godoy-Veiga, M., Ceccantini, G., Pitsch, P., Krottenthaler, S., Anhof, D., Locosselli, G.M., 2018. Shadows of the edge effects for tropical emergent trees: the impact of lianas on the growth of *Aspidosperma polyneuron*. *Trees - Struct. Funct.* 32, 1073–1082. <https://doi.org/10.1007/s00468-018-1696-x>.

- GRASS Development Team, 2017. Geographic Resources Analysis Support System (GRASS) Software, Version 7.2. Open Source Geospatial Foundation. Electronic document: <http://grass.osgeo.org>.
- Hammerschlag, I., Macario, K. D., Barbosa, A. C., De Assis Pereira, G., Farrapo, C. L., & Cruz, F., 2019. Annually verified growth of *Cedrela fissilis* from central Brazil. *Radiocarbon*, 61(4), 927–937. <https://doi.org/10.1017/RDC.2019.52>
- Hietz, P., 2011. A simple program to measure and analyse tree rings using Excel, R and SigmaScan. *Dendrochronologia* 29, 245–250. <https://doi.org/10.1016/j.dendro.2010.11.002>.
- Holmes, R., 1983. Computer-assisted quality control in tree-ring dating and measurement.
- Hua, Q., Barbetti, M., Rakowski, A., 2013. Atmospheric radiocarbon for the period 1950–2010 55.
- IPCC, V. Masson-Delmotte, P. Zhai, H. O. Pörtner, D. Roberts, J. Skea, P. R. Shukla, A. Pirani, W. Moufouma-Okia, C. Péan, R. Pidcock, S. Connors, J. B. R. Matthews, Y. Chen, X. Zhou, M. I. Gomis, E. Lonnoy, T. Maycock, M. Tignor, T. Waterfield (eds.). 2018: Summary for Policymakers. In: Global warming of 1.5°C. An IPCC Special Report on the impacts of global warming of 1.5°C above pre-industrial levels and related global greenhouse gas emission pathways, in the context of strengthening the global response to the threat of climate change, sustainable development, and efforts to eradicate poverty. World Meteorological Organization, Geneva, Switzerland, 32 pp.
- Kitoh, A., Endo, H., Krishna Kumar, K., Cavalcanti, I.F.A., Goswami, P., Zhou, T., 2013. Monsoons in a changing world: A regional perspective in a global context. *J. Geophys. Res. Atmos.* 118, 3053–3065. <https://doi.org/10.1002/jgrd.50258>.
- Konter, O., Büntgen, U., Carrer, M., Timonen, M., Esper, J., 2016. Climate signal age effects in boreal tree-rings: Lessons to be learned for paleoclimatic reconstructions. *Quat. Sci. Rev.* 142, 164–172. <https://doi.org/10.1016/j.quascirev.2016.04.020>.
- Kriegler, F.J., Malila, W.A., Nalepka, R.F., and Richardson, W., 1969. Preprocessing transformations and their effects on multispectral recognition. *Proceedings of the Sixth International Symposium on Remote Sensing of Environment*, p. 97-131.
- Krottenthaler, S., Pitsch, P., Helle, G., Locosselli, G.M., Ceccantini, G., Altman, J., Svoboda, M., Dolezal, J., Schleser, G., Anhof, D., 2015. A power-driven increment borer for sampling high-density tropical wood. *Dendrochronologia* 36, 40–44. <https://doi.org/10.1016/j.dendro.2015.08.005>.

- Leite, E. J. (2005). State-of-knowledge on *Amburana cearensis* (Fr. Allem.) A.C. Smith (Leguminosae: Papilionoideae) for genetic conservation in Brazil. *Journal for Nature Conservation*, 13(1), 49–65. <https://doi.org/10.1016/j.jnc.2004.07.003>.
- Levine, N. M., Zhang, K., Longo, M., Baccini, A., Phillips, O. L., Lewis, S. L., ... Moorcroft, P. R. (2016). Ecosystem heterogeneity determines the ecological resilience of the Amazon to climate change. *Proceedings of the National Academy of Sciences of the United States of America*, 113(3), 793–797. <https://doi.org/10.1073/pnas.1511344112>.
- Linick, T.W., Long, A., Damon, P.E., Ferguson, C.W., 1986. High-precision radiocarbon dating of bristlecone pine from 6554 to 5350 BC. *Radiocarbon* 28, 943–953. <https://doi.org/10.1017/s0033822200060227>
- Lloyd, J., Farquhar, G.D., 2008. Effects of rising temperatures and CO<sub>2</sub> on the physiology of tropical forest trees. *Philos. Trans. R. Soc. B Biol. Sci.* 363, 1811–1817. <https://doi.org/10.1098/rstb.2007.0032>.
- Locosselli, G.M., Buckeridge, M.S., 2017. Dendrobiochemistry, a missing link to further understand carbon allocation during growth and decline of trees. *Trees - Struct. Funct.* 31, 1745–1758. <https://doi.org/10.1007/s00468-017-1599-2>.
- Locosselli, G.M., Cardim, R.H., Ceccantini, G., 2016. Rock outcrops reduce temperature-induced stress for tropical conifer by decoupling regional climate in the semiarid environment. *Int. J. Biometeorol.* 60, 639–649. <https://doi.org/10.1007/s00484-015-1058-y>.
- Lombardi, J.A., Salino, A., Temoni, L.G., 2005. Diversidade florística de plantas vasculares no município de Januária, Minas Gerais, Brasil. *Lundiana* 6, 3–20.
- López, J. A., 1987. *Árboles Comunes del Paraguay*. Nãnde Yvirá Mata Kuera, Cuerpo de Paz, Asunción.
- López, L., & Villalba, R., 2016. Reliable estimates of radial growth for eight tropical species based on wood anatomical patterns. *Journal of Tropical Forest Science*, 28(2), 139–152.
- López, L., Rodríguez-Catón, M., Villalba, R., 2019. Convergence in growth responses of tropical trees to climate driven by water stress. *Ecography (Cop.)*. 42, 1899–1912. <https://doi.org/10.1111/ecog.04296>.
- López, Lidio, Villalba, R., & Bravo, F., 2013. Cumulative diameter growth and biological rotation age for seven tree species in the Cerrado biogeographical province of

Bolivia. *Forest Ecology and Management*, 292, 49–55.  
<https://doi.org/10.1016/j.foreco.2012.12.011>.

López, Lidio, Villalba, R., & Peña-Claros, M., 2012. Ritmos de crecimiento diamétrico en los bosques secos tropicales: Aportes al manejo sostenible de los bosques de la provincia biogeográfica del cerrado boliviano. *Bosque*, 33(2), 211–219.  
<https://doi.org/10.4067/S0717-92002012000200011>.

Lorenzi, H., Matos, FJA. 2008. *Plantas medicinais no Brasil: nativas e exóticas*. 2 ed. Nova Odessa, São Paulo, Instituto Plantarum, 544p.

McLaughlin, B. C., Ackerly, D. D., Klos, P. Z., Natali, J., Dawson, T. E., & Thompson, S. E., 2017. Hydrologic refugia, plants, and climate change. *Global Change Biology*, 23(8), 2941–2961. <https://doi.org/10.1111/gcb.13629>.

Ministério do Meio Ambiente, 2002. Termo de referência para a contratação de serviços para a elaboração do plano de manejo do Parque Nacional Cavernas do Peruaçu – MG. IBAMA, Brasília, DF.

Morelli, T. L., Barrows, C. W., Ramirez, A. R., Cartwright, J. M., Ackerly, D. D., Eaves, T. D., ... Thorne, J. H., 2020. Climate-change refugia: biodiversity in the slow lane. *Frontiers in Ecology and the Environment*, 18(5), 228–234.  
<https://doi.org/10.1002/fee.2189>.

Mori, H., Yamashita, K., Saiki, S.T., Matsumoto, A., Ujino-Ihara, T., 2020. Climate sensitivity of *Cryptomeria japonica* in two contrasting environments: Perspectives from QTL mapping. *PLoS One* 15, 1–14. <https://doi.org/10.1371/journal.pone.0228278>.

Murphy, P.G., Lugo, A.E., 1986. Ecology of tropical dry forest. *Annu. Rev. Ecol. Syst.* Vol. 17 17, 67–88. <https://doi.org/10.1146/annurev.es.17.110186.000435>.

Ogle D.H., Wheeler P., Dinno A. (2020). FSA: Fisheries Stock Analysis. R package version 0.8.30.9000.

Paine, C.E.T., Baraloto, C., Chave, J., Hérault, B., 2011. Functional traits of individual trees reveal ecological constraints on community assembly in tropical rain forests. *Oikos* 120, 720–727. <https://doi.org/10.1111/j.1600-0706.2010.19110.x>.

Paredes-Villanueva, K., López, L., Brookhouse, M., Cerrillo, R.M.N., 2015. Rainfall and temperature variability in Bolivia derived from the tree-ring width of *Amburana cearensis* (Fr. Allem.) A.C. Smith. *Dendrochronologia* 35, 80–86.  
<https://doi.org/10.1016/j.dendro.2015.04.003>.



- Peel, M.C., Finlayson, B.L., McMahon, T.A., 2007. Updated world map of the Köppen-Geiger climate classification. *Hydrol. Earth Syst. Sci.* 11, 1633–1644. <https://doi.org/10.5194/hess-11-1633-2007>
- Pennington, R. T., Prado, D. E., and C. A. Pendry, 2006. Neotropical seasonally dry forests and Quaternary vegetation changes. *Journal of Biogeography* 27:261–273.
- Pereira, G. de A., Barbosa, A. C. M. C., Torbenson, M. C. A., Stahle, D. W., Granato-Souza, D., Santos, R. M. Dos, & Barbosa, J. P. D., 2018. The climate response of *Cedrela fissilis* annual ring width in the Rio São Francisco basin, Brazil. *Tree-Ring Research*, 74(2), 162–171. <https://doi.org/10.3959/1536-1098-74.2.162>.
- Peters, R. L., Groenendijk, P., Vlam, M., & Zuidema, P. A., 2015. Detecting long-term growth trends using tree rings: A critical evaluation of methods. *Global Change Biology*, 21(5), 2040–2054. <https://doi.org/10.1111/gcb.12826>.
- Prous, A., Rodet, M.J., 2009. Arqueologia do vale do rio Peruaçu e adjacências - Minas Gerais. *Arq. Mus. Hist. Nat. Jard. Bot. - UFMG. Belo Horizonte. Volume XIX.*
- QGIS Development Team, 2015. QGIS Geographic Information System. Open Source Geospatial Foundation Project. <http://qgis.osgeo.org>.
- R Core Team, 2020. R: a language and environment for statistical computing. R foundation for statistical computing, Vienna, Austria. <https://www.R-project.org>.
- Ramsey, C.B., 2008. Deposition models for chronological records. *Quaternary Science Reviews*, 27(1-2): 42–60
- Ramsey, C.B., 2009. Bayesian analysis of radiocarbon dates. *Radiocarbon* 51, 337–360. [https://doi.org/10.2458/azu\\_uapress\\_9780816530595-ch039](https://doi.org/10.2458/azu_uapress_9780816530595-ch039).
- Ramsey, C.B., van der Plicht, J., & Weninger, B., 2001. 'Wiggle matching' radiocarbon dates. *Radiocarbon*, 43(2A), 381-389.
- Regev, L., Steier, P., Shachar, Y., Mintz, E., Wild, E. M., Kutschera, W., & Boaretto, E., 2017. D-REAMS: a new compact AMS system for radiocarbon measurements at the Weizmann Institute of Science, Rehovot, Israel. *Radiocarbon*, 59(3), 775–784. <https://doi.org/10.1017/RDC.2016.96>.
- Rodet, J., Willems, L., Pouclet, A., 2015. The Rio Peruaçu basin: an impressive multiphased karst system, in: Vieira, B.C., Salgado, A.A.R., Santos, L.J.C. (Eds.), *Landscapes and Landforms of Brazil*. Springer Netherlands, Dordrecht, pp. 171–181. [https://doi.org/10.1007/978-94-017-8023-0\\_15](https://doi.org/10.1007/978-94-017-8023-0_15).

- Rouse, J.W., Haas, R.H., Scheel, J.A., and Deering, D.W., 1974. Monitoring Vegetation Systems in the Great Plains with ERTS.' Proceedings, 3rd Earth Resource Technology Satellite (ERTS) Symposium, vol. 1, p. 48-62. <https://ntrs.nasa.gov/archive/nasa/casi.ntrs.nasa.gov/19740022592.pdf>
- Sala, A., Woodruff, D.R., Meinzer, F.C., 2012. Carbon dynamics in trees: Feast or famine? *Tree Physiol.* 32, 764–775. <https://doi.org/10.1093/treephys/tp143>.
- Santos, G. M., Linares, R., Lisi, C. S., & Tomazello Filho, M. 2015. Annual growth rings in a sample of Paraná pine (*Araucaria angustifolia*): Toward improving the <sup>14</sup>C calibration curve for the Southern Hemisphere. *Quaternary Geochronology*, 25, 96–103. <https://doi.org/10.1016/j.quageo.2014.10.004>.
- Schongart, J., Bräuning, A., Barbosa, A.C.M.C., Lisi, C.S., de Oliveira, J.M., 2017. Dendroecological studies in the neotropics: history, status and future challenges. [https://doi.org/10.1007/978-3-319-61669-8\\_8](https://doi.org/10.1007/978-3-319-61669-8_8).
- Soliz-Gamboa, C.C., Rozendaal, D.M.A., Ceccantini, G., Angyalossy, V., van der Borg, K., Zuidema, P.A., 2011. Evaluating the annual nature of juvenile rings in Bolivian tropical rainforest trees. *Trees - Struct. Funct.* 25, 17–27. <https://doi.org/10.1007/s00468-010-0468-z>.
- Speer, B.J.H., 2010. Fundamentals of tree-ring research 509. <https://doi.org/10.1002/gea.20357>.
- Stillman, R.A., Railsback, S.F., Giske, J., Berger, U., Grimm, V., 2015. Making predictions in a changing world: The benefits of individual-based ecology. *Bioscience* 65, 140–150. <https://doi.org/10.1093/biosci/biu192>.
- Townsend, A. R., Asner, G. P., & Cleveland, C. C., 2008. The biogeochemical heterogeneity of tropical forests. *Trends in Ecology and Evolution*, 23(8), 424–431. <https://doi.org/10.1016/j.tree.2008.04.009>.
- Trouillier, M., van der Maaten-Theunissen, M., Harvey, J.E., Würth, D., Schnittler, M., Wilmking, M., 2018. Visualizing individual tree differences in tree-ring studies. *Forests* 9, 1–14. <https://doi.org/10.3390/f9040216>.
- Uriarte, M., Muscarella, R., & Zimmerman, J. K., 2018. Environmental heterogeneity and biotic interactions mediate climate impacts on tropical forest regeneration. *Global Change Biology*, 24(2), e692–e704. <https://doi.org/10.1111/gcb.14000>.

- van der Maaten-Theunissen, M., van der Maaten, E., Bouriaud, O., 2015. PointRes: An R package to analyze pointer years and components of resilience. *Dendrochronologia* 35, 34–38. <https://doi.org/10.1016/j.dendro.2015.05.006>.
- Vera, C., Higgins, W., Amador, J., Ambrizzi, T., Garreaud, R., Gochis, D., Gutzler, D., Lettenmaier, D., Marengo, J., Mechoso, C.R., Nogues-Paegle, J., Silva Dias, P.L., Zhang, C., 2006. Toward a unified view of the American monsoon systems. *J. Clim.* 19, 4977–5000. <https://doi.org/10.1175/JCLI3896.1>.
- Ward, J.H., Hook, M.E., 1963. Application of a hierarchical grouping procedure to a problem of grouping profiles. *Educ. Psychol. Meas.* XXIII, 69–81.
- Warnes, G., Bolker, B., Bonebakker, L., Gentleman, R., Liaw, W., Lumley, T., Maechler, M., Magnusson, A., Moeller, S., Schwartz, M., Venables, B., R., 2015. *gplots: Various R Programming Tools for Plotting Data*.
- Wickham, H., 2016. *Ggplot2: elegant graphics for data analysis*.
- Wiegand, T., Gunatilleke, C.V.S., Gunatilleke, I.A.U.N., Huth, A., 2007. How individual species structure diversity in tropical forests. *Proc. Natl. Acad. Sci. U. S. A.* 104, 19029–19033. <https://doi.org/10.1073/pnas.0705621104>.
- Worbes, M., 1989. Growth rings, increment and age of trees in inundation forests, savannas and a mountain forest in the neotropics. *IAWA Journal*, 10(2), 109–122. <https://doi.org/10.1163/22941932-90000479>.
- Worbes, M., 2002. One hundred years of tree-ring research in the tropics—a brief history and an outlook to future challenges. *Dendrochronologia* 20, 217–231.
- Wright, S.J., 2002. Plant diversity in tropical forests: A review of mechanisms of species coexistence. *Oecologia* 130, 1–14. <https://doi.org/10.1007/s004420100809>.
- Zar, J.H. 2010. *Biostatistical Analysis*, 5th ed. Pearson Prentice Hall: Upper Saddle River, NJ.
- Zhou, J., Lau, K.M., 1998. Does a monsoon climate exist over South America? *J. Clim.* 11, 1020–1040. <https://doi.org/10.1175/1520-0442>.
- Zuidema, P.A., Baker, P.J., Groenendijk, P., Schippers, P., van der Sleen, P., Vlam, M., Sterck, F., 2013. Tropical forests and global change: filling knowledge gaps. *Trends Plant Sci.* 18, 413–419. <https://doi.org/10.1016/j.tplants.2013.05.006>.

## Supplementary Material

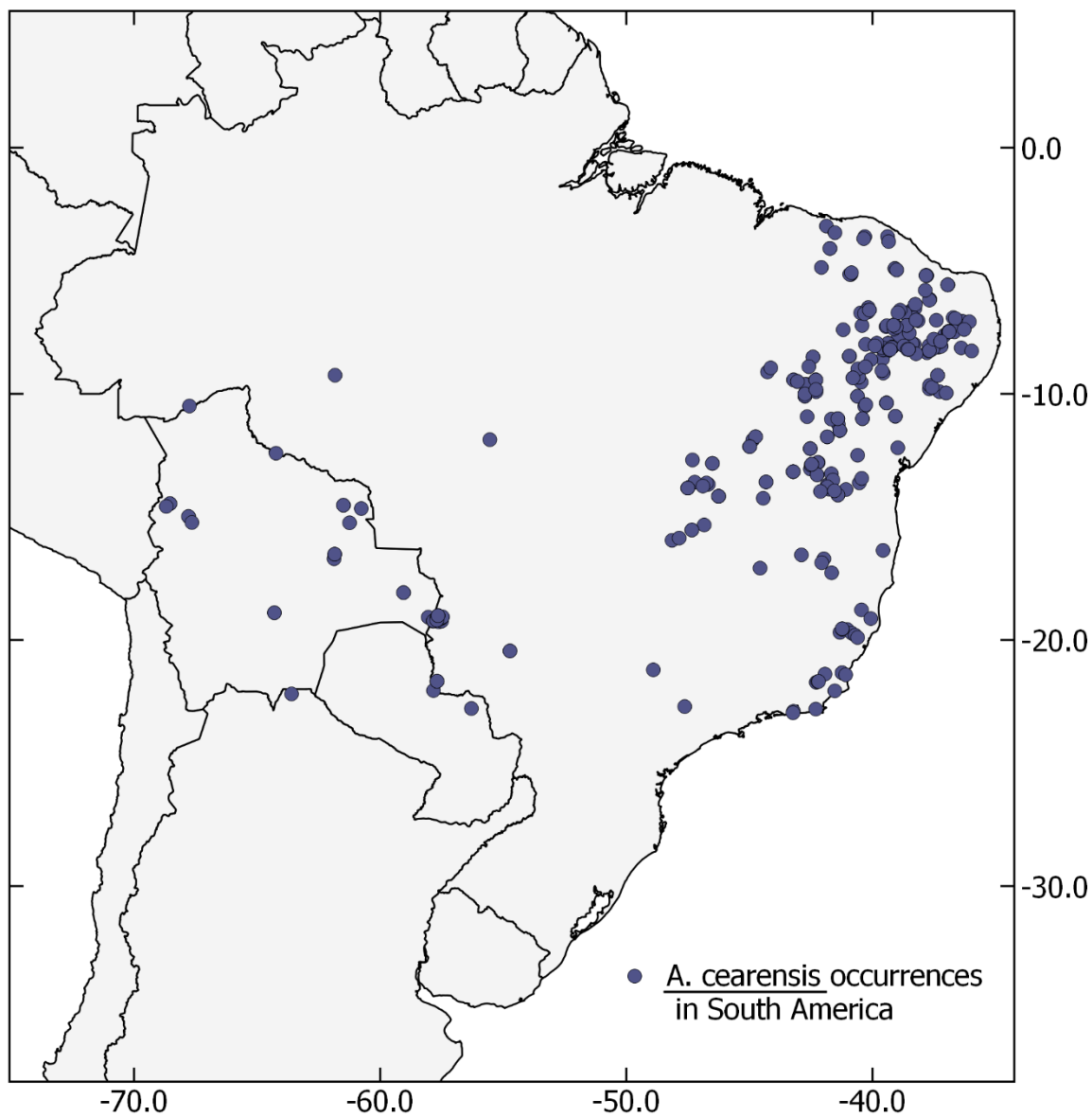


**Figure S1** – Map showing *Amburana cearensis* wide distribution across South America. Data from 516 records in (blue circles) the Global Biodiversity Information Facility – GBIF (available at GBIF.org; <https://doi.org/10.15468/dl.6vnbcy>). Decimal coordinates are show on the right and at the bottom.

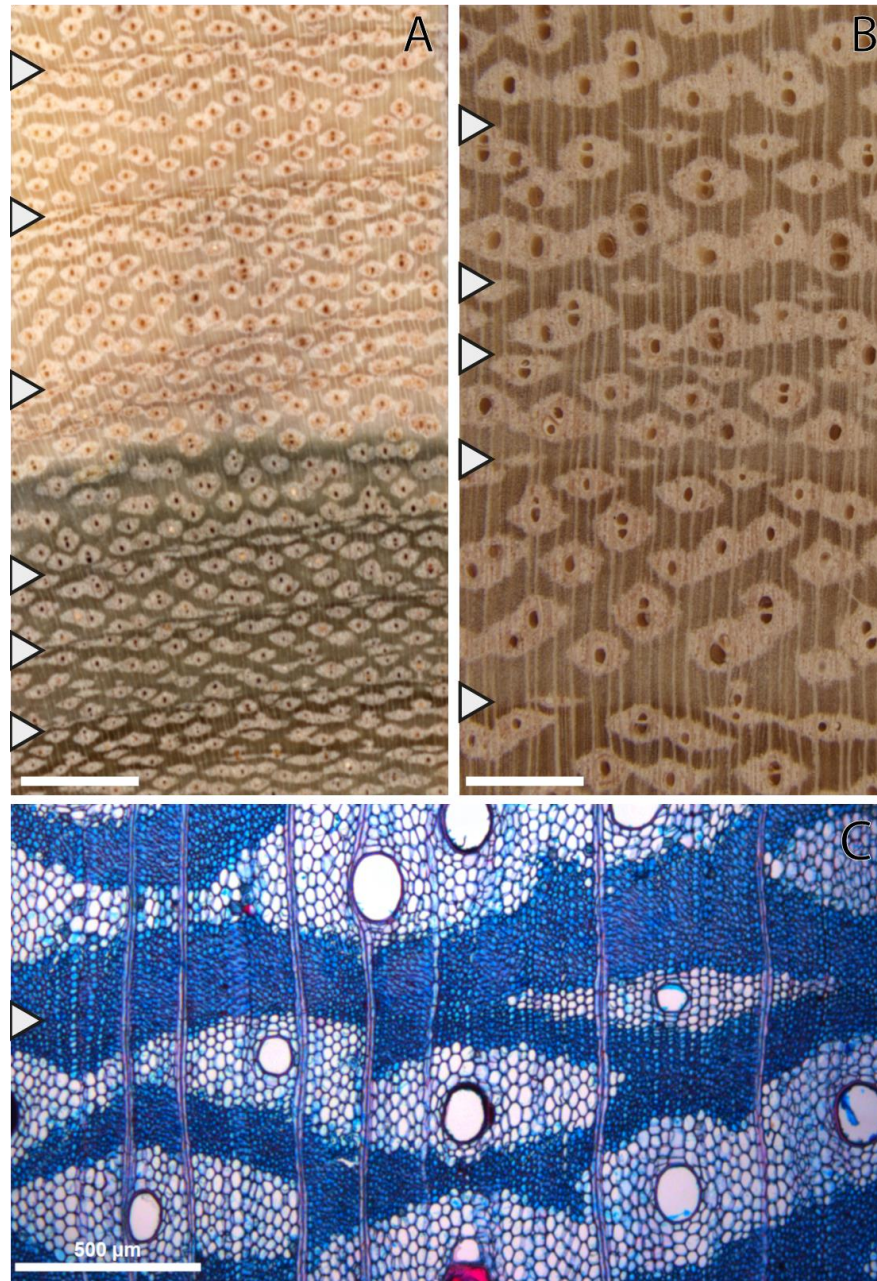


**Figure S2** - *Amburana cearensis* tree rings from macroscopic to microscopic view. In A the scanned core shows the color difference between sapwood and heartwood. B) stereomicroscope image of the core. Tree rings are delimited by half-flattened aliform parenchyma around small vessels, often with a fibre zone without vessels in the beginning of the tree ring. In C a microscopic transverse section shows in detail the tree-ring boundary, with a small vessel surrounded by half-flattened parenchyma on the right. White arrowheads indicate tree-ring boundary; Scale bars: A = 3 mm, B = 1 mm and C = 500  $\mu\text{m}$ .

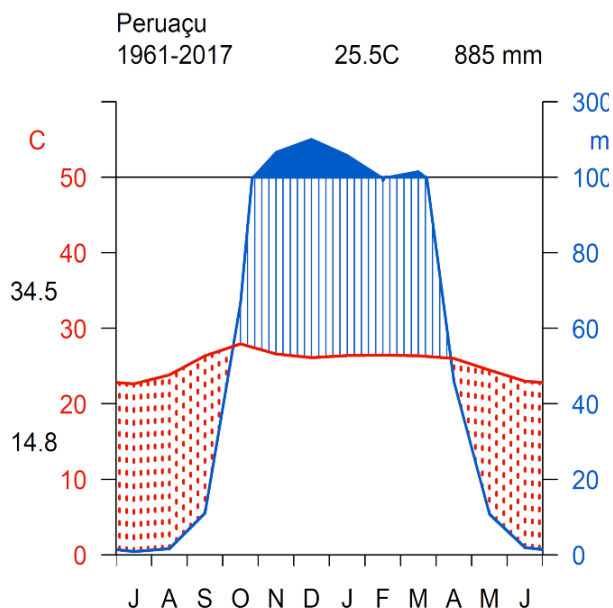


**Figure S3-** Walter-Lieth climate diagram of the local climate near the “Cavernas do Peruaçu” National Park - Minas Gerais, Brazil. Red line represents monthly averages temperature and blue line represents the monthly precipitation. Dotted area indicates the dry season and vertical lines the wet season. Data from 2017 - 1961 shows that the mean temperature in the site is around 25.5°C and total annual rainfall is 885 mm. Precipitation is below 50 mm from March until September. Mean maximum temperatures reaches 34.5°C and minimum 14.8°C.

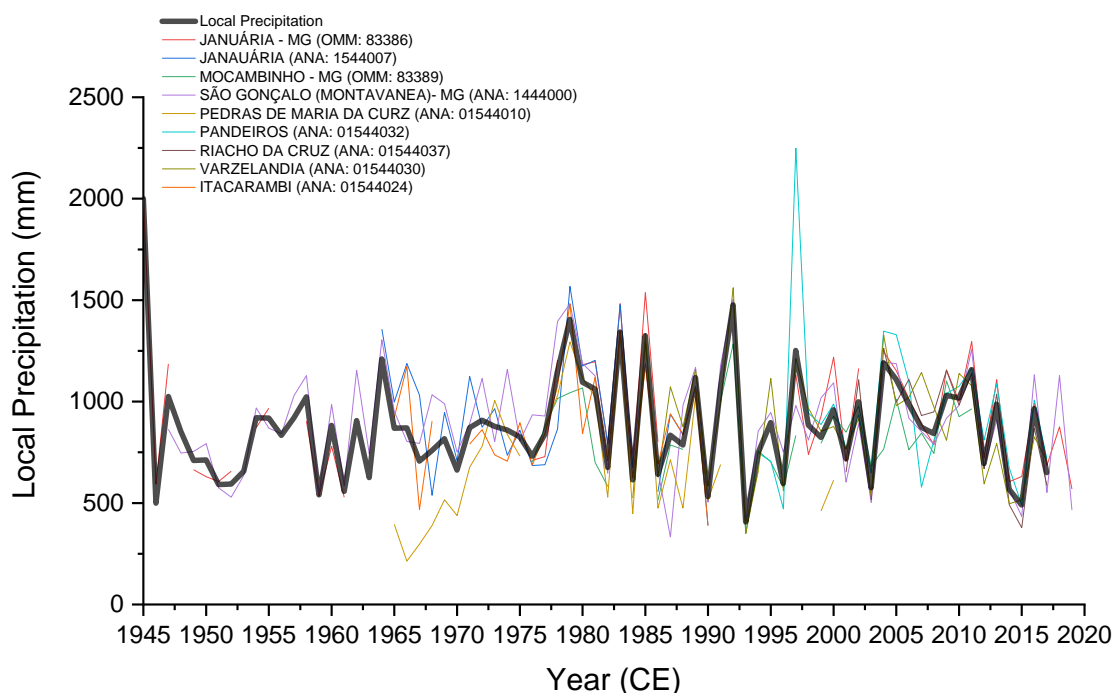


**Figure S4** – Local precipitation calculated using mean annual precipitation obtained from local meteorological stations from *Agência Nacional de Águas (ANA)* and *Instituto Nacional de Meteorologia (INMTE)*. See figure S5 for station location.



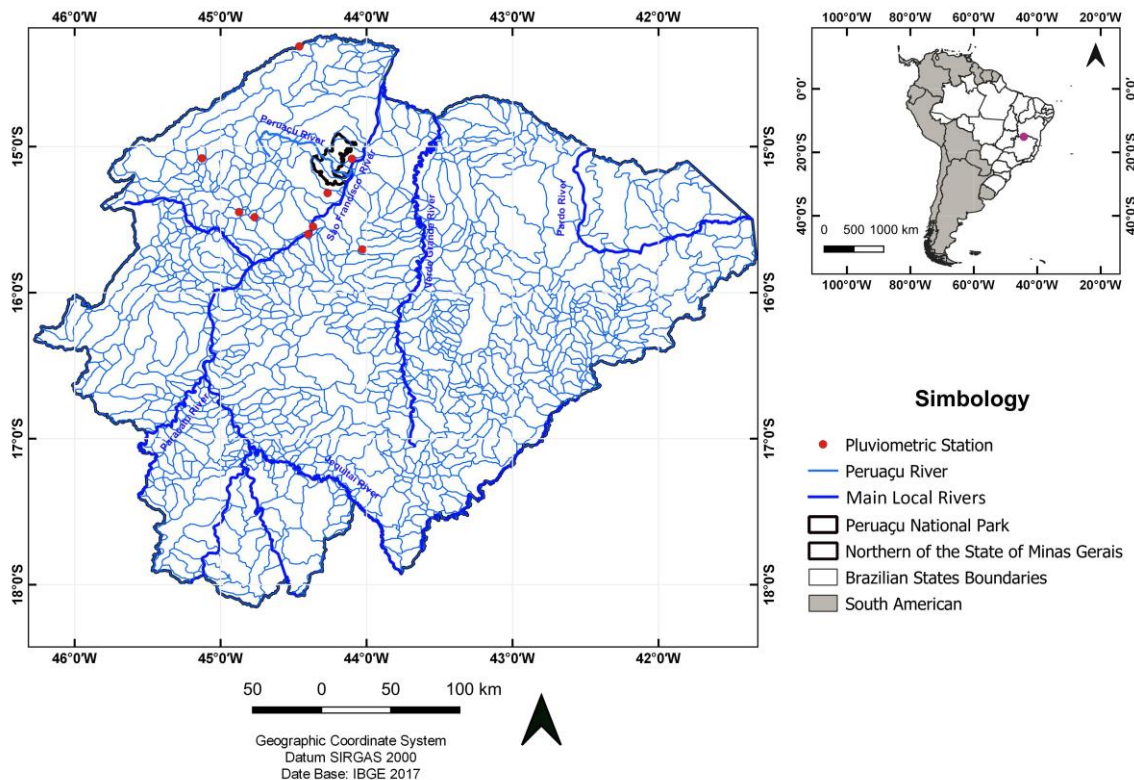


**Figure S5** – Location of the meteorological stations used in this study.

**Table S1**

List of meteorological Stations from *Instituto Nacional de Meteorologia* (INMET) and *Agência Nacional de Águas* (ANA) used in this study.

<b>Meteorological Stations</b>	<b>Latitude</b>	<b>Longitude</b>
JANUÁRIA - MG (OMM: 83386)	15°26'53.22"S	44°21'58.08"w
JANUÁRIA (ANA: 1544007)	15°28'59.88"S	44°22'0.12"w
MOCAMBINHO - MG (OMM: 83389)	15°4'48.00"S	44°0'36.00"w
SÃO GONÇALO (MONTAVANEA) - MG (ANA: 1444000)	14°18'48.96"S	44°27'37.08"w
PEDRAS DE MARIA DA CRUZ (ANA: 01544010)	15°36'0.00"S	44°24'0.00"w
PANDEIROS (ANA: 01544032)	15°28'59.16"S	44°46'1.92"w
RIACHO DA CRUZ (ANA: 01544037)	15°19'4.08"S	44°16'0.12"w
VARZELANDIA (ANA: 01544030)	15°42'15.12"S	44°1'42.96"w
ITACARAMBI (ANA: 01544024)	15°5'0.00"S	44°6'0.00"w



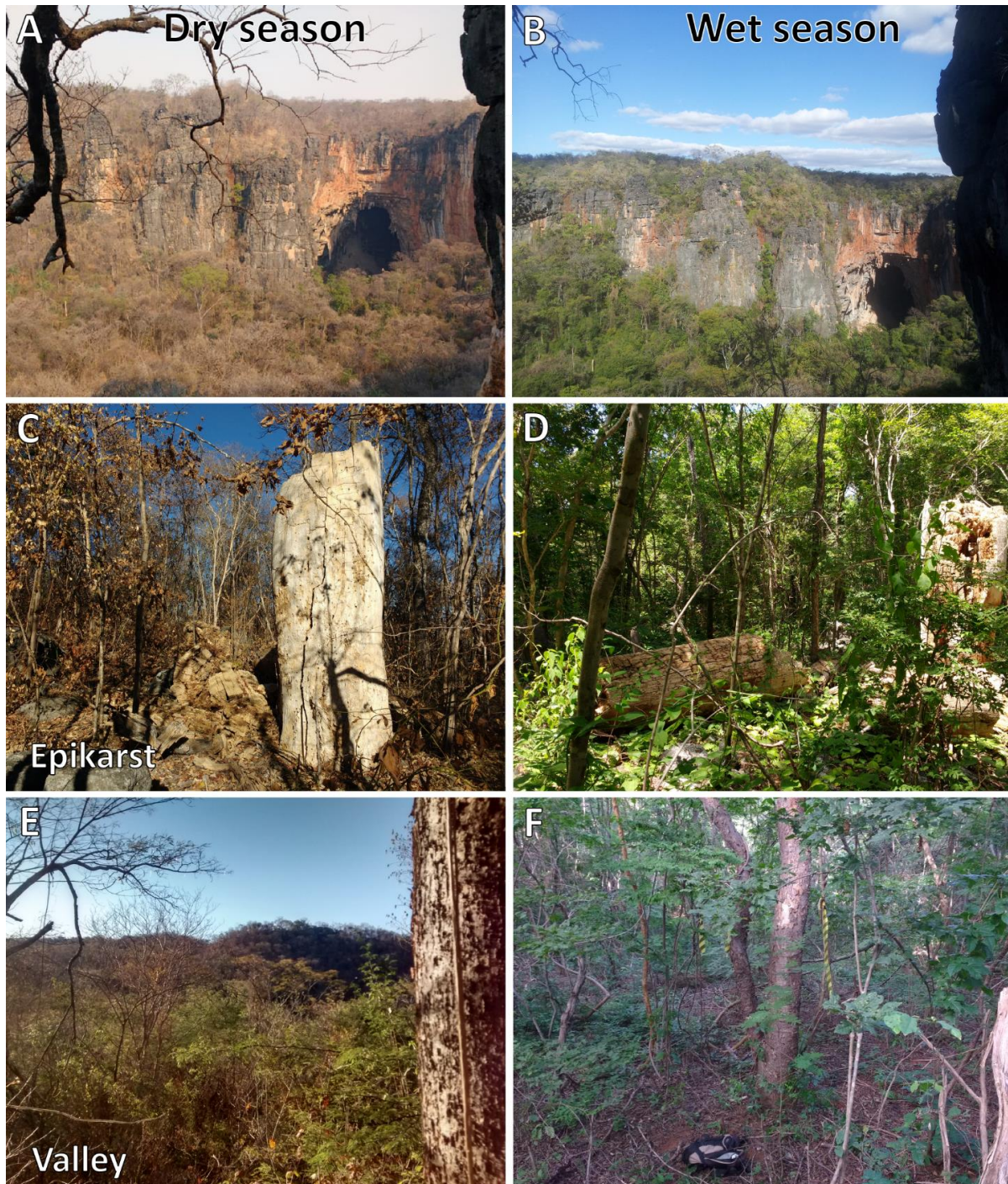


**Figure S6** – Different sampling sites in different seasons. The pictures on the left were obtained in dry season and the panels on the right in the wet season, kindly provided by Luciano Fioroto Redondo. The pictures show different landscapes (A and B) and micro-environments at the epikarst (C and D) and at the valley (E and F).



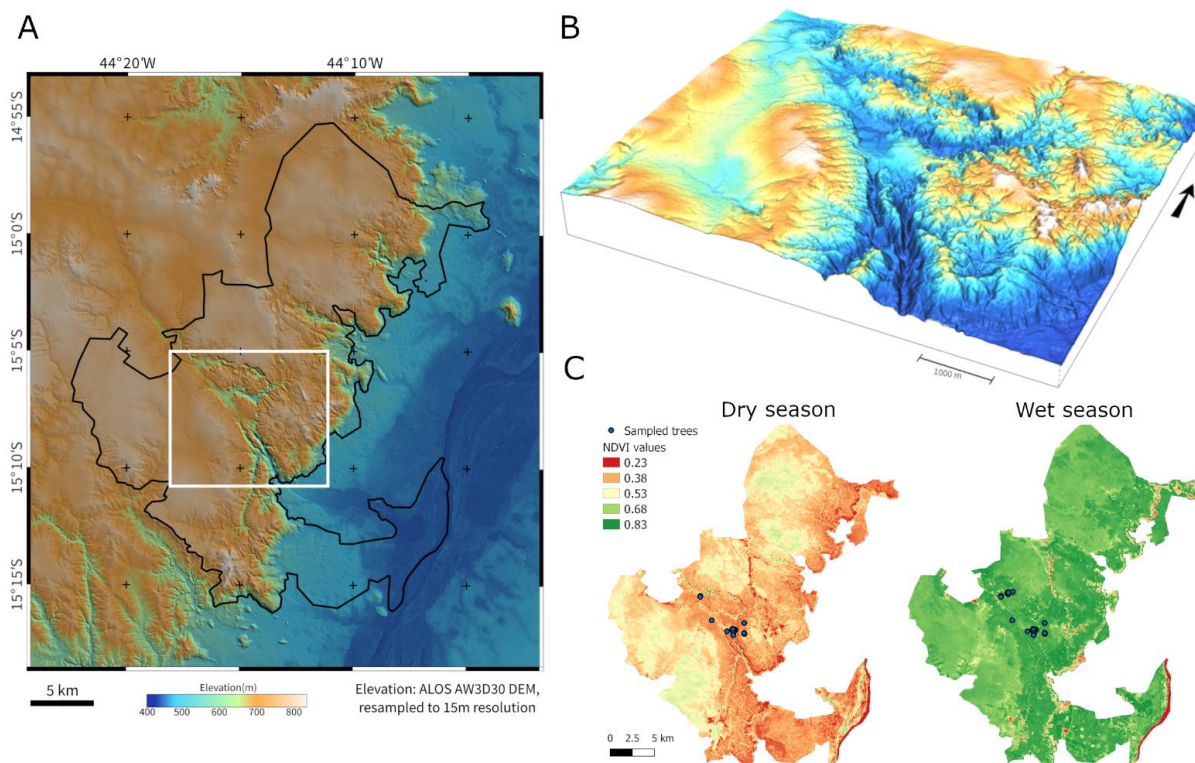


**Figure S7** – Site characterization using satellite images. In A the elevation profile of the region is shown. The white square is detailed in B in a 3D model, highlighting the elevation difference in the landscape. In C are shown the images used to calculate the Normalized Difference Vegetation Index (NDVI) ratio. Images were taken in the dry Season (Landsat 8 OLI satellite image LO82190702019197CUB00) and the wet season (LO82190702018354CUB00) both downloaded from the Brazilian National Institute of Space Research web catalog - INPE - <http://www.dgi.inpe.br/catalogo/>.



**Figure S8** – Anatomical markers in removed radii from trees still in the chronology and radii from removed trees. For every common problem cited on the left, two scanned images are showed. For scale reference, the maximum diameter of the wood core is showed: the cores without numbers are 5mm standard cores; the others are from 10mm; or 15 mm samples. Because these samples were removed due to lack of satisfying cross-date or even before, the white arrowheads aim to indicate true tree rings and the gray arrowheads points the anatomical marker in question. Sample number from the top left to bottom right: 7562G, 7492C, 7558B, 7554D, 8004C, 7544B, 7489B, 7541D, 7506C (10 mm), 7541B, 7557A, 7549A, 8012C (15 mm), 7546A (10 mm).

**Table S2**

Radiocarbon results for every tree and selected tree ring. The most likely results are in bold letters.

RTD	SPFw	Dendro year	Dating difference	F <sup>14</sup> C ±1σ		Calibrated year (1σ) AD	Calibrated year (2σ) AD	δ <sup>13</sup> C (‰) ±0.02
							<b>1959.9 to 1962.3 (48.5%)</b>	
10284	8005	1960	0 to 1 year	1.19553	0.00314	1960.6 to 1961.4 (32.9%) 1986.2 to 1987.1 (35.3%)	1963.0 to 1963.1 (1.0%) 1985.3 to 1985.7 (5.6%) 1986.1 to 1987.2 (36.5%) 1987.9 to 1988.2 (3.8%)	-29.49
10283	8005	1965 Earlywood 1	0	1.62877	0.00377	1964.8 to 1965.0 (18.5%) 1966.2 to 1966.9 (49.7%)	1964.7 to 1965.5 (35.8%) <b>1965.7 to 1967.1 (59.6%)</b>	-28.04
10282	8005	1965 Earlywood 2	0	1.63445	0.00377	1964.7 to 1965.3 (24.0%) 1965.8 to 1966.8 (44.2%)	<b>1964.7 to 1967.0 (95.4%)</b>	-27.8
10281	8005	1965 Earlywood 3	0	1.63978	0.00371	1964.9 to 1965.4 (21.3%) 1965.7 to 1966.4 (46.9%)	<b>1964.8 to 1966.9 (95.4%)</b>	-27.53
10280	8005	1965 Earlywood 4	0	1.63423	0.00378	1964.7 to 1965.3 (24.1%) 1965.8 to 1966.9 (44.1%)	<b>1964.7 to 1967.0 (95.4%)</b>	-26.98
10279	8005	1965 Latewood 5	0	1.62884	0.00374	1964.8 to 1965.0 (18.6%) 1966.2 to 1966.9 (49.6%)	<b>1964.7 to 1967.1 (95.4%)</b>	-26.88
10278	8005	1965 Latewood 6	0	1.62563	0.00372	1964.8 to 1965.0 (14.0%) 1966.3 to 1966.9 (54.2%)	1964.7 to 1965.6 (31.3%) <b>1966.1 to 1967.2 (64.1%)</b>	-26.64
10277	8005	1965 Latewood 7	0	1.62606	0.00378	1964.8 to 1964.9 (13.8%) 1966.2 to 1966.9 (54.4%)	1964.7 to 1965.6 (32.4%) <b>1966.1 to 1967.2 (63.0%)</b>	-26.67
10276	8005	1965 latewood 8	0	1.6221	0.0037	1966.3 to 1967.2 (68.2%)	1964.7 to 1965.6 (21.6%) <b>1966.1 to 1967.4 (73.8%)</b>	-25.8
10438	8005	1980 Earlywood	0 to 1 year	1.27629	0.0031	1980.3 to 1981.3 (68.2%)	1962.5 to 1963.4 (17.9%) <b>1980.2 to 1981.4 (71.8%)</b>	-26.4
10437	8005	2001 Latewood	0 to 1 year	1.09414	0.00282	2000.2 to 2001.6 (68.2%)	1981.9 to 1982.2 (5.7%) 1958.6 to 1958.7 (0.4%) <b>1999.5 to 2002.4 (91.2%)</b>	-26.42
							2002.9 to 2003.2 (3.8%)	

10212	7486	1960	1 to 2 years	1.22236	0.00241	1983.5 to 1983.5 (0.7%) 1983.8 to 1985.1 (67.5%)	<b>1961.9 to 1962.5 (8.2%)</b> 1963.0 to 1963.1 (1.9%) 1983.3 to 1985.2 (85.3%)	-27.62
10211	7486	1965 Earlywood	0 to 1 year	1.62897	0.00287	1964.7 to 1965.0 (21.2%) 1966.2 to 1966.8 (47.0%)	<b>1964.7 to 1967.0 (95.4%)</b>	-27.56
10210	7486	1965 Latewood	0 to 1 year	1.62529	0.00282	1964.8 to 1965.0 (13.4%) 1966.3 to 1967.0 (54.8%)	1964.7 to 1965.5 (30.3%) <b>1966.1 to 1967.2 (65.1%)</b>	-27.8
10440	7486	1980 Latewood	0 to 1 year	1.27268	0.0031	1962.7 to 1962.9 (8.6%) 1980.4 to 1981.4 (59.6%)	1962.6 to 1963.3 (17.8%) <b>1980.3 to 1981.5 (70.3%)</b> 1981.9 to 1982.2 (7.3%)	-26.78
10439	7486	2001 Latewood	0 to 1 year	1.09235	0.00284	2000.3 to 2002.3 (68.2%)	1958.6 to 1958.7 (1.3%) 1999.5 to 1999.8 (2.9%) <b>2000.1 to 2002.5 (81.9%)</b> 2002.7 to 2003.4 (9.4%)	-26.41
10390	7538	1960 Earlywood	0 to 1 years	1.20592	0.00297	1961.8 to 1962.2 (8.9%) 1985.1 to 1986.7 (59.3%)	<b>1960.7 to 1962.4 (26.5%)</b> 1962.9 to 1963.2 (2.3%) 1984.5 to 1984.8 (2.5%) 1985.1 to 1986.8 (64.2%)	-27.6
10391	7538	1960 Latewood	0 to 1 year	1.20704	0.00299	1961.8 to 1962.2 (11.3%) 1985.1 to 1986.2 (56.9%)	<b>1960.8 to 1962.4 (23.5%)</b> 1962.9 to 1963.2 (2.4%) 1984.5 to 1986.8 (69.5%)	-26.2
10392	7538	1964 Earlywood	0 to 1 year	1.62402	0.00342	1966.3 to 1967.1 (68.2%)	<b>1964.7 to 1965.6 (27.1%)</b> 1966.1 to 1967.2 (68.3%)	-28.2
10393	7538	1964 Latewood	0 to 1 year	1.62436	0.00354	1964.8 to 1964.9 (8.4%) 1966.3 to 1967.1 (59.8%)	<b>1964.7 to 1965.6 (28.1%)</b> 1966.1 to 1967.2 (67.3%)	-27.9

RTD: Radiocarbon laboratory access number; SPFW: Xylarium number of the sample; Dendro Year: the cross-dated year; Dating difference: The difference between the year attributed with cross-dating minus 14C year; F14C: Fraction of modern carbon and measurement uncertainty; Calibration: Probability (one and two sigma) distribution after calibration using the Southern Hemisphere Zones 1&2, from Hua *et al.*, 2013;  $\delta^{13}C$ : obtained with IRMS (fixed standard deviation).



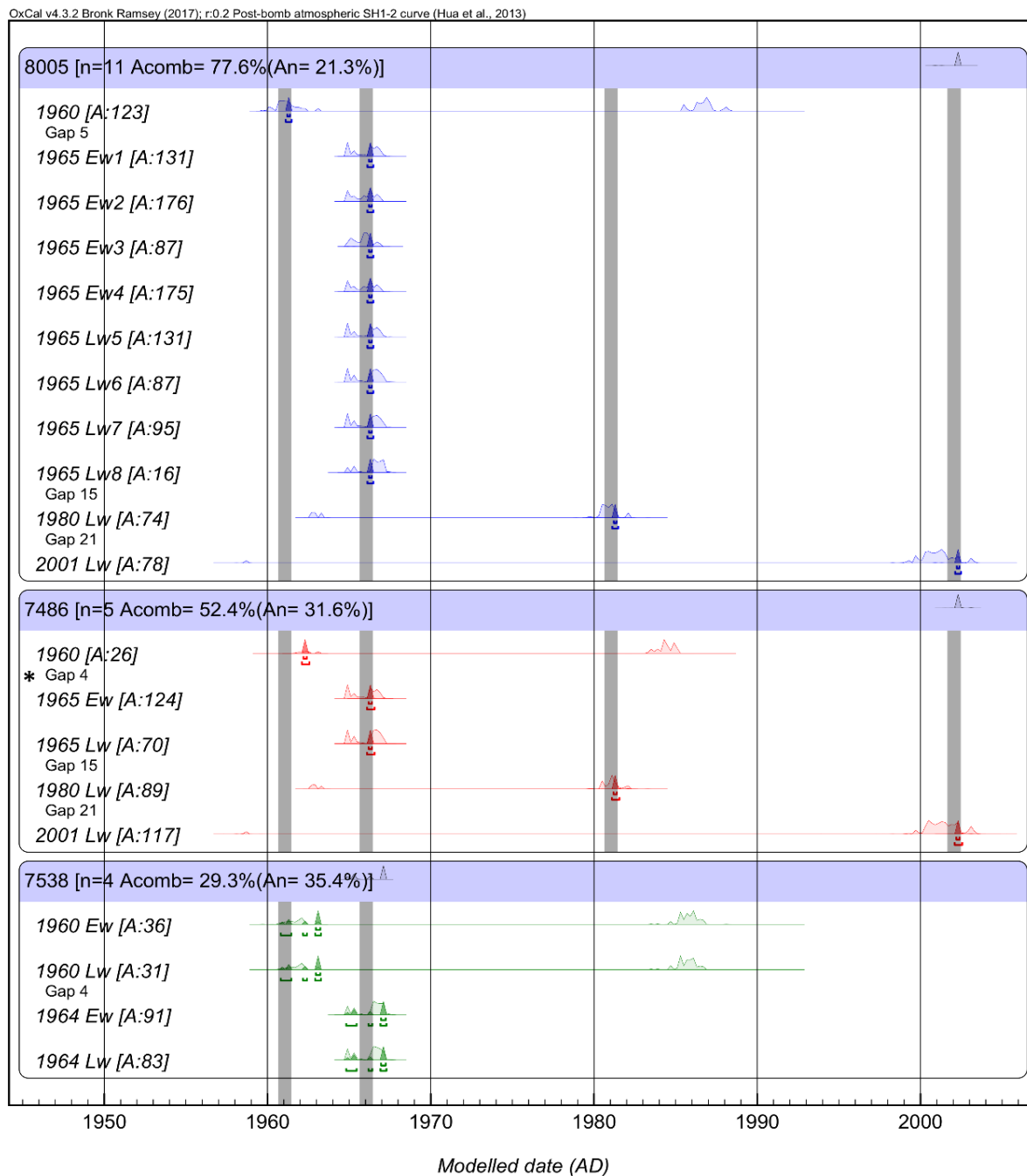


**Figure S9** – Multiplot of modeled  $^{14}\text{C}$  probability distribution for all samples (OxCal v4.3.2 Ramsey (2009); using the D\_sequence according to Ramsey et al., (2001)), based on the Post-bomb atmospheric Southern Hemisphere zones 1-2 curve (Hua et al., 2013). Tree identification of each sample is enlarged (four numbers from the SPFW collection). The cross dated year is showed on the left, followed by the measured region of the ring (Ew = earlywood, defined as the first half of the tree ring; Lw = the second half of the tree ring).

The shaded bars indicate the expected date. \* = the dendrochronological gap is actually 5 years; however, the calibration starts with the oldest ring and this order pushed the following dates one year forward. Therefore, it is more likely the dating error is on the oldest rings, because of higher sample coverage in the recent years and the cross-dating method that starts with last year formed, so the amount of dating errors increase from bark to pith and we choose to present the best model.

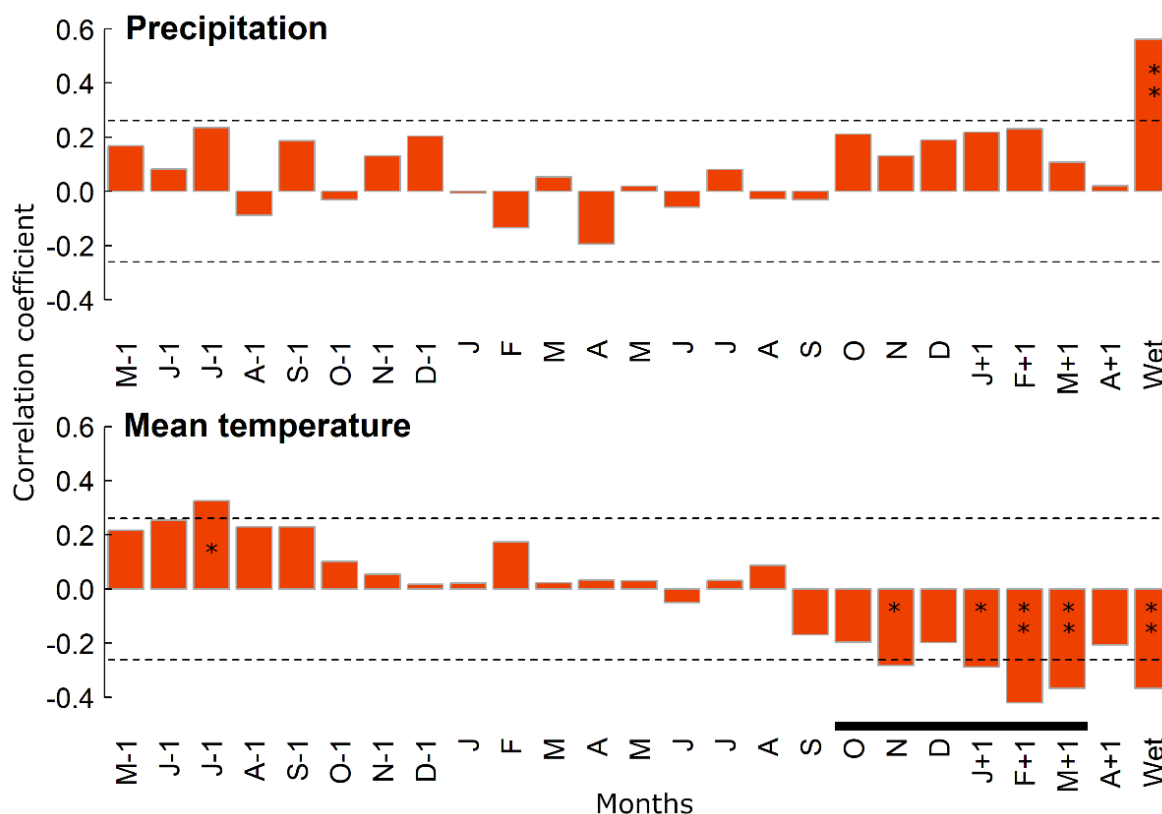


**Figure S10** – Monthly climate correlations of the chronology with mean temperature and precipitation. Dotted line is the 95% confidence interval. Asterisks indicate statistical significance: \* $p < 0.05$ , \*\*  $p < 0.01$  for the correlation analysis between monthly temperature and growth. Black thick line is indicating the current growing season.

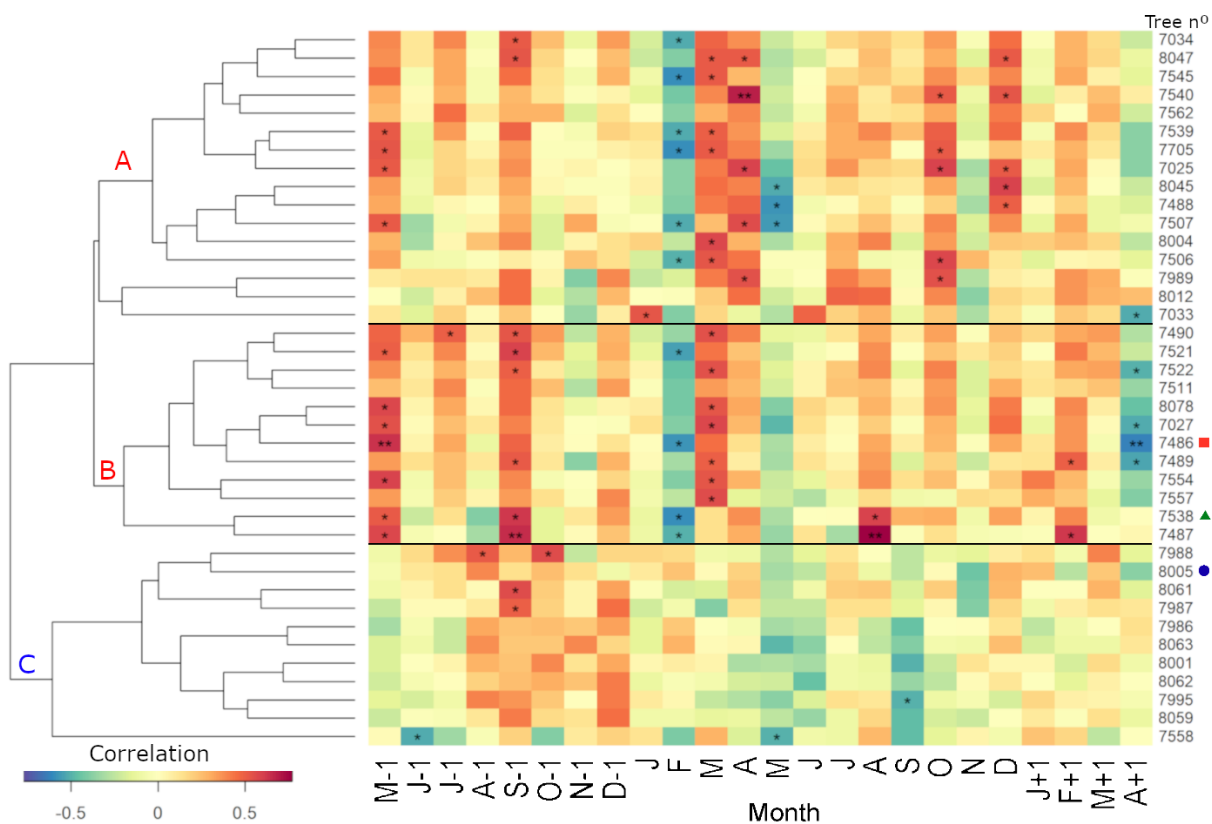


**Figure S11** – Heatmaps detailing the results of hierarchical clustering analysis based on the monthly correlation values between growth of individual trees and precipitation. The number of the sampled trees are indicated on the right; symbols indicate the trees selected for <sup>14</sup>C dating (same as in Figure 2). Asterisks indicate statistical significance: \*p < 0.05, \*\* p < 0.01 for the correlation analyses between monthly precipitation and growth. Black thick line is indicating the current growing season.

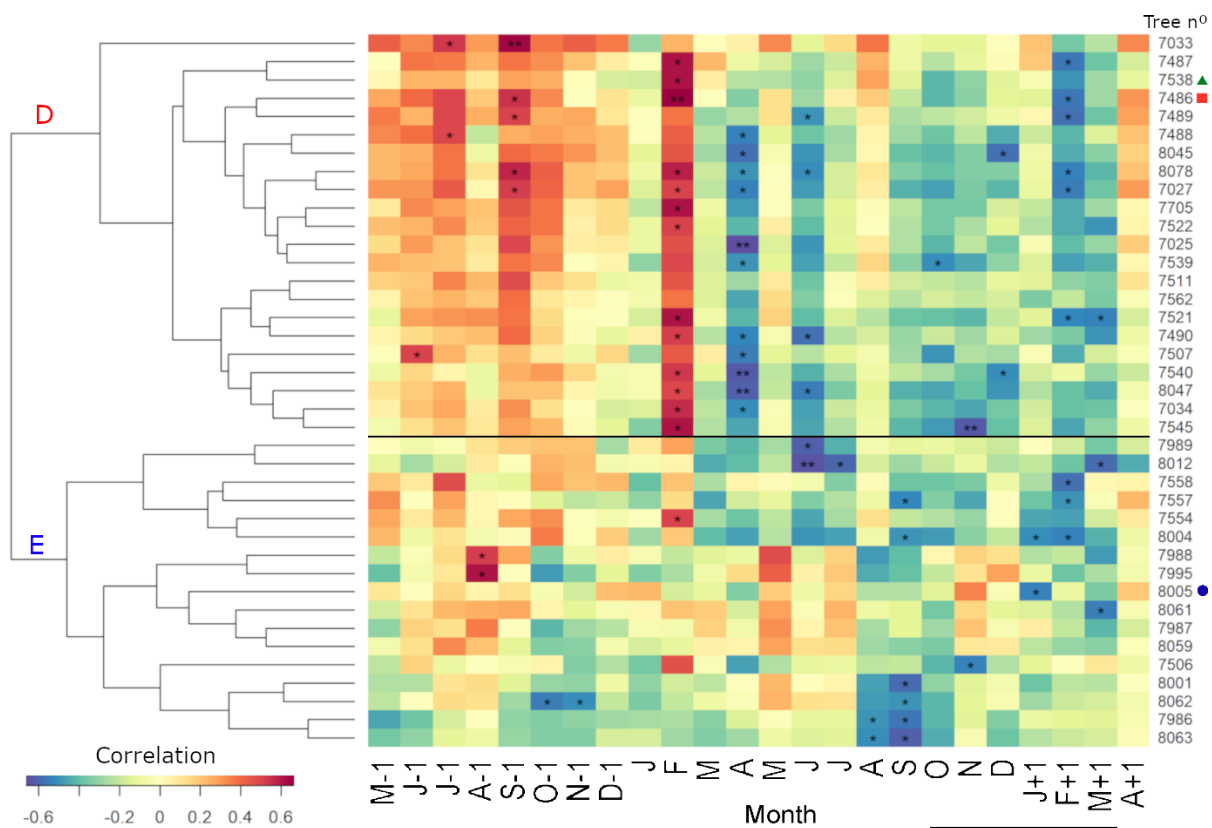
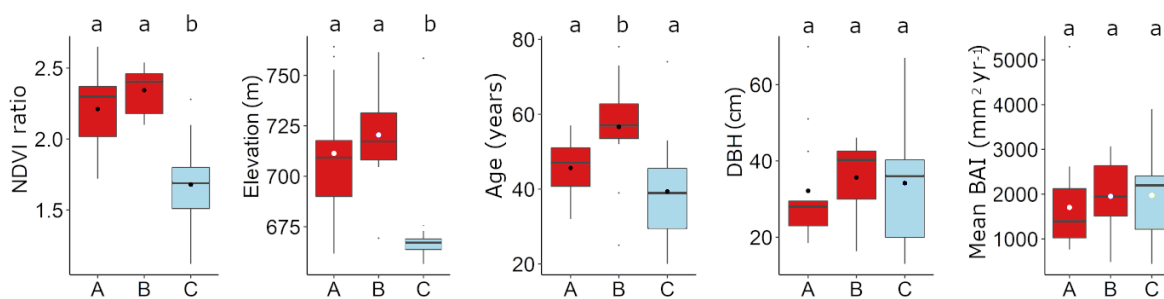


**Figure S12** – Heatmaps detailing the results of hierarchical clustering analysis based on the monthly correlation values between growth of individual trees and temperature. The number of the sampled trees are indicated on the right; symbols indicate the trees selected for 14C dating (same as in Figure 2 and 4). Asterisks indicate statistical significance: \* $p < 0.05$ , \*\*  $p < 0.01$  for the correlation analyses between monthly temperature and growth. Black thick line is indicating the current growing season.

## Precipitation



## Temperature

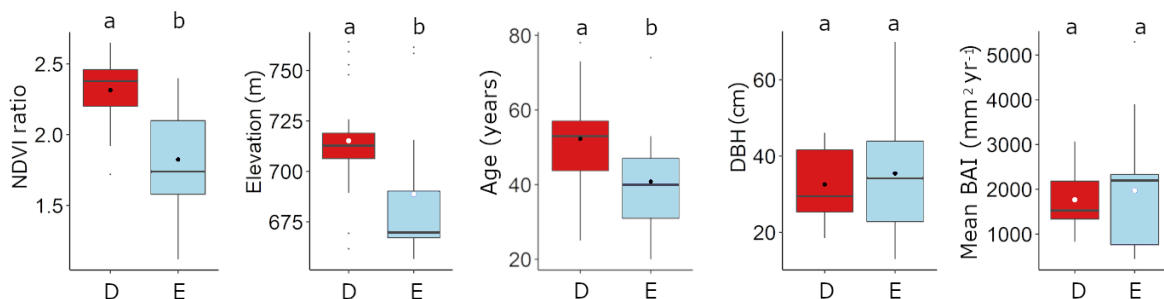


**Figure S13** – Individual-tree metadata to characterize the possible drivers of the observed climate-growth clusters for precipitation (top) and temperature (bottom). The boxplots are the individual trees' score of NDVI ratio (value from the wet season divided by dry season), age, elevation, BAI and height compared per group. Red boxplots is the sensitive group and blue is the complacent group. Letters "a" and "b" in small case are indicate statistically different statistical groups.



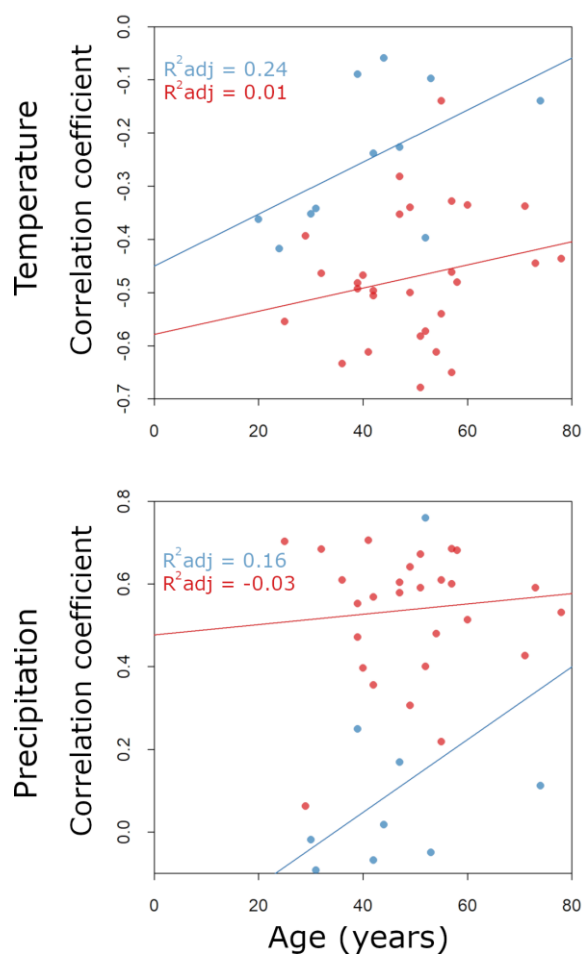


**Figure S14** – Scatter plots and linear models of individual tree correlation with wet season climate according to age. There is no significant correlation (all  $p$  values were above 5%) between tree age and tree sensitivity. Red dots are the sensitive trees and blue are the complacent trees.

**Table S3**

Diagnostics of the two *Amburana cearensis* tree-ring width chronologies built after the cluster analysis

	Sensitive	Complacent
Number of trees/radii	28/83	11/29
Series intercorrelation <sup>a</sup>	0.68	0.62
Sensitivity <sup>a</sup>	0.51	0.54
Absent rings (%) <sup>a</sup>	0.37	0.78
Time Span	1947-2018	1945-2018
rbar	0.49	0.46
EPS	0.91	0.81

<sup>a</sup>data from COFECHA

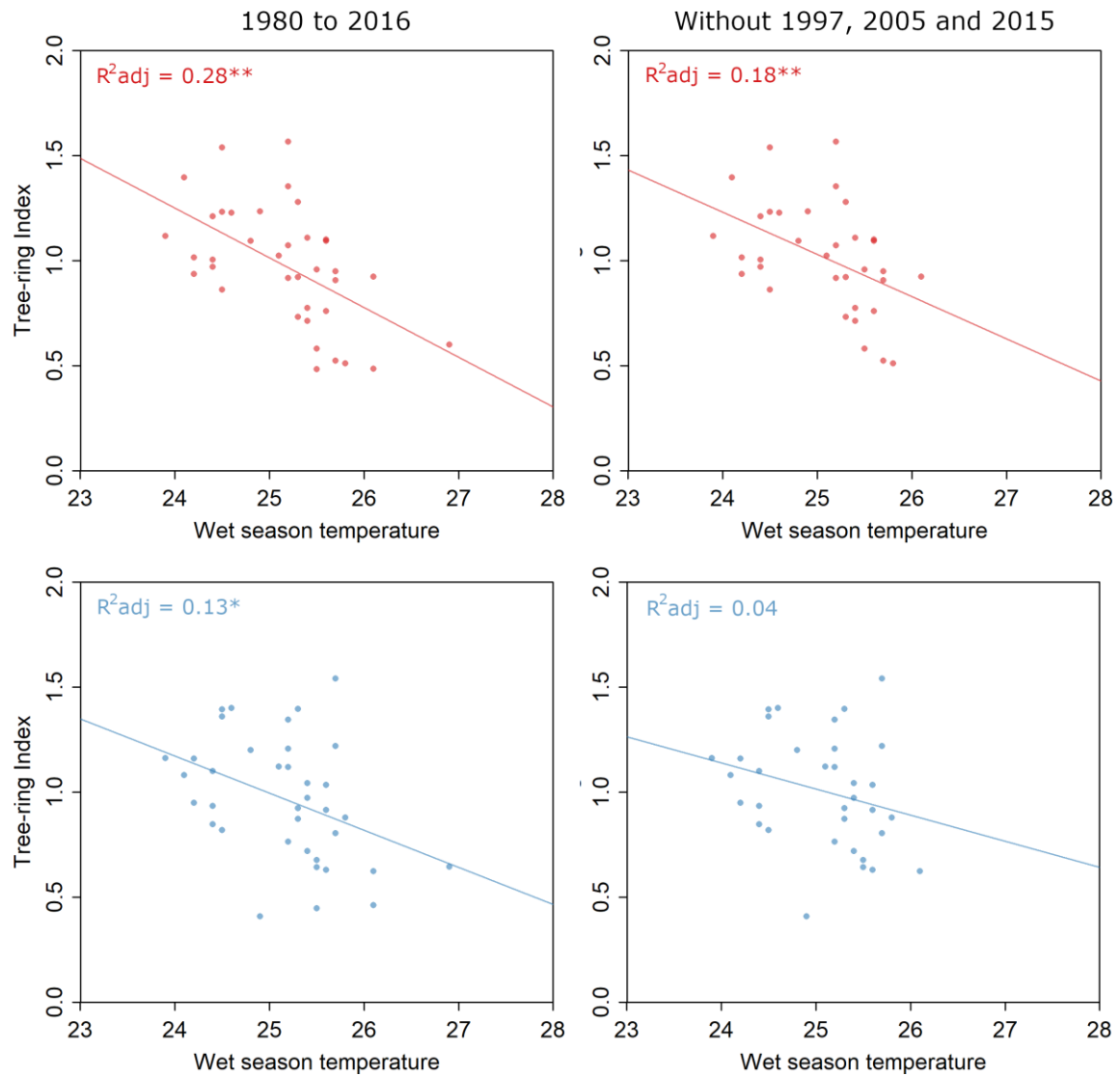


**Figure S15** – Scatter plots of tree-ring index and wet season temperature for sensitive and complacent chronologies covering the whole period from 1980 to 2016 and without the pointer years (1997 and 2005) and the hottest year of the climate record (2015). Red and top panels are for sensitive trees; blue and bottom panels for the complacent trees chronology. The adjusted R squared of the linear models show is shown for every case. Asterisks indicate statistical significance: \* $p < 0.05$ , \*\*  $p < 0.01$  for the correlation analyses between monthly temperature and growth.

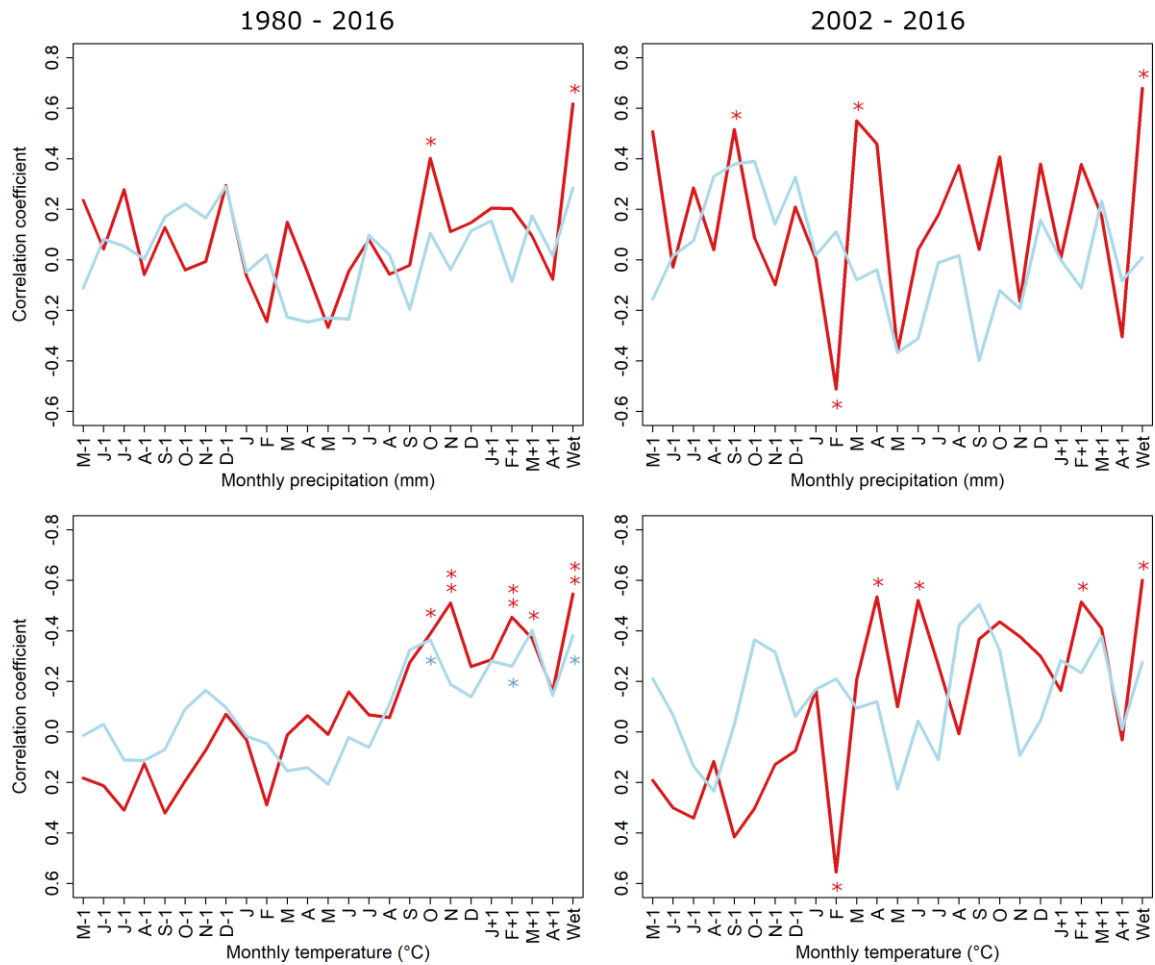


**Figure S16** – Monthly climate correlations of the two chronologies with mean temperature and precipitation for two periods. Red line is the sensitive trees chronology and blue is the complacent trees chronology. Asterisks indicate statistical significance: \* $p < 0.05$ , \*\*  $p < 0.01$  for the correlation analysis between monthly temperature and growth.

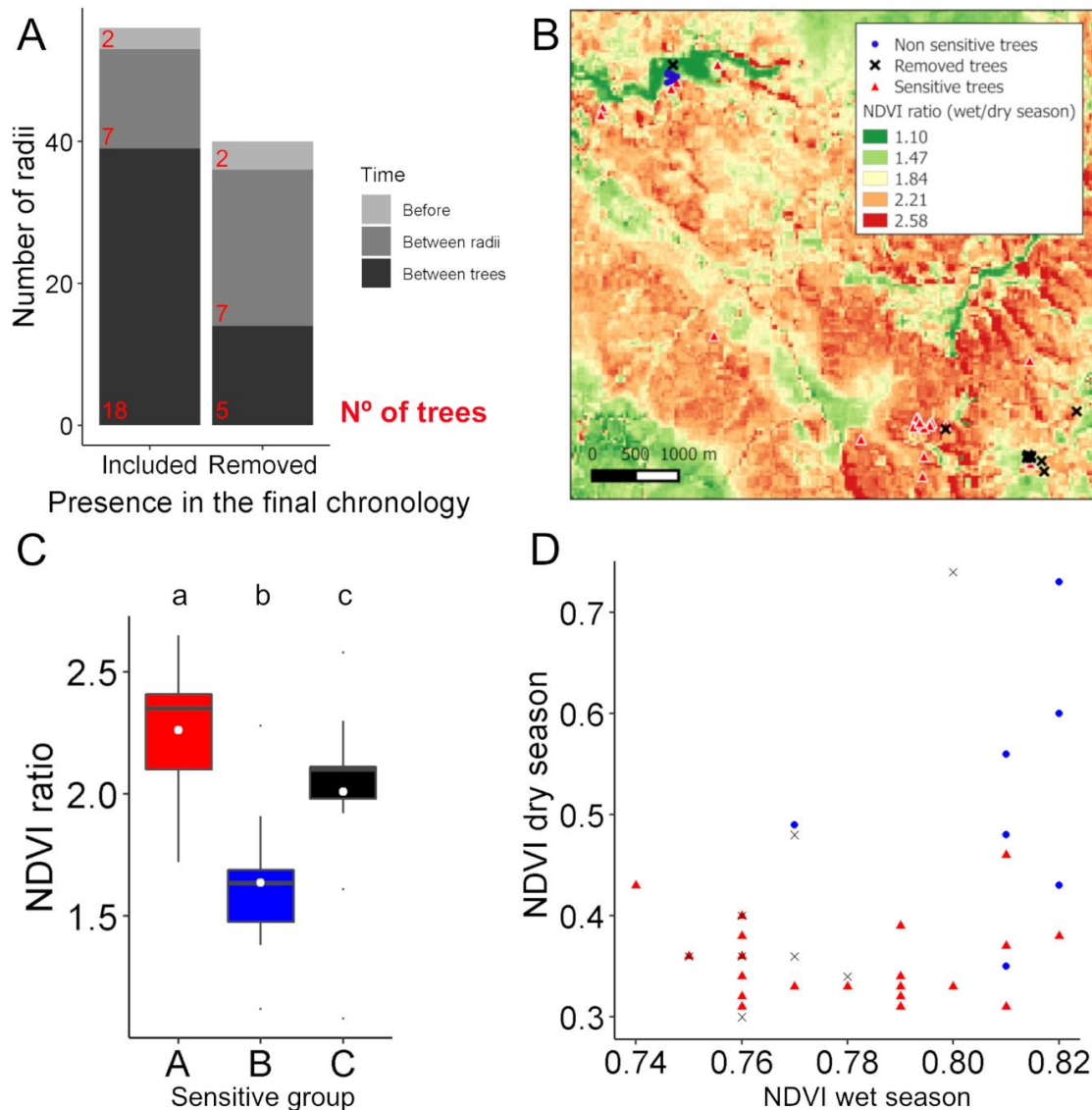


**Figure S17** – Analysis of removed radii and trees. A) Number of radii of trees that have at least two radii in the chronology, and number of radii of trees entirely removed from the final chronology. The removal of samples happened in three different moments (Time), from the light gray to dark gray: radii removed before tree-ring counting (e.g. scars, twisted core); during visual cross-dating amongst radii of the same tree; and after verification with COFECHA. B) Location in the study site of all sampled trees. C) NDVI ratio of the sensitive trees (red), non-sensitive/complacent trees (blue) and removed trees (black), A, B, C, respectively. The letters in small case are different statistical groups. D) NDVI values of the wet and dry season. Colors for the different groups are the same in all figures: red for sensitive trees; blue for non-sensitive/complacent trees; black for removed trees.

## Capítulo 3

---

*Tree growth does not decline due to increasing VPD in seasonally  
dry tropical forest*

Crescimento de árvores expostas ao aumento de VPD não é afetado  
em floresta tropical sazonalmente seca

Milena Godoy-Veiga, Gabriel Assis-Pereira, Bruno Barçante Ladvocat Cintra,  
Nicolás Misailidis Stríkis, Marília Harumi Shimizu, Francisco William da Cruz,  
Lior Regev, Elisabetta Boaretto, Ana Carolina Maioli Campos Barbosa, Mario  
Tomazzelo-Filho, Gregório Ceccantini, Veronica Angyalossy, Laia Andreu-Hailes,  
Giuliano Maselli Locosselli.

Artigo será submetido à *Nature*, *PNAS* ou *Global Change Biology*



## Abstract

The intensification of atmospheric vapor pressure deficit (VPD) caused by global warming is known to negatively impact trees and forest biomass gain in the tropics. The largest Seasonally Dry Tropical Forests (SDTF) in South America are located in central-eastern Brazil, in a tropical hotspot of warming. High evaporative demands during recent decades may be increasing the vulnerability of SDTF, which are intrinsically constrained by water availability. However, long-term effects of high VPD are poorly understood in situ yet. Instrumental climate data, air mass back trajectories, recent  $\delta^{18}\text{O}$  rainfall monitoring, and millennium-long  $\delta^{18}\text{O}$  records from local speleothems consistently show an increase in evaporative demands since the 1980s. Local trees share similar increasing  $\delta^{18}\text{O}$  trend ( $\beta = 0.05\text{‰ yr}^{-1}$ ) in multi-centennial tree-ring series from *Amburana cearensis* and *Cedrela fissilis* populations. Most of our stable isotope models estimates up to 70% of tree-ring  $\delta^{18}\text{O}$  enrichment explained by the observed changes in VPD, but despite the increasing evaporative demand, no growth decline in any diameter class of trees was observed. Furthermore, a rare set of subfossil tree-ring records of *A. cearensis* do not show any clear growth changes during the Little Ice Age when abrupt changes in radiative forcing also led to increases in tree-ring  $\delta^{18}\text{O}$ . Therefore, no evidence has been found so far indicating a VPD induced sustained decline on tree growth in this SDTF, except during extreme years. This points out that rainfall is still the main driver of biomass gain in this hotspot of warming. The results indicate large resistance of the SDTF to abrupt changes in climate, suggesting an overestimation of VPD impacts on the carbon cycle and vegetation models.

**Keywords:** Global warming, tree resistance, oxygen isotopes, speleothems, paleoclimate.

## Resumo

A intensificação no déficit de vapor hídrico (VPD) causada pelo aquecimento global é tida como prejudicial ao ganho de biomassa de árvores e florestas nos trópicos. A maior área contínua de florestas tropicais sazonalmente secas (SDTF) na América do Sul está localizada na região centro-leste do Brasil, um *hot spot* de aumento de temperaturas nos trópicos. A alta demanda evaporativa nas últimas décadas pode aumentar a vulnerabilidade das SDTF as quais já são intrinsecamente restringidas pela disponibilidade hídrica local. Entretanto, os efeitos a longo prazo do aumento no VPD ainda são poucos compreendidos. Registros climáticos instrumentais, trajetórias de massas de ar, monitoramento de  $\delta^{18}\text{O}$  da água da chuva e registros milenares de  $\delta^{18}\text{O}$  de espeleotemas locais mostram o aumento de VPD a partir da década de 1980. As árvores locais compartilham deste aumento em cronologias centenárias de  $\delta^{18}\text{O}$  ( $\beta = 0.05\text{‰ yr}^{-1}$ ) de *Amburana cearensis* e *Cedrela fissilis*. A maioria dos nossos modelos isotópico estimou até 70% do enriquecimento na série de  $\delta^{18}\text{O}$  explicada pelo aumento no VPD, mas mesmo com o aumento na demanda evaporativa não foi observada redução nas taxas de crescimento em nenhuma classe de diâmetro. Além disso, os registros subfósseis de *A. cearensis* não mostram nenhum sinal claro de mudanças de crescimento durante um período de alterações nas forçantes radiativas locais na metade da Pequena Idade do Gelo que também ocasionou um aumento na série de  $\delta^{18}\text{O}$ . Portanto, nenhuma evidência foi encontrada de que o VPD limita o crescimento das árvores analisadas nessa SDTF. Esses resultados apontam para a quantidade de chuva como principal fator limitante ao acúmulo de biomassa nesse *hot spot* de aumento de temperatura nos trópicos. Isso indica uma resistência das SDTF às mudanças abruptas no clima, sugerindo uma superestimação dos impactos de alto VPD no balanço de carbono em modelos de resposta de vegetação nos trópicos.

**Palavras-chave:** Aquecimento global, resitência de árvores, isótopos de oxigênio, espeleotemas, paleoclima.

## Introduction

Global warming increases the capacity of atmosphere to hold water pushing vapor pressure deficit (VPD) worldwide<sup>1,2</sup>. Increases in VPD are of great concern because it is currently known to be one of the main drivers of leaf physiology and consequently plant development<sup>3-5</sup>. By affecting growth, high evaporative demands can directly constrain biomass gain of forests worldwide that are major sinks in the global carbon cycle<sup>6,7</sup>. This is especially relevant for tropical forests which are the most productive terrestrial ecosystems<sup>8</sup> and hold around 262 Pg C of above and below ground biomass<sup>7</sup>. Trees link with the carbon cycle through stomatal conductance and assimilation through photosynthesis, both of which may be limited under high VPD as a safety measure to avoid hydraulic imbalances and maintain plant's water status<sup>9,10</sup>. Negative impacts of high VPD on plants' physiology and growth have been largely reported in short-term experiments conducted under controlled conditions<sup>11</sup>. Sensitivity to VPD increases of stomatal conductance is usually higher than photosynthesis<sup>12</sup>, nonetheless, assimilation (A) may be limited under prolonged high evaporative conditions and low soil moisture<sup>3,11,13</sup>. These negative effects on carbon assimilation are alarming since these are the expected climate conditions in future scenarios of global warming<sup>14</sup>. This effect of VPD on plants' physiology may be especially critical in naturally hot and dry forests that likely operate near their physiological limits at the cost of primary productivity<sup>15,16</sup>.

In such scenario, biomass gain is at risk in Seasonally Dry Tropical Forests (SDTF), one the world's most threatened biome that covers more than 40% of tropical woodland (4.9 million km<sup>2</sup>) with current rates of deforestation at 11%<sup>17</sup>. The estimates of SDTF aboveground biomass range from 39 to 334 Mg ha<sup>-1</sup>, corresponding to 8.7 Pg of stored aboveground carbon worldwide<sup>18,19</sup> and almost one third of the interannual variability of global net primary productivity<sup>20</sup>. This biomass accumulation in SDTF is mainly regulated by rainfall and dry-season length<sup>18,21-22</sup> and alarming reductions from 30% up to 60% of SDTF aboveground biomass were predicted for the end of the 21 century in Bolivia and Brazil using rainfall model projections<sup>21,23</sup>. The existing data come from short-term monitoring plots or experiments and most diverge from Global Vegetation Models (GVMs) for long term and inter-annual variability projections of carbon dynamics<sup>24</sup>. Additionally, rainfall projections are more uncertain than temperature's, and vegetation models yet have low resolution to pinpoint effects in diverse SDTF<sup>25,26</sup>, and the effects of the recent VPD increase is still overlooked in most models<sup>3,11</sup>. For instance in a SDTF from northeastern Brazil, the seasonal variability of CO<sub>2</sub> fluxes suffer direct impacts of global radiation, air

and soil temperature<sup>26</sup> and the drought conditions will worsen with warming<sup>24,25</sup>. A carbon sink decline is already observed in seasonal forests from southeastern Brazil with pronounced effects in the warmest and driest sites since 1987<sup>25</sup>. Thus, negative impacts in SDTF functioning due to rising VPD will impact the global carbon cycle and yet need to be better represented in GVMs<sup>21,25</sup>.

Central-eastern Brazil is a hot spot of warming in the tropics, where increases in temperature of around 2°C have been observed in the last century (**Figure 1**) in an area that supports the continent's largest continuous extensions of SDTF<sup>30,31</sup>. This region is at the core of the South American Monsoon System (SAMS), under direct influence of the South Atlantic Convergence Zone (SACZ)<sup>32,33</sup>, and it is affected by climate modes like El Niño, episodic volcanic eruptions and changes in radiative forcing that regulate SAMS activity<sup>34-36</sup>. Millennium long speleothems series from the entrance of caves, next to the SDTF where this study took place, revealed significant changes in their ratio of stable oxygen isotopes ( $\delta^{18}\text{O}$ ) in the present and in pre-industrial period. In the last 40 years there is a clear increase in speleothem  $\delta^{18}\text{O}$  annual layers associated with the increasing evaporative conditions that mirrors the trend in the instrumental records of VPD since the 1980s (Strikis *et al.*, in press). Still an open question is the long term effects of increasing VPD on tree physiology of SDTF, which can also be analyzed with  $\delta^{18}\text{O}$ , but in tree-ring layers from local trees. Centuries long tree-ring records are the only real alternative to assess long-term changes in tree growth and biomass gain in forests worldwide. Dendrochronology is particularly successful in SDTF, where tree rings are excellent records of climate variability and where an increase in evaporative demands and drought conditions is expected to exert the strongest impacts in tropical forests<sup>15,37,38</sup>. Therefore, this region gathers a unique assemblage of natural records to evaluate the effects of abrupt changes in radiative forcing and long-term changes in VPD on tree growth using tree-ring width and  $\delta^{18}\text{O}$ .

Tree-ring width and growth are intimately coupled to regional climate<sup>37,38</sup>. Local and global climate can also affect the stable oxygen isotope ratios ( $\delta^{18}\text{O}$ ) in tree rings, offering an additional proxy to improving cross-dating, understanding tree physiological responses, enhancing climate signal intensity, spatial coverage<sup>39-40</sup>, and enabling comparison with other archives<sup>41</sup>. Trees absorb water from rainfall with an  $\delta^{18}\text{O}$  signal determined by the temperature of condensation, which have little variation in tropical lowlands, and the amount of rainfall, both local or upstream<sup>42</sup>. Thus, the most common  $\delta^{18}\text{O}$  signal in tropical trees is related to the enhanced removal of heavy isotopes ( $\text{H}_2\text{O}^{18}$ ) along the air mass trajectory according to the rainout upstream or to local amount effects

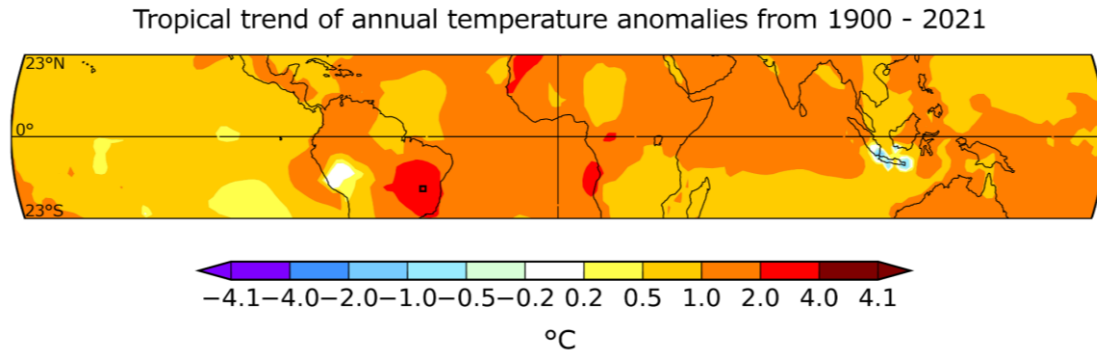


**Figure 1** - Global map of tropical region annual temperature anomalies from 1900 to 2021. The study site is located in the region that stands out as a tropical hot spot (black square in central eastern Brazil). Obtained and modified from GISS Surface Temperature Analysis (GISTEMP).

regulated by site rainfall intensity and duration<sup>40,43</sup>. However, there is another signal, which can be hard to dissociate from the amount effect, that is the leaf-level  $\delta^{18}\text{O}$  enrichment associated with high VPD conditions that increases the rate of evaporation of light water molecules ( $\text{H}_2\text{O}^{16}$ )<sup>44,45</sup>. Therefore, the  $\delta^{18}\text{O}$  of tree-ring cellulose will record VPD when the enrichment at the leaf level is higher than the exchange with stem water during the synthesis of tree-ring cellulose, which is more likely to occur in dry forests<sup>40,45</sup>.

Given the lack of comprehensive knowledge on the responses of mature trees from one of the largest physiognomies of tropical forests, and one of the most endangered, we aimed at understanding the effects of the observed increasing VPD and evaporative demands since 1980s on tree growth from an STDF in a tropical hotspot of global warming. We produced accurately-dated centennial-long tree-ring chronologies of *Amburana cearensis* and *Cedrela fissilis*, two widely distributed neotropical tree species known for their strong common growth signal and climate sensitivity<sup>46-50</sup>. Despite the records of increasing evaporative demands shared by different proxies including present study's tree-ring  $\delta^{18}\text{O}$  series, tree-ring width chronologies reveal no growth decline even when analyzed by diameter class of trees. Furthermore, tree-ring  $\delta^{18}\text{O}$  series of *Amburana cearensis* subfossil wood and local  $\delta^{18}\text{O}$  speleothem records also revealed a past change in radiative forcing during the Little Ice Age that similarly did not result in lower growth rates of trees. Thus, there is no evidence that vapor pressure deficit alone has limited the growth of the trees in these tropical dry forests up to this point.

## Results and Discussion

### *Increasing VPD recorded in multi-proxies*

We produced an accurately dated 179-years long tree-ring series of living trees of *Amburana cearensis*, *Cedrela fissilis*, and a 162-years long tree-ring floating series of *Amburana cearensis* subfossil samples, which were compared to local climate and speleothem series (**Figure 2**). Tree-ring chronologies of both species are well replicated, have a strong common signal (Figures S1) are accurately dated and supported by radiocarbon analysis<sup>47,51</sup>. Furthermore, dating accuracy is confirmed by the good agreement between the two species chronologies within the same site (Figure S2). The site tree-ring width chronology composed by trees of both species (from now on referred to as Peruaçu *spp.* chronology) show a mean  $\bar{r}$  of 0.37 and  $\epsilon$  higher than 0.95 from 1842 to 2020, with higher values in recent years. Individual chronologies and climate analysis supporting the use of both species in a site chronology are shown in Supplementary information. The Peruaçu *spp.*  $\delta^{18}\text{O}$  chronology were composed by 9 and 6 trees, respectively of *Amburana cearensis* and *Cedrela fissilis*, that even though sampled in different site conditions share similar variability (Figure S3), with an average correlation among time series of both species of  $r = 0.54$ , reaching  $r = 0.73$  from 1960 to the present (Figure S4). This 179-year long series is 70 years longer than the local instrumental records and coupled with speleothems and subfossil series can offer valuable insight into the effects of climate change on tropical tree growth.

Tropical tree-ring width and  $\delta^{18}\text{O}$  chronologies show a strong convergence towards interannual changes in rainfall volume, but less is known for medium and low frequency variability<sup>46,47,52,53</sup>. Because data selection, treatment, sampling design can influence the final results<sup>54</sup>, we used different approaches to depict their strengths and limitations. Thus, the interannual variability was accessed in chronologies detrended with a smoothing spline (SP\_TRW, Figure 2), while medium and high-frequency variability were accessed in chronologies detrended with a regional curve (RC\_TRW, Figure 3). The monthly climate correlations revealed that SP\_TRW highly correlates with the entire growing season (Figure S5 A-F), while the  $\delta^{18}\text{O}$  signal is stronger during the summer (Figure S5 G-L). This strong interannual correlation with rainfall was observed for the Peruaçu *spp.* chronology from the beginning of the 20th century until 1980s, when both SP\_TRW and  $\delta^{18}\text{O}$  chronologies were significantly associated with total rainfall during the growth season ( $r = 0.45$ ,  $p < 0.01$  for TRW and  $r = -0.32$ ,  $p < 0.05$  for  $\delta^{18}\text{O}$ ) (Figures S06 to S07). While the SP\_TRW chronology strengthen its correlation with precipitation from early 1980s to the



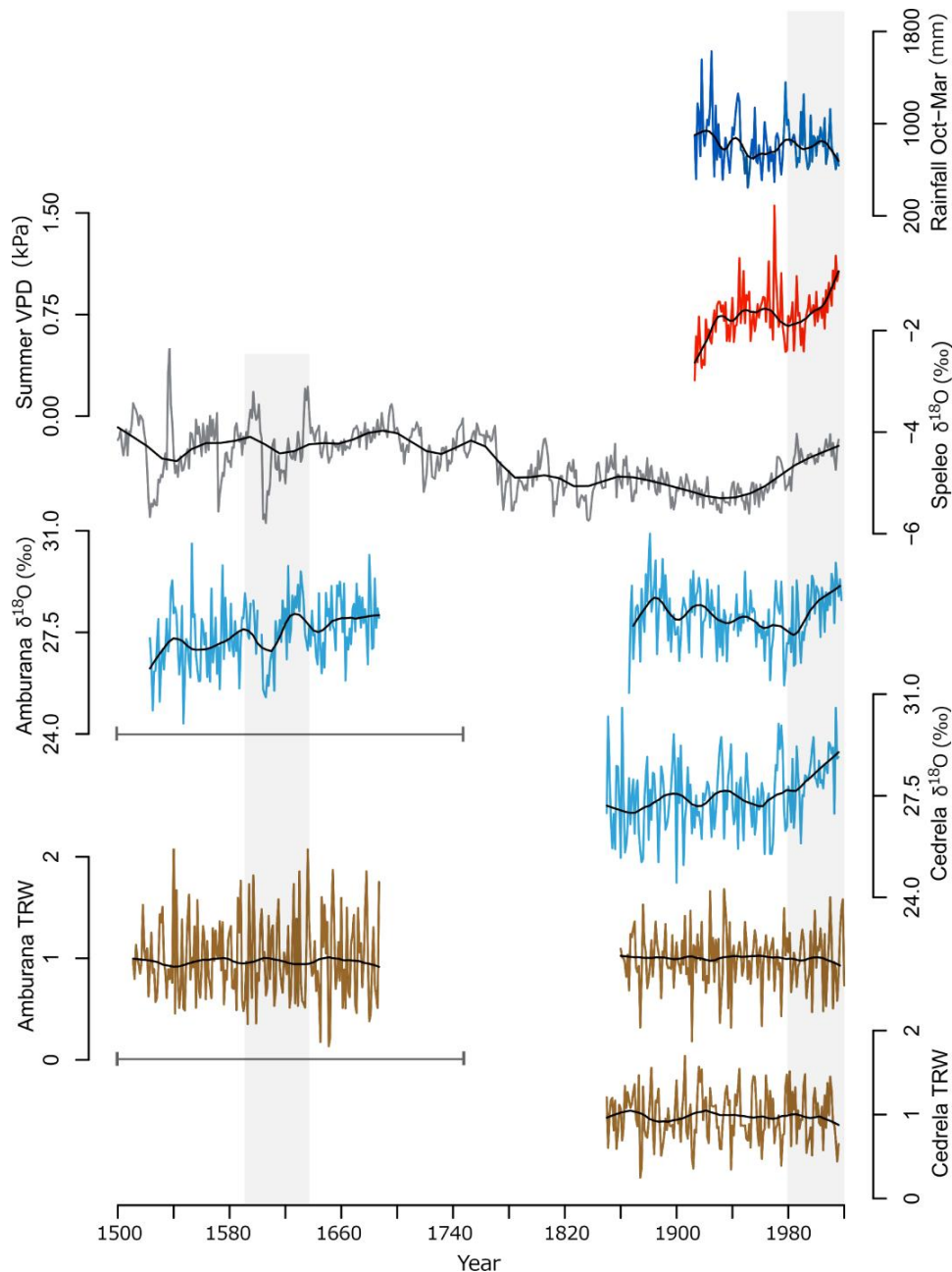


**Figure 2** - Temporal series of local climate and proxy records with 15 years moving average (smooth black lines). From top to bottom, blue: Instrumental total amount of growth season rainfall (October to March); red: Instrumental summer Vapor Pressure Deficit (VPD); gray: Local speleothem  $\delta^{18}\text{O}$  (Strikis *et al.*, in press); Light blue: Tree-ring  $\delta^{18}\text{O}$  of *Amburana* and *Cedrela*, respectively; brown: Tree-ring width index (TRW) of *Amburana* and *Cedrela*, respectively. Dark gray bars below subfossil floating series are the radiocarbon wiggle match dating age range.

present day ( $r = 0.65$ ,  $p < 0.01$ , Figure S06), the  $\delta^{18}\text{O}$  series correlation with rainfall overall are barely significant ( $r = -0.32$  and  $r = -0.34$   $p < 0.05$ , 07). Piecewise linear regressions detected a precise changing point in 1984 for the tree-ring  $\delta^{18}\text{O}$  mean series (Figure S08 for piecewise of the different species and subfossil trees) and the site  $\delta^{18}\text{O}$  mean series

becomes enriched at  $0.05 \text{ ‰ year}^{-1}$ , resulting in a predicted  $1.55 \text{ ‰}$  enrichment by 2015. Thus, after 1984 there is a unique increasing trend in tree-ring  $\delta^{18}\text{O}$  that is not present in the total amount of rainfall during the growing season, which only shows a small decline after 2010 (from October to March, **Figure 2, blue line**). Actually, the tree-ring  $\delta^{18}\text{O}$  increasing trend mirrors the summer VPD regional series (**Figure 2, red line**), and after 1980 they reach a correlation of  $r = 0.70$ , that are consistent after smoothing series (Figure S09). This medium frequency changes in VPD and  $\delta^{18}\text{O}$  are not detected in the SF\_TRW (**Figure 3**). After 1980, the series decouples from the  $\delta^{18}\text{O}$  series, show an increase followed by a brief stabilization, and drop around 2010, similar to what is observed for rainfall (**Figure 3**). These results indicate that VPD takes over as the main driver of  $\delta^{18}\text{O}$  variability in the 1980s, but this trend is not clear in the tree-ring width series which is mainly regulated by rainfall.

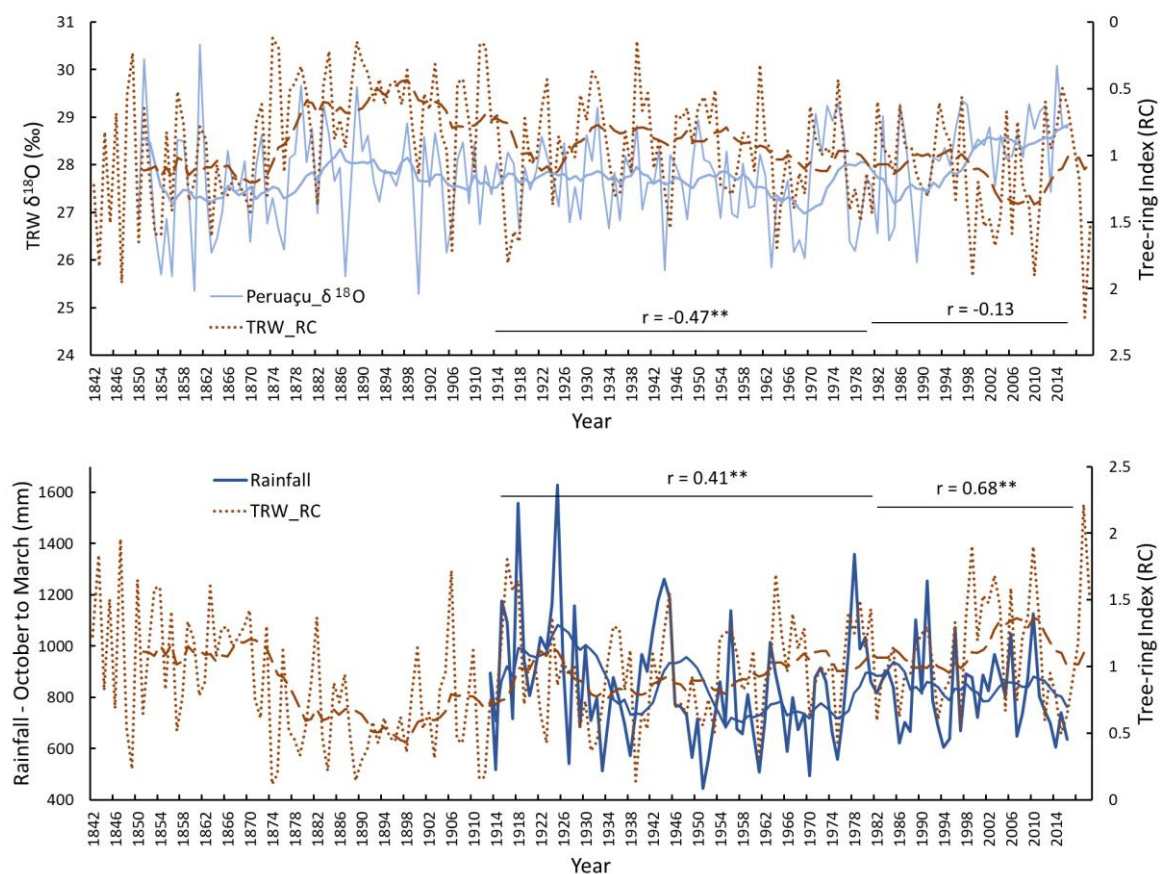


**Figure 3** - Site standard regional curve tree-ring series (brown dotted line) with tree-ring  $\delta^{18}\text{O}$  series (light blue line) and total rainfall of growth season (dark blue line). For each series a 10 year moving mean is shown to highlight medium frequency co-variation of series. Correlation coefficients between series are given for before and after 1984. \*\*  $p < 0.01$ .

While the trend of increasing VPD since the 1980s is a fact revealed by the regional climate stations dataset, we had to exhaust any alternative explanation for the observed trend in tree-ring  $\delta^{18}\text{O}$ . Regional and local changes in source water can lead to a similar trend to that observed in the tree rings  $\delta^{18}\text{O}$ <sup>40,45</sup>. The analysis of the accumulated rainfall during moisture transport covering the period between 2000 to 2018 shows a small, but still non-significant trend since 2010, when correlations between air mass back trajectories and tree-ring  $\delta^{18}\text{O}$  weakens from  $r = -0.79$  ( $p < 0.01$ ) to  $r = -0.21$  ( $p > 0.05$ ) (Figure S10). Similarly, data from recent local  $\delta^{18}\text{O}$  rainfall monitoring (2000 to 2017) show a slight negative trend, that strengthens after 2010 (Figure S11, data obtained by Strikis *et al.*, in press), but without association or changes in tree-ring  $\delta^{18}\text{O}$ . The effect of evapotranspiration is also supported by local speleothems records (Strikis et al in prep). The local speleothem  $\delta^{18}\text{O}$  record sampled at the cave entrance where fractionation is driven by evaporation shares similar  $\delta^{18}\text{O}$  enrichment (**Figure 2, gray**) and significant association with living trees oxygen isotopes ratios (Figures S12).

Alternatively, soil water enrichment through evaporation could lead to the observed trend in tree-ring  $\delta^{18}\text{O}$ <sup>40,45</sup>. Nonetheless, we observed the same increasing tree-ring  $\delta^{18}\text{O}$  in different types of forests including canopy-exposed trees from low density forests in the epikarst where the exposed soil is prone to evaporation, open fields inside farms, as well as in trees growing in the valley (Figures S03C-D) where the soil is protected by dense canopy, lower seasonal contrast, thick litter layer, or shading by rock outcrops, all common to SDTF<sup>47,55-56</sup>. Finally, to test the leaf water enrichment contribution to tree-ring  $\delta^{18}\text{O}$ , we used a tree-ring isotope fractionation model<sup>45,53,57</sup> comparing the expected cellulose  $\delta^{18}\text{O}$  in the climate conditions of 1970 to 1980 and 2005 to 2015. **Figure 4** shows that 66.67% of our models explains more than half of the observed difference in  $\delta^{18}\text{O}$  values comparing the mean conditions of the two periods (observed mean  $\delta^{18}\text{O}$  difference of 1970 to 1980 compared to 2005 to 2015 was 0.68‰). The model can be underestimating the trend for the use of conservative climate assumptions such the VPD calculated from air temperature and not leaf temperature that might be even higher<sup>45,58</sup>. Still, seven of our models explained more than 70% of the observed changes in tree-ring  $\delta^{18}\text{O}$  due to higher VPD values. Thus, all evidence points that the source water signal, usually strong in tropical tree-ring  $\delta^{18}\text{O}$ , is overridden by the enrichment at the leaf level and the evidences point out VPD as the main driver of tree-ring  $\delta^{18}\text{O}$  enrichment since the 1980s.

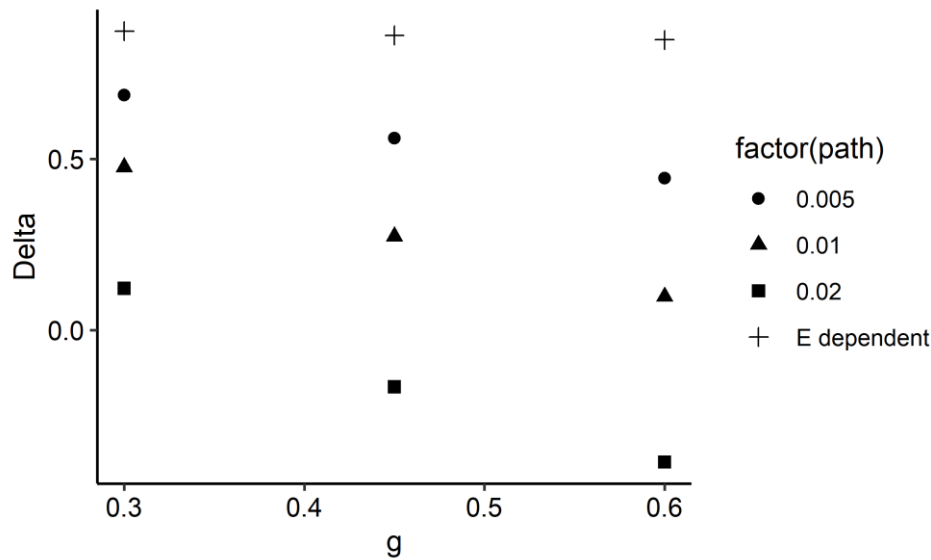


**Figure 4** - Stable isotope model the test the influence of VPD on tree-ring  $\delta^{18}\text{O}$  between 1980 and 2015. The different inputs (g: stomatal conductance and path lengths) and outputs (Delta: difference between the simulated  $\delta^{18}\text{O}$  value in cellulose) are represented by the different symbols.

#### *Effects of VPD on living trees growth*

Short-term experiments have proven the role of VPD on physiological constraints and growth restrictions under controlled conditions<sup>3,4,11,13</sup>. These results establish a clear link between VPD and plant carbon fixation, tree growth and biomass gain<sup>3,11</sup>. In the last decades of the last century, tree-rings revealed a climate sensitivity shift worldwide and trees are becoming more limited by atmospheric water demand<sup>24</sup>. However, our field work in one of the most demanding tropical biomes in terms of evapotranspiration reveal no long term effects of VPD on the growth of trees (**Figure 5**). The analysis in diameter classes to avoid metric biases inherent to tree-ring data also show no significant changes when comparing more spaced periods, from 1940 to 1970 against 1988 to 2018 (**Figure 5B**, and Figure S13). Alternative growth analyzes with tree-ring chronologies built using conservative detrendings as linear regressions (Figures S14) and basal area increment (Figures S15) all converge showing no significant growth changes in any species after 1980, although from 2010 there is a slight decrease trend likely caused by the decreasing rainfall and consecutive years of extreme VPD, also present in the RC\_TRW series (Figure 2). During these years of extreme (more than one standard deviation from series mean) low rainfall and high VPD (**Figure 5C**) the growth rate of trees are smaller than in regular (mean) years (**Figure 5D**), but is not possible to untangle the effects of rainfall and VPD in the reduction observed during the last 10 years. Moreover, the low growth increments are

not unprecedented in the series and there is no sustained decline that mirrors the magnitude of the increasing VPD and  $\delta^{18}\text{O}$  trends (Figure 2, Figures S14 and S15). Thus, one can state that trees from this SDTF sustained their growth rate despite the physiological changes recorded in the recent tree-ring  $\delta^{18}\text{O}$  series as an unprecedented rising in the last 200 years due to VPD.

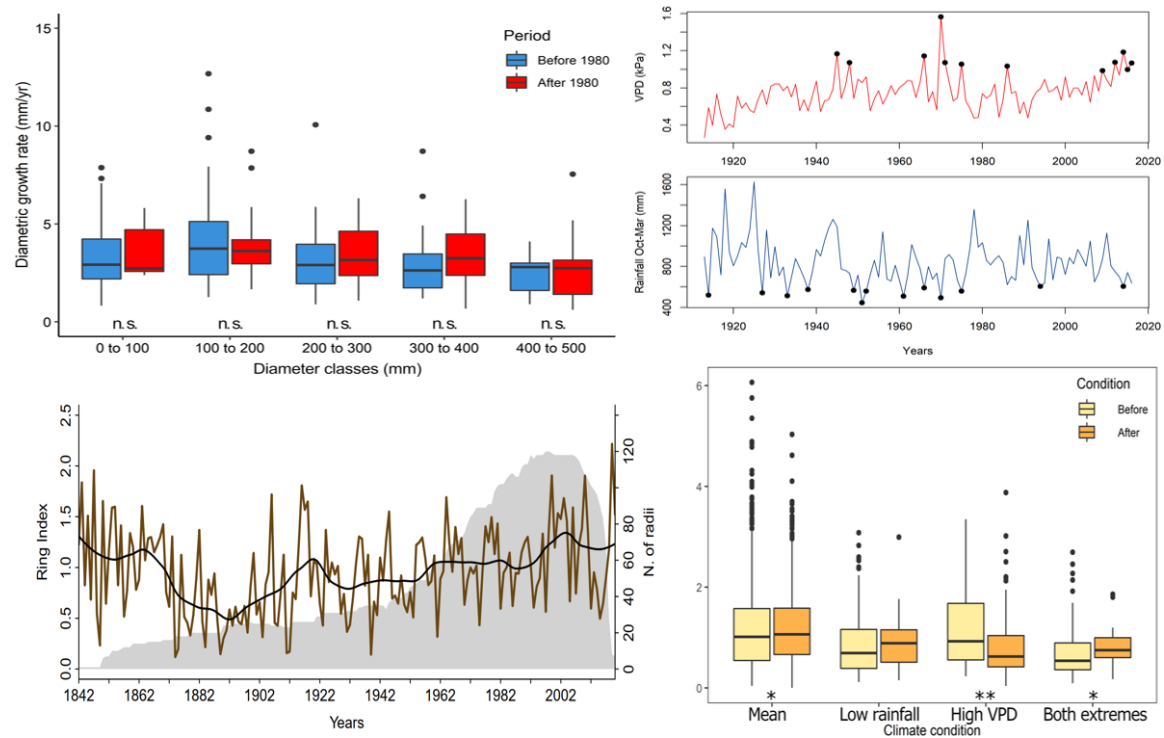


**Figure 5** – Growth analysis in years of increasing and extreme VPD. A) Diametric growth rate in diameter classes of *A. cearensis* and *C. fissilis*. The blue (left) boxplots represent the growth rate before 1980 and the red boxplots for after 1980, and in B, the blue (left) boxplots represent the growth rate from 1940 to 1970 and the red boxplots for 1988 to 2018. No difference was observed between growth rate comparing the two periods in any class. (n. s.: no significant difference in groups means between periods using Wilcoxon non-parametric tests). Years of extreme high VPD and low rainfall were identified (C) and tree growth rates were compared with mean years (D). Wilcoxon pairwise tests showed that growth during mean years differs from extreme years. Different letters (“a”, “b”) indicate statistically different groups.

### *Effects of VPD in a broader temporal context*

The subfossil series, also revealed a previous period of abrupt increase in  $\delta^{18}\text{O}$  around 1610 to 1635 that was a period of drier conditions in Central-eastern Brazil<sup>36</sup> (Figure 6). The subfossil samples found in the caves (Figure S16) radiocarbon ( $^{14}\text{C}$ ) dates were wiggle matched against the Southern Hemisphere calibration curve<sup>59-60</sup>, and indicated

an overlap of two *A. cearensis* during the Little Ice Age (LIA) (Figure S17-18). Then, synchronization of this tree-ring  $\delta^{18}\text{O}$  floating record with local speleothem  $\delta^{18}\text{O}$  series, that share a common source water  $\delta^{18}\text{O}$  signal<sup>41</sup> and have similar inter-annual and decadal variability in the recent decades (Figure S12, and S19), pointed out a position of significant correlation between records from 1527 to 1690 ( $r = 0.34$   $p < 0.01$ , Figure S19). During this period, and similar to recent years, climate model simulations for the site (CESM-LME) show a temperature increase (**Figure 6A**), a decrease in relative humidity (**Figure 6B**) and small decrease in precipitation (**Figure 6C**). As expected by the observed in the records nowadays, the increase in VPD matches and increase in the  $\delta^{18}\text{O}$  series of trees and speleothems during the LIA, and both records have inter-annual and decadal variability similar to the modeled rainfall and VPD (Table S1). The correlations between tree-ring  $\delta^{18}\text{O}$  and rainfall during the period of increasing VPD were high ( $r = -0.57$   $p < 0.01$ ) as the correlation between natural records ( $r = 0.47$   $p < 0.01$ ). The increase trend in the series likely represents the intensification of the dry conditions, when once more no positive nor negative growth changes can be easily observed in *Amburana* tree-ring width (Figure S20). These results are expected, as we observed in the living trees, but impressive given the small replication of this rare set of subfossil samples in tropical regions.

Also impressive, was the match between the lowest subfossil tree-ring  $\delta^{18}\text{O}$  values in the record, 1599 and 1604, with the speleothem series lowest  $\delta^{18}\text{O}$  years from 1604 to 1606 (Figure S18-19). The climate model simulation for the period shows three years with high rainfall rate from 1600 to 1603 that could cause the extremely low values observed in the records. These extreme rainfall years and  $\delta^{18}\text{O}$  depletions could reflect changes in radiative forcing caused by one of the largest eruptions in the last 500 years of Huaynaputina in Peru, whose effects were detected worldwide<sup>61-62</sup>. Such an eruption in Peru can likely disrupted the climate of Central-eastern and Northeastern Brazil because of the teleconnections through atmospheric circulation cells over South America that causes the east-west moisture dipole patterns<sup>34</sup>. The eruption took place around 1600, falling within the dating accuracy of both tree-ring  $^{14}\text{C}$  and speleothem U-Th ( $\pm 5$  years), thus even though both records only have two samples, their relative dating do not appear to be more than 5 to 10 years off. Moreover, our climate models testing for individual forcings shows that the volcanic and solar forcings, similar to the records  $\delta^{18}\text{O}$ , have an increase around 1610 to 1630, reflecting in the changes in local temperature and relative humidity simulations for this period (**Figure 6A-C**). An additional indication of this teleconnection was observed in the site tree-ring  $\delta^{18}\text{O}$  chronology of living trees that shows antiphase



correlations between Peru and central-eastern and northeastern Brazil gridded precipitation, especially during years with high evaporative demand (Figure S21). However, there are still a lot of uncertainties and spatial variability from proxy records in these areas regarding past conditions during the LIA and no certain associations can be made yet. This calls out to the need of more research and benchmark studies on subfossil materials of tropical areas, which are rare but can provide useful paleoclimate information.

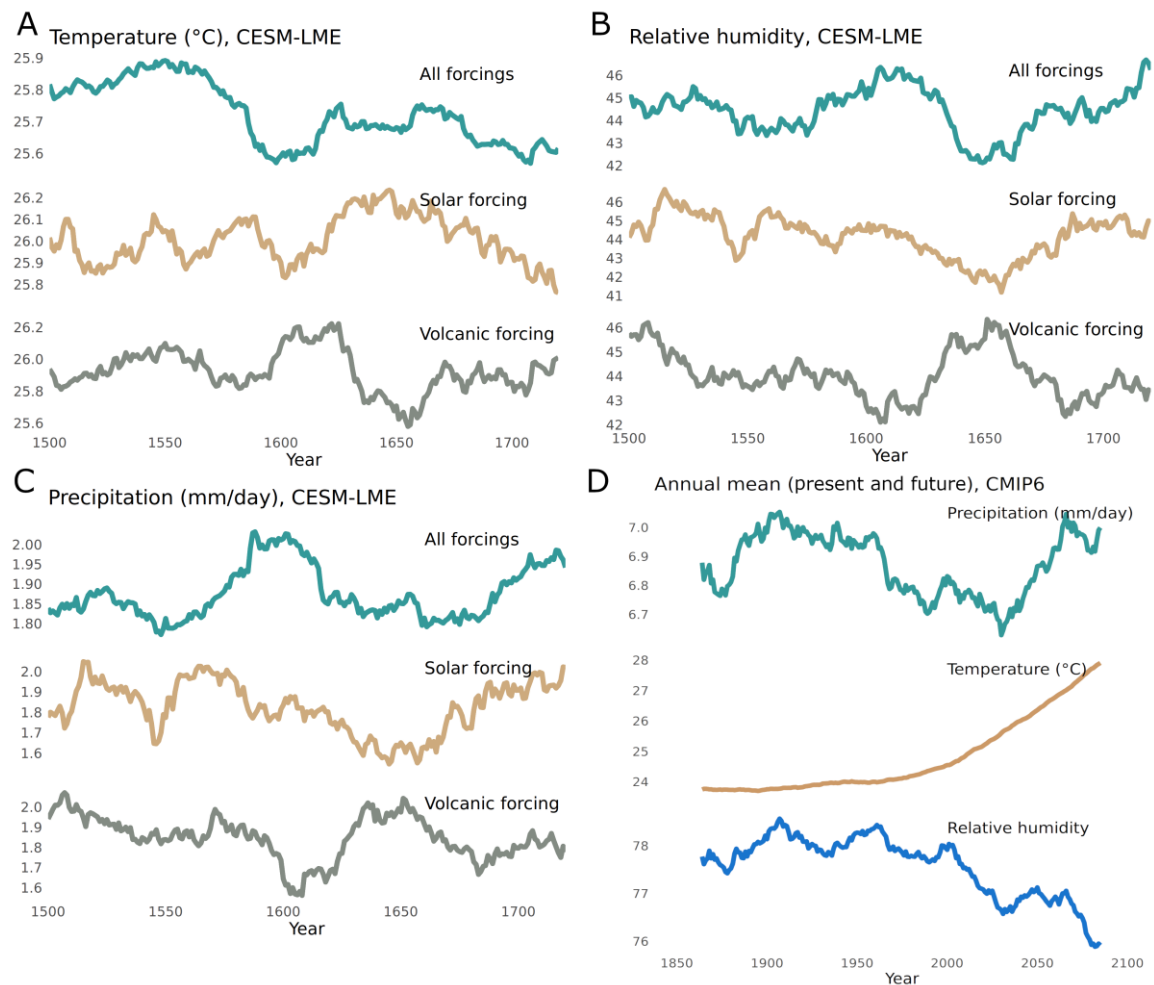


**Figure 6** – Growth analysis in years of increasing and extreme VPD. A) Diametric growth rate in diameter classes of *A. cearensis* and *C. fissilis*. The blue (left) boxplots represent the growth rate before 1980 and the red boxplots for after 1980, and in B, the blue (left) boxplots represent the growth rate from 1940 to 1970 and the red boxplots for 1988 to 2018. No difference was observed between growth rate comparing the two periods in any class. (n. s.: no significant difference in groups means between periods using Wilcoxon non-parametric tests). Years of extreme high VPD and low rainfall were identified (C) and tree growth rates were compared with mean years (D). Wilcoxon pairwise tests showed that growth during mean years differs from extreme years. Different letters (“a”, “b”) indicate statistically different groups.

Regarding future growth of this trees, no strong assumptions can be made, however the increase in temperature and drop in relative humidity can be counter balanced by the

projections of increased rainfall (**Figure 6D**), which would sustain rates of carbon assimilation of trees. Thus, it is still unclear to what point trees will remain resistant to VPD because the increase in temperature, with temperatures exceeding 26°C is unprecedented in the 500 years' period analysed. This 2°C increase in mean temperature could reduce trees growth rate and age<sup>63</sup> and consecutive years of extreme conditions can reduce carbon assimilation and eventually lead to carbon starvation or hydraulic failure, increasing the risk of tree mortality<sup>15</sup>.

## Conclusion

Disagreeing with the evidence of negative impacts of VPD on plant growth from short-term controlled experiments<sup>3,9,11</sup>, we observed sustained growth of trees facing recent high evaporative conditions and temperature increases in a SDTF highly affected by global warming. Using multi-centennial tree-ring width and  $\delta^{18}\text{O}$  series from a unique set of living and subfossil trees, we demonstrate that fluctuations in tree-ring  $\delta^{18}\text{O}$  and speleothems series share demanding evaporative conditions now and back in the Little Ice Age. Despite the changes in VPD, no growth decline has been recorded during these periods of abrupt changes in global radiative forcing, except during extreme years. The two representative tree species from this SDTF<sup>46,47</sup> kept their growth rate even with high transpiration rates that should limit turgor pressure for cell division and growth<sup>6</sup>. The SDTF are expected to be more drought tolerant than rainforests over evolutionary time-scales, even though there is a wide range of species and some might not be as drought tolerant<sup>25</sup>. The common light-wooded tree species present in SDTF, such *A. cearensis* and *C. fissilis*, considered vulnerable to hydraulic imbalances may invest in alternative strategies to couple with high evaporative demands like high sapwood water storage and deciduous short-lived leaves<sup>25,64–67</sup>. Thus, our consistent results point to the long resistance of SDTF trees to warming and VPD increase likely pointing to an overestimation of the impacts of warming and high evaporative demand on tropical forests growth in low resolution models<sup>27,28</sup>. Counter effects caused by CO<sub>2</sub> fertilization also could have sustained tree growth, but our data cannot discern this effect and there might be a physiological limit to how much trees would benefit from the fertilization, after which the VPD may start to limit growth<sup>68,69</sup>. Thus, it is still unclear to what point trees will remain resistant to VPD given the prospects of unprecedented high temperature, low relative humidity and prolonged droughts, that endangers future SDTF biomass gain and functioning<sup>14,22,25</sup>.

## References

1. Willett, K. M. *et al.* HadISDH land surface multi-variable humidity and temperature record for climate monitoring. *Clim. Past* **10**, 1983–2006 (2014).
2. Hatfield, J. L. & Prueger, J. H. Temperature extremes: Effect on plant growth and development. *Weather Clim. Extrem.* **10**, 4–10 (2015).
3. Grossiord, C. *et al.* Plant responses to rising vapor pressure deficit. *New Phytol.* **226**, 1550–1566 (2020).
4. Pennington, R. T., Lehmann, C. E. R. & Rowland, L. M. Tropical savannas and dry forests. *Curr. Biol.* **28**, 541–R545 (2018).
5. Rawson, H. M., Begg, J. E. & Woodward, R. G. The effect of atmospheric humidity on photosynthesis, transpiration and water use efficiency of leaves of several plant species. *Planta* **134**, 5–10 (1977).
6. Franks, P. J. & Farquhar, G. D. A relationship between humidity response, growth form and photosynthetic operating point in C3 plants. *Plant, Cell Environ.* **22**, 1337–1349 (1999).
7. Pan, Y., Birdsey, R. A., Phillips, O. L. & Jackson, R. B. The structure, distribution, and biomass of the world's forests. *Annu. Rev. Ecol. Evol. Syst.* **44**, 593–622 (2013).
8. Beer, C. *et al.* Terrestrial gross carbon dioxide uptake: Global distribution and covariation with climate. *Science.* **329**, 834–838 (2010).
9. Wong, S. C., Cowan, I. R., & Farquhar, G. D. (1979). Stomatal conductance correlates with photosynthetic capacity. *Nature* **282**, 424–426 (1979).
10. Flexas, J. *et al.* Decreased Rubisco activity during water stress is not induced by decreased relative water content but related to conditions of low stomatal conductance and chloroplast CO<sub>2</sub> concentration. *New Phytol.* **172**, 73–82 (2006).
11. López, J., Way, D. A. & Sadok, W. Systemic effects of rising atmospheric vapor pressure deficit on plant physiology and productivity. *Glob. Chang. Biol.* **27**, 1704–1720 (2021).
12. Zhang, Q. *et al.* Response of ecosystem intrinsic water use efficiency and gross primary productivity to rising vapor pressure deficit. *Environ. Res. Lett.* **14**, (2019).
13. Yuan, W. *et al.* Increased atmospheric vapor pressure deficit reduces global vegetation growth. *Sci. Adv.* **5**, 1–13 (2019).
14. WGI, I. A. Climate Change 2021 The Physical Science Basis WGI. *Bulletin of the Chinese Academy of Sciences* vol. 34 (2021).
15. Allen, K. *et al.* Will seasonally dry tropical forests be sensitive or resistant to future changes in rainfall regimes? *Environ. Res. Lett.* **12**, (2017).
16. Smith, M. N. *et al.* Empirical evidence for resilience of tropical forest photosynthesis

- in a warmer world. *Nat. Plants* **6**, 1225–1230 (2020).
17. Ocón, J. P. *et al.* Global tropical dry forest extent and cover: A comparative study of bioclimatic definitions using two climatic data sets. *PLoS One* **16**, (2021).
  18. Becknell, J. M., Kissing Kucek, L. & Powers, J. S. Aboveground biomass in mature and secondary seasonally dry tropical forests: A literature review and global synthesis. *For. Ecol. Manage.* **276**, 88–95 (2012).
  19. Saatchi, S. S. *et al.* Benchmark map of forest carbon stocks in tropical regions across three continents. *Proc. Natl. Acad. Sci. U. S. A.* **108**, 9899–9904 (2011).
  20. Poulter, B. *et al.* Contribution of semi-arid ecosystems to interannual variability of the global carbon cycle. *Nature* **509**, 600–603 (2014).
  21. Castanho, A. D. A. *et al.* Potential shifts in the aboveground biomass and physiognomy of a seasonally dry tropical forest in a changing climate. *Environ. Res. Lett.* **15**, (2020).
  22. Murphy, P. G. & Lugo, A. E. Ecology of tropical dry forest. *Annu. Rev. Ecol. Syst.* **17**, 67–88 (1986).
  23. Seiler, C., Hutjes, R. W. A., Kruijt, B. & Hickler, T. The sensitivity of wet and dry tropical forests to climate change in Bolivia. *J. Geophys. Res. Biogeosciences* **120**, 399–413 (2015).
  24. Babst, F. *et al.* Twentieth century redistribution in climatic drivers of global tree growth. 1–10 (2019).
  25. Meir, P. & Pennington, R. T. Seasonally Dry Tropical Forests. *Seas. Dry Trop. For.* 279–299 (2011) doi:10.5822/978-1-61091-021-7.
  26. Sitch, S. *et al.* Evaluation of ecosystem dynamics, plant geography and terrestrial carbon cycling in the LPJ dynamic global vegetation model. *Glob. Chang. Biol.* **9**, 161–185 (2003).
  27. Mendes, K. R. *et al.* Seasonal variation in net ecosystem CO<sub>2</sub> exchange of a Brazilian seasonally dry tropical forest. *Sci. Rep.* **10**, 1–16 (2020).
  28. Ocón, J. P. *et al.* Global tropical dry forest extent and cover: A comparative study of bioclimatic definitions using two climatic data sets. *PLoS One* **16**, 1–20 (2021).
  29. Maia, V. A. *et al.* The carbon sink of tropical seasonal forests in southeastern Brazil can be under threat. *Sci. Adv.* **6**, 1–12 (2020).
  30. Prado, D. E. Seasonally dry forests of tropical South America: From forgotten ecosystems to a new phytogeographic unit. *Edinburgh J. Bot.* **57**, 437–461 (2000).
  31. Apgaua, D. M. G. *et al.* Floristic variation within seasonally dry tropical forests of the Caatinga Biogeographic Domain, Brazil, and its conservation implications. *Int. For. Rev.* **17**, 33–44 (2015).

32. Marengo, J. A. *et al.* Recent developments on the South American monsoon system. *Int. J. Climatol.* **32**, 1–21 (2012).
33. Vera, C. *et al.* Toward a unified view of the American monsoon systems. *J. Clim.* **19**, 4977–5000 (2006).
34. Cruz, F. W. *et al.* Orbitally driven east – west antiphasing of South American precipitation. *Nat. Geosci.* **2**, 210–214 (2009).
35. Orrison, R. *et al.* South American Summer Monsoon variability over the last millennium in paleoclimate records and isotope-enabled climate models. *Clim. Past* **18**, 2045–2062 (2022).
36. Campos, J. L. P. S. *et al.* Coherent South American Monsoon variability during the last millennium revealed through high-resolution proxy records. *Geophys. Res. Lett.* **46**, 8261–8270 (2019).
37. Fritts, H. C. Growth rings of trees: Their correlation with climate. *Science.* **154**, 973–979 (1966).
38. Fritts, H. C. Tree rings and climate. *Elsevier* (2012).
39. Libby, L. M. *et al.* Isotopic tree thermometers. *Nature* **261**, 284–288 (1976).
40. van der Sleen, P., Zuidema, P. A. & Pons, T. L. Stable isotopes in tropical tree rings: theory, methods and applications. *Funct. Ecol.* **31**, 1674–1689 (2017).
41. Managave, S. R. Model evaluation of the coherence of a common source water oxygen isotopic signal recorded by tree-ring cellulose and speleothem calcite. *Geochemistry, Geophys. Geosystems* **15**, 905–922 (2014).
42. Dansgaard, W. Stable isotopes in precipitation. *Tellus A Dyn. Meteorol. Oceanogr.* **16**, 436–468 (1964).
43. Brienen, R. J. W., Helle, G., Pons, T. L., Guyot, J.-L. & Gloor, M. Oxygen isotopes in tree rings are a good proxy for Amazon precipitation and El Niño-Southern Oscillation variability. *Proc. Natl. Acad. Sci.* **109**, 16957–16962 (2012).
44. Cintra, B. B. L. *et al.* Tree-ring oxygen isotopes record a decrease in Amazon dry season rainfall over the past 40 years. *Clim. Dyn.* **59**, 1401–1414 (2022).
45. Cintra, B. B. L. *et al.* Contrasting controls on tree ring isotope variation for Amazon floodplain and terra firme trees. *Tree Physiol.* **39**, 845–860 (2019).
46. Pereira, G. de A. *et al.* The climate response of *Cedrela fissilis* annual ring width in the Rio São Francisco Basin, Brazil. *Tree-Ring Res.* **74**, 162–171 (2018).
47. Godoy-Veiga, M. *et al.* The value of climate responses of individual trees to detect areas of climate-change refugia, a tree-ring study in the Brazilian seasonally dry tropical forests. *For. Ecol. Manage.* **488**, (2021).
48. Brienen, R. J. W. & Zuidema, P. A. Relating tree growth to rainfall in Bolivian rain

- forests: a test for six species using tree ring analysis. *Oecologia* **146**, 1–12 (2005).
49. Granato-Souza, D. *et al.* Multidecadal changes in wet season precipitation totals over the eastern Amazon. *Geophys. Res. Lett.* **47**, 1–9 (2020).
  50. López, L., Villalba, R. & Stahle, D. High-fidelity representation of climate variations by *Amburana cearensis* tree-ring chronologies across a tropical forest transition in South America. *Dendrochronologia* **72**, (2022).
  51. Hammerschlag, I. *et al.* Annually verified growth of *Cedrela fissilis* from central Brazil. *Radiocarbon* **61**, 927–937 (2019).
  52. Brien, R. J. W., Schöngart, J. & Zuidema, P. A. Tree rings in the tropics: insights into the ecology and climate sensitivity of tropical trees. *Tropical tree physiology: adaptations and responses in a changing environment*. 439-461. (2016).
  53. Cintra, B. B. L. *et al.* Tree-ring oxygen isotopes record a decrease in Amazon dry season rainfall over the past 40 years. *Clim. Dyn.* **59**, 1401–1414 (2022).
  54. Büntgen, U., *et al.* The influence of decision-making in tree ring-based climate reconstructions. *Nature Communications*, **12**, 3411 (2021).
  55. Toby Pennington, R., Prado, D. E. & Pendry, C. A. Neotropical seasonally dry forests and Quaternary vegetation changes. *J. Biogeogr.* **27**, 261–273 (2000).
  56. Locosselli, G. M., Cardim, R. H. & Ceccantini, G. Rock outcrops reduce temperature-induced stress for tropical conifer by decoupling regional climate in the semiarid environment. *Int. J. Biometeorol.* **60**, 639–649 (2016).
  57. McCarroll, D. & Loader, N. J. Stable isotopes in tree rings. *Quat. Sci. Rev.* **23**, 771–801 (2004).
  58. Holloway-Phillips, M. *et al.* Leaf vein fraction influences the Péclet effect and <sup>18</sup>O enrichment in leaf water. *Plant Cell Environ.* **39**, 2414–2427 (2016).
  59. Ramsey, C. B., Johannes van der P., and Bernhard W. ‘Wiggle matching’ radiocarbon dates. *Radiocarbon* **43**, 381–389 (2001).
  60. Hogg, A. G. *et al.* SHCal20 Southern hemisphere calibration, 0–55,000 years Cal BP. *Radiocarbon* **62.4**, 759–778 (2020).
  61. Silva, S. L. De & Zielinski, G. A. Global influence of the AD 1600 eruption of Huaynaputina, Peru. *Nat. Lett.* **393**, 455–458 (1998).
  62. Verosub, K. & Lippman, J. Global Impacts of the 1600 Eruption of Peru’s Huaynaputina Volcano. *Eos, Trans. Am. Geophys. Union* **89**, 141–142 (2008).
  63. Locosselli, G. M. *et al.* Global tree-ring analysis reveals rapid decrease in tropical tree longevity with temperature. *Proc. Natl. Acad. Sci. U. S. A.* **117**, 33358–33364 (2020).
  64. Wright, C. L., de Lima, A. L. A., de Souza, E. S., West, J. B. & Wilcox, B. P. Plant functional types broadly describe water use strategies in the Caatinga, a seasonally dry



- tropical forest in northeast Brazil. *Ecol. Evol.* **11**, 11808–11825 (2021).
65. Brito, N. D. S., Medeiros, M. J. S., Souza, E. S. & Lima, A. L. A. Drought response strategies for deciduous species in the semiarid Caatinga derived from the interdependence of anatomical, phenological and bio-hydraulic attributes. *Flora Morphol. Distrib. Funct. Ecol. Plants* **288**, 152009 (2022).
66. de Souza, B. C. *et al.* Drought response strategies of deciduous and evergreen woody species in a seasonally dry neotropical forest. *Oecologia* **194**, 221–236 (2020).
67. Brodribb, T. J., Holbrook, N. M., Edwards, E. J. & Gutiérrez, M. V. Relations between stomatal closure, leaf turgor and xylem vulnerability in eight tropical dry forest trees. *Plant, Cell & Environment*, **26**, 443–450 (2003).
68. Van Der Sleen, P. *et al.* No growth stimulation of tropical trees by 150 years of CO<sub>2</sub> fertilization but water-use efficiency increased. *Nat. Geosci.* **8**, 24–28 (2015).
69. Brienen, R. J. W., Gloor, E. & Zuidema, P. A. Detecting evidence for CO<sub>2</sub> fertilization from tree ring studies: The potential role of sampling biases. *Global Biogeochem. Cycles* **26**, (2012).

## Material and Methods

### Study Site

Seasonally Dry Tropical Forests (SDTF) have mean annual temperatures around 17–20°C, rainfall between 250–2000 mm of rain per year and a strong dry season of at least 3–4 months, and negative water balance in a year<sup>22</sup>. Besides precipitation, SDTF have nutrient-rich soils in contrast to some rainforests and neotropical savannas that occurs under similar climatic conditions<sup>22</sup>. SDTF are very diverse in terms of species diversity and local climate conditions suggesting that different responses to drought are expected<sup>15,25</sup>. The region of the Cavernas do Peruaçu National Park is located in northwestern Minas Gerais State (14°54' and 15°15'S / 44°03' and 44°22'W), central eastern Brazil, South America. The karstic area is at ~600–700 m above sea level in the São Francisco craton, crossed by the lesser course of the Peruaçu river<sup>70</sup> a perennial left-bank tributary of the Rio São Francisco river. This is the largest and most diverse continuous patch of dry tropical forests in South America<sup>30,31</sup>. Climate is tropical savanna-like with dry winters (Aw) according to the Köppen system, and mean total annual precipitation is 930 mm which 90% falls in the spring and summer months (ONDJF) and it is almost absent (less than 50 mm per month) during winter (JJA)<sup>33</sup>.

## Tree species

SDTF usually have a dense canopy and are dominated by Leguminosae and Bignoniaceae tree species<sup>55</sup>. *Amburana cearensis* (Allemão) A.C. Sm., (Leguminosae) is a deciduous tree species widely spread and common in calcareous and limestone-rich soil, typical of karstic areas, but due to its wood quality, beauty and smell, the species was highly explored and is currently endangered<sup>71</sup>. This is a characteristic species of South America tropical forests<sup>30</sup>, and across South America<sup>72,73</sup> and at the study site<sup>47</sup>, its tree rings are annual and growth is highly correlated with local climate<sup>48,50</sup>. The tree rings of *A. cearensis* are characterized by the presence of small vessels surrounded by half-flattened aliform axial parenchyma, sometimes associated with a fibrous zone without vessels, and non-continuous marginal parenchyma bands may be present in the oldest individuals with relatively lower growth rates<sup>47</sup>. *Cedrela fissilis* is also a widespread tree species in SDTF with clear tree rings characterized by the presence of marginal parenchyma bands and semi-porosity in wider rings and with several established tree-ring chronologies in many tropical regions<sup>43,46-47</sup>.

Here we opted for establishing a single chronology with the two species, something unusual in the tropics. Differences in species physiology, phenology and genetics can cause differences in climate responses and strategies to couple with high evaporative demands<sup>19,20</sup>. However, tree-ring investigations can be made using the assumption that evolutionary and biogeographic patterns are stronger than differences at the species level<sup>24</sup>. Accordingly, here the climate and growth tests with both species showed the same results, pointing that climate exerts a strong influence in this region (Barbosa et al., 2018) and using trees of different species could increase the common climate signal, length and the replication of the site chronology, all of which are bottlenecks for advancing tropical dendroclimatology<sup>63,74</sup>.

## Tree-ring width analyses

### *Sampling and preparation*

For *A. cearensis* we sampled trees with various diameters at breast height, ranging from 10 cm to 70 cm, to have a better representation of the tree population<sup>75</sup>. Also the trees were sampled in different microsite conditions<sup>47</sup>, but trees from the two contrasting sites show similar variation in tree-ring stable isotopes (Figure S03). The *C. fissilis* trees were mostly growing in open fields and farms. Some standing dead trees of both species were found and had entire cross sections obtained that aided tree-ring crossdating. From living

trees, we obtained two to four cores from each individual tree using manual increment borers or a special borer coupled to a motor drill<sup>76</sup>. After sampling, we applied a solution of copper sulfate and calcium carbonate in the sampling hole and closed it with natural cork to avoid infections. Metadata for each tree was obtained (e.g. geographical location, diameter at breast height (DBH), tree height, injuries) in the field. All wood samples were included in the Xylarium Nanuza Luiza de Menezes and in the ESALQ Xylarium (online information of samples in <http://splink.cria.org.br/>). The samples were left to dry while glued on wooden holders, and sanded to obtain a clean cross-section for proper tree ring observation using sandpaper with different grits (80–400). All samples were scanned at 2400dpi resolution (EPSON Expression 12000XL) and tree-ring width was measured in WinDendro<sup>TM</sup> (Regents Instruments Inc., Canada) and in CoRecorder<sup>TM</sup>. Because a few *A. cearensis* trees missed the pith, we estimated their age assuming a position for the pith through the rays in the last rings<sup>77,78</sup>.

#### *Cross-dating, chronology building and statistics*

For the cross-dating we conducted a visual cross-dating in within the radii of the same tree to spot any false and missing rings, then the software COFECHA<sup>79</sup> was used to guarantee the dating quality and guide the dating between trees<sup>75</sup>. The calendar year was attributed according to the year tree rings started to be produced (Schulman, 1956). For *Amburana*, 6 fallen trees were added to a previous established chronology<sup>47</sup>, to build a longer one composed by 37 trees, 96 radii and 4962 tree rings counted. As for *Cedrela*, the dataset is composed by 21 trees, 43 radii and 3576 tree rings counted. Therefore, the Peruaçu spp. chronology established using both species have 58 trees, 139 radii and a total of 8538 tree rings counted in all series. From now when we refer to the site chronology it is the one using both species. Tests in the single species chronologies can be found in supplementary material for every analysis, but the main discussion is focused on the Peruaçu spp. chronology that showed stronger common signal, higher replication and is supported by the consistent results of the tests with the species individually.

The selection of a proper detrending can influence climate reconstructions<sup>54</sup> and climate growth inferences<sup>80</sup>. We built two main chronologies: the first to retain climatic signals, high-frequency variability, remove ontogenetic trends and test climate and growth relations using a 20-year cubic smoothing spline curve, removing autocorrelation<sup>81</sup>. The second one, build to retain medium to low frequency variability, was established using the Regional Curve Standardization, possible due to the big dataset gathered using two species

and the three subfossil samples of *A. cearensis*. We calculated the  $\bar{r}$  (mean correlation coefficient of all pairwise combinations of trees) to quantify the common-growth signal and the EPS (Expressed Population Signal) to test chronology sample depth and representation of a population signal<sup>82</sup>. Analysis were performed in the Dendrochronology Program Library - dplR<sup>83</sup> in R<sup>84</sup>, and in ARSTAN<sup>79</sup>.

### *Growth tests*

To test differences in growth from before and after 1980, we tested differences in growth rate by diameter classes<sup>80</sup>. The diameter classes were defined in 10 cm increments, up to a DBH of 50 cm and differences in growth rate between the two periods were evaluated using Wilcoxon non-parametric test. A second test for difference in growth was performed in a more spaced time window, comparing the period of 1940 to 1970 with 1988 to 2018, because growth changes might have a delay due mechanisms of tree resistance like use of stored reserves or plasticity to cope with climate variation<sup>25,65,66</sup>. To exhaust the methods available to verify growth changes in tree-ring data and select the most cohesive result, two other chronologies were build to retain growth changes and local forest dynamics: one detrend using linear regressions with any slope and one of Basal Area Increment (BAI)<sup>80</sup>. Finally, we tested the growth in extreme years before and after 1980 usign the regional curve detrended tree-ring data. All analyses were carried in R<sup>84</sup>.

## **Tree-ring stable isotopes analyses**

### *Sampling, preparation and chronology building*

We selected 9 *Amburana cearensis* and 6 *Cedrela fissilis* trees with ages between 16 to 167 and DBH from 18 to 59.4 (Table S2) to measure the isotopic ratio of oxygen in tree-ring cellulose and removed the first 5 to 10 rings to exclude juvenile effects. Thin 2mm slices were cut from clean samples (washed with high pressure water or polished in microtomes), then the chemical treatment for cellulose extraction was performed in several laths at a time (modified from<sup>85,86</sup>). Tree rings were individualized using a razor blade under a stereomicroscope and placed in clean Eppendorfs. Individual rings were homogenized with distilled water, left to frozen and lyophilized before being weighted in silver capsules for analysis at the Stable Isotope Laboratory of the Geosciences Institute of the University of São Paulo (LIESP-CPGeo-IGc-USP) using a Thermo-Finnigan Delta Plus Advantage mass spectrometer. The oxygen isotopic ratios are expressed in ‰ relative to the Vienna Standard Mean Ocean Water.

### *Untagling the change in source water from the evaporative enrichment signal*

We assessed changes in rainout during air mass trajectory to the site calculating site air mass back trajectories<sup>53</sup> using daily precipitation data from the Tropical Rainfall Measuring Mission (TRMM), and local  $\delta^{18}\text{O}$  rainfall monitoring from 2000 to 2018 (Strikis *et al.*, in press).

To explore the effect of leaf water enrichment on the isotope ratios we used an isotope model that considers changes in equilibrium and kinetic fractionation resulting from variations in temperature and vapor pressure deficit, stomatal conductance (gs), and changes during cellulose synthesis<sup>44,45</sup>. Because the parameters are chosen based on literature data of the species and region<sup>65</sup> and not directly from the sampled trees, we tested different path lengths, stomatal conductance and changing the path length according to the transpiration rate<sup>87</sup>.

### **Climate data**

The climate data for temperature, relative humidity and rainfall was compiled from surrounding meteorological stations that cover an area of nearly  $1.5^\circ \times 1.5^\circ$ , centered over the Cavernas do Peruaçu National Park, using the same list of meteorological stations in<sup>47</sup>. VPD was calculated using local temperature and relative humidity. We tested monthly climate correlations from May to April (next year) because the growing season starts in October and ends around March and whole growing season, summer means and totals to search the most relevant periods for the inferences about climate and growth.

Local past conditions of rainfall, relative humidity and temperature were accessed using a general circulation model (GCM) of the National Center for Atmospheric Research (NCAR) Community Earth System Model (CESM) Last Millennium Ensemble (LME)<sup>88</sup>. Simulations correspond to a  $2^\circ$  cell grid centered at  $14^\circ 04'S$ ,  $44^\circ 13'W$ .

### **Tree-ring relation with instrumental and local speleothem records**

To assess growth responses to climate, we compared our tree-ring series with regional and local climate and speleothem records. The tests were performed for both species separately (check supplementary material) and together. Because the climate responses were coherent between species and stronger in the multi-species chronology, the main results discussed are from the series composed of both *A. cearensis* and *C. fissilis* trees. The standard Pearson's correlation coefficients<sup>89</sup> were used in different time

windows to understand high-frequency climate correlations. The existence of trends was tested using Piecewise linear regressions<sup>90</sup>. All analyses were carried in R<sup>84</sup>.

## **Subfossil trees analyses**

### *Sample context and tree-ring analyses*

To associate any trees response to anthropogenic climate change the observations need to be put in a longer context within the local natural climate variability. This is a challenge for tropical trees that reach 200 years in average<sup>63</sup> and the construction of long records of environmental variability relies on tree rings from long dead trees<sup>75</sup>. It is unlikely to find preserved wood in the tropics because the warm and moist conditions are not ideal for preservation. But these conditions were found in the karstic regions from Central-Eastern Brazil, where tall conduits inside the caves created an environment that allowed the preservation of trunks (Figure S16). Such trunks were probably removed from the surrounding vegetation by large flooding events that transported them into the caves<sup>91</sup> and here were dated using the radiocarbon wiggle-match approach<sup>59</sup> (Figure S10, Table S3). With this unique set of data for tropical lowlands, the natural variability of the climate in a pre-industrial period was accessed using two subfossils trunk samples and local annual layered speleothem. Because of the strong common signal of *A. cearensis*<sup>47</sup>, the strong common signals in cellulose  $\delta^{18}\text{O}^{40}$ , the independent techniques used to thoroughly date both tree ring and speleothems, and climate modeling for the past, all of this allowed that climate inferences using both living and subfossil trees could be made.

### *Radiocarbon “wiggle match” dating*

To obtain an accurate dating of these fossil trunks, we used the radiocarbon wiggle matching dating method<sup>59,92</sup>. This method consists of the radiocarbon dating of several years in a known interval to find a precise region of correspondence in the known <sup>14</sup>C calibration curve. We found three *Amburana cearensis* inside cave conduits in the site, from each sample we selected from 3 to 5 tree rings with a known gap (number of rings between two consecutive samples), depending on how old and where in the calibration curve the sample was dated (Figure S17). We extracted the  $\alpha$ -cellulose from the whole wood to perform the measurements<sup>93</sup> with an acid-base-acid and bleaching extraction of individual rings as described by Ehrlich et al. (2017)<sup>94</sup>. Between 2-3mg of  $\alpha$ -cellulose were graphitized using an EA-AGE3 system, composed of an elemental analyzer (EA, 'vario ISOTOPE SELECT' by Elementar), coupled to an automatic graphitization equipment



(AGE3 by Ionplus). The  $^{14}\text{C}$  content determination was made using an Accelerator Mass Spectrometer at the Dangoor Research Accelerator Mass Spectrometry (D-REAMS) laboratory at the Weizmann Institute<sup>95</sup>, and the results were calibrated and modelled using OxCal v 4.4.4<sup>96</sup> to the Southern Hemisphere calibration curve, SHCal20<sup>60</sup> and the Post-bomb atmospheric SH1-2 curve<sup>97</sup>.

### Acknowledgments

Funding: this work was supported by the São Paulo Research Foundation – FAPESP (grant numbers: PIRE-CREATE project 2017/50085-3; MG V grant 2018/07632-6 and BEPE 2019/09813-0. The radiocarbon research was supported by the Exilarch Foundation that supports the Dangoor Research Accelerator Mass Spectrometer (D-REAMS) Laboratory. We wish to thank the Kimmel Center for Archaeological Science and the George Schwartzman Fund for the laboratory and funding support for MG V in Israel. This study was partially financed by the Coordenação de Aperfeiçoamento de Pessoal de Nível Superior - CAPES (Finance Code 001). The authors are deeply indebted to fieldwork support personnel, such as our cooks, Mrs. Anita and Nildinha dos Santos and our field guides, Mr. Lucimar dos Santos and Mr. Vandey Batista de Jesus whose help and knowledge are immeasurable for this research. The authors also thank Paula Alecio and Eugenia Mintz for helping with sample preparation and laboratory procedures.

### Methods references

70. Ministério do Meio Ambiente. diagnóstico do macrozoneamento ecológico-econômico da bacia hidrográfica do Rio São Francisco. (2011).
71. Leite, E. J. State-of-knowledge on *Amburana cearensis* (Fr. Allem.) A.C. Smith (Leguminosae: Papilionoideae) for genetic conservation in Brazil. *J. Nat. Conserv.* **13**, 49–65 (2005).
72. Baker, J. C. A. *et al.* Oxygen isotopes in tree rings show good coherence between species and sites in Bolivia. *Glob. Planet. Change* **133**, 298–308 (2015).
73. Paredes-Villanueva, K., López, L., Brookhouse, M. & Cerrillo, R. M. N. Rainfall and temperature variability in Bolivia derived from the tree-ring width of *Amburana cearensis* (Fr. Allem.) A.C. Smith. *Dendrochronologia* **35**, 80–86 (2015).
74. Zuidema, P. A. *et al.* Tropical tree growth driven by dry-season climate variability.

- Nat. Geosci.* **15**, 269–276 (2022).
75. Speer, B. J. H. Fundamentals of tree-ring research. 509 (2010).
76. Krottenthaler, S. *et al.* A power-driven increment borer for sampling high-density tropical wood. *Dendrochronologia* **36**, 40–44 (2015).
77. Godoy-Veiga, M. *et al.* Shadows of the edge effects for tropical emergent trees: the impact of lianas on the growth of *Aspidosperma polyneuron*. *Trees - Struct. Funct.* **32**, 1073–1082 (2018).
78. Hietz, P. A simple program to measure and analyze tree rings using Excel, R and SigmaScan. *Dendrochronologia* **29**, 245–250 (2011).
79. Holmes, R. Computer-assisted quality control in tree-ring dating and measurement. (1983).
80. Peters, R. L., Groenendijk, P., Vlam, M. & Zuidema, P. A. Detecting long-term growth trends using tree rings: A critical evaluation of methods. *Glob. Chang. Biol.* **21**, 2040–2054 (2015).
81. Cook, E. R. The Decomposition of Tree-Ring Series for Environmental Studies. *Tree-Ring Bull.* **47**, 37–59 (1987).
82. Wigley, T. M. L., Briffa, K. R. & Jones, P. D. On the average value of correlated time series with applications in dendroclimatology and hydrometeorology. *Journal of Climate & Applied Meteorology* **23**, 201–213 (1984).
83. Bunn, A. G. A dendrochronology program library in R (dplR). *Dendrochronologia* **26**, 115–124 (2008).
84. R Core Team (2022). R: A language and environment for statistical computing. *R Found. Stat. Comput. Vienna, Austria* (2022).
85. Kagawa, A., Sano, M., Nakatsuka, T., Ikeda, T. & Kubo, S. An optimized method for stable isotope analysis of tree rings by extracting cellulose directly from cross-sectional laths. *Chem. Geol.* **393–394**, 16–25 (2015).
86. Wieloch, T., Helle, G., Heinrich, I., Voigt, M. & Schyma, P. A novel device for batch-wise isolation of  $\alpha$ -cellulose from small-amount whole wood samples. *Dendrochronologia Technical note*, **29**, 115–117 (2011).
87. Pereira, G. A. The climate response of *Cedrela fissilis* annual ring width in the Rio São Francisco Basin, Brazil. *Tree-Ring Research*, **74**, 162–171 (2018).
88. Otto-Bliesner, B. L., Brady, E. C., Fasullo, J., Jahn, A., Landrum, L., Stevenson, S., Rosenbloom, N., Mai, A., Strand, G., Climate variability and change since 850 CE an ensemble approach with the community earth system model. *Bull. Am. Meteorol. Soc.* **97**, 787–801 (2016).
89. Blasing, T. J., Solomon, A. M. & Duvick, D. N. Response Functions Revisited. *Tree-Ring Bull.* **44**, 1–15 (1984).

90. Muggeo, V. segmented: an R Package to Fit Regression Models with Broken-Line Relationships. *R news* **8**, 20–25 (2008).
91. Coelho, M., Fernandes, G. & Sánchez-Azofeifa, A. Brazilian Tropical Dry Forest on Basalt and Limestone Outcrops. *Trop. Dry For. Am.* 55–68 (2013).
92. Galimberti, M., Ramsey, C. B. & Manning, S. W. Wiggle-match dating of tree-ring sequences. *Radiocarbon* **46**, 917–924 (2004).
93. Linick, T. W., Long, A., Damon, P. E. & Ferguson, C. W. High-precision radiocarbon dating of bristlecone pine from 6554 to 5350 BC. *Radiocarbon* **28**, 943–953 (1986).
94. Ehrlich, Y., Regev, L., Kerem, Z. & Boaretto, E. Radiocarbon dating of an olive tree cross-section: New insights on growth patterns and implications for age estimation of olive trees. *Front. Plant Sci.* **8**, 1–9 (2017).
95. Regev, L. *et al.* D-REAMS: A New Compact AMS System for Radiocarbon Measurements at the Weizmann Institute of Science, Rehovot, Israel. *Radiocarbon* **59**, 775–784 (2017).
96. Ramsey, C. B. Bayesian analysis of radiocarbon dates. *Radiocarbon* **51**, 337–360 (2009).
97. Hua, Q., *et al.* Atmospheric radiocarbon for the period 1950 –019. *Radiocarbon* **64**, 723–745 (2022).

## Supplementary information

### Tree growth does not decline due to increasing VPD in seasonally dry tropical forest

Milena Godoy-Veiga<sup>1</sup>, Gabriel Assis-Pereira<sup>2</sup>, Bruno Barçante Ladvocat Cintra<sup>3</sup>, Nicolás Misailidis Stríkis<sup>4</sup>, Marília Harumi Shimizu<sup>5</sup>, Francisco William da Cruz<sup>6</sup>, Lior Regev<sup>7</sup>, Elisabetta Boaretto<sup>7</sup>, Ana Carolina Maioli Campos Barbosa<sup>8</sup>, Mario Tomazzelo-Filho<sup>9</sup>, Gregório Ceccantini<sup>1</sup>, Veronica Angyalossy<sup>1</sup>, Laia Andreu-Hayles<sup>9,10,11</sup>, Giuliano Maselli Locosselli<sup>12,13</sup>.

<sup>1</sup>Institute of Biosciences, University of São Paulo, Rua do Matão 277, 05508-090 São Paulo, Brazil

<sup>2</sup>Forestry Sciences Department, University of São Paulo, Av. Pádua Dias 11, 13418-900, Piracicaba, Brazil

<sup>3</sup>School of Geography, University of Leeds, Garstang North Building, Leeds LS2 9JT, UK

<sup>4</sup>Geochemistry Department, Fluminense Federal University, 24020-141 Niterói, Brazil

<sup>5</sup>General Coordination of Earth Sciences, National Institute for Space Research—INPE, São Paulo, Brazil

<sup>6</sup>Institute of Geosciences, University of São Paulo, Rua do Lago 562, 05508-080 São Paulo, Brazil

<sup>7</sup>D-REAMS Laboratory, Scientific Archaeology Unit, Weizmann Institute of Science, 7610001 Rehovot, Israel

<sup>8</sup>Department of Forest Sciences, Federal University of Lavras, PO Box 3037, Lavras, Minas Gerais, Brazil

<sup>9</sup>Lamont-Doherty Earth Observatory, Columbia University, 61 Route 9W, Palisades, NY 10964, USA;

<sup>10</sup>CREAF, Bellaterra (Cerdanyola del Vallés), Barcelona, Spain

<sup>11</sup>ICREA, Pg. Lluís Companys 23, Barcelona, Spain

<sup>12</sup>Center for Nuclear Energy in Agriculture, University of São Paulo, Piracicaba, Brazil

<sup>13</sup>Environmental Research Institute of the State of São Paulo, São Paulo, Brazil

#### List of supplementary figures:

**Figures S1 to S4** - Individual and multi-species tree-ring series, metrics, and tests.

**Figures S05 to S09** - Tree-ring chronologies correlations with local rainfall and VPD.

**Figures S10 to S12** - Tests for untangling the source signal from the evaporative enrichment signal in tree-ring  $\delta^{18}\text{O}$ .

**Figures S13 to S15** - Testing the effect of VPD on trees growth.

**Figures S16 to S21** - Subfossil samples context, dating and tests.

**Figures S1 to S4 - Individual and multi-species tree-ring series, metrics, and tests.**

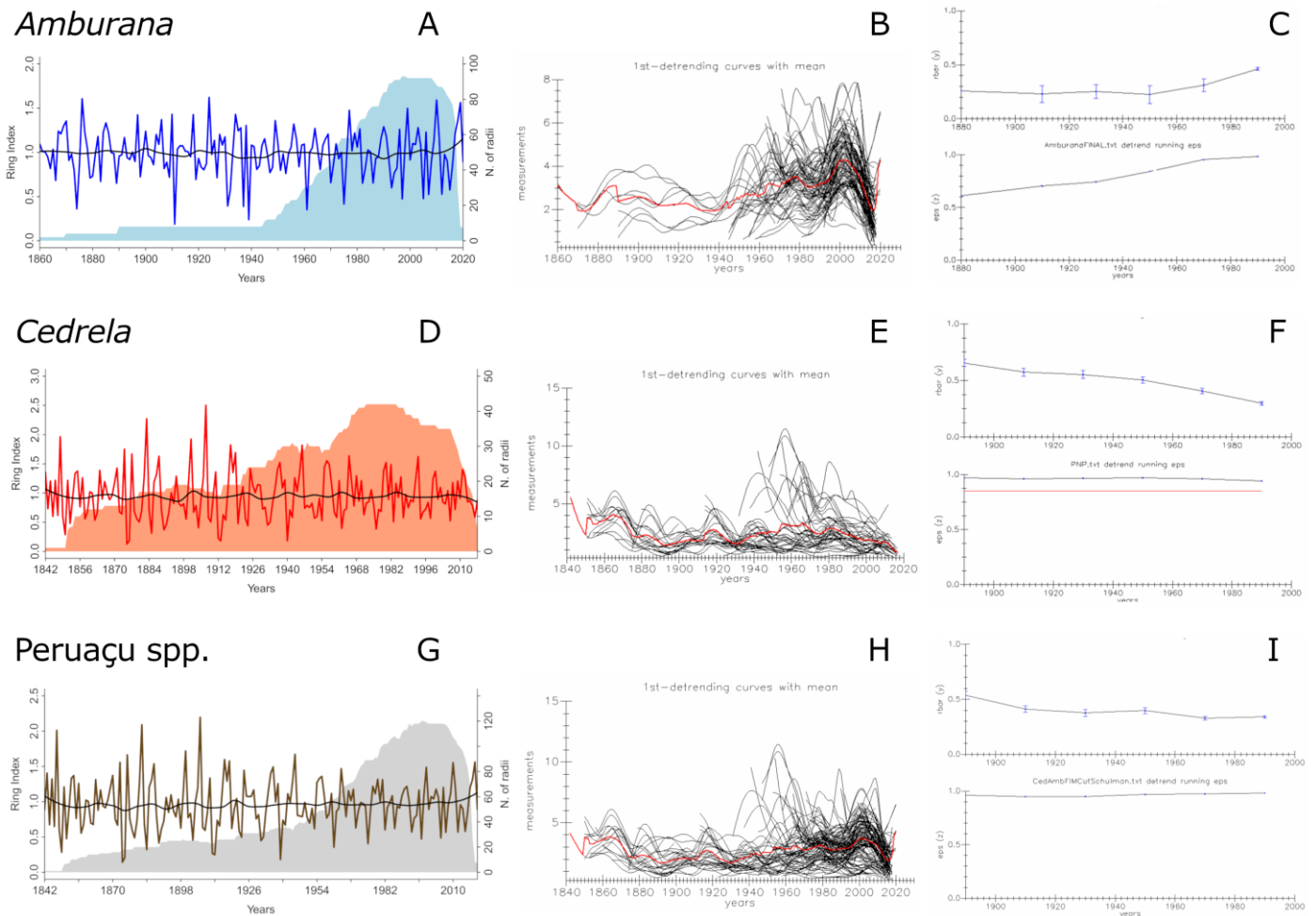


**Figure S01 – Tree-ring width chronologies, smoothing spline detrending curves, rbar and EPS for both species and site chronology using both.**

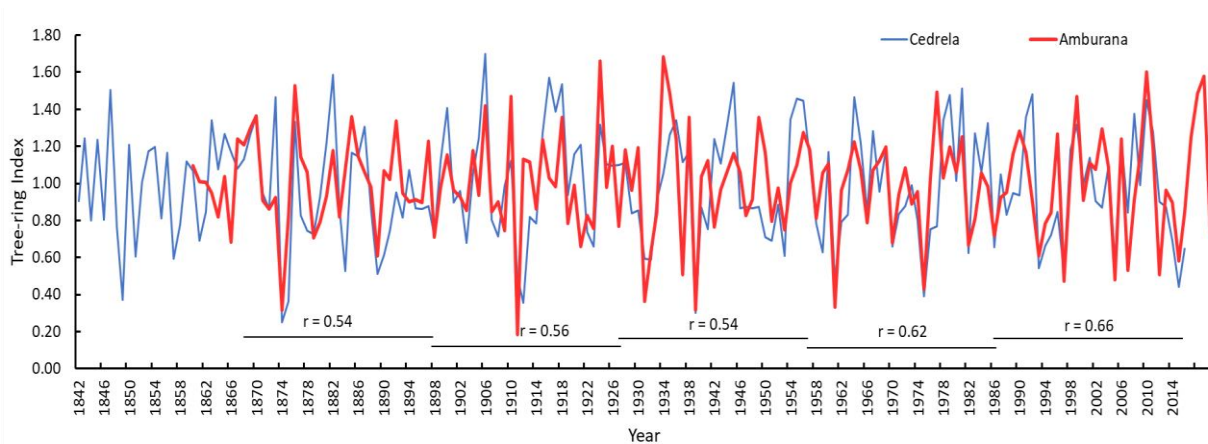


**Figure S02 – *Amburana cearensis* and *Cedrela fissilis* tree-ring width chronology with correlations coefficient in 30-years windows. Correlations are significant ( $p < 0.01$ ).**

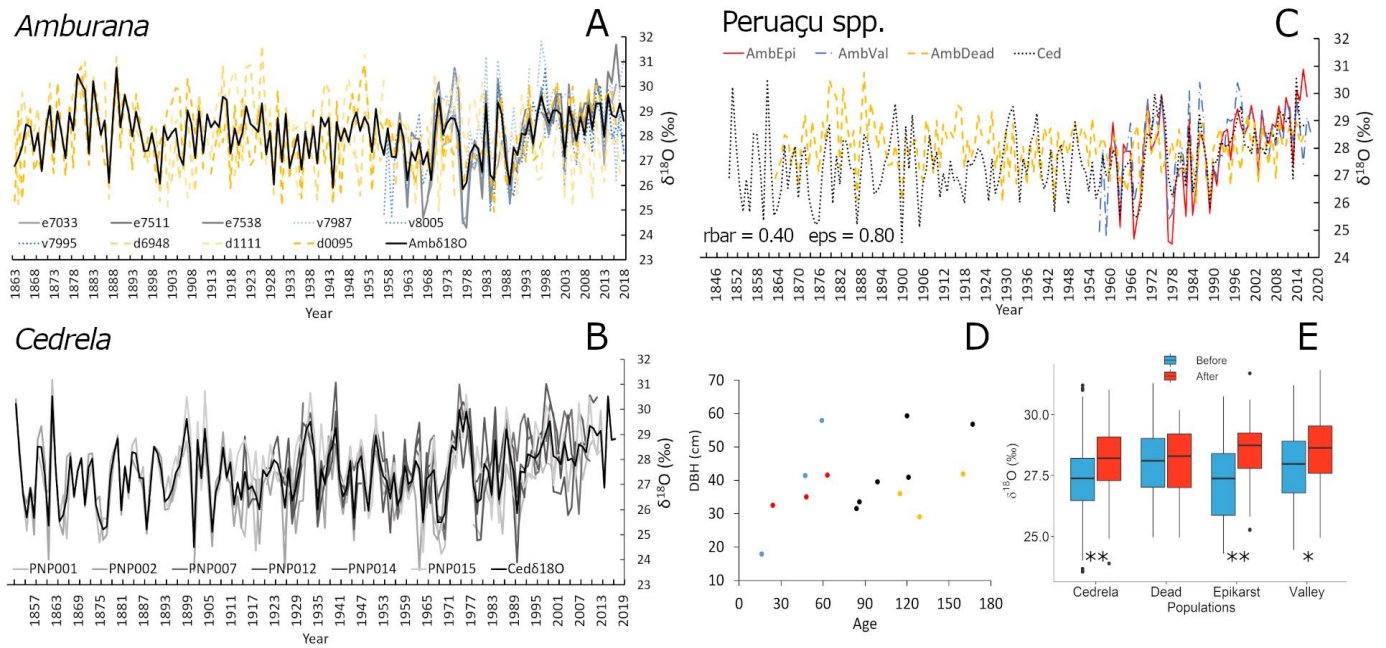


**Figure S03** – Tree-ring ratio of oxygen isotopes ( $\delta^{18}\text{O}$ ) of individual species and site mean. In A: *Amburana cearensis* individual tree and population tree-ring oxygen  $\delta^{18}\text{O}$  series. Letter before samples ID represent the sampling site, e: from driest epikarst areas; v: trees from less seasonal areas in the valley or deep soiled karstic areas; D: dead trees from valley or unknown origin. In B: *Cedrela fissilis* individual and population tree tree-ring  $\delta^{18}\text{O}$  series. In C: Different populations of *Amburana cearensis* and *Cedrela fissilis* mean tree-ring  $\delta^{18}\text{O}$  series. AmbEpi: *A. cearensis* trees from driest epikarst areas; AmbVal: *A. cearensis* trees from less seasonal in the valley or deep soiled karstic areas; AmbDead: dead *A. cearensis* trees from valley or unknown origin; Ced: *C. fissilis* trees sampled in more uniform microsite conditions in open areas. In D: Age and diameter at breast height (DBH) of trees. Different colors correspond to the different populations in C. In E: Isotopic values of the different populations before and after 1980. Using Wilcoxon non-parametric to test difference between periods, the asterisk indicate significant difference (\*  $p < 0.05$ , \*\*  $p < 0.01$ ).

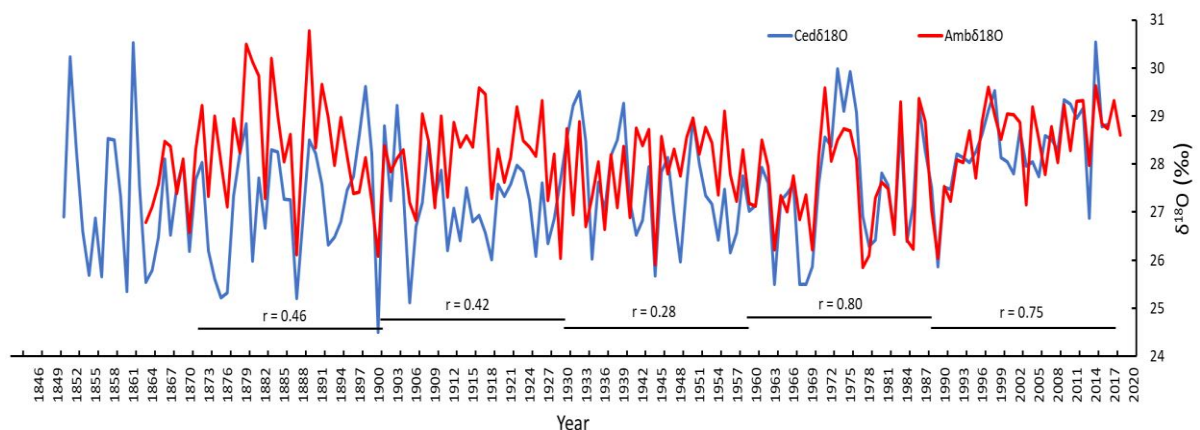


**Figure S04** - *Amburana cearensis* and *Cedrela fissilis* tree-ring  $\delta^{18}\text{O}$  chronology with correlations coefficient in 30-years windows. Low correlations are only observed in the same period the TRW chronologies also decreases, probably due to low sample replication and/or local disturbances since correlations are strong in the beginning of the series.



**Figures S05 to S09 – Tree-ring chronologies correlations with local rainfall and VPD.**

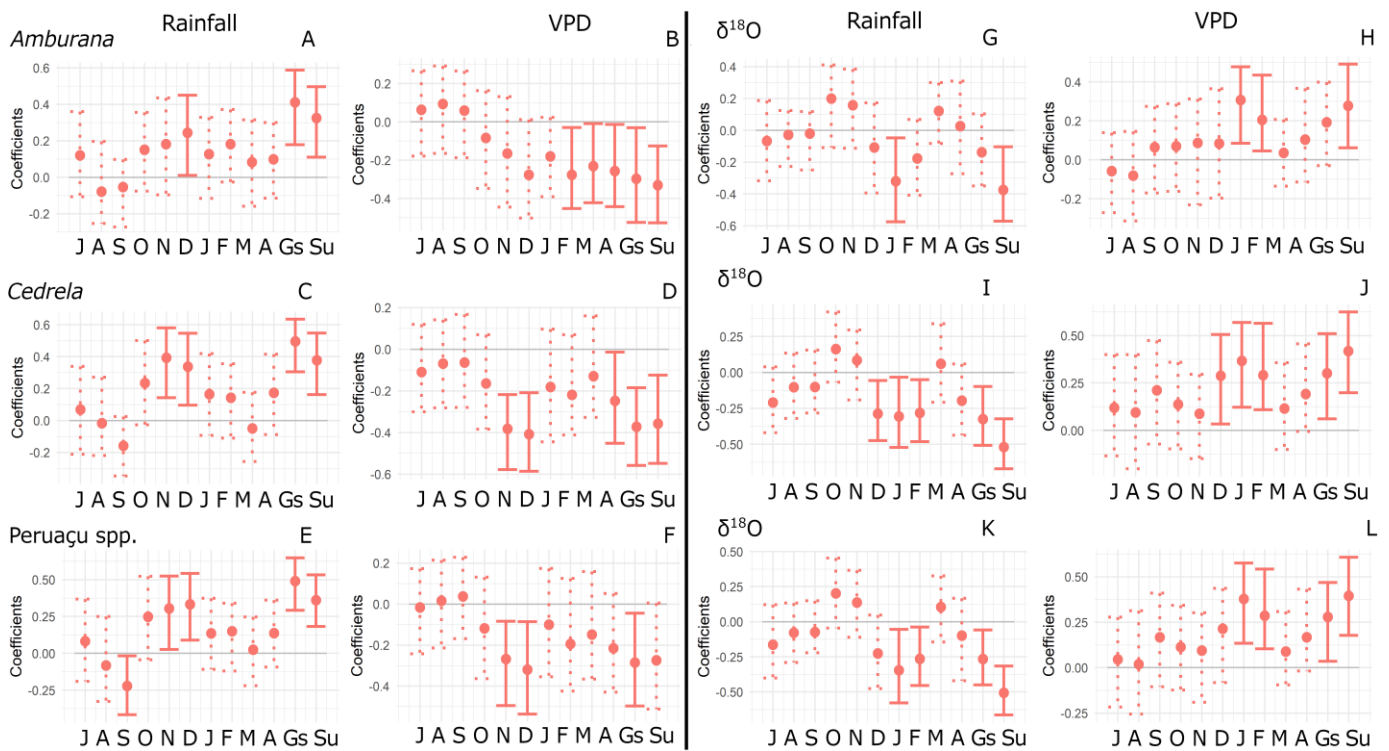


**Figure S05 –** Tree-ring width (A-F)  $\delta^{18}\text{O}$  (G-L) series correlation with montly rainfall and VPD for both species separetly and togheter. Significant correlations in of the bootstrapped analisys are indicated by continous lines. The letters bellow are the respective months from July to April, followed by the Gs: Growth season, and Su: Summer months.

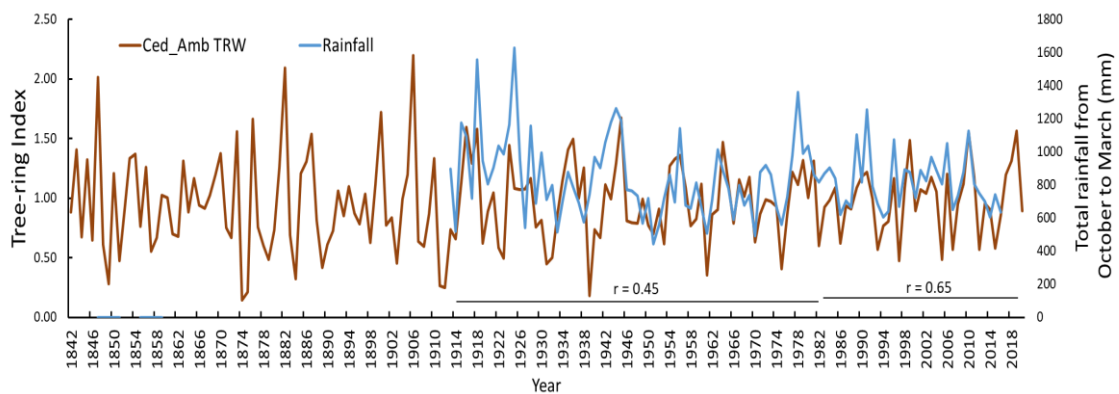


**Figure S06 –** Site tree-ring width chronology (brown) and total local rainfall from October to March (blue). Pearson correlation are shown for the period before and after 1980. Correlations are significant ( $p < 0.01$ ).

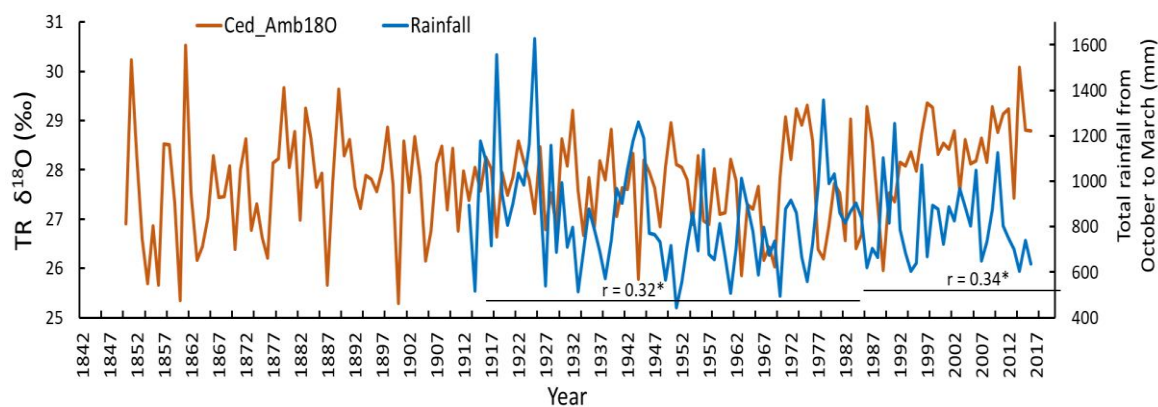


**Figure S07** – Site tree-ring  $\delta^{18}\text{O}$  chronology (orange) and local rainfall (blue). Pearson correlation are shown for the period before and after 1980. Correlations are significant (\*  $p < 0.05$ ). With a 5 years moving average in the tree-ring series, the correlations are  $r = -0.17$  (before 1980, not significant) and  $r = 0.35^*$  (after 1980,  $p < 0.05$ ).

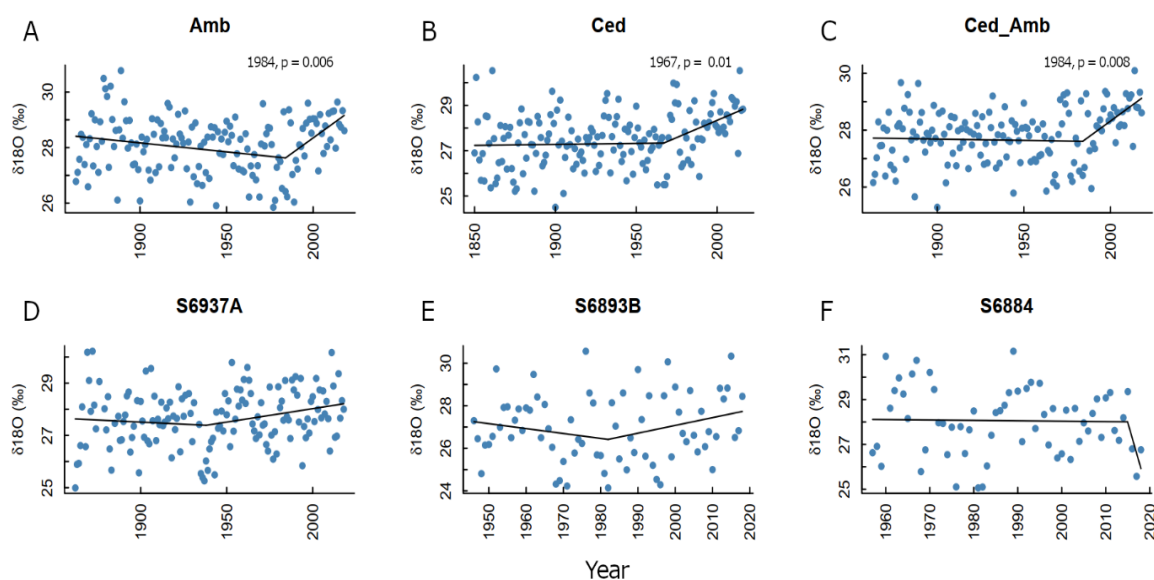


**Figure S08** – Piecewise linear regressions of  $\delta^{18}\text{O}$  series from both species (Amb, Ced), multispecies (Ced\_Amb) and the three subfossil samples of *Amburana*. Significant breakpoints are indicated in each plot by the year of the breakpoint and the  $p$  value.

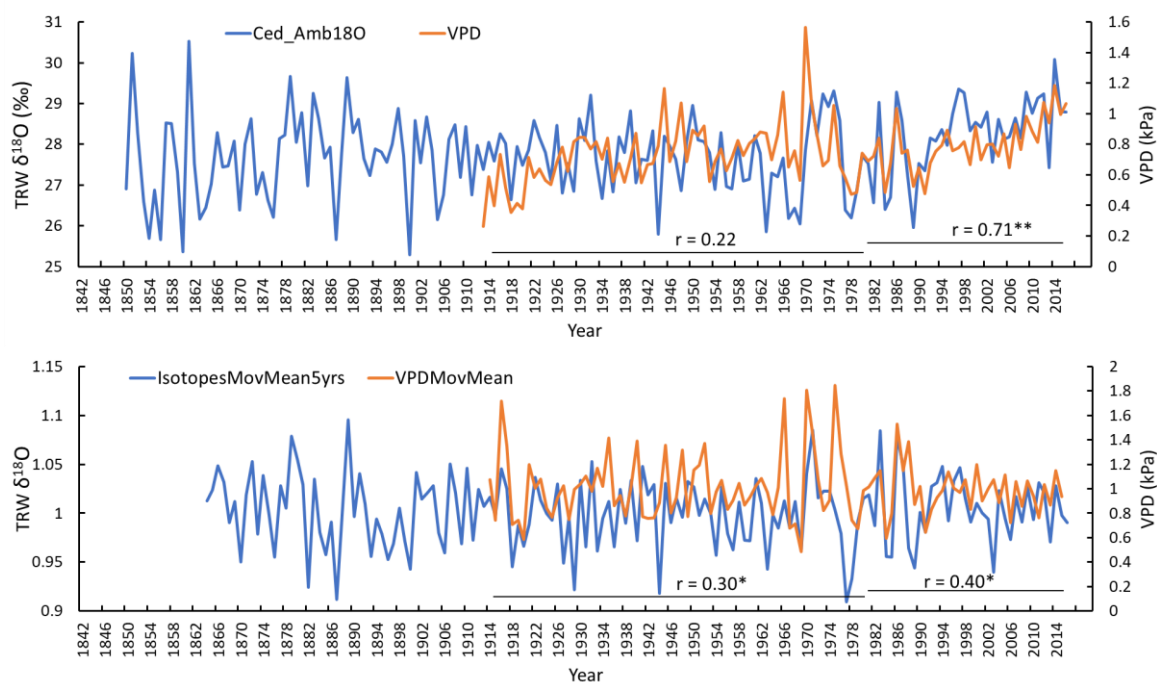


**Figure S09** – Multi species tree-ring  $\delta^{18}\text{O}$  chronology (light blue) and local summer VPD (red) raw and with a 5 years moving mean in both series. Pearson correlation are shown for the period before and after 1980. \*  $p < 0.05$ , \*\*  $p < 0.01$ .

### Figures S10 to S12 – Tests for untangling the source signal from the evaporative enrichment signal in tree-ring $\delta^{18}\text{O}$

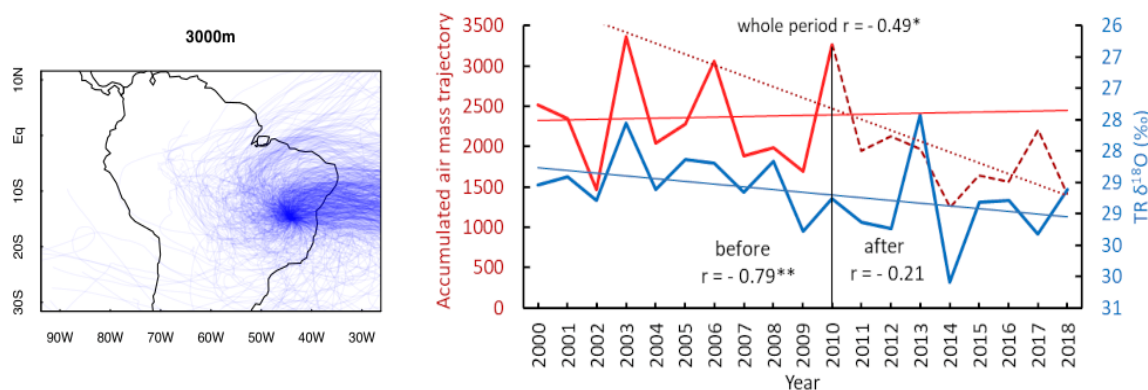


**Figure S10** – Air mass back trajectories calculated for the site. On the right panel the air mass total from October to March (top line, red) overall has no trend, but there is signs of the beginning of a decrease in 2010 (dashed red line), still not significant according to piecewise linear regression analysis. The blue line is the tree-ring  $\delta^{18}\text{O}$  and the correlations coefficients between series for the whole period, before, and after 2010. \*  $p < 0.05$ , \*\*  $p < 0.01$ .

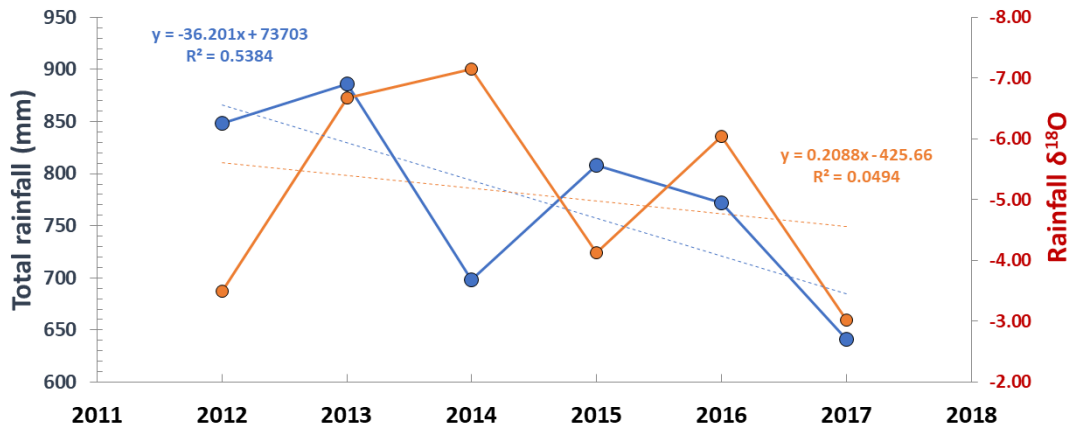


**Figure S11** – Local rainfall  $\delta^{18}\text{O}$  monitoring (orange) and local rainfall amount (blue). There is a negative trend in total rainfall in recent years (blue line, top left linear regression values), but the trend is less pronounced in the isotopes. Data collected by Strikis et al in press.

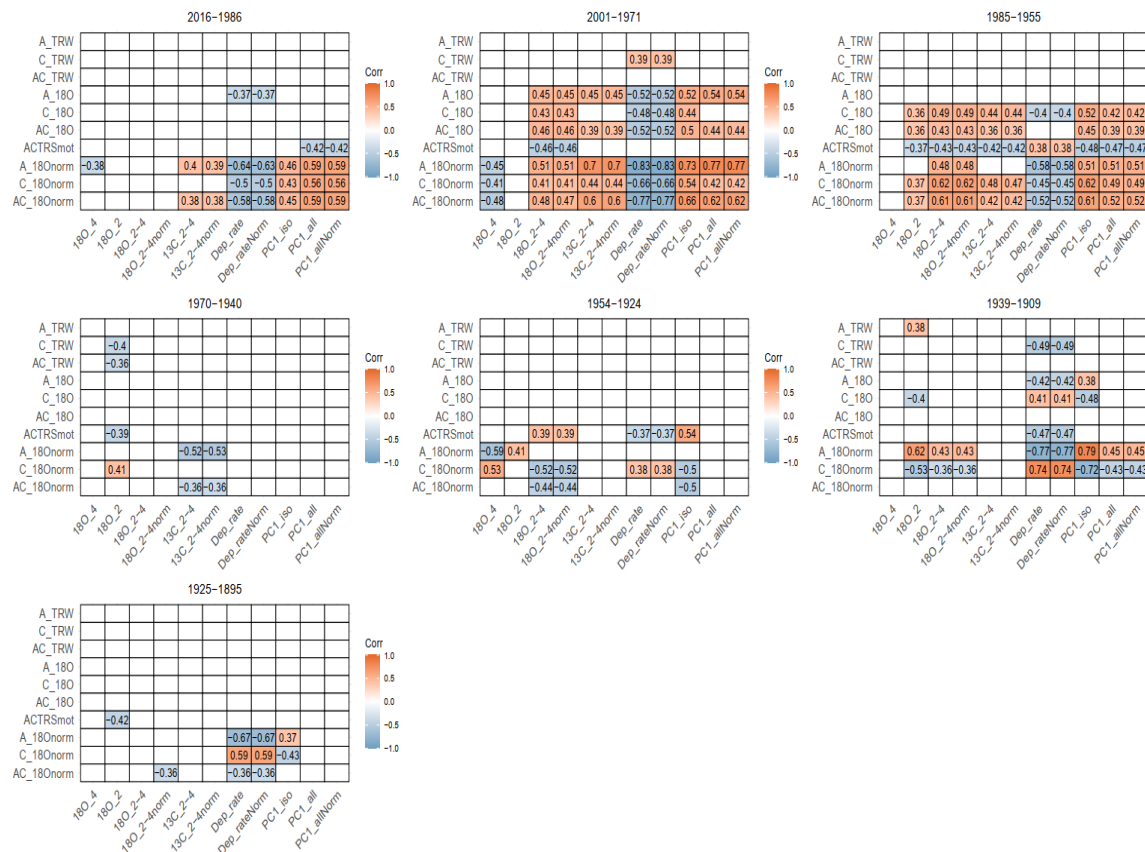


**Figure S12** – Heatmap of correlations between tree-ring series and speleothems (ONÇA 2-4, Strikis et al.) proxies. Tests were performed for *Amburana cearensis* tree-ring width chronology (A\_TRW), *Cedrela fissilis* tree-ring width chronology (C\_TRW), site tree-ring width chronology (AC\_TRW), followed by the tree-ring oxygen  $\delta^{18}\text{O}$  chronologies of *Amburana cearensis* (A\_18O), *Cedrela fissilis* (C\_18O) and site chronology (AC\_18O). The TRW was smoothed (ACTRSmot) and the last three tests are with the previous three  $\delta^{18}\text{O}$  chronologies smoothed with a loess function with span = 0.1 (A\_18Onorm, C\_18Onorm, AC\_18Onorm). The speleothem proxies, from left to right are:  $\delta^{18}\text{O}$  ONÇA 4,  $\delta^{18}\text{O}$  ONÇA 2,  $\delta^{18}\text{O}$  ONÇA 2-4,  $\delta^{18}\text{O}$  ONÇA 2-4 detrended,  $\delta^{13}\text{C}$  ONÇA 2-4,  $\delta^{13}\text{C}$  ONÇA 2-4 detrended, speleothem deposition rate, deposition rate detrended, principal

component of isotopic proxies, principal component of all proxies and principal component of all proxies detrended.

**Figures S13 to S15 – Testing the effect of VPD on trees growth.**

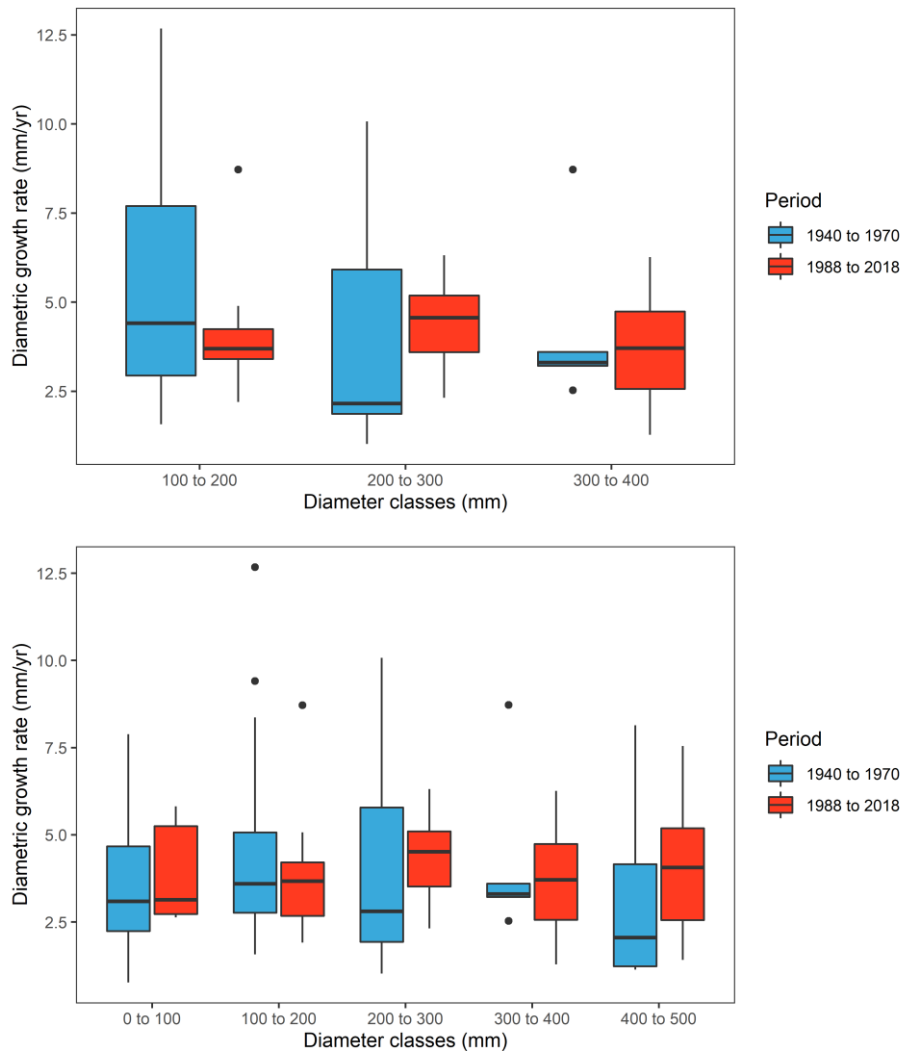


**Figure S13** – Diametric growth rate in diameter classes of *A. cearensis* and *C. fissilis* from the Peruaçu region (top) and together with data from the Juvenilia population, 50-100km from the site (Pereira *et al.*, 2018). The blue boxplots represent the growth rate from 1940 to 1970 and the red boxplots for 1988 to 2018. No difference was observed between growth rate comparing the two periods in any class.

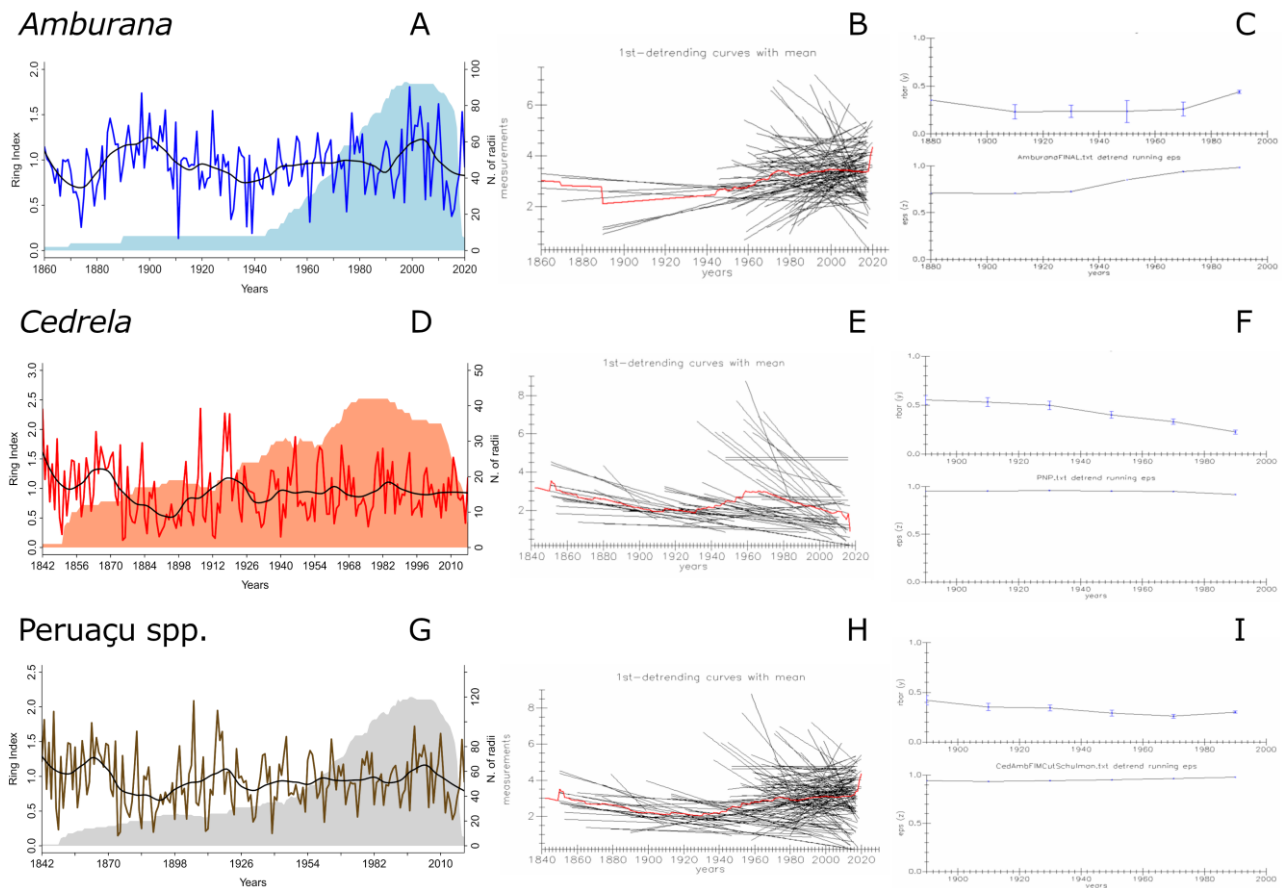


**Figure S14** – Tree-ring width chronologies, linear detrending lines,  $\bar{r}$  and EPS for both species and site chronology using both. The series do not show signs of decrease in growth after 1980. Instead there is an increase in growth around 1990 followed by a decrease caused by a few extreme years after 2010.

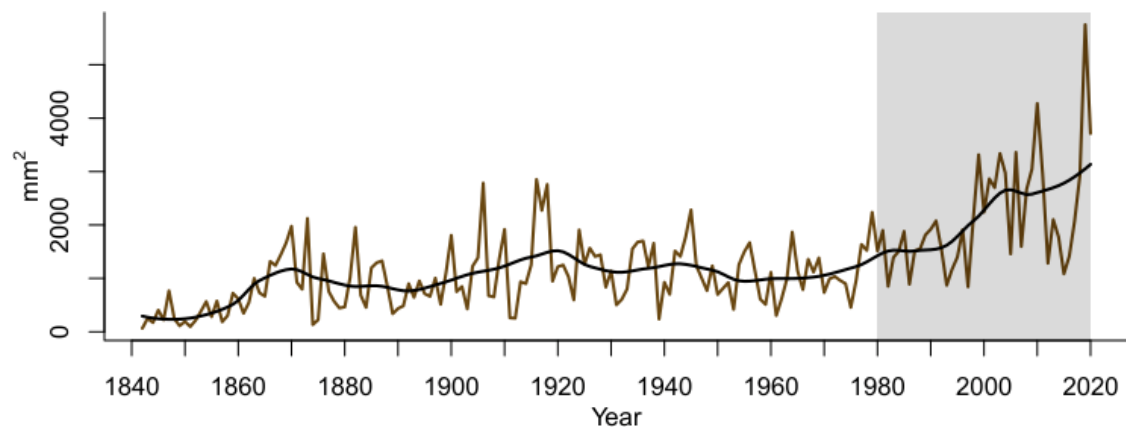


**Figure S15** – Peruaçu spp. Tree-ring width Basal Area Increment (BAI) series. Period after 1980 is highlighted, where an increase in growth is observed around 2000, then an stabilization, a few extreme years after 2010 and return to increase in the last years.



**Figures S16 to S21 – Subfossil samples context, dating and tests.**

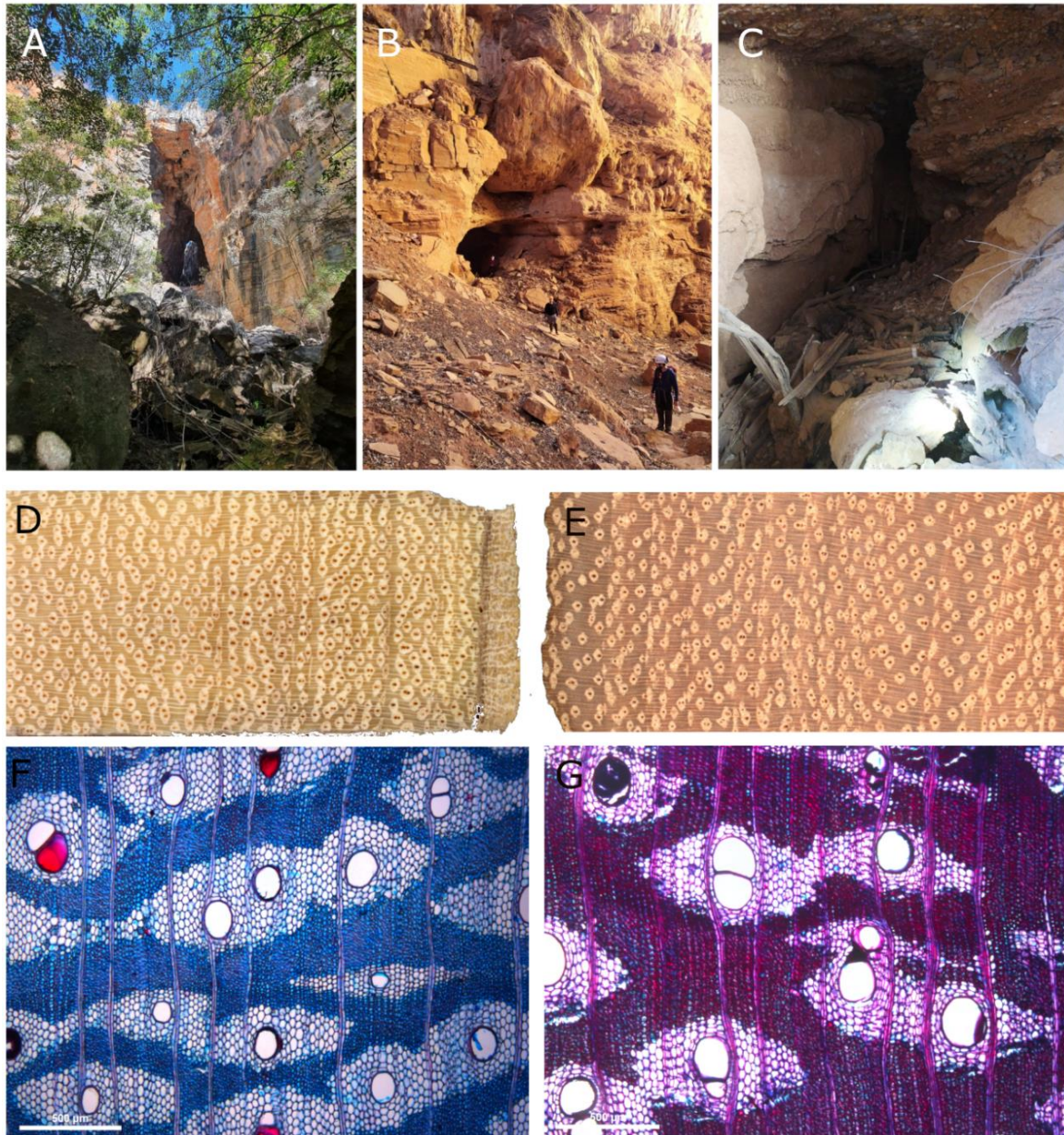


**Figure S16** – Subfossil samples of *Amburana cearensis* site context and wood anatomy. In A is the view of the Arco do André (André's Arch), one of the many arches and caves were conduits (B) are found filled with wood debris of many species (C). Macroscopic view of a 15mm core of a living tree (D) and a subfossil sample (E), with the transversal microscopic cross-section view below (scale bar = 500 $\mu$ m).

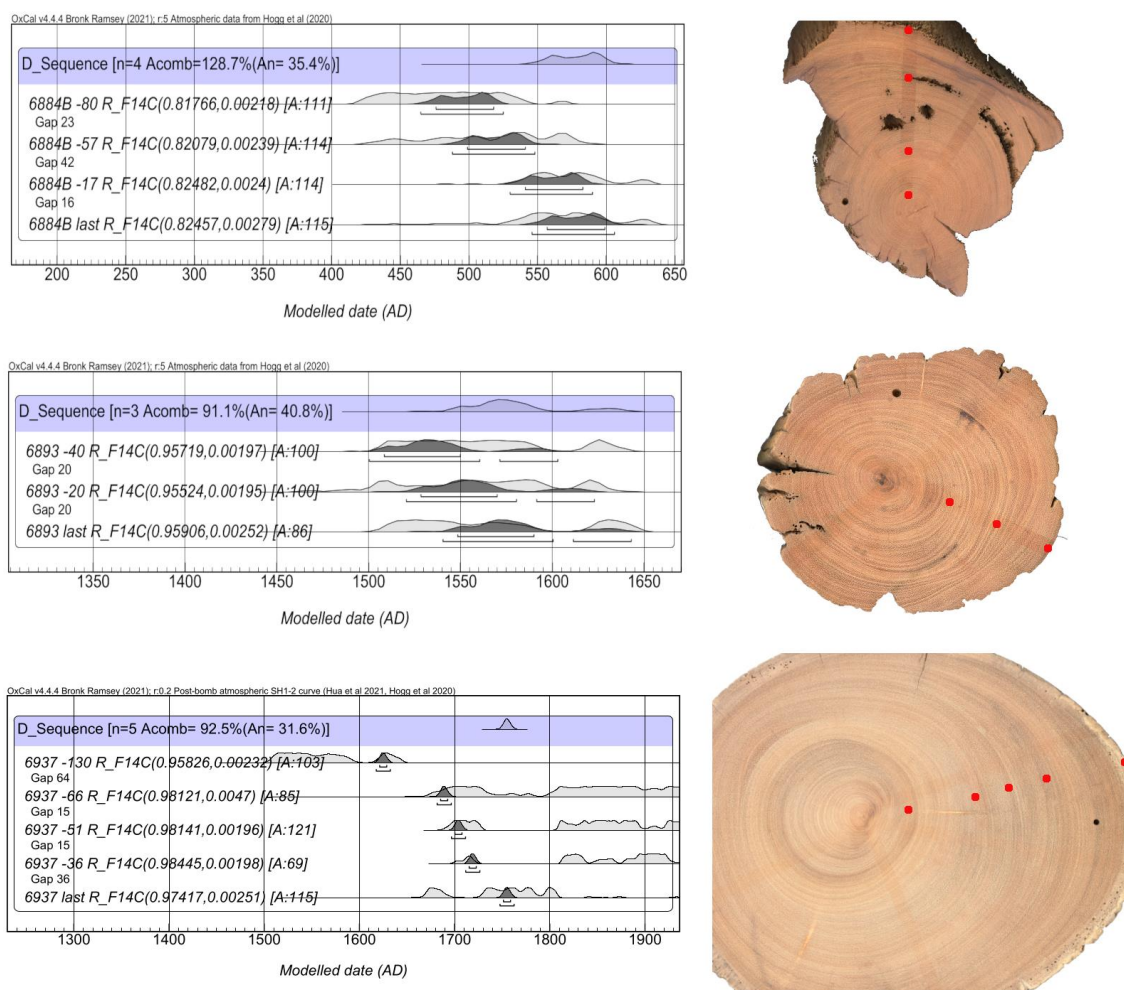


**Figure S17** – Modelled age of subfossil samples. The red dots on the scanned image of the samples represent the rings selected for the wiggle matching. In the panels are shown the parameters (fraction of  $^{14}\text{C}$  with measurement standard deviation, gap between rings, agreement of each sample in the model, and calibration curves) used in the D\_sequence in OxCal to calibrate and date the subfossil samples. The results are in Table S3.



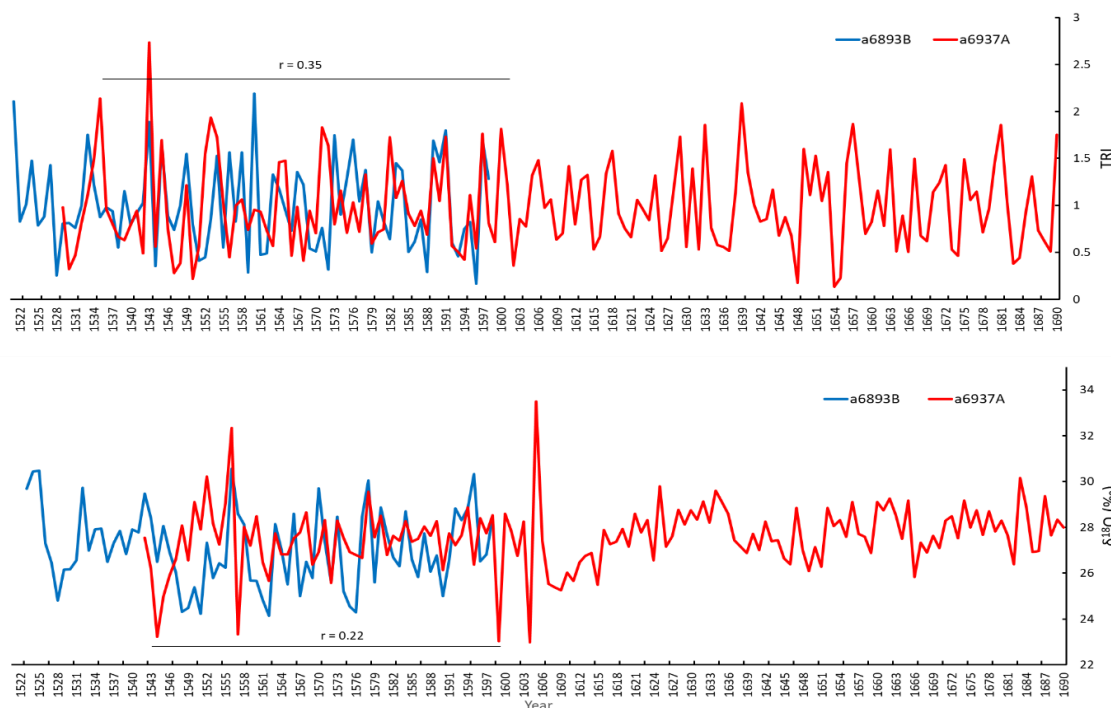


**Figure S18** – Subfossil tree-ring width (detrended with smooth spline) and  $\delta^{18}\text{O}$  floating series of the two *Amburana cearensis* samples that overlap 70 (TRW) and 57 ( $\delta^{18}\text{O}$ ) years with correlation coefficient between series.

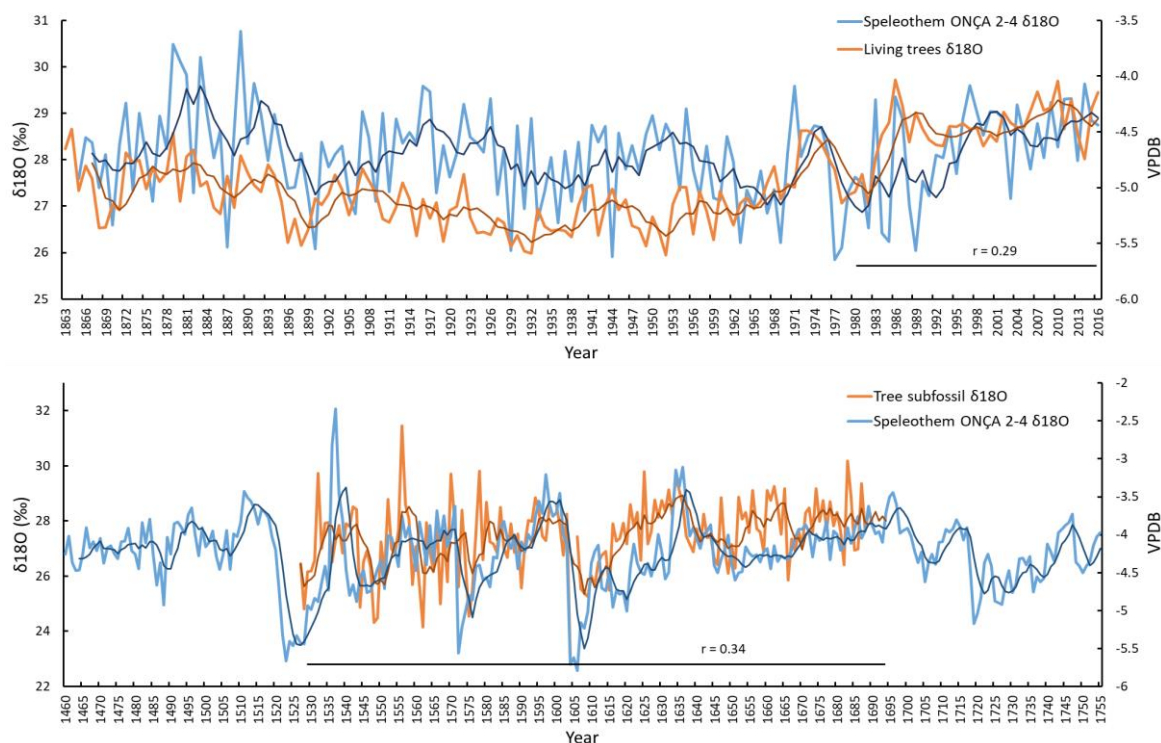


**Figure S19** –  $\delta^{18}\text{O}$  series of living and subfossil trees of *Amburana* (orange) with local speleothem ONÇA 2-4  $\delta^{18}\text{O}$  (light blue). Top panel: Living trees, correlation coefficient for the whole period is  $r = 0.21$  and from 1980 to 2016,  $r = 0.29$ . Bottom panel: series are shown for the period from 1460 to 1755 (widest range of possible ages for the subfossil trunks according to the  $^{14}\text{C}$  wiggle matching). Both raw and smoothed with 5 year moving mean (thin line) are shown.

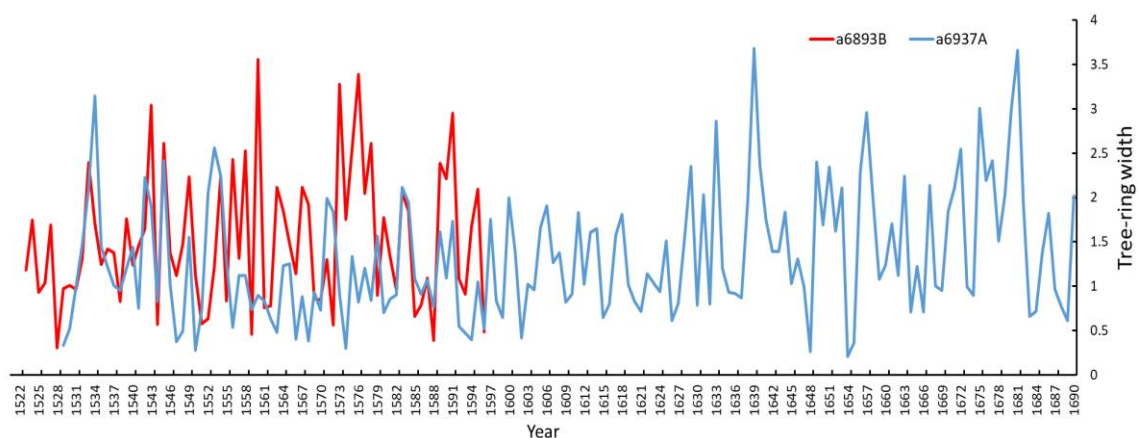


**Figure S20** – Raw subfossil tree-ring width series. No significant growth changes are apparent besides the growth release common to species attaining the canopy in 6937.

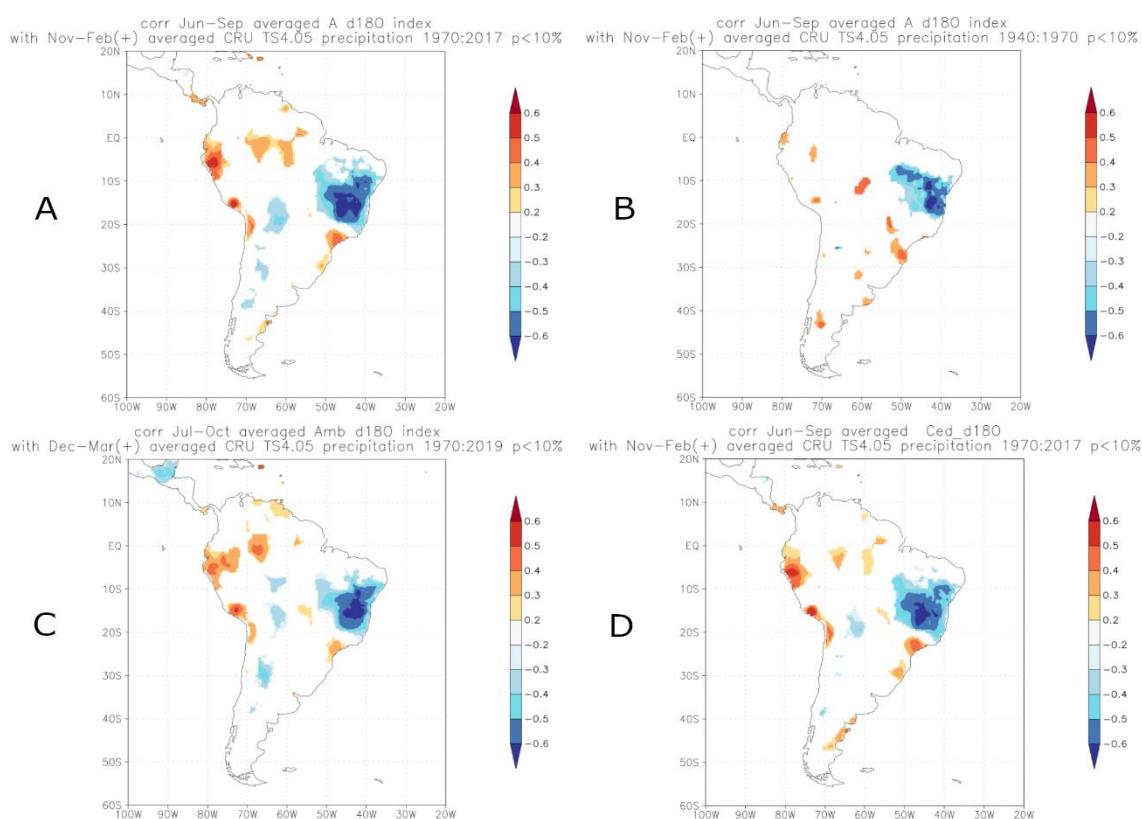


**Figure S21** – Spatial correlations of tree-ring  $\delta^{18}\text{O}$  with CRU gridded rainfall data over South America. The chronology using both species was correlated with rainfall from 1970 to 2017 (A) and 1940 to 1970 (B). C and D are the results for the species separately from 1970 to 2017.

**Table S1** - Correlation among *Amburana* tree-ring  $\delta^{18}\text{O}$  (amb), speleothem  $\delta^{18}\text{O}$ , and CESM-LME model series of VPD and rainfall raw values and smoothed with a 15 year moving mean.

The time windows correspond to an initial less arid period, followed by a period with increasing VPD and natural  $\delta^{18}\text{O}$  series increase, and a final period where VPD values drop but are higher than the initial state.

<b>Raw values</b>	<b>amb x vpd</b>	<b>amb x rainfall</b>	<b>amb x speleo</b>	<b>speleo x vpd</b>	<b>n</b>	<b>df</b>	<b>p 5%</b>	<b>p 1%</b>
<b>1530 - 1608</b>	-0.20	0.17	0.27	-0.11	79	77	<b>0.22</b>	<b>0.29</b>
<b>1608 - 1637</b>	0.34	-0.57**	0.47**	0.25	30	28	<b>0.36</b>	<b>0.46</b>
<b>1637 - 1690</b>	0.07	0.06	0.05	-0.31*	54	52	<b>0.27</b>	<b>0.35</b>
<b>15 yr moving mean</b>	<b>amb x vpd</b>	<b>amb x rainfall</b>	<b>amb x speleo</b>	<b>speleo x vpd</b>	<b>n</b>	<b>df</b>	<b>p 5%</b>	<b>p 1%</b>
<b>1530 - 1608</b>	-0.09	0.00	0.53**	-0.26*	79	77	<b>0.22</b>	<b>0.29</b>
<b>1608 - 1637</b>	0.41*	-0.87**	0.86**	0.75**	30	28	<b>0.36</b>	<b>0.46</b>
<b>1637 - 1690</b>	-0.51**	-0.25	0.20	-0.60**	54	52	<b>0.27</b>	<b>0.35</b>

n : number of observations ; df : degrees of freedom ; and critical p values. \*  $p < 0.05$ , \*\*  $p < 0.01$ .

**Table S2** - Statistics of extreme years analysis.

Four climate states are compared: Mean state, and years where the observed Rainfall or VPD was more than 1 standard deviation higher than record mean. Some years experienced extreme values in both parameters.

<b>climate</b>	<b>count</b>	<b>mean</b>	<b>sd</b>	<b>median</b>	<b>IQR</b>	<b>min</b>	<b>max</b>	<b>amp</b>
<b>Mean</b>	3512	3.09	2.1	2.7	2.78	0	17.5	17.5
<b>Rain</b>	234	2.4	1.88	1.94	2.18	0.22	11	10.8
<b>VPD</b>	399	2.28	1.74	1.83	2.09	0	12.1	12.1
<b>VPD_Rain</b>	210	2.53	2	1.91	2.02	0.23	14.1	13.8

$p$  values of pairwise comparisons between groups using Wilcoxon rank sum test with continuity correction

	<b>Mean</b>	<b>Rain</b>	<b>VPD</b>
<b>Mean</b>	-	-	-
<b>Rain</b>	4.50E-08	-	-
<b>VPD</b>	1.10E-15	0.57	-
<b>VPD_Rain</b>	9.50E-06	0.5	0.15

count: observations; mean; sd: standard deviation; median; IQR: interquartile range; min: minimum; max: maximum; amp: amplitude.

**Table S3** Calibrated and modelled results for each *Amburana* subfossil sample.

A D\_Sequence was used in OxCal calibration software, using the known gap between each two dated individual rings. The results were calibrated with SHCal20 (samples 6884B and 6893) or Post-bomb SH1-2 (sample 6937) calibration curves.

Sample/ring	F <sup>14</sup> C, sd	Unmodelled (BC/AD), 68.3%	Unmodelled (BC/AD), 95.4%	Modelled (BC/AD), 68.3%	Modelled (BC/AD), 95.4%
<b>6884B -80</b>	0.81766, 0.00218	434AD (15.9%) 454AD 466AD (52.3%) 526AD 474AD (23.7%) 511AD	419AD (95.4%) 542AD	476AD (68.3%) 518AD	464AD (95.4%) 524AD
<b>6884B -57</b>	0.82079, 0.00239	520AD (27.2%) 550AD 556AD (17.5%) 577AD	432AD (95.4%) 581AD	498AD (68.3%) 540AD	488AD (95.4%) 548AD
<b>6884B -17</b>	0.82482, 0.0024	540AD (68.3%) 595AD	523AD (95.4%) 638AD 476AD (5.0%) 510AD	540AD (68.3%) 582AD	530AD (95.4%) 590AD
<b>6884B last</b>	0.82457, 0.00279	536AD (68.3%) 596AD	520AD (90.4%) 638AD	556AD (68.3%) 598AD	546AD (95.4%) 606AD
<b>6893 -40</b>	0.95719, 0.00197	1510AD (63.5%) 1582AD 1622AD (4.8%) 1628AD 1503AD (9.7%) 1514AD	1502AD (79.6%) 1595AD 1615AD (15.9%) 1640AD	1508AD (68.3%) 1550AD	1500AD (80.2%) 1560AD 1571AD (15.2%) 1602AD
<b>6893 -20</b>	0.95524, 0.00195	1542AD (48.8%) 1595AD 1615AD (9.7%) 1626AD 1510AD (38.0%) 1549AD	1490AD (95.4%) 1632AD	1528AD (68.3%) 1570AD	1520AD (80.2%) 1580AD 1591AD (15.2%) 1622AD
<b>6893 last</b>	0.95906, 0.00252	1561AD (12.9%) 1577AD 1623AD (17.3%) 1641AD 1510AD (39.5%) 1550AD	1506AD (71.4%) 1592AD 1617AD (24.1%) 1648AD	1548AD (68.3%) 1590AD	1540AD (80.2%) 1600AD 1611AD (15.2%) 1642AD
<b>6937 -130</b>	0.95826, 0.00232	1560AD (17.0%) 1579AD 1623AD (11.7%) 1635AD 1693AD (16.9%) 1728AD 1809AD (7.7%) 1825AD 1830AD (31.4%) 1894AD	1505AD (75.2%) 1593AD 1617AD (20.3%) 1645AD  1674AD (25.4%) 1739AD 1757AD (1.0%) 1763AD	1621.32AD (68.3%) 1628.74AD	1617.7AD (95.4%) 1632.5AD
<b>6937 -66</b>	0.98121, 0.0047	1922AD (10.3%) 1943AD 1943AD (1.1%) 1946AD 1946AD (0.5%) 1948AD 1948AD (0.4%) 1949AD 1698AD (18.5%) 1724AD 1810AD (3.8%) 1816AD	1775AD (0.6%) 1779AD 1798AD (67.8%) 1950AD 1952AD (0.7%) 1955AD  1691AD (22.9%) 1728AD 1808AD (53.2%) 1896AD	1685AD (68.3%) 1693AD	1682AD (95.4%) 1697AD
<b>6937 -51</b>	0.98141, 0.00196	1844AD (19.1%) 1871AD 1875AD (11.3%) 1892AD 1923AD (11.6%) 1941AD	1905AD (2.4%) 1914AD 1920AD (17.0%) 1950AD	1700AD (68.3%) 1708AD	1697AD (95.4%) 1712AD



		1942AD (0.2%) 1943AD			
		1945AD (0.3%) 1946AD			
		1712AD (5.6%) 1719AD			
		1813AD (20.8%) 1836AD	1699AD (11.7%) 1723AD		
		1863AD (0.7%) 1865AD	1811AD (22.9%) 1839AD		
<b>6937 -36</b>	0.98445, 0.00198	1881AD (3.1%) 1887AD	1845AD (11.3%) 1870AD		
		1888AD (0.3%) 1889AD	1877AD (44.4%) 1931AD	1715AD (68.3%) 1723AD	1712AD (95.4%) 1727AD
		1890AD (35.7%) 1925AD	1936AD (4.8%) 1947AD		
		1942.3AD (1.0%) 1944AD	1949AD (0.1%) 1949AD		
		1945.3AD (1.1%) 1947AD	1954AD (0.3%) 1955AD		
		1671AD (14.3%) 1686AD			
		1732AD (16.1%) 1748AD	1665AD (21.3%) 1697AD		
		1752AD (15.0%) 1767AD	1724AD (68.4%) 1810AD		
<b>6937 last</b>	0.97417, 0.00251	1772AD (10.9%) 1782AD	1839AD (0.5%) 1844AD		
		1796AD (9.5%) 1806AD	1871AD (0.5%) 1875AD	1751AD (68.3%) 1759AD	1748AD (95.4%) 1763AD
		1950AD (0.5%) 1951AD	1944AD (0.2%) 1945AD		
		1952AD (2.0%) 1954AD	1947AD (4.5%) 1955AD		

---

F<sup>14</sup>C (fraction modern carbon) is the measured value by the AMS. sd is the measurement standard deviation

## Discussão Geral e Conclusões

---

A presente tese deu um passo significativo para estudos dendroclimatológicos e isotópicos na região central do Brasil utilizando a espécie *Amburana cearensis* em um dos *hot spots* de aquecimento global nos trópicos. Os resultados obtidos a partir dos anéis de crescimento puderam ser analisados conjuntamente com espeleotemas locais, cumprindo um dos principais objetivos do projeto temático no qual esta tese se insere. Primeiramente, foi desenvolvida uma nova metodologia para melhorar a observação dos anéis de crescimento e para explorar a diversidade de espécies encontradas na região. A espécie escolhida no local foi *Amburana cearensis*, previamente utilizada na América do Sul e com grande potencial dendroclimático (Baker *et al.*, 2015; Brienen & Zuidema, 2005; López *et al.*, 2022; Paredes-Villanueva *et al.*, 2015) e dela foram construídas cronologias da largura e dos isótopos estáveis de oxigênio dos anéis de crescimento. As cronologias de largura e isótopos estáveis de oxigênio de *A. cearensis* e *Cedrela fissilis* mostraram um excelente sinal climático de precipitação (largura dos anéis) e déficit de pressão de vapor (VPD, com os isótopos de oxigênio). Portanto, a tese consolidou uma nova espécie em uma nova região do Brasil, trazendo desde avanços metodológicos a discussões de questões fundamentais relacionadas ao aquecimento global e como o crescimento de espécies arbóreas responde em um local extremamente exposto (Figura 1). Isso foi realizado com a colaboração de especialistas em diversas áreas de conhecimento para explorar um conjunto único em regiões tropicais de amostras subfósseis e fazer correlações com espeleotemas locais para verificar quais os efeitos de mudanças climáticas atuais e passadas árvores de matas tropicais sazonalmente secas.

### **Capítulo 1** – Desafio: *Dificuldade de visualização dos anéis de crescimento em áreas com grande diversidade anatômica*

No primeiro capítulo, uma nova metodologia para melhorar a visualização dos anéis de crescimento foi testada explorando a autofluorescência da madeira. Utilizando um estereomicroscópio de fluorescência e um conjunto de filtros em

diferentes comprimentos de onda, comumente encontrados em institutos de pesquisa, espécies com diferentes características anatômicas foram testadas em busca de melhoras na visualização das camadas de crescimento. Dentre as 38 espécies testadas, mais da metade das mostrou melhoras na visualização e interpretação de algum aspecto anatômico. Por exemplo, uma espécie emblemática nessas regiões de matas secas, a barriguda (*Cavanillesia arborea*), previamente descrita como não possuindo camadas de crescimento visíveis em uma área próxima (Barbosa *et al.*, 2018), teve suas camadas de crescimento reveladas devido à autofluorescência mais intensa dos limites do anel em relação a matriz de células produzidas durante a estação de crescimento. Já em espécies muito utilizadas na dendrocronologia tropical, como *Cedrela* sp. e *Hymenaea* sp., a técnica também auxiliou na distinção entre anéis de crescimento verdadeiros e falsos, mostrando sua utilidade na datação cruzada em porções das amostras de difícil interpretação. As diferenças anatômicas entre os anéis verdadeiros e falsos, como células de parênquima maiores e mais finas nos anéis falsos de *Hymenaea* (Locosselli *et al.*, 2016) são rapidamente localizadas com a técnica. Portanto conseguimos desenvolver e testar uma nova metodologia para observação e interpretação de camadas de crescimento em madeira que pode auxiliar cientistas no processo de contagem e datação cruzada, além de também oferecer imagens de qualidade e com grande contraste para estudos anatômicos quantitativos.

## **Capítulo 2** – Desafio: *Estabelecer uma nova cronologia em região tropical*

No segundo capítulo, foi estabelecida a primeira cronologia brasileira da largura dos anéis de *Amburana cearensis*, com um forte sinal climático a nível populacional e individual que permitiu a identificação de áreas de refúgio climático no PNCP (Godoy-Veiga *et al.*, 2021). Graças a cronologia com árvores bem datadas, confirmado por análises detalhadas de radiocarbono no período do pico-da-bomba (Hua *et al.*, 2013), foi possível adotar uma estratégia menos conservadora e fazer inferências para além do sinal populacional. Exploramos a nível individual a sensibilidade climática de cada árvore em uma paisagem com diferentes níveis de sazonalidade mensurados por índices de vegetação obtidos de imagens de satélite.

Utilizando uma análise de agrupamento hierárquico dos coeficientes de correlação entre as séries de anéis normalizadas de cada árvore com dados mensais de temperatura e precipitação, foram encontrados grupos de árvores com sensibilidade climática distinta. Nas áreas com sazonalidade mais intensa, onde os valores do índice de vegetação (NDVI) variavam mais entre as estações secas e chuvosas, as árvores apresentam grande sensibilidade as variações de precipitação e temperatura. Já nas áreas mais baixas e com solos mais profundos do PNCP, a largura dos anéis das árvores não é tão sensível as variações médias do clima.

Essas árvores estão menos expostas às mudanças climáticas, demorando mais para sofrerem os impactos negativos dos previstos aumentos de temperatura e provável redução em precipitação (IPCC WGI, 2021). Isso traz repercussões ao local visto que a abordagem adotada permitiu identificar árvores em chamados refúgios climáticos (Morelli *et al.*, 2020), que no caso do PNCP correspondem a um quarto de sua área. Entretanto, em anos de condições extremas de alta temperatura e pouca chuva, todas as árvores do local sofrem impactos negativos no crescimento. Portanto, esta espécie e nossa abordagem podem auxiliar na confecção de propostas de manejo em locais com paisagem complexa indicando regiões em que as medidas serão mais efetivas (Morelli *et al.*, 2020; Trouillier *et al.*, 2018). Isso é útil em locais com poucos recursos, como normalmente é o caso dos Parques Nacionais e Unidades de Conservação no geral, que podem usar essa abordagem para focar em áreas de refúgio climático e garantir o desenvolvimento das espécies locais.

### **Capítulo 3** – Desafio: *Aumentar o poder de inferências paleoclimáticas em regiões tropicais unindo diferentes arquivos naturais.*

No terceiro capítulo investigamos o efeito de mudanças climáticas no crescimento de árvores em uma região de intenso aumento de temperatura nos últimos anos utilizando um conjunto único em regiões tropicais de amostras subfósseis e correlacionando os dados de anéis de árvores com espeleotemas. Utilizando cronologias multicentenárias de *Amburana cearensis* que já continham um forte sinal comum, e unindo dados de *Cedrela fissilis* para a construção de séries robustas e bem datadas, a largura e isótopos estáveis puderam ser analisadas com

espeleotemas anuais locais. Isso foi possível após a obtenção dos resultados do segundo capítulo investigando todas as possíveis respostas individuais e populacionais de *A. cearensis* e de uma extensiva datação por radiocarbono de amostras de tronco preservadas, algo raro em regiões tropicais. Todos os registros analisados mostram um enriquecimento nos isótopos de oxigênio, reflexo do aumento de VPD no local, mas o crescimento das árvores ainda não foi impactado. O enriquecimento dos valores isotópicos observados recentemente é majoritariamente devido ao enriquecimento a nível da folha provocado pelo aumento de VPD, mas alterações no sinal da fonte podem começar a contribuir para esse aumento nos próximos anos.

Aumentos na demanda evaporativa, regulados pelos aumentos de temperatura e déficit de vapor de pressão, podem causar fechamento dos estômatos, reduzir a taxa fotossintética e assim reduzir o ganho de biomassa das árvores, importantes componentes do ciclo de carbono terrestre (Grossiord *et al.*, 2020; Pan *et al.*, 2013; Running, 1975). Estes períodos de alta demanda evaporativa podem ocorrer naturalmente e provavelmente ocorreram no período da Pequena Idade do Gelo como apontado pelos registros de espeleotemas (Novello *et al.*, 2012; Strikis *et al.* in press) e amostras subfósseis de *A. cearensis*, em que mais uma vez, nenhuma alteração no crescimento foi encontrada. Isso ocorre porque as árvores do local crescem reguladas pela disponibilidade hídrica entre os meses de outubro a março, e não são tão sensíveis as condições de alta demanda evaporativa. Porém vale notar que os valores de  $\delta^{18}\text{O}$  observados nos últimos anos são maiores do que o das amostras subfósseis, assim como o período de exposição a altas condições de VPD. Portanto, as consequências dessa longa exposição a condições de altas temperaturas e demanda evaporativa podem ter efeitos negativos no crescimento dessas árvores caso o local fique mais seco.

Dessa forma, o último capítulo desta tese mostrou que a união de espécies, indicadores e registros naturais podem auxiliar a elucidar os efeitos das mudanças climáticas que já afetam o meio biótico (fisiologia das árvores) e abiótico (sinal isotópico dos espeleotemas). Os dados de amostras de árvores subfósseis e espeleotemas que cresceram antes da intensa liberação de carbono na atmosfera

provém um amplo contexto para verificar os efeitos das atuais mudanças climáticas no sistema hídrico regulado pela Monção da América do Sul. Visto que as projeções de quantidade de chuvas na região não são tão claras como as de temperatura (IPCC WGI, 2021), continuar a produzir séries isotópicas de registros naturais pode auxiliar a entender as variações no Sistema de Monção da América do Sul, principalmente no funcionamento da Zona de Convergência do Atlântico Sul, responsável pela chuva no local e abastecimento de milhões de pessoas. Nossos resultados apontam uma superestimação dos efeitos do aumento de temperatura no crescimento dessas florestas e podem subsidiar modelos de resposta de vegetação mais realistas.

**Do projeto inicial aos resultados finais:** *Dificuldades práticas, resultados negativos, dados em aberto e indicação de próximas investigações*

Este projeto foi iniciado em maio de 2018, resistiu a uma pandemia e foi defendido em julho de 2023. Durante os cinco anos de sua execução, alguns pontos mudaram em relação ao planejamento inicial, seja pelas dificuldades inerentes à dendrocronologia tropical, ou pelas restrições impostas pela pandemia de corona vírus. Inicialmente, foi proposto a criação de cronologias de duas espécies do PNCP: *Amburana cearensis* e *Commiphora leptophloeos*. Para *A. cearensis*, a delimitação dos anéis e a datação cruzada foram feitas à contento comparado a espécies que tínhamos experiência em outros locais, como *Aspidosperma polyneuron* (Godoy-Veiga *et al.*, 2018), *Hymenaea courbaril* (Locosselli *et al.*, 2016, Locosselli *et al.*, 2017), *Podocarpus lambertii* (Locosselli *et al.*, 2016b), e as espécies do PNCP que começamos a analisar, como *Goniorrhachis marginata*, *Parapiptadenia zehnteneri*, *Handroanthus* sp. e *Commiphora leptophloeos*. Para esta última, a contagem dos anéis foi iniciada, mas a dificuldade de visualização dos anéis em imagens escaneadas dificultou o estabelecimento de uma cronologia durante a pandemia. As análises com autofluorescência (Godoy-Veiga *et al.*, 2019) mostraram bons resultados para a espécie, mas devido ao acesso restrito aos laboratórios durante a pandemia e não foi possível finalizar uma cronologia para esta espécie.



Até o momento foram contados 27 raios de 11 indivíduos de *C. leptophloeos*, e, tudo indica que a espécie pode atingir idades elevadas, de mais de 180 anos (Figura 2A). Apesar de possuir madeira de densidade mais baixa que *A. cearensis*, a taxa de crescimento diamétrica é de apenas 0.38 cm/ano, menor do que os 0.70 cm/ano de *A. cearensis* no mesmo local (Godoy-Veiga *et al.*, 2021). Dois desses indivíduos tiveram três anéis datados por radiocarbono ( $^{14}\text{C}$ ), e mesmo sem uma cronologia e sem a datação entre árvores, aparentemente algumas árvores podem apresentar poucos anéis problemáticos. A diferença entre o ano esperado pela contagem de anéis e pela datação por  $^{14}\text{C}$  foi de apenas um ano até 1974 para uma das amostras (Figura 2B). Já a segunda árvore analisada tinha mais anéis ausentes, sendo que o anel contado para 1985 foi datado e calibrado em 1980 (5 anéis ausentes) e o anel contado para 1974 tinha um conteúdo de  $^{14}\text{C}$  que indicou o ano de 1963, portanto, 10 anéis ausentes nesse período (Figura 2C). Dessa forma, esta espécie pode ter potencial para estudos dendrocronológicos, mas a construção das cronologias pode tomar mais tempo do que de outras espécies. Dentre as dificuldades estão à dificuldade de visualizar os anéis em imagens, anéis localmente ausentes e grande diferenças na anatomia da madeira do cerne e do alburno. Contudo, a longevidade e a dominância de *C. leptophloeos* na região a torna uma espécie chave para entender a dinâmica do local. Os problemas anatômicos podem ser superados dada a grande quantidade de discos de árvores mortas (mais de dez) e subfósseis (7 amostras) e assim permitir com que longas cronologias sejam construídas e informações valiosas sejam retiradas dos anéis desta espécie.

Além dos dados em aberto com árvores vivas, 21 amostras subfósseis de pelo menos 7 espécies também tiveram os anéis mais externos datados por radiocarbono ( $^{14}\text{C}$ ), compondo um material raríssimo em regiões tropicais para obter informações paleoclimáticas e paleoecológicas (Tabela 1). As amostras de madeira preservada são discos completos em boas condições e têm em média 80 anos, sendo que 13 deles têm mais de 60 camadas visíveis. Estudos dendrocronológicos usando madeira preservada em regiões tropicais são muito raros e nesta tese já conseguimos obter informações paleoclimáticas utilizando *A. cearensis* graças a uma abordagem multi proxy. De acordo com nossos resultados, outras espécies como a *C. leptophloeos* e

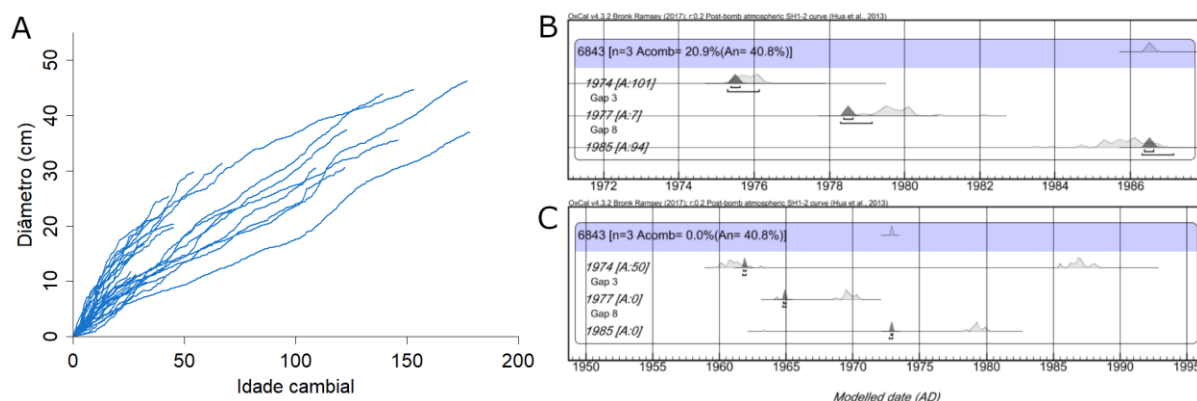


**Figura 2** – Em A, diâmetro (cm) por idade cambial dos raios de *Commiphora leptophloeos* analisados. Em B e C são apresentadas as datações de radiocarbono ( $^{14}\text{C}$ ) de duas amostras, sendo que para cada uma, três anos (1974, 1977 e 1985) contados pelos anéis de crescimento foram calibrados de acordo com seu conteúdo de  $^{14}\text{C}$ .

*P. zehntneri* também podem oferecer informações paleoecológicas ou paleoclimáticas inéditas. Ambas as espécies têm pelo menos 5 amostras, com pelo menos duas próximas dos 100 anos. Essas espécies possuem características ecológicas distintas, por exemplo em relação a densidade da madeira e riqueza no parque. Pelo observado durante as expedições ao PNCP, quando comparado à *C. leptophloeos* existe uma aparente alta taxa de mortalidade de *P. zehntneri*, evidente pela grande quantidade de árvores mortas e maior dificuldade em localizar árvores vivas. Portanto, essas duas espécies podem oferecer registros complementares do local para serem exploradas em estudos futuros.

**Tabela 1** - Amostras subfósseis encontradas na região, explicitando a quantidade de anéis observados e quantas datações de  $^{14}\text{C}$  foram feitas.

Espécie	SPFw	Local	Anéis	Datações
<i>Amburana cearensis</i>	6884	Arco do André (Central)	80	4
<i>Amburana cearensis</i>	6893	Arco do André (Superior)	86	4
<i>Amburana cearensis</i>	6937	Arco da Brejal	177	5
<i>Parapiptadenia zehntneri</i>	6896	Arco do André	51	Anel externo
<i>Parapiptadenia zehntneri</i>	6891	Arco do André	64	Anel externo
<i>Parapiptadenia zehntneri</i>	6963	Arco do André	88	Anel externo

<i>Parapiptadenia zehntneri</i>	6965	Arco do André	103	Anel externo
<i>Parapiptadenia zehntneri</i>	8231	Arco do André (Cobra)	100	Anel externo
<i>Commiphora leptophloeos</i>	6887	Arco do André (Grutinha)	54	Anel externo
<i>Commiphora leptophloeos</i>	6889	Arco do André (Superior)	75	Anel externo
<i>Commiphora leptophloeos</i>	6962	Arco do André	65	Anel externo
<i>Commiphora leptophloeos</i>	6966	Arco do André	99	Anel externo
<i>Commiphora leptophloeos</i>	6967	Arco do André	105	Anel externo
<i>Commiphora leptophloeos</i>	6968	Arco do André	52	Anel externo
<i>Commiphora leptophloeos</i>	6976	Arco do André	71	Anel externo
<i>Handroanthus</i> sp.	6919	Arco da Brejal	-	Anel externo
<i>Handroanthus</i> sp.	6972	Arco do André	89	Anel externo
<i>Handroanthus</i> sp.	7036	Arco do Boi - Carlúcio	-	Anel externo
<i>Hymenaea</i> sp.	6888	Arco do André (Grutinha)	56	Anel externo
<i>Lecythidaceae</i> cf.	8232	Arco do André (Cobra)	44	Anel externo
<i>Maclura tinctoria</i>	6890	Arco do André (Superior)	57	Anel externo

A partir desse conjunto de amostras subfósseis, obtivemos muitos dados de datações de  $^{14}\text{C}$ , apresentados na Figura 3. Na figura destaca-se os períodos da Pequena Idade do Gelo Antiga, do inglês *Late Antique Little Ice Age* (LALIA), Anomalia Climática Medieval, do inglês *Medieval Climate Anomaly* (MCA) e Pequena Idade do Gelo, do inglês *Little Ice Age* (LIA). Nota-se uma boa sobreposição das amostras na pequena idade do gelo, período que vai de 1400 a 1900 CE (IPCC, 2021), de grande importância para estudos paleoclimáticos dentro do contexto da Monção Sul-Americana e de estudos relacionados a ocorrência de mudanças climáticas abruptas. Nesse período, a forçante vulcânica aparentemente exerceu forte influência sobre o local de estudo, como observado no mundo todo (IPCC, 2021). Erupções vulcânicas que de alguma forma deslocam a Zona de Convergência Intertropical para o hemisfério Sul, ou que intensifiquem a atividade convectiva da Zona de Convergência do Atlântico Sul poderiam causar eventos de precipitação extrema na região (Strikis *et al.*, 2012; Vera *et al.*, 2006) e mega-enchentes no rio Peruaçu (Coelho, 2013) que levaram. Estes eventos potencialmente mobilizaram essas árvores subfósseis da floresta para o interior das cavernas, sendo

que algumas amostras foram encontradas em condutos a mais de 30 metros acima do nível atual do rio Peruaçu. Próximos trabalhos podem medir a composição dos isótopos estáveis de oxigênio e elementos traço para reconstruir esses eventos extremos de chuva. Além disso, também se abre também caminhos para medir a composição dos isótopos estáveis de carbono, comparar às árvores vivas e explorar efeitos do aumento da concentração de gás carbônico no crescimento das árvores nos dias atuais. Tanto os resultados já publicados, quanto os ainda em análise, reforçam a singularidade da região do PNCP como um local ideal para estudos paleoclimáticos unindo os já estabelecidos resultados de espeleotemas com os anéis de crescimento de árvores.

Tanto os dados em aberto das árvores vivas de *Commiphora leptophloeos*, quanto as datações e medições dos subfósseis não puderam ser extensamente analisados durante a duração deste projeto, mas continuarão sendo analisados. As dificuldades em relação a visualização dos anéis e datação cruzada encontradas durante esta tese são comuns a outras regiões e espécies tropicais (Worbes, 2002). Entretanto, foi possível finalizar a publicação de dois trabalhos e a organização de um terceiro artigo para submissão em uma revista de alto impacto, mesmo tendo focando em apenas uma espécie. Para garantir que as conclusões a partir de uma espécie resultassem em um trabalho de alto impacto no último capítulo da tese, fizemos colaborações, facilitadas pelo Projeto Temático PIRE-CREATE. Assim, incluímos a cronologia de *Cedrela fissilis*, a comparação com espeleotemas e modelos climáticos para o passado produzidos por colaboradores. Portanto, os produtos finais da tese foram resultado de tomadas de decisões que optaram por investir as análises na espécie da região cuja cronologia tinha um forte sinal climático e complementar o conjunto de dados através de colaborações, assim os resultados puderam ser discutidos com robustez na duração da tese.

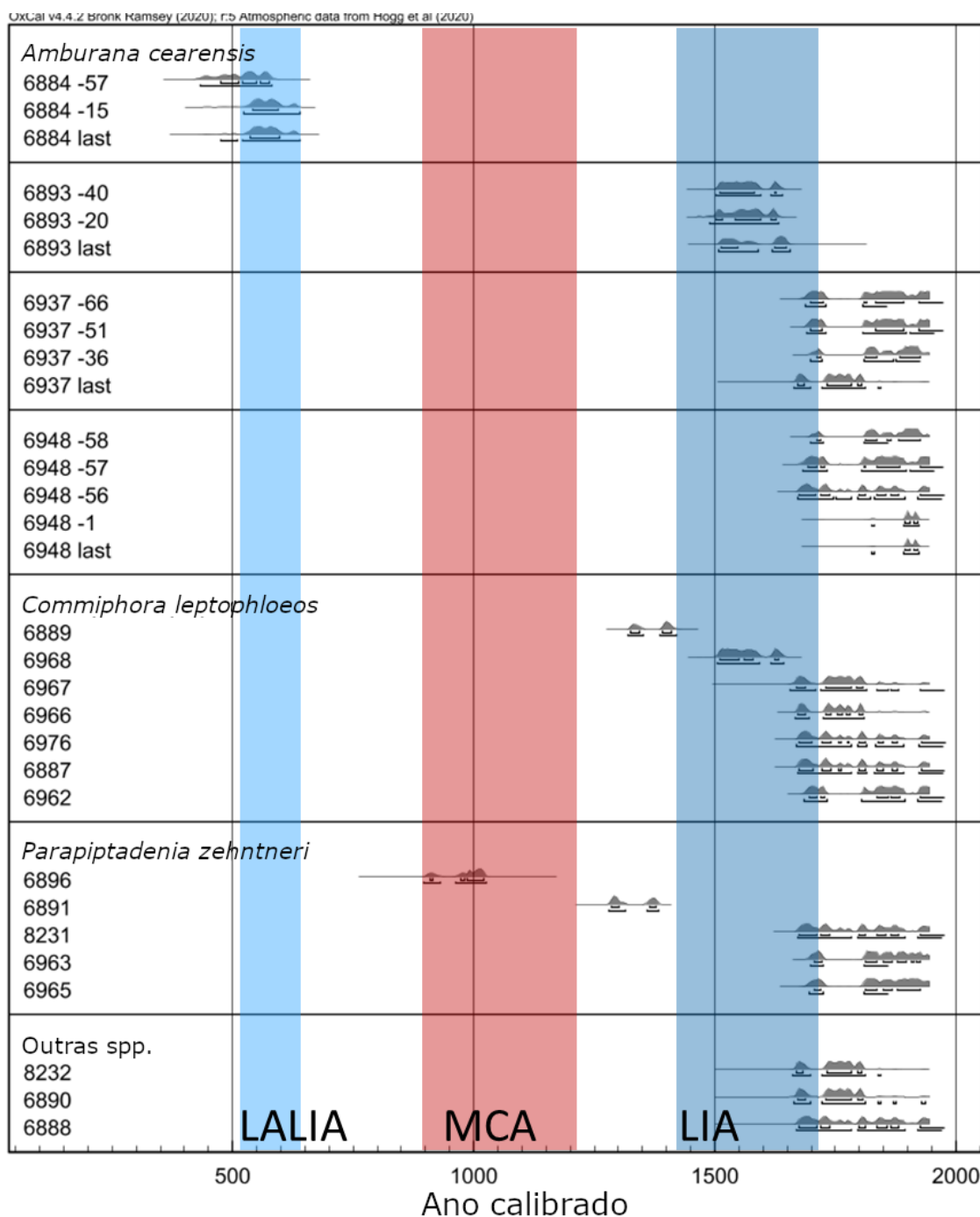


**Figura 3** - Amostras subfósseis datadas com número da coleção SPFW e anel datado por radiocarbono ( $^{14}\text{C}$ ). Em destaque estão os períodos climáticos com mudanças abruptas no clima descritos no texto. Para cada indivíduo é apresentado a distribuição de probabilidades de idades (ano) resultantes da calibração com a curva de  $^{14}\text{C}$  para a América do Sul.

## Conclusões

A produção de séries de dados centenárias de largura e de razão dos isótopos estáveis de oxigênio ( $\delta^{18}\text{O}$ ) dos anéis de crescimento de árvores permitiu entender respostas de crescimento das árvores da região frente as mudanças climáticas. Além de compreender a distribuição e intensidade dessas variações climáticas nos últimos 500 anos na região, com enfoque no sistema hidroclimático estabelecido pelo Sistema de Monção da América do Sul. O Parque Nacional Cavernas do Peruaçu está inserido em uma das regiões tropicais de *hot spot* de aquecimento global, e em sua paisagem e florestas complexas foram encontrados refúgios climáticos. Nesses refúgios, as árvores crescem em um microambiente desacoplado das variações regionais médias de chuva e temperatura. Entretanto, em anos extremos de pouca chuva e altas temperaturas, até mesmo as árvores nesses refúgios sofrem efeitos negativos em seu crescimento. Já os aumentos de VPD que causam o aumento na demanda evaporativa e a tendência de enriquecimento nas cronologias de  $\delta^{18}\text{O}$  a partir da década de 1980 ainda não afetam o crescimento dessas árvores e a quantidade de chuva se mantém como o principal fator limitante ao crescimento. Dentre as possibilidades de trabalhos futuros a partir desta tese estão estudos mensurando a composição de isótopos estáveis de carbono e análise de elementos traço. Também é interessante a procura por discos de árvores mortas ou madeira preservada para estender as cronologias atuais e tentar construir séries flutuantes quando amostras preservadas forem encontradas. Com mais registros como estes, teremos ferramentas para mensurar as consequências das mudanças climáticas e assim auxiliar na produção de medidas de mitigação para a população.



## Referências Bibliográficas

---

- Baker, J. C. A., Hunt, S. F. P., Clerici, S. J., Newton, R. J., Bottrell, S. H., Leng, M. J., Heaton, T. H. E., Helle, G., Argollo, J., Gloor, M., & Brienen, R. J. W. (2015). Oxygen isotopes in tree rings show good coherence between species and sites in Bolivia. *Global and Planetary Change*, 133, 298–308. <https://doi.org/10.1016/j.gloplacha.2015.09.008>
- Barbosa, A. C. M., Pereira, G. A., Granato-Souza, D., Santos, R. M., & Fontes, M. A. L. (2018). Tree rings and growth trajectories of tree species from seasonally dry tropical forest. *Australian Journal of Botany*, 66(5), 414–427. <https://doi.org/10.1071/BT17212>
- Brienen, R. J. W., & Zuidema, P. A. (2005). Relating tree growth to rainfall in Bolivian rain forests: a test for six species using tree ring analysis. *Oecologia*, 146(1), 1–12. <https://doi.org/10.1007/s00442-005-0160-y>
- Coelho, A. H. F. 2013. Registros de grandes alagamentos no cânion do rio Peruaçu, Parque Nacional Cavernas do Peruaçu – PNCP, MG. Master Thesis defended at the Geography department of the University of Minas Gerais.
- Godoy-Veiga, M., Ceccantini, G., Pitsch, P., Krottenthaler, S., Anhof, D., & Locosselli, G. M. (2018). Shadows of the edge effects for tropical emergent trees: the impact of lianas on the growth of *Aspidosperma polyneuron*. *Trees - Structure and Function*, 32(4), 1073–1082. <https://doi.org/10.1007/s00468-018-1696-x>
- Godoy-Veiga, M., Cintra, B. B. L., Stríkis, N. M., Cruz, F. W., Grohmann, C. H., Santos, M. S., Regev, L., Boaretto, E., Ceccantini, G., & Locosselli, G. M. (2021). The value of climate responses of individual trees to detect areas of climate-change refugia, a tree-ring study in the Brazilian seasonally dry tropical forests. *Forest Ecology and Management*, 488(January). <https://doi.org/10.1016/j.foreco.2021.118971>
- Godoy-Veiga, M., Slotta, F., Alecio, P. C., & Ceccantini, G. (2019). Improved tree-ring visualization using autofluorescence. *Dendrochronologia*, 55(April), 33–42. <https://doi.org/10.1016/j.dendro.2019.03.003>
- Grossiord, C., Buckley, T. N., Cernusak, L. A., Novick, K. A., Poulter, B., Siegwolf, R. T. W., Sperry, J. S., & McDowell, N. G. (2020). Plant responses to rising vapor pressure deficit. *New Phytologist*, 226(6), 1550–1566. <https://doi.org/10.1111/nph.16485>
- Hua, Q., Barbetti, M., & Rakowski, A. (2013). Atmospheric radiocarbon for the period 1950–2010. 55(4).

- IPCC WGI, I. A. (2021). Climate Change 2021 The Physical Science Basis WGI. In Bulletin of the Chinese Academy of Sciences (Vol. 34, Issue 2).
- Locosselli, G. M., Cardim, R. H., & Ceccantini, G. (2016b). Rock outcrops reduce temperature-induced stress for tropical conifer by decoupling regional climate in the semiarid environment. *International Journal of Biometeorology*, *60*(5), 639–649. <https://doi.org/10.1007/s00484-015-1058-y>
- Locosselli, G. M., Krottenthaler, S., Pitsch, P., Anhuf, D., & Ceccantini, G. (2017). Age and growth rate of congeneric tree species (*Hymenaea* spp. - Leguminosae) inhabiting different tropical biomes. *Erdkunde*, *71*(1), 45–57. <https://doi.org/10.3112/erdkunde.2017.01.03>
- Locosselli, G. M., Schöngart, J., & Ceccantini, G. (2016). Climate/growth relations and teleconnections for a *Hymenaea courbaril* (Leguminosae) population inhabiting the dry forest on karst. *Trees - Structure and Function*, *30*(4), 1127–1136. <https://doi.org/10.1007/s00468-015-1351-8>
- López, L., Villalba, R., & Stahle, D. (2022). High-fidelity representation of climate variations by *Amburana cearensis* tree-ring chronologies across a tropical forest transition in South America. *Dendrochronologia*, *72*(December 2021). <https://doi.org/10.1016/j.dendro.2022.125932>
- Morelli, T. L., Barrows, C. W., Ramirez, A. R., Cartwright, J. M., Ackerly, D. D., Eaves, T. D., Ebersole, J. L., Krawchuk, M. A., Letcher, B. H., Mahalovich, M. F., Meigs, G. W., Michalak, J. L., Millar, C. I., Quiñones, R. M., Stralberg, D., & Thorne, J. H. (2020). Climate-change refugia: biodiversity in the slow lane. *Frontiers in Ecology and the Environment*, *18*(5), 228–234. <https://doi.org/10.1002/fee.2189>
- Novello, V. F., Cruz, F. W., Karmann, I., Burns, S. J., Strikis, N. M., Vuille, M., Cheng, H., Lawrence Edwards, R., Santos, R. V., Frigo, E., & Barreto, E. A. S. (2012). Multidecadal climate variability in Brazil's Nordeste during the last 3000 years based on speleothem isotope records. *Geophysical Research Letters*, *39*(23), 1–6. <https://doi.org/10.1029/2012GL053936>
- Pan, Y., Birdsey, R. A., Phillips, O. L., & Jackson, R. B. (2013). The structure, distribution, and biomass of the world's forests. *Annual Review of Ecology, Evolution, and Systematics*, *44*(November), 593–622. <https://doi.org/10.1146/annurev-ecolsys-110512-135914>
- Paredes-Villanueva, K., López, L., Brookhouse, M., & Cerrillo, R. M. N. (2015). Rainfall and temperature variability in Bolivia derived from the tree-ring width of *Amburana cearensis* (Fr. Allem.) A.C. Smith. *Dendrochronologia*, *35*, 80–86. <https://doi.org/10.1016/j.dendro.2015.04.003>

- Running, S. W. (1975). Environmental control of leaf water conductance in conifers. *Canadian Journal of Forest Research*, 6, 104–112.  
<https://doi.org/https://doi.org/10.1139/x76-013>
- Strikis, N. M., Cruz, F. W., Cheng, H., Karmann, I., Edwards, R. L., Vuille, M., Wang, X., de Paula, M. S., Novello, V. F., & Auler, A. S. (2012). Abrupt variations in South American monsoon rainfall during the Holocene based on a speleothem record from central-eastern Brazil. *Geology*, 39(11), 1075–1078.  
<https://doi.org/10.1130/G32098.1>
- Trouillier, M., van der Maaten-Theunissen, M., Harvey, J. E., Würth, D., Schnittler, M., & Wilmking, M. (2018). Visualizing individual tree differences in tree-ring studies. *Forests*, 9(4), 1–14. <https://doi.org/10.3390/f9040216>
- Vera, C., Higgins, W., Amador, J., Ambrizzi, T., Garreaud, R., Gochis, D., Gutzler, D., Lettenmaier, D., Marengo, J., Mechoso, C. R., Noguez-Paegle, J., Silva Dias, P. L., & Zhang, C. (2006). Toward a unified view of the American monsoon systems. *Journal of Climate*, 19(20), 4977–5000.  
<https://doi.org/10.1175/JCLI3896.1>
- Worbes, M. (2002). One hundred years of tree-ring research in the tropics—a brief history and an outlook to future challenges. *Dendrochronologia*, 20, 217–231.
- Zuidema, P. A., Baker, P. J., Groenendijk, P., Schippers, P., van der Sleen, P., Vlam, M., & Sterck, F. (2013). Tropical forests and global change: filling knowledge gaps. *Trends in Plant Science*, 18(8), 413–419.  
<https://doi.org/10.1016/j.tplants.2013.05.006>

## Biografia

---

Milena de Godoy Veiga, nascida em Amparo, interior de São Paulo, estudou em escola pública no Ensino médio, entrou e permaneceu na Universidade de São Paulo graças às ações de inclusão e permanência estudantil como INCLUSP e moradia no CRUSP. Formou-se em ciências biológicas pelo Instituto de Biociências da USP (IB-USP) em 2017, e seguiu para a pós-graduação, participando ativamente das atividades do departamento como monitorias de disciplinas de graduação, representante no Conselho do Departamento, na Comissão Coordenadora do Programa de Pós-Graduação, e na Congregação do IB-USP. Iniciou mestrado para investigar os efeitos de borda em duas espécies tropicais em floresta estacional semi-decidual, mas transferiu-se para curso de doutorado direto em 2018. No Departamento de Botânica do IB-USP, desenvolveu projeto de doutorado direto *“Impacto das mudanças climáticas nos últimos 500 anos por meio de estudos dendroclimatológicos e isotópicos de árvores na região do Parque Nacional Cavernas do Peruaçu”* com bolsa FAPESP (projeto 2018/07632-6 dentro do Temático 2017/50085-3). Dentro desse período, usufruiu de 11 meses de Bolsa de Estágio e Pesquisa no Exterior (BEPE, 2019/09813-0) desenvolvendo o projeto *“Datação com radiocarbono para confirmar anualidade dos anéis de crescimento e datar precisamente troncos fósseis de espécies arbóreas no Parque Nacional Cavernas do Peruaçu para estudos paleoclimáticos”* nos laboratórios de arqueologia e datação por radiocarbono do Instituto Weizmann em Israel. Mesmo durante a pandemia, participou de 4 congressos internacionais, revisou artigos para periódicos internacionais, publicou os dois primeiros capítulos e submeteu o terceiro. Além disso, colaborou em outros dois trabalhos já publicados e um terceiro em preparação, colaborou em três resumos para congressos, participou de dois capítulos e lecionou no curso Botânica no Inverno do IB-USP e deu curso de princípios de dendrocronologia para o público geral na 23ª Semana temática da Biologia.

### Lista de publicações

1. Godoy-Veiga, M. *et al.*, 2021. The value of climate responses of individual trees to detect areas of climate-change refugia, a tree-ring study in the Brazilian seasonally dry tropical forests. *Forest Ecology and Management*, 488. <https://doi.org/10.1016/j.foreco.2021.118971>
2. Godoy-Veiga, M. *et al.*, 2019. Improved tree-ring visualization using autofluorescence. *Dendrochronologia*, 55. <https://doi.org/10.1016/j.dendro.2019.03.003>
3. Godoy-Veiga, M. *et al.*, 2018. Shadows of the edge effects for tropical emergent trees: the impact of lianas on the growth of *Aspidosperma polyneuron*. *Trees Structure and Function*. <https://doi.org/10.1007/s00468-018-1696-x>
4. Godoy-Veiga, M. and Teixeira-Costa, L. 2018. Chapter 13 – Anatomy basis for wood function attributes comprehension (in Portuguese). *Em livro: Apostila – VII Botânica no Inverno 2018*. ISBN: 978-85-85658-77-9

### Colaborações

5. Teixeira-Costa, L and Godoy-Veiga, M. 2022. Chapter 9 - Microtomography for three dimensional study of plant anatomy. *Em livro: Apostila – VII Botânica no Inverno 2018* ISBN: 978-65-88234-10-5
6. Amais *et al.*, 2021 - Trace elements distribution in tropical tree rings through high-resolution imaging using LA-ICP-MS analysis - *Journal of Trace Elements in Medicine and Biology*. <https://doi.org/10.1016/j.jtemb.2021.126872>
7. Borrego *et al.*, 2019 – The trajectory and digital reconstitution of a canoe of Museu Paulista - USP. *Anais do Museu Paulista: História e Cultura Material*, v. 27. <https://doi.org/10.1590/1982-02672019v27e18d1>

### Resumos em congresso

1. Godoy-Veiga, M. *et al.*, *AGU Fall Meeting, apresentação oral*, 12-16 Dec 2022 - “Recent Increase in Water Deficit in Central Brazil is Recorded in the Oxygen Isotopes of Dry-forest Tree Species” na seção: Changes and Impacts of Climate Variability in South America III. Chicago, IL. ID do resumo: 1146979. Final Paper Number: GC25B-04
2. Godoy-Veiga, M. *et al.*, *AmeriDendro 4th edition, apresentação oral presencial* 27-30 Junho 2022 - “Using wood autofluorescence to explore the diversity of wood anatomy in the tropics and improve tree-ring visualization” in: Symposium 8 - Dendrochronological progress in tropical Americas. Montreal, Canadá.

3. Godoy-Veiga, M. *et al.*, *TRACE 2021 Conference, painel online*, 16-17 Junho 2021 - “Integrating multiple-proxies from tree rings and speleothems to allow paleoclimate studies in Central Brazil using a unique set of subfossil wood” In: Edvardsson, J., Chen, T.T., Gunnarson, B., Hansson, A., Linderholm, H.W. (eds.) *Book of Abstracts.*, Lund, Sweden. p. 122.

4. Godoy-Veiga, M. *et al.*, *22nd EGU General Assembly, painel online* 4-8 Maio, 2020 – “First *Amburana cearensis* (Fabaceae) tree-ring chronology in Brazil in a dry forest shows great potential for climate reconstruction” DOI: 10.5194/egusphere-egu2020-11379

### **Colaborações**

5. Fontana, C. *Et al.*, *CONFLAT - Congreso Forestal Latinoamericano, apresentação oral presencial*, 27-30 Março 2023. “Multiproxy approach in dendrochronology: a case study for a specimen of *Aspidosperma australe* MÜLL.ARG (Apocynaceae).”

6. Fontana, C. *et al.*, *V CBCTEM – Brazilian Conference of Wood Science and Technology, poster apresentado pessoalmente*, 19-21 Outubro 2022. “Anatomical characterization of the growth rings of *Ocotea porosa* (Lauraceae).”

7. Ganiko-Dutra, M. *et al.*, *71º Congresso Nacional de Botânica e XIII Encontro de Botânicos do Centro-Oeste*, poster online, 27-02 Junho 2021. “Diferentes estratégias do uso da água em ervas-de-passarinho sustentam sua atividade em plantas hospedeiras decíduas.”

### **Cursos ministrados**

1. Curso: Princípios e práticas em dendrocronologia tropical, durante a *23ª Semana Temática da Biologia do IB-USP*, nos dias 19 e 20 de outubro de 2020, carga horária de 6 horas.

2. Orientação de pequeno projeto: Aspectos da funcionalidade do lenho na relação parasita-hospedeira, durante o *VII Curso Botânica no Inverno*, realizado no Departamento de Botânica do Instituto de Biociências da Universidade de São Paulo, no período de 10 a 27 de julho 2018, carga horária aproximadamente 24 horas.

### **Revisão de artigos em periódicos internacionais**

- 1 trabalho revisado para *Theoretical and Applied Climatology* em 2023
- 6 trabalhos revisados para *Dendrochronologia* entre 2021 e 2022